Towards a novel polio VLP vaccine:
Stabilising the PV-1 capsid by thermal selection

Oluwapelumi Olufemi Adeyemi

Submitted in accordance with the requirements for the degree of

Doctor of Philosophy

The University of Leeds
School of Molecular and Cellular Biology

January 2017

The candidate confirms that the work submitted is his own, except where work which has formed part of jointly authored publications has been included. The contribution of the candidate and the other authors to this work has been explicitly indicated below. The candidate confirms that appropriate credit has been given within the thesis where reference has been made to the work of others.

The work in Chapter 3 and part of Chapter 4 of the thesis has appeared in publication as follows:

Increasing type-1 poliovirus capsid stability by thermal selection. Journal of virology 91:e01586-16., Accepted manuscript posted online 7 December 2016, doi:10.1128/JVI.01586-16. Oluwapelumi O Adeyemi, Clare Nicol (CN), Nicola J Stonehouse (NJS), and David J Rowlands (DJR).

The author (OOA) was responsible for carrying out all experiments and drafting the manuscript. CN assisted with some of the preliminary experimental work. NJS and DJR conceived the idea, supervised the project, prepared and edited the manuscript.

Acknowledgements

Let not the wise boast of their wisdom or the strong boast of their strength or the rich boast of their riches, but let the one who boasts, boast about this: that they have the understanding to know me, that I am the Lord... Jeremiah 9:23 (NKJV).

The novel polio VLP vaccine research consortium (2015). A priceless photograph [to me] of the research team members. Picture was taken after a scientific retreat at the Edward Jenner Museum, Thackeray, by an anonymous volunteer. Front: Dave Rowlands (Lead), Dave Stuart, Luigi De Colibus, Helen Fox, Mai Uchida, Sarah Knowlson, Sinead Lyons, Liz Fry, Oluwapelumi Adeyemi (self), Johanna Marsian, Nicola Stonehouse, Ellie Ehrenfeld, Phil Minor. Back: Jeff Almond, George Lomonossoff, Claudine Porta, Ian Jones, Toby Tuthill, Andy Macadam, Joe Newman, Jim Hogle, Mohammad Bahar, and

Clare Nicol (not in the photo). Insert: The official logo of the Edward Jenner museum.

I would also like to thank my undergraduate lecturers at the Lagos State University, Nigeria, especially Prof. K.O. Akinyemi, who encouraged me to complete my Microbiology studies in my years of uncertainties. Many thanks also to my lecturers at the University of Ilorin, Nigeria, during my Master's program, especially my project supervisor, Dr. O.O. Agbede, who taught me a lesson I would always remember: *"a good student is one who teaches his teachers"*, and to Prof L.D. Edungbola, for his professional mentoring and guidance.

To my family: Mom, you "cranked up" my quest in Virology and fuelled it all the way!!! Thank you for the countless times you stooped down to get me back on my feet *as I rode the edge of "the storms..."* Dad, you've always been my hero and mentor. Thank you, for your support, constant words of encouragement and exemplary leadership. I love it when you say, *"The reward of hard work is more work!"* To my siblings, bro' Ogo (MD), bro' 'Seun (MD), sis' Ola (PhD) and 'Sanmi: you make the best team anyone could ever ask for! And to two lovely ladies who've transformed my world: Valerie and Victoria, thank you for your patience and love; we've got a long road ahead – buckle up, please.

Not to forget my friends too many to mention by name… thanks for the dynamic support.

Every good and perfect gift is from above, coming down from the Father of the heavenly lights, with whom there is no change or shifting shadow. James 1:17 (NKJV).

Abstract

Poliomyelitis (polio) is a highly infectious and debilitating viral disease caused by poliovirus (PV). The use of an oral (OPV) and an inactivated (IPV) polio vaccine over the years has led to remarkable progress towards the eradication of polio. In order to safeguard against reintroduction of polio, post-eradication, vaccination will continue. However, current OPV and IPV require the propagation of live virus and therefore constitute biological hazards post-eradication.

Genome-free empty capsids (ECs) are produced during the PV lifecycle but are conformationally unstable at physiological temperatures, rapidly losing native antigenicity. If stabilised in the native conformation, recombinantly expressed PV ECs could have applications as alternative virus-free vaccines for use post-eradication.

In this study, thermally-stable variants were selected through cycles of increasing thermal pressures from 51°C through 53°C to 57°C. Selected viruses were shown to have evolved thermally-stable ECs that retained native antigenicity at elevated temperatures. The capsid-stabilising mutations were identified and stabilising combinations were further investigated.

The structural precursor protein (P1) of two mutant virus candidates were co-expressed with the viral protease (3CD) in a plant system which resulted in the production of thermally-stable PV-1 ECs, some of which retained the native antigenicity at temperatures higher than current IPV. The investigated potential for expression of thermally-stable VLPs in yeast is also discussed.

Table of Contents

Table of Figures

Table of Tables

Table of Abbreviations

µCi/ ml	Micro curie per millilitres
AFP	Acute flaccid paralysis
APS	Ammonium persulfate
BMGY	Buffered Glycerol-Complex Medium
BMMY	Buffered Methanol-Complex Medium
bOPV	Bivalent OPV
BRP	Biological Reference Preparation
CDC	Centre for Disease control
CL	Cloverleaf
Cryopreservation	Cryogenic preservation
CsCl	Caesium chloride
CSF	Cerebrospinal fluid
CV	*Coxsackievirus*
cVDPV	Circulating vaccine derived PV
Cys/Meth	Cysteine/ methionine
ddH$_2$O	Double distilled water
DEPC	Diethylpyrocarbonate [C$_6$H$_{10}$O$_5$]
dH$_2$O	Distilled water
DMEM	Dulbecco's Modified Eagles Medium
DNA	Deoxy nucleic acid
dNTP	Dinucleotide triphosphate
DTT	Dithiothreitol
EC	Empty capsid
EDTA	Ethylenediaminetetraacetic
EDTA	Diaminoethanetetra-acetic acid
ELISA	Enzyme-linked immunosorbent assay
EP	European Pharmacopoeia
EV	Enterovirus
FCS	Foetal calf serum
GPEI	Global Polio Eradication Initiative
GuHCl	Guanidine hydrochloride

h.p.i	Hours post-infection
H_2O	Water
HBc	Hepatitis B virus core
HCl	Hydro chloric acid
HeLa:	Henrietta Lax
HEPES	N-(2-hydroxyethyl) piperazine-K-(2-ethane-sulfonic acid)
HPV	Human Papillomavirus
HRP	Horse radish protein
ICTV	International Committee on the Taxonomy of viruses
IgG	Immunoglobulin G
IP	Immunoprecipitated
IPV	Inactivated polio vaccine
IRES	Internal ribosome entry site
iVDPV	Immunodeficient vaccine-derived poliovirus
KCl	Potassium chloride
KH_2PO_4	Potassium phosphate
mAb	Monoclonal antibodies
MAFFT	Multiple sequence alignment fast Fourier transform
MOPS	3-morpholinopropane-1-sulfonic acid
$Na_2HPO_4 \cdot 2\ H_2O$	Sodium di-hydrogen phosphate
NaCl	Sodium Chloride
NaOH	Sodium hydroxide
NFIP	National Foundation for Infantile Paralysis
NIBSC	National Institute of Biological Standards and Control
OD	Optical density
OPV	Oral polio vaccine
ORF	Open reading frame
PAD	Pichia Adenine-dropout
PaSTRy	Particle stability RNA releaser assay
PBS	Phosphate buffered saline
PCR	Polymerase chain reaction
PFU/ml	Plaque forming units per millilitre

PIPES	Piperazine-N,N′-bis
Polio	Poliomyelitis
PV	Poliovirus
RdRp	RNA-dependent RNA-polymerase
RIPA	Radio Immunoprecipitation assay
RSBEC	Re-suspension buffer for EC
RSBVir	Re-suspension buffer for virion
RT	Reverse Transcription
SDM	Site-directed mutagenesis
SDS-PAGE	Sodium dodexycholate-Poly acrylamide gel electrophoresis
SDT	Sequence Demarcation Tool
ssRNA	Single-stranded RNA
TAE	Tris Acetic Acid EDTA
TB	Tris-buffer
TBE	Tris Borate EDTA
TBST	Tris-Buffered Saline and Tween 20
TEMED	Tetramethylethylenediamine
Tm	Melting temperature
Ts	Transitional
Tv	Transversional
UNICEF	United Nations Children's Fund
UTR	Untranslated region
VAPP	Vaccine-associated paralytic poliomyelitis
VDPV	Vaccine derived PV
VLPs	Virus-like particles
VPg	Viral protein
WHA	World Health Assembly
WHO	World Health Organisation
wt	Wild type

Chapter 1

Introduction

1.1. Poliomyelitis

The term "poliomyelitis" is derived from two Greek words, "polios" (grey) and myelos (marrow or spinal cord), which describe the site of infection i.e. the grey matter of the spinal cord (Erasmus, 2011; Glass *et al.*, 2002). Poliomyelitis (also known as polio) is caused by three serotypes of *Poliovirus* (i.e. PV-1, PV-2 and PV-3). Outbreaks of polio have been responsible for numerous irreversible paralysis and deaths for over 12 decades (CDC, 2012; De Jesus, 2007; Horstmann, 1985). Polio or infantile paralysis (as it was popularly known) is clinically defined as a highly infectious viral disease that presents as fever, meningitis, and acute flaccid paralysis (AFP), and may lead to death (Knowles, 2012b). For the purpose of this work, polio or poliomyelitis refers to infectious poliomyelitis caused by PV (figure 1.1).

100 nm
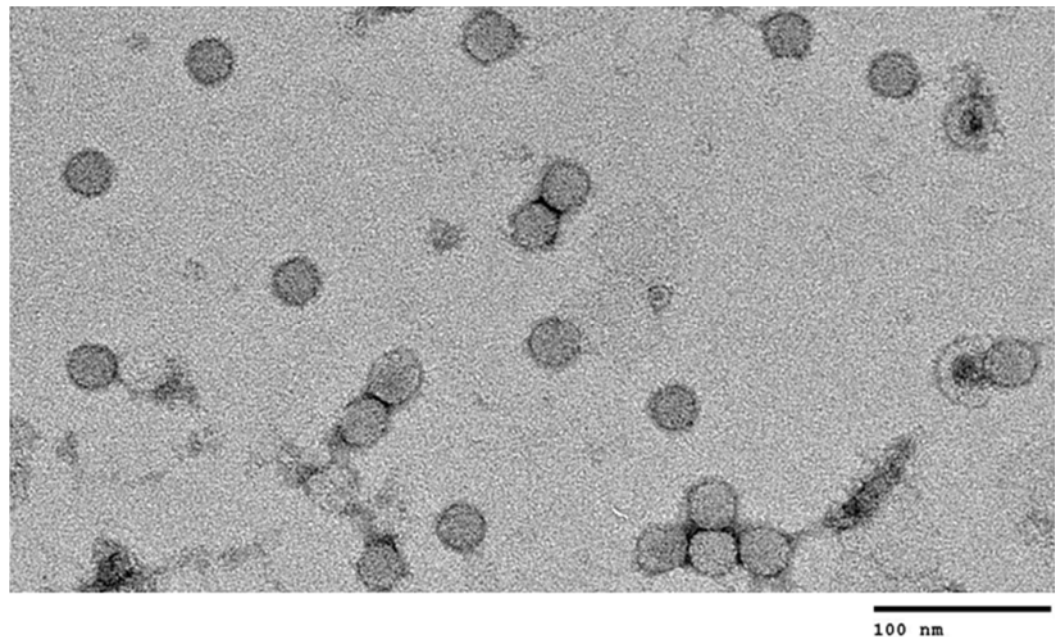
Figure 1.1 Negatively stained electron micrograph of PV-1 particles.

1.2. Four centuries of polio: a historical account

Polio is alleged to be an ancient disease of man that pre-dates documented history. The discovery of an Egyptian stele of the second millennium BC that portrays a man with asymmetric flaccid paralysis and an atrophic limb, as well as mummified Egyptian bodies of this era having similar conditions, have provided additional evidence for this claim (Bunimovich-Mendrazitsky & Stone, 2005; Glass *et al.*, 2002; Kirienko A., 2011). While this claim may be true for AFP and atrophy of the limb, it does not take into account other causes of AFP such as non-polio enteroviruses, bacteria and non-pathogenic causes (extensively reviewed in Marx *et al, 2000)* (Knowles, 2012b; Marx *et al.*, 2000). This section gives an account of polio, its aetiology and remedial efforts over four centuries (figure 1.2).

1.2.1. The 18th Century

The first documented evidence of poliomyelitis as an entity was in 1789, by a British physician, Michael Underwood, who reported the occurrence of a fatal epidemic "debility of the lower extremities" among infants in England (Underwood, 1789). In 1840, a German orthopaedist, Jacob Heine, published a monograph in which he recognised polio as a disease. His clinical interest, which included paralysis of arms and legs, prompted his extensive work on polio (Baicus, 2012a). The industrial revolution in Europe from the 18th to 20th Century is believed to have triggered the western epidemics and outbreaks of polio that culminated to the 20th Century polio epidemics (Cassel, 1913; CDC, 2012; Cross, 1912; De Jesus, 2007; Horstmann, 1985). Polio was termed "acute anterior poliomyelitis" by Erb in 1875 (Baicus, 2012a) and later published as polio by Putnam in 1893 (PUTNAM & TAYLOR 1893). In early 20th century, polio was

given the name, *Heine-Medin disease*, in honour of the clinical contributions of Jacob Heine – who was an orthopaedic surgeon with major interest in paralyses (Baicus, 2012a; Hewitt, 1912) (figure 1.2).
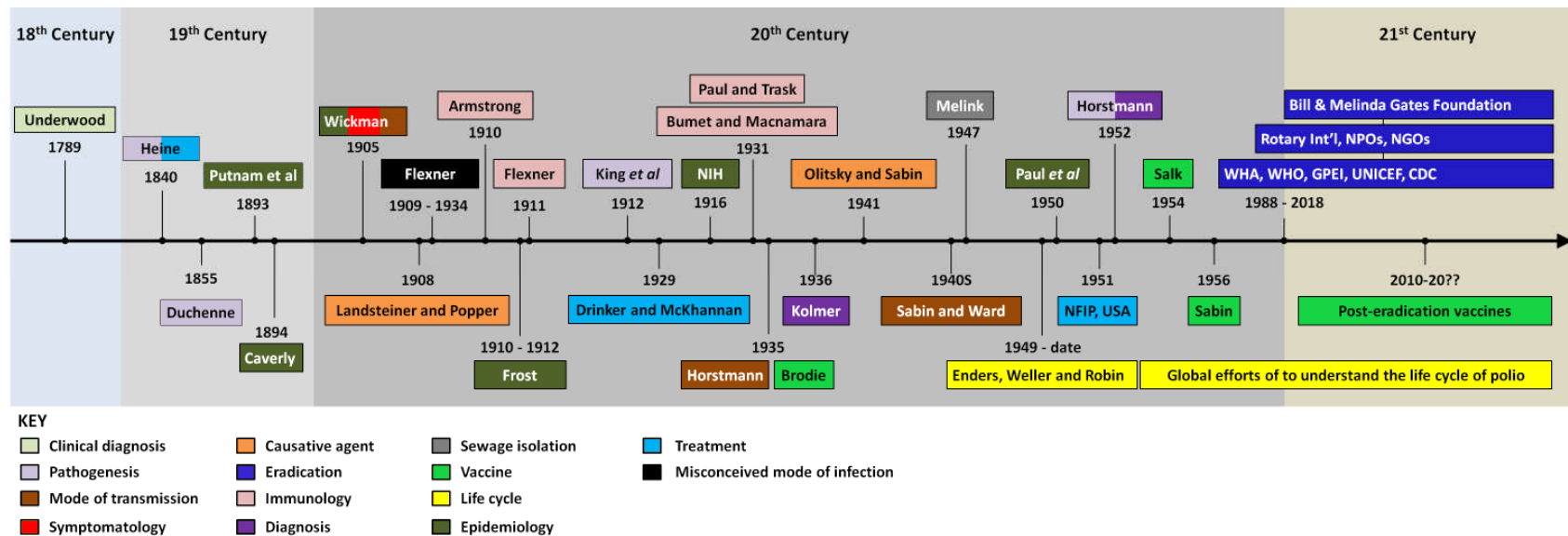
Figure 1.2. A timeline of contributions towards the eradication of polio. *Polio was recorded briefly in the 18th century, with clinical descriptions documented by Michael Underwood and later Heine. Following outbreaks of the 19th Century, focus shifted to its pathogenesis, while highlighting its contagious nature. Efforts were made to describe its contagious nature and asymptomatic forms in this period. By early 20th century, the viral aetiology was established and this accelerated research towards its eradication. Neutralizing antibodies against polio, were also discovered also and this opened up the possibility of a vaccine. A dark period of polio research occurred when researchers were misguided on its mode of infection for 25 years. This was followed by a breakthrough that culminated to rapid progresses with vaccine attempts. Antigenic differences among serotypes were discovered with much progress in symptomatology, laboratory diagnosis, immunology, serology, and treatment by immunotherapy. Towards the mid-20th century two vaccines had been licenced and at the end of the 20th century large-scale efforts to eradicate the disease globally were in place and are still ongoing. The dark arrow in the figure above represents a timeline of collective efforts towards polio eradication through the centuries (large shaded arears). Coloured boxes represent the areas indicated. Dates beneath boxes represents time in history. Acronyms: Centre for Disease control (CDC), National Foundation for Infantile Paralysis (NFIP), United Nations Children's Fund (UNICEF), Global Polio Eradication Initiative (GPEI), World Health Assembly (WHA), World Health Organisation (WHO)*

5

1.2.2. The 19th and early-20th Centuries

Following outbreaks in the 19th Century, focus began to shift towards the pathogenesis of polio. During this period, Ivar Wickman, described the contagious nature of polio as well as its asymptomatic forms (Wickman, 1911; 1980). By the early 20th century, Landsteiner and Popper established its viral aetiology (Landsteiner & Levaditi, 1909; Levaditi & Landsteiner, 1909), which accelerated research towards eradication. Flexner later reported on neutralising antibodies against polio in humans and monkeys (Flexner & Clark, 1911; Flexner & Lewis, 1910b), thus opening the possibility of a polio vaccine. Unfortunately, his submission on the neurotropic mode of infection (Flexner, 1910a; b; Flexner & Amoss, 1914; Flexner & Lewis, 1910a; b) is believed to have misguided researchers on the pathogenesis of polio for 25 years (Eggers, 1999). Polio transmission in this era, was wrongly regarded as neurotropic, however, Howe and Bodian in their neurotropic submission, reiterated an oral-faecal possibility (Burr, 1942), which had previously been demonstrated in 1912 by Carl Kling and his team from Sweden (Eggers, 1999; Kling *et al.*, 1912; Melnick, 1996), but had been ignored until Horstmann re-demonstrated the oral mode of polio infections (Carleton, 2011; Horstmann, 1952). However, Burnet and Macnamara in 1931, established antigenic differences among serotypes (Burnet & MacNamara, 1931; Eggers, 1999) (figure 1.2).

1.2.3. The mid-20th and early 21st Centuries

The mid-20th century witnessed remarkable progress in understanding the polio mode of transmission (Sabin & Ward, 1941), symptomatology (Paul & Trask, 1935), immunology (Paul & Trask, 1935), epidemiology (Frost, 1913; Lavinder *et al.*, 1918; Trevelyan *et al.*, 2005), pathogenesis (in clearer details) (Horstmann,

1952), treatment (serum therapy) (Smellie, 1933; Stewart & Haselbauer, 1928), environmental surveillance (i.e. polio-contaminated sewage) (Melnick, 1947) and *In vitro* propagation of PV in cell culture (Enders *et al.*, 1949; Weller & Robbins, 1950; Weller *et al.*, 1949) – the foundation of polio virology. This era marked the formative years of polio vaccines development against polio, which was first attempted by Brodie in 1935 – but resulted in thousands of polio cases (Baicus, 2012b). Further progress was however recorded by Sabin and Salk who developed the oral polio vaccine (OPV) and IPV, respectively with grant funding provided by the National Foundation for Infantile Paralysis (NFIP), (CDC, 2012; Eggers, 1999; Horstmann, 1985; Sabint, 1973).

In 1988, the World Health Assembly (WHA) resolved to eradicate polio with the use of OPV and IPV. Through sustained commitments of the Global Polio Eradication Initiative (GPEI), which is led by national governments and supported by five partners: WHO, Rotary, the CDC, UNICEF and the Bill & Melinda Gates Foundation; there has been a remarkable reduction in the number of cases in the last three decades (figure 1.3).
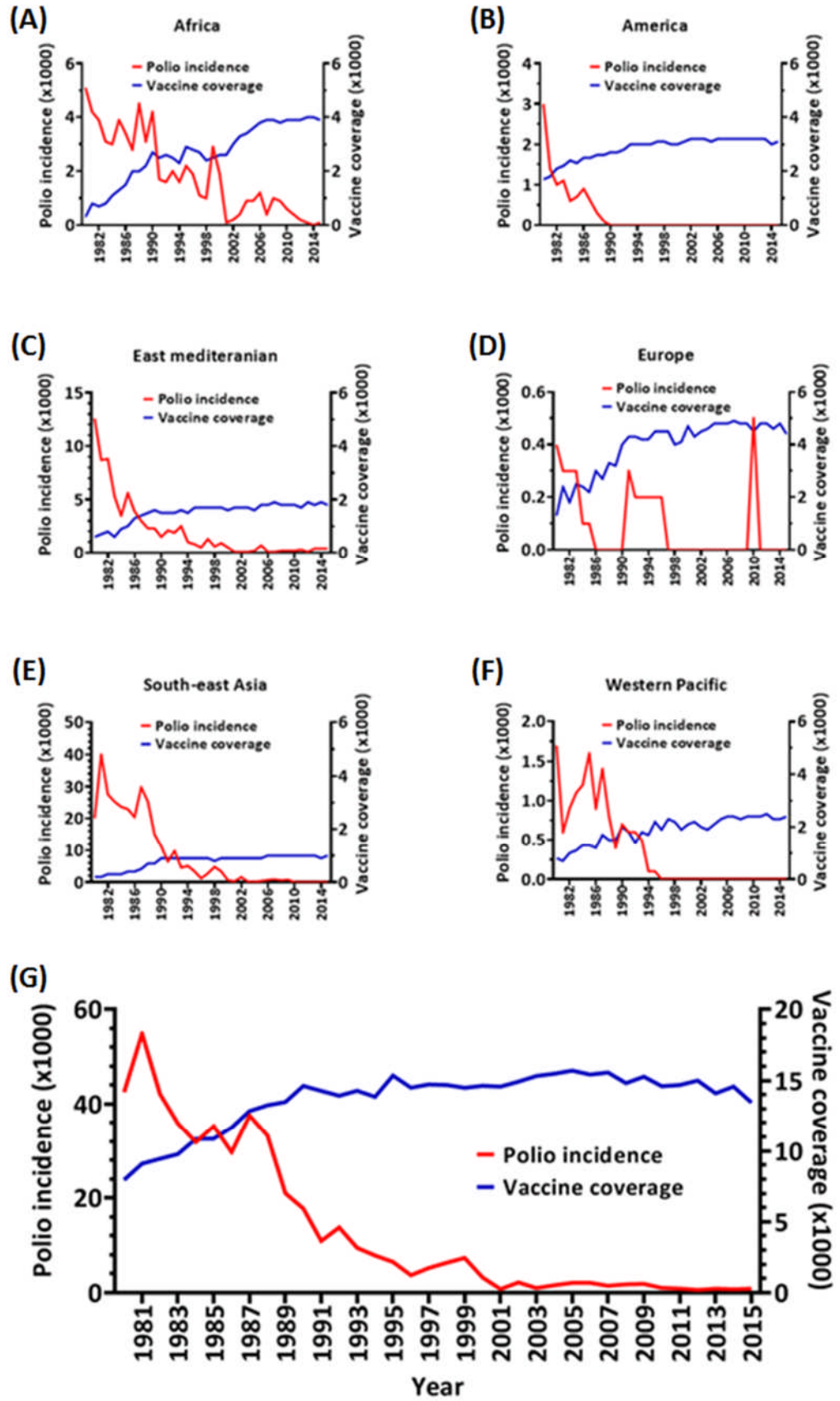
Figure 1.3. Effect of immunisation (IPV and OPV) on polio incidence worldwide. *The incidence of polio from 1980 – 2015, together with vaccine*

8

coverage from six intercontinental WHO regions in (A) Africa, (B) the Americas, (C) Eastern Mediterranean region, (D) Europe, (E) South-East Asia (F) the Western Pacific region (G) and a combination of all regions. In all regions, vaccine coverage resulted to steep decline in polio incidence. Source: WHO vaccine-preventable diseases: monitoring system 2016 global summary.

The use of OPV and IPV have remarkably reduced incidence from thousands of cases worldwide to a few cases in three endemic countries (Morales *et al.*, 2016).

1.3. Causative Agents

Karl Landsteiner and Erwin Popper identified PV as the causative agent of polio in 1908 and 43 years later, the NFIP described three antigenically distinct serotypes of the virus (PV-1, PV-2 and PV-3), (Hogle, 2002a; Minor, 1986; Rossmann *et al.*, 2002b). All three serotypes are structurally similar and belong to the *Picornaviridae* family of viruses (Knowles, 2012b) (discussed further in section 1.8.3.). With the existence of other virus-related paralytic diseases of non-polio origin, polio-related paralysis remains distinctive by its rapid onset within a few hours to 2 days and pathology (Solomon & Willison, 2003).

1.4. Transmission, pathogenesis and clinical features of polio

PV can be transmitted from an infected person to another via the oral-faecal route (Horstmann, 1985). The first site of multiplication is in the tonsils, Payer's patches or the lymph nodes that drain these tissues. The virus begins to appear in the throat and in the faeces, and is thereby shed to the environment. Secondary virus spread occurs via the bloodstream to other lymph nodes, brown fat, muscle and ultimately to the central nervous system by means of peripheral or cranial nerve retrograde axonal flow. High level of viral replication within the CNS leads to the death of the anterior horn cells of the lower motor neurons and the onset of flaccid paralysis (Pallansch M., 2007). The incubation period for polio is commonly 6 to 20 days with a range of 3 to 35 days. The response to PV infection is highly variable and has been categorised on the basis of the severity of clinical presentation (CDC, 2009).

1.5. Symptoms

Polio presents initially as fever, fatigue, headache, vomiting, stiff-neck and pain in the limbs. Irreversible paralysis occurs from 1/200 infections; among these,

5% – 10% develop muscular paralysis and this may be fatal. However, about 95% of all polio cases are asymptomatic. Infections could be abortive (i.e. with mild illness, with viral-like symptoms and diarrhoea), non-paralytic (i.e. with the additional neurological symptoms, such as sensitivity to light and neck stiffness) and paralytic (i.e. with loss of superficial reflexes and muscle pain or spasms and asymmetric flaccid paralysis) (CDC, 2009; WHO, 2013).

1.6.   Laboratory Diagnosis

PV can be isolated from the stools and the cerebrospinal fluid of infected patients. Under the International Health Regulation (IHR) of the WHO, a notifiable case of polio due to wild-type PV is clinically defined as a suspected case (i.e. any child under 15 years of age with AFP, or any person of any age with paralytic illness if polio is suspected), with isolation of wild PV in stool specimens collected from the suspected case or from a close contact of the suspected case (WHO, 2005a). Therefore, the WHO-recommended diagnosis is the isolation of wild-type PV from stool specimens collected from the suspected case or from a close contact of the suspected case as notifiable. The isolated virus is cultured and mapped by oligonucleotide fingerprinting or genome sequencing. Serological diagnosis can also be carried out but should demonstrate a four-fold rise in neutralizing antibody titres over time (CDC, 2009).

1.7.   Epidemiology

Poliomyelitis initially had a world-wide occurrence. Since the introduction of OPV and IPV at different periods around the world, polio cases [including vaccine derived PV (VDPV)] have significantly declined from its tens of thousands incidences to single digit incidences all around the world (figure 1.3) (WHO, 2013). Man is the only known reservoir of PV. Transmission is most

frequent by persons with asymptomatic infections mostly from 7 to 10 days before and after the onset of symptoms (if shown), although PV may be shed in the stool from 3 to 6 weeks post-infection. Polio typically peaks in the summer months in temperate climates but is without a seasonal pattern in tropical climates (CDC, 2009). In 2010, there was an outbreak of polio in Europe, which were investigated as imported cases due to territorial conflicts (figure 1.3). This event as well as others (e.g. Boko Haram insurgencies in Nigeria) highlights the importance of an outbreak response vaccine that can be as effective as OPV.

1.8.   Treatment and Prevention

Polio symptoms can be treated to alleviate debility e.g. by heat and physical therapy (to stimulate muscles) and anti-spasmodic drugs (to relax the muscles). However, these treatments cannot reverse the polio paralysis. The use of convalescent serum (i.e. from a person that recovered from polio) was first demonstrated as therapeutic in monkeys (Flexner & Lewis, 1910b). As an immediate response to outbreak in the early 18th century, convalescent serum from previously infected individuals were applied as therapeutic immune serum by lumber puncture. (Smellie, 1933; Stewart & Haselbauer, 1928). Anti-picornavirus capsid-binding drugs such as pleconaril (Florea *et al.*, 2003; Pevear *et al.*, 1999), disoxaril (Zeichhardt *et al.*, 1987a; b), and pirodavir (Andries *et al.*, 1992) have been reported as effective against polio, but a study also showed that the virus readily becomes resistant and drugs were ineffective in a PV-infected immunodeficient individual (MacLennan *et al.*, 2004). Other approaches such as protease inhibitors (e.g. rupintrivir), protein 3A inhibitors (e.g. enviroxime, C_2- and vinylacetylene analogs), nucleoside analogues (e.g. $2'$-C-methylcytidine, valopicitabine, and $4'$-azidocytidine), 2C inhibitors (e.g. MRL-1237 and 2-(α-

hydroxybenzyl)-benzimidazole), as well as a compounds with unknown mechanism of action (i.e. MDL-860) (De Palma *et al.*, 2008a) have inhibited PV replication at various levels and may be somewhat effect in outbreak situations, however, owing to high rates of drug-resistance due to the error-prone PV RNA-dependent RNA polymerases (RdRp) (Elde, 2012; Karakasiliotis *et al.*, 2005) there remains no known cure for polio. Prevention is through immunisation in multiple doses for a life-long protection (Guttman & Baltimore, 1977).

1.8.1. Current anti-polio vaccines

The first attempt at making a vaccine against polio was by Brodie in 1935. He inactivated PV with 10% formalin and tested it on 20 monkeys and then 3,000 children in California. The results were poor and trials were stopped. That same year, Kollmer attempted to produce a live attenuated virus consisting of a 4% suspension of PV from infected monkey spinal cord, treated with sodium ricinoleate. The result of his clinical trials on 10,000 individuals was disastrous with some fatal cases (Baicus, 2012b). It was not until the discovery of the 3 serotypes of PV that successful polio vaccines (IPV and OPV) were independently produced by Jonas Salk (Salk *et al.*, 1954) and Albert Sabin (CDC, 2009; Sabint, 1973)

1.8.1.1. Inactivated polio vaccine (IPV)

Jonas Salk successfully produced the first potent vaccine against polio in 1953. He cultured all three serotypes of PV in African green monkey kidney (Vero) cells and inactivated them using formaldehyde (Salk *et al.*, 1954). The success of his clinical trial in inducing serum immunity to protecting individual from poliomyelitis earned his inactivated polio vaccine (IPV) an immediate licence.

1.8.1.2. Oral polio vaccine (OPV)

Immediately after Salk's IPV was Jonas Sabin's oral polio vaccine (OPV). The road to the OPV involved over 40 passages of *wt* strains at high multiplicity of infection (MOI) in various hosts ranging from monkey testis, kidneys, skin and live monkeys. It also involved selecting the strain that yielded the best neutralising antibody responses at varying optimal concentrations. OPV mimics natural (wild) PV infection and is able to induce cellular and humoral immunity. This made it an ideal vaccine candidate for the eradication of polio and the most widely used vaccine (Baicus, 2012b; CDC, 2009; De Jesus, 2007; Horstmann, 1985; Sabint, 1973).

1.8.2. Challenges of current polio vaccines

Despite the successes recorded by the use of OPV and IPV worldwide, both vaccines have contributed to polio outbreaks directly through reversions and/ or recombination of OPV (Liu *et al.*, 2013; Liu *et al.*, 2000; WHO, 2005b) as well as unsuccessful inactivation of IPV (Baicus, 2012b) or indirectly through spillage of PV from manufacturing facilities. Hence, the continued use of live poliovirus at any stage of vaccine production in a polio-free world may pose a challenge.

1.8.2.1. IPV

The cutter incident of 1955 during which a defective PV-inactivation process resulted to 40,000 polio cases in the USA (Fitzpatrick, 2006; Nathanson & Langmuir, 1995) stands out as a major concern for a polio-free world. In addition, the inability of IPV to produce mucosal immunity against subsequent wild PV infections as well as its high cost of production are factors to consider in the interruption of PV-transmission in endemic regions where PV transmission is predominantly faecal-oral (Baicus, 2012b; De Jesus, 2007; Horstmann, 1985).

1.8.2.2. OPV

Three challenges that raise concerns about its suitability as a post-eradication vaccine. Associated with OPV, have been cases of vaccine-associated paralytic polio (VAPP), circulating vaccine derived PV (cVDPV) and immune-deficient vaccine derived PV (iVDPV) (John, 2001; Minor, 1986).

1.8.2.2.1.   VAPP

After receiving the vaccine, OPV recipients are known to shed the virus in their stools for 30 to 60 days. During this period, reversions of attenuation as well as recombination of the non-virulent vaccine strain with other enteroviruses can occur. It has been shown that such recombination may result in regained virulence and may lead to transmissible VAPP (Liu, *et al.*, 2000).

1.8.2.2.2.   cVDPV

PV is prone to sequence drift as well as recombination with other Enteroviruses such as Coxsackie A viruses to regain neurovirulence and transmissibility in poorly immunised human populations. This has led to the emergence of cVDPV, which have caused outbreaks of polio in areas where the virus had been previously eradicated (Jegouic *et al.*, 2009; Liu *et al.*, 2000).

1.8.2.2.3.   iVDPV

Some individuals have B-cell deficiency disorders and are unable to produce a humoral response against PV infections. This can lead to asymptomatic chronic long term excretion of iVDPV. Although transmission of polio from iVDPV excreting individuals has not yet been documented, hypogammaglobulinaemic patients constitute a pool of seeding carriers (Liu *et al.*, 2000). Such chronic careers may serve as virus depots and re-seed populations, post-eradication.

1.8.3. Biology of polioviruses

1.8.3.1. Picornaviruses

The *Picornaviridae* family comprise non-enveloped positive-sense viruses, with a single-stranded RNA (ssRNA) genome of 7,200 to 8,500 nucleotides. The mRNA genome is enclosed in a 25 to 35 nm icosahedral capsid that comprises 60 copies of four proteins, VP1, VP2, VP3 and VP4 encoded at the 5' end of the single open reading frame (ORF) (Raciniello, 2007; Stanway, 1990). Members possess highly similar genomes with some members known for distinct features as highlighted in a cartoon structure of the genomic components of picornaviruses (figure 1.4).In this section, key features of picornaviruses are briefly discussed, highlighting some distinguishing genetic features among genera.
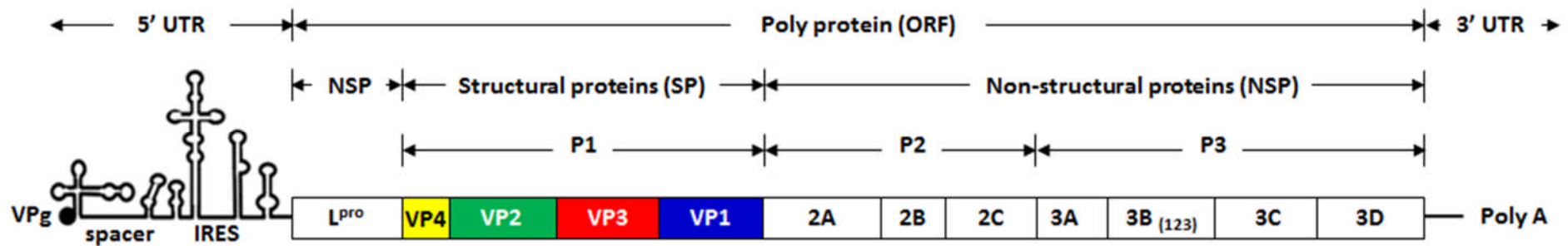
Figure 1.4. A generalised cartoon structure showing genomic regions of picornaviruses. *Covalently attached to the 5' UTR is the VPg (product of 3B), which is followed by a cloverleaf, spacer and the IRES. The length of the 5' UTR varies among picornaviruses but are structurally similar. Some picornaviruses possess a leader protein (Lpro) that also varies in sizes among genera, while other do not have the Lpro. All picornaviruses have a similar organisation of the region. Processed products are in yellow (VP4 or 1A), green (VP2 or 1B), red (VP3 or 1C) and blue (VP1 or 1D). Genes that code for non-structural proteins (NSP) are shown in white boxes and comprise the P2 and P3 region. Structural organisation within this region is highly similar among picornaviruses, however except with FMDV (an Aphthovirus) peculiar for its 3 tandem copies of 3B as well as a very short 2A.*

1.8.3.2. The picornavirus genome

1.8.3.2.1.   The 5' un-translated region (UTR)

The 5' UTR of picornaviruses is highly structured and conserved among members comprising a VPg, a distinct cloverleaf (CL) element (Rohll *et al.*, 1994), and an internal ribosome entry site (IRES). The length of the 5' UTR ranges from 307 – 1,500 nucleotides among members (Table 1.1).

1.8.3.2.1.1.   The viral genome protein (VPg)

At the 5'-terminus of the untranslated region (5' UTR) of the genome is a covalently-linked viral protein (VPg) (Barco & Carrasco, 1998). The VPgs vary in length among picornaviruses with PV having 22 amino acids (Takegami *et al.*, 1983) and other picornaviruses having 22 to 24 amino acid residues [VPg] and between 500 and 1,200 nucleotides [5' UTR], respectively. Although the functions of VPg have not been fully exhausted (Goodfellow, 2011), it is associated with the initiation of viral replication by becoming uridylated and acting as a primer for RNA synthesis (Pathak *et al.*, 2007b). Unlike cellular RNAs that are capped, picornaviruses possess VPgs.

1.8.3.2.1.2.   The cloverleaf

Next to the VPg is a "cloverleaf" (CL) structure which has been identified to form ribonucleoprotein complexes (RNPs) made up of poly r(C) binding protein (PCBP) and 3CD that are required for RNA replication as a cis-replication element (CRE), also involved in RNA translation (Barton *et al.*, 2001; Herold & Andino, 2001).

Table 1.1: Classification of the picornaviruses highlighting genome sites, length of 5'UTR and L^{pro} (Knowles, 2012b).

S/N	Genus	Genome size (kb)	5' UTR	L^{pro}
1.	Aphthovirus	8,500	1,050	+
2.	Aquamavirus	6,718	506	-
3.	Avihepatovirus	7,800	652	-
4.	Avisivirus	7,500	552	-
5.	Cardiovirus	8,000	827	+
6.	Cosavirus	7,300	1,164	-
7.	Dicipivirus	8,700	972	-
8.	Enterovirus	7,500	750	-
9.	Erbovirus	8,800	894	+
10.	Gallivirus	8,500	769	+
11.	Hepatovirus	7,500	713	-
12.	Hunnivirus	7,500	732	+
13.	Kobuvirus	8,300	808	+
14.	Kunsagivirus	7,500	500	-
15.	Limnipivirus	8,000	712	-
16.	Megrivirus	9,000	700	-
17.	Mischivirus	8,500	1,407	+
18.	Mosavirus	8,500	660	+
19.	Oscivirus	7,600	650	+
20.	Parechovirus	7,500	511	-
21.	Pasivirus	6,900	420	-
22.	Passerivirus	8,000	400	+
23.	Potamipivirus	7,500	490	-
24.	Rosavirus	9,000	752	-
25.	Sakobuvirus	7,500	591	+
26.	Salivirus	7,900	763	+
27.	Sapelovirus	7,500	668	+
28.	Senecavirus	7,200	667	-
29.	Sicinivirus	9,000	790	+
30.	Teschovirus	7,000	307	-
31.	Tremovirus	7,000	414	-

1.8.3.2.1.3.   The internal ribosome entry site (IRES)

All picornaviruses possess IRES elements, which may differ among genus in nucleotide sequence, length, RNA secondary structure and requirements for trans-acting factors. However all IRES are known to direct cap-independent internal initiation of protein synthesis by governing the recruitment of the ribosomal subunits (Pelletier & Sonenberg, 1988; Trono *et al.*, 1988). Based on uniqueness in RNA secondary structure, IRES elements can be grouped into four major classes with two sub-types (i.e. I, II, III, and HCV-like that, in turn, include subtypes A and B) - reviewed by Martinez-Sales et al (Martinez-Salas *et al.*, 2015) and Belsham (Belsham, 2009)). Possibly owing to its unique role, the IRES is positioned prior to the open reading frame which codes for the structural and non-structural proteins (figure 1.4).

1.8.3.2.2.   The Leader protein (L^{pro})

The leader protein (also known as L^{pro}) is a virally encoded protease (Strebel & Beck, 1986) that is present only in some picornavirus genera (Table 1.1). There are two fomrs of L^{pro} both of which perform the same function and self-cleave off the VP4 (or 1A) end of P1 at the same position but differ at the AUG start position during translation. Functionally, the L^{pro} inhibits host-cellular RNA translation by preventing cellular mRNA capping through the cleavage of eIF-4γ at residues Gly$_{479}$–Arg$_{480}$ (Kirchweger *et al.*, 1994; Seipelt *et al.*, 1999). Other picornaviruses that do not possess the L^{pro}, achieve cleavage of eIF-4γ by the 2A^{pro} with equal effect but at a different position (discussed in section 1.8.2.2.4.1).

1.8.3.2.3.   The P1 region

The Picornavirus P1 region comprises four structural proteins i.e. VP4 (or 1A), VP2 (or 1B), VP3 (or 1C) and VP1 (or 1D). Post translation, the P1 region is cleaved off the polyprotein by 3C or 3CD. Further processing of this region is carried out by 3C^{pro} into VP1, VP3 and VP0 a precursor of VP2 and VP4. At early stages of morphogenesis, equal numbers of the cleaved proteins in conformation self-assemble into an icosahedral capsid (further discussed in section 1.8.3.3.3). At the later stages of morphogenesis, the VP0 is by autocatalytic means into VP2 and VP4. This event marks the encapsidation of the viral RNA (Guttman & Baltimore, 1977).

1.8.3.2.4.   The P2 region

In the life cycle of picornaviruses, a first proteolytic processing of the transcribed genome occurs in *Trans* as well as in *cis* by mature proteins and/ or precursor non-structural proteins. The P2 region comprises three non-structural proteins known as the 2A, 2B and 2C. Post-translation of the polyprotein, the P2 region is self-cleaved off the 3' end of P1 by 2A and cleaved off the 5' end of P3 end by a 3CD or the mature 3C (Guttman & Baltimore, 1977).

1.8.3.2.4.1.   2A

At the 5' end of the P2 region encodes a protease (2A) that varies in length among picornaviruses. The 2A ranges from 18 amino acid in FMDV (a member of the Aphthovirus genus) to over 149 amino acid residues in polioviruses (which belong to the enterovirus genus). In the course of the virus life cycle, 2A is has been shown to carry out a number of functions. With the use of a cell-free replication assay, a study has shown that 2A improves RNA stability as well as prolongs viral RNA translation (Jurgens *et al.*, 2006). It has been shown that the

C-terminus residues of 2A have been implicated in RNA replication (Li *et al.*, 2001) by an independent initiation of negative strand synthesis (Jurgens *et al.*, 2006). In addition, as a virally encoded protease, 2A also inhibits host protein synthesis by cleaving eIf 4γ – the host-cell mRNA capping recruitment factor. In some picornaviruses with significantly small 2A, the L^{pro} has been shown inhibit host-celluar RNA synthesis (Kirchweger *et al.*, 1994; Seipelt *et al.*, 1999).

1.8.3.2.4.2.   2B

Next to the 2A is a hydrophobic non-structural protein (2B) that has been associated with host cellular membrane complexes (Bienz *et al.*, 1987; Sandoval & Carrasco, 1997) where it plays roles in membrane permeability along with its 2BC precursor (Aldabe *et al.*, 1996; van Kuppeveld *et al.*, 1997). It has also been suggested to inhibit cellular protein trafficking (de Jong *et al.*, 2008).

1.8.3.2.4.3.   2C

The picornavirus 2C is a hexametric protein with diverse roles in the virus lifecycle. It has been shown to play roles in vesicle formation, NTpase activities (Sweeney *et al.*, 2010) and negative strand RNA synthesis (Banerjee & Dasgupta, 2001; Barton & Flanegan, 1997). Treatment of poliovirus with 2 mM guanidine hydrochloride has been shown to inhibit 2C activities that involve negative-strand RNA synthesis (Barton & Flanegan, 1997) thereby forcing the virus to produce more genome-free capsids (Jacobson & Baltimore, 1968).

1.8.3.2.5.   The P3 region

1.8.3.2.5.1.   3A

Within the P3 region is 3A, which is known to inhibit cellular protein transport from the endoplasmic reticulum to the Golgi apparatus (Doedens *et al.*, 1997; Doedens & Kirkegaard, 1995). In association with a precursor, 3AB, the 3A

region has been shown to play an anchorage role for 3D in the replication complex (Xiang *et al.*, 1995).

1.8.3.2.5.2. 3B

The picornavirus 3B proteins are small peptides, which have been shown to be uridylated as primers for RNA synthesis (Paul *et al.*, 1998; Pettersson *et al.*, 1978). The 3B is a distinct among picornaviruses with FMDV possessing three tandem repeats of 3B (Forss & Schaller, 1982), which have been suggested to contribute to its rapid replication (Gebauer *et al.*, 1988)..

1.8.3.2.5.3. 3C

The 3C^{pro} is a proteases involved in the viral polyprotein-processing as well as inhibition of host-protein synthesis (extensively reviewed by Di Sun *et al* (Sun *et al.*, 2016)). The 3C^{pro} precursor (i.e. 3CD^{pro}) has also been shown to be highly involved in both activities with great efficiency (Ypmawong *et al.*, 1988), both of which are encoded by picornaviruses.

1.8.3.2.5.4. 3D

The 3D region encodes an RNA-dependent RNA-polymerase (RdRp) responsible for the synthesis of positive and negative RNA strands during replication (Van Dyke & Flanegan, 1980). When fused to its 3CD precursor, 3D remains inactive until its proteolytic cleavage from 3CD (Thompson & Peersen, 2004). RdRp has been shown to uridylylate VPg for priming activities as a first step of replication (Paul *et al.*, 2003). As a fused protein, 3CD regulates translation as an RNA-binding protein (Andino *et al.*, 1993) in addition to polyprotein processing (Sun *et al.*, 2016). Structurally, the finger-thumb-palm shape of the RdRp (Hansen *et al.*, 1997) is important to its function (Ng *et al.*,

2008) with highly conserved motifs among picornaviruses (O'Reilly & Kao, 1998). (Paul *et al.*, 2003)

1.8.3.2.6.   The 3'UTR

The picornavirus genome terminates with a highly conserved 3'UTR and a poly A tail. Genome replication begins at the 3' end proceeds having a great impact on replication in poliovirus toward the 5' end *(Rohll et al., 1995b)*. In PV, the 3'UTR has been shown to be a binding site for 3AB and 3CD (Harris *et al.*, 1994) and in encephalomyocarditis virus it binds the 3D (Rohll *et al.*, 1995a).

1.8.3.3. Classification of picornaviruses

The *Picornaviridae* family is of the order *Picornavirales* (Adams *et al.*, 2016). Members of this family are ubiquitous and have been isolated from a wide range of vertebrates including fish (Phelps *et al.*, 2014), birds (Boros *et al.*, 2014a; Boros *et al.*, 2014b), reptiles (Marschang, 2011; Ng *et al.*, 2015); small and large mammals (Jones *et al.*, 2007) including bats (Kemenesi *et al.*, 2015), seals (Boros *et al.*, 2013), ungulates (Ley *et al.*, 2002; Rowlands, 2003); humans (de Crom *et al.*, 2016) and other primates (Oberste *et al.*, 2013; Oberste *et al.*, 2002), etc.

The classification of viruses could be quite challenging, some of which have been surmounted with the advancement of molecular virology. Current guidelines on the classification of viruses by the International Committee on the Taxonomy of viruses (ICTV), groups species into genera on bases of L^{pro}, $2A^{pro}$, 2B and 3A polypeptide homology, IRES structure and phylogenetically related P1, P2 and P3 genome regions, that share >40%, >40% and >50% amino acid identity, respectively (Adams *et al.*, 2016; Knowles, 2012b). Other basis for classification include natural and experimental host range, cell and tissue

tropism, pathogenicity, vector specificity, antigenicity, proteolytic processing and genetic recombination (Knowles, 2012b) (Table 1.1). Based on these classifications, the three PV serotypes (i.e. PV-1, PV-2 and PV-3) belong to the *Enterovirus* C species, which currently consists of 23 serologically distinct viruses (Table 1.2) known to infect humans.

Table 1.2: Serotypes of *Enterovirus C* species. Source: ICTV (Knowles, 2012b).

S/N	Serotype
1.	PV 1 (PV-1)
2.	PV-2
3.	PV-3
4.	Coxsackievirus A1 (CV-A1)
5.	CV-A11
6.	CV-A13
7.	CV-A17
8.	CV-A19
9.	CV-A20
10.	CV-A21
11.	CV-A22
12.	CV-A24
13.	Enterovirus (EV)-C 95
14.	EV-C96
15.	EV-C99
16.	EV-C102
17.	EV-C104
18.	EV-C105
19.	EV-C109
20.	EV-C113
21.	EV-C116
22.	EV-C117
23.	EV-C118

1.8.3.4. Evolution of picornaviruses

RNA viruses have very high rates of mutations, and naturally exists as a quasi-species of viruses (Lauring *et al.*, 2013b) within a genetically robust environment that constantly drives their evolution (Fares, 2015; Lauring *et al.*, 2013b). Another interesting phenomenon and an important adaptive strategy of viruses is the recombination among species. Studies have shown that recombination is a common occurrence among picornaviruses (Kew *et al.*, 2005; Lauring *et al.*, 2013b; Rakoto-Andrianarivelo *et al.*, 2007). It is often limited to the non-structural regions of the viral genome (e.g. 5' UTR, P2 and P3) (Santti *et al.*, 1999; Simmonds & Welch, 2006) with no recorded effect on virus serotype.

Two models have been proposed to suggest how recombination occurs.

- The earliest model, which has been extensively studied, suggests a recombination on the basis of a template switch mechanism by the viral polymerase, during replication. In this model, which is also referred to as copy-choice, the viral RdRp during replications, jumps with the nascent RNA to a different region of the same template or to another template and continues RNA synthesis .(Kirkegaard & Baltimore, 1986; Nagy *et al.*, 1998)

- Recombination has also been shown to occur in the absence of replication, by means of replication incompetent variants through mechanisms that are not fully understood. Earlys speculations suggest that such models could involve the cleavage of phosphodiester bonds by neutrophils followed by a ligation of cleaved products through the activation of the 5'-phosphate group or by transesterification (Gallei *et al.*, 2004; Gmyl *et al.*, 1999; Gmyl *et al.*, 2003; Simmonds, 2006).

Through various means that could possibly include contributions from these models, picornaviruses have evolved as a genetically and antigenically diverse family of viruses that are ubiquitous in nature (Gmyl *et al.*, 1999; Simmonds, 2006); members include *Enterovirus A, B, C, D, E, F, G, H, I* and *J*, as well as *Rhinovirus A, B* and *C* (Table 1).

1.8.4. Poliovirus

1.8.4.1. Physico-chemical properties

Picornaviruses particle has a buoyant density in caesium chloride (CsCl) of 1.33-1.45 g/cm^3, and a sedimentation coefficient of 140S-165S, and a pH stability range of 3.0 – 8.0, depending on species. Picornaviruses are not sensitive to treatment with chloroform, ether, and non-ionic detergents (Büchen-Osmond, 2006; Newman *et al.*, 1973). Studies have shown that PV is sensitive to formaldehyde (Gard, 1960), ultraviolet and infrared lights, as well as heat (Le Bouvier, 1955; Lwoff, 1962; Mikhejev.A & Ghendon, 1974).

1.8.4.2. Capsid Structure

PV has a 7.5 kb positive sense RNA genome enclosed in a 30 nm icosahedral capsid that comprises 60 copies each of viral proteins VP1, VP3, VP2, and VP4 (Raciniello, 2007; Stanway, 1990). The capsid is reinforced by a network of N-termini of capsid surface proteins VP1, VP2, VP3, and internal protein, VP4, which could be referred to as the detached N-terminal extension of VP2 (Hogle, 2002a). VP1, VP2 and VP3 differ in amino acid sequences but each forms a structurally-similar, wedge-shaped, 8-stranded β-barrel, that comprises two antiparallel β-sheets (Hogle, 2002a). Within the 8-stranded β-fold of VP1 lies a pocket, which contains a sphingosine-like lipid (pocket factor) and is essential for host-attachment and uncoating; hence, the viral pocket contains the most-conserved structural PV amino acids (Rossmann *et al.*, 2002b).

Studies have revealed the structural details of the PV particles, which are based on icosahedral symmetry with 5-fold, 3-fold and 2-fold axes of symmetry. The five-fold axis is characterised by a prominent star-shaped mesa, and is surrounded by a canyon that serves as receptor binding site for the virion (figure

1.5) (He *et al.*, 2003; Iizuka *et al.*, 1989; Minor, 1986; Pathak *et al.*, 2007a; Wang, 2012). VP1, VP2 and VP3 have a triangular arrangement on the outer capsid surface giving rise to a propeller like protrusion of the 3-fold axis (figure 1.5).
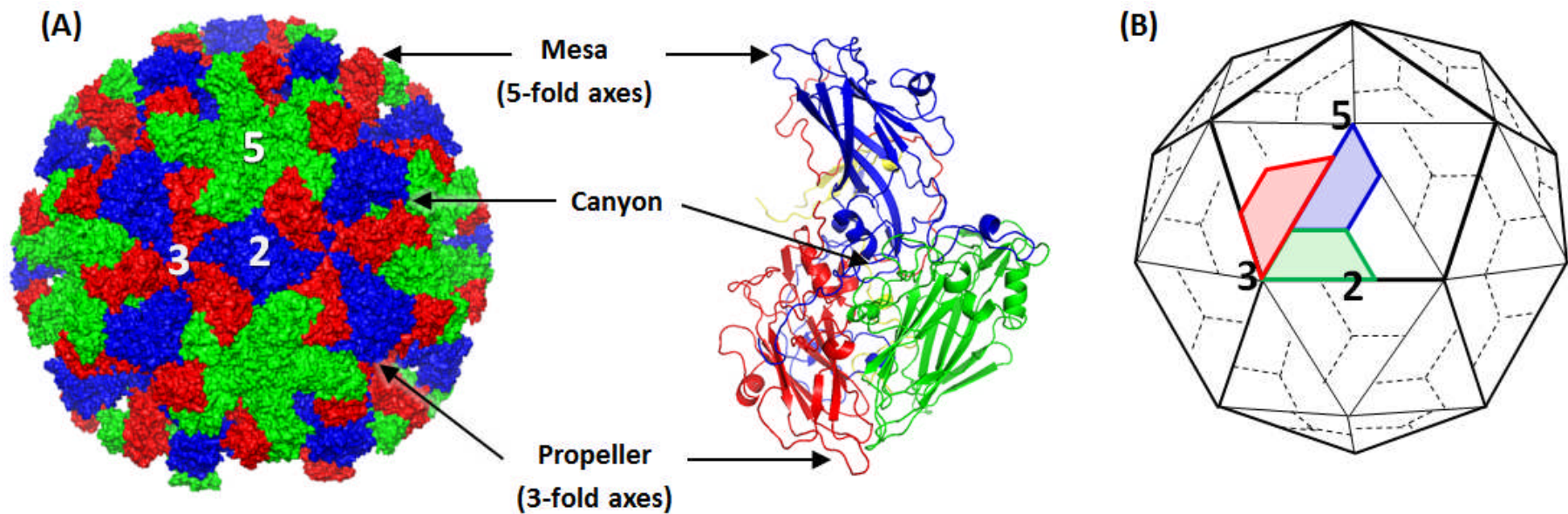
Figure 1.5: **Structure of PV particle.** *(A) Left panel shows a crystalline structure of a PV particle (PDB-1ASJ). A large star-shaped plateau formed by loops at the narrow end of the capsid protein VP1 (blue) at the fivefold axes (5); a prominent three-bladed propeller formed by the narrow ends of VP2 (green) and VP3 (red) at the particle threefold axes (3); a large surface loop of VP2 near the particle twofold axes (2); and a deep pentagonal canyon which separates the star-shaped and propeller-shaped features. Right panel shows an expanded representation of a single protomer showing ribbon diagrams of VP1 (blue), VP2 (green), VP3 (red), and VP4 (yellow). Panel was generated using Pymol (PDB-1ASJ). Figure adapted from Wien et al, 1996 and Bubeck et al., 2005 (Bubeck et al., 2005; Wien et al., 1996) (B) cartoon structure of PV particle, showing capsid proteins VP1 (blue), VP2 (green), VP3 (red), and VP4 (yellow) as well as 5-fold, 3-fold and 2-fold axes.*

This wedge shape is thought to contribute to the stability of the virion in that it facilitates packaging to form a dense, rigid protein shell (Pathak *et al.*, 2007a). The closed end of the barrel of VPI is located near the five-fold axis; while those of VP2 and VP3 alternate around the three-fold axis (figure 1.6).
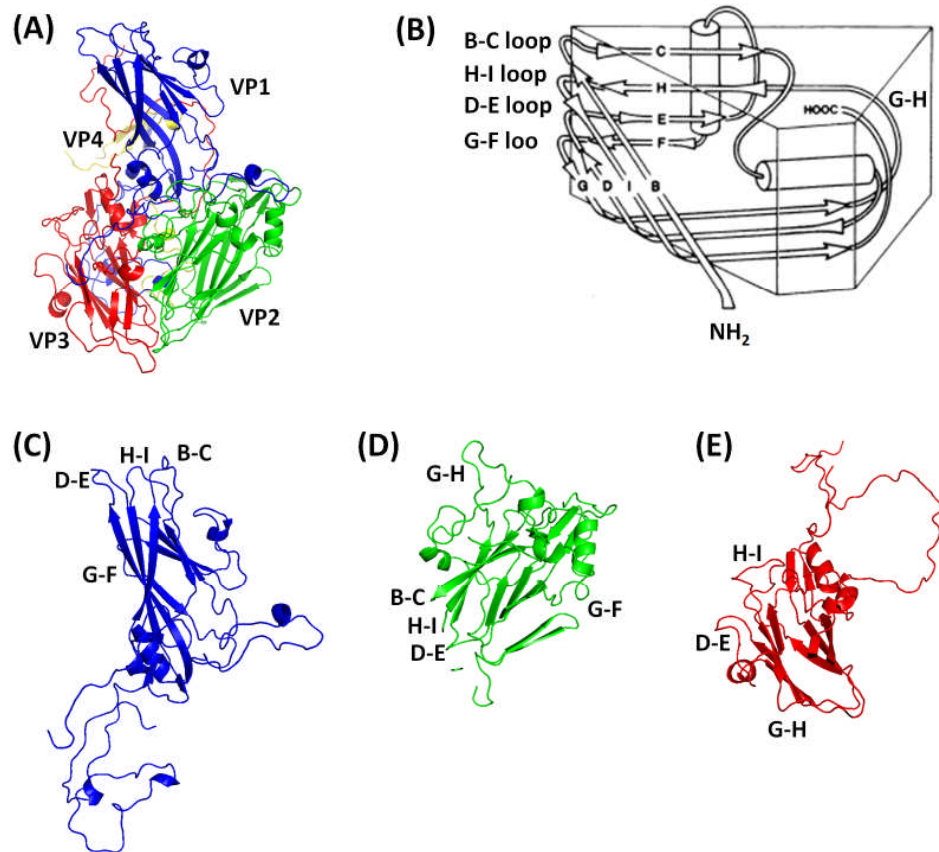
Figure 1.6. β-barrel shape of PV monomeric sub-units. (A) Single protomer showing ribbon diagrams of VP1 (blue), VP2 (green), VP3 (red), and VP4 (yellow). (B) Schematic diagram of the eight β-strands of VP1 (C), VP2 (D) or VP3 (E) of PV

The canyons that surround the five-fold axes are separated from the adjacent 3-fold axis by saddled surfaces which make up the 2-fold axes (Hogle *et al.*, 1985). Each icosahedron of PV comprises of 12 pentamers that together make up 60 units of each of the structural proteins (VP1-VP4). It has been suggested that the

PV genome is released from the capsid at or near to an axis of 2-fold symmetry (Bostina *et al.*, 2011). Within the core of the VP1, just beneath the canyon floor, is a hydrophobic pocket, which contains a fatty acid pocket factor (e.g. sphingosine) that stabilises the viral capsid and is the binding site for a class of antiviral drugs (Bubeck *et al.*, 2005; Minor, 1986; Pathak *et al.*, 2007a; Wang, 2012; Wien *et al.*, 1996).

1.8.4.2.1. Antigenic Sites

1.8.4.2.2. Monoclonal antibody (mAb) binding sites

Amongst the three viral proteins (VP1, VP2, and VP3) of PV, there are structural differences within the loops that connect the β-sheets as well as in the terminal sequences that extend from the beta-domain. Peculiar to each protein within these loops are the major neutralisation antigenic sites, which define the viral serotype (Porter, 1993). All three PV serotypes have been shown to possess four neutralising antigenic sites, termed N-AgI [VP1 residue positions 90-104], N-AgII [VP1 residues 220-222 and VP2 residues 164-175] and N-AgIIIa [VP1 residues 286-290] and N-AgIIIb [VP3 residues 58-60 and 71-79] (Murdin *et al.*, 1992; Murray *et al.*, 1988; Rombaut *et al.*, 1990) (figure 1.7). In PV-1, N-AgII and N-AgIII have been shown to have immunodominance over N-AgI (Murdin *et al.*, 1992; Murray *et al.*, 1988).

	N-AgI	VP1 (90 – 104)
	N-AgII	VP1 (220 – 222), VP2 (164 – 175)
	N-AgIIIa	VP1 (164 – 175)
	N-AgIIIb	VP3 (58 – 60, 71 – 79)
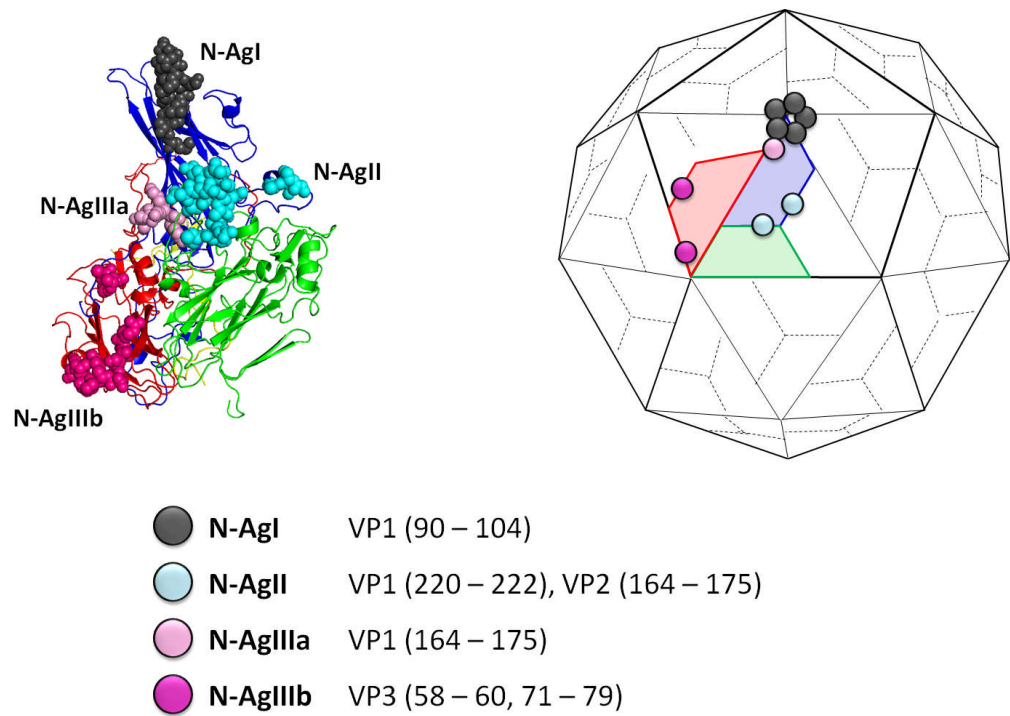
Figure 1.7. Neutralising antigenic sites. Neutralising antigenic sites located on the surface of the capsid are shown on a single protomer (top left panel), and cartoon image of a capsid (top right panel) as coloured balls. Color-coded positions of antigenic sites are also shown (lower panel) (Le Bouvier, 1955; Porter, 1993). Figure not drawn to scale.

PV particles occur in two antigenic forms: the native (N) antigenicity of infectious virions and the non-native or heated (H) antigenicity of non-infectious EC particles, or infectious particles after heating at 60 °C (Breindl, 1971; Le Bouvier, 1955). Protomers and pentamers are known to exhibit epitopes specific for H or C antigenicity, while provirion as well as mature viruses exhibit epitopes specific for N or D antigenicity (Basavappa *et al.*, 1994b; Rombaut *et al.*, 1990; Rombaut *et al.*, 1983; Rossmann *et al.*, 2002b; Zhang *et al.*, 2008).

1.8.4.2.3. Neutralising VHH nanobodies

Conventionally, most antibodies are composed of two heavy chains (50 kDa) and two light chains (25 kDa), which together make up the two identical antigen-

binding sites (Nelson, 2010). Unconventionally, camelids and sharks are known to possess antibodies composed only of heavy chains, which possess single domain binding sites (known as VHH for camelids) and are the smallest known antigen-binding fragments (Kontermann, 2010; Wesolowski *et al.*, 2009). VHH nanobodies have robust affinities and readily access hidden sites, which are inaccessible to conventional antibodies. As a result of these, as well as their ability to tolerate low/high-pH and wide temperature ranges, VHH have gained fast acceptance in scientific and clinical research applications (de Marco, 2011; Spiess *et al.*, 2015). A group of highly specific pocket-binding PV VHHs have been selected against native and non-native PV particles (Thys *et al.*, 2010) and have been successfully characterised and applied to neutralisation (Schotte *et al.*, 2015; Strauss *et al.*, 2016) and immuno-capture assays (Schotte *et al.*, 2012).

1.8.4.2.4. PV Receptors

Located within the canyons on the surface of the PV capsid are more conserved amino acid residues, where the PV receptor binding sites are protected from host immune surveillance by the inability of neutralising antibodies to penetrate far into the canyon on account of their large surface area (Rossmann *et al.*, 2002b). Studies have shown that all three serotypes of PV (PV-1, -2, 3) cause polio in man; they also have a common cellular receptor (CD155) for attachment and entry (Pathak *et al.*, 2007a). CD155 is a membrane-anchored glycoprotein with three immunoglobulin-like domains: D1, D2 and D3, which have a total of 8 glycosylation sites (Burnet & MacNamara, 1931). There are four known isotypes (or spliced variants) of human CD155 (α, β, γ and δ) of which CD155-β and −γ lack the trans-membrane domain and are released from cells after expression.

Membrane-bound CD155-α and -δ are used as receptors of all three serotypes of PV (Iizuka *et al.*, 1989; Zhang *et al.*, 2008).

Some pocket-binding compounds were developed by Sterling-Winthrop Inc. and are otherwise known as the WIN compounds (De Palma *et al.*, 2008b) and have been shown to possess antiviral properties against picornaviruses (Andries *et al.*, 1994; Dove & Racaniello, 2000; Smyth & Martin, 2002). These compounds characteristically stabilise the hydrophobic pocket and thereby inhibit both attachment and uncoating. Such antiviral properties have also been reported with the use of camelid-derived VHH nanobodies (Schotte *et al.*, 2014). Clearer insight into this mechanism has been shown by CryoEM studies, which suggests that the initial binding of CD155 to PV residues pushes on the roof of the VP1 pocket, thus resulting in the expulsion of the pocket factor. Loss of this hydrophobic pocket factor therefore permits CD155 to move further into the canyon to increase its binding affinity, thereby decreasing virus stability and thus initiating uncoating (Basavappa *et al.*, 1994b).

1.8.4.3. Replication

The viral lifecycle can be broadly divided into cell entry, genome replication and virus assembly otherwise known as morphogenesis (figure 1.9).

1.8.4.3.1. Cell entry

Replication of PV begins with the attachment of the virus to the cell receptor, CD155. The attached virus particle is internalised by endocytosis within an endosome. As the virus interacts with the receptor (within the endosome), its capsid becomes unstable and these interactions serve as a catalyst for the uncoating of the virus RNA. Studies have shown that myristoylation of VP4 is involved in inducing membrane interaction *in vitro* (Davis *et al.*, 2008; Zhang *et*

al., 2008); and possible pore-formation for the RNA delivery into the cell (Panjwani, 2013).

1.8.4.3.2. Genome replication

Picornaviruses replicate in the cytoplasm of the host cell, during which the genomic RNA directly acts as an mRNA. Viral RNA replicates in complexes associated with cytoplasmic membranes via distinct, partially double-stranded RNAs - the "replicative intermediates" (Pathak *et al.*, 2007a). The viral RNA serves as template for complementary negative-strand synthesis, thereby producing a double-stranded RNA (replicative form, RF); this initiates synthesis of positive strands from a single negative strand that produces the partially single-stranded replicative intermediate (RI) (De Jesus, 2007).

1.8.4.3.3. Particles assembly and morphogenesis

On delivery of the RNA into the cytoplasm, the VPg, (a 22 amino acid peptide which functions as primer) is removed by a cellular unlinking enzyme (Basavappa *et al.*, 1994b). The removal of the VPg initiates translation of viral genome into a single large open reading frame of approximately 220 kDa. Proteolytic cleavages by non-structural proteins (2A^{pro} and 3C^{pro}) result in the three precursors, P1, P2 and P3. The first protein to be formed is P1, a 100 kDa precursor capsid protein. In the P2 and P3 are the cis-acting non-structural proteins required for the replication process. These include 2A^{pro} and 3C^{pro}, the 3D^{pol}, which is a RNA-dependent RNA polymerase and VPg (3B) (Basavappa *et al.*, 1994b; Goodfellow *et al.*, 2003). The P1 is further cleaved into four structural proteins (VP0, VP1, and VP3 by 3CD). The monomeric VP0, VP1 and VP3 exist as a 5S structural subunit (protomer), five of which aggregate into a 14S pentamer and twelve pentamers form the 74S procapsid. The viral RNA is

37

encapsulated into the procapsid to form a 125S provirion. At this stage VP0 is cleaved into VP2 and VP4 and this transforms the provirion into a 150S virion: a mature infectious virus particle (Guttman & Baltimore, 1977). ECs (containing VP0) are also found in infected cells. Lysis of the infected cell results in release of infectious progeny virions (Figure 1.8) (De Jesus, 2007).
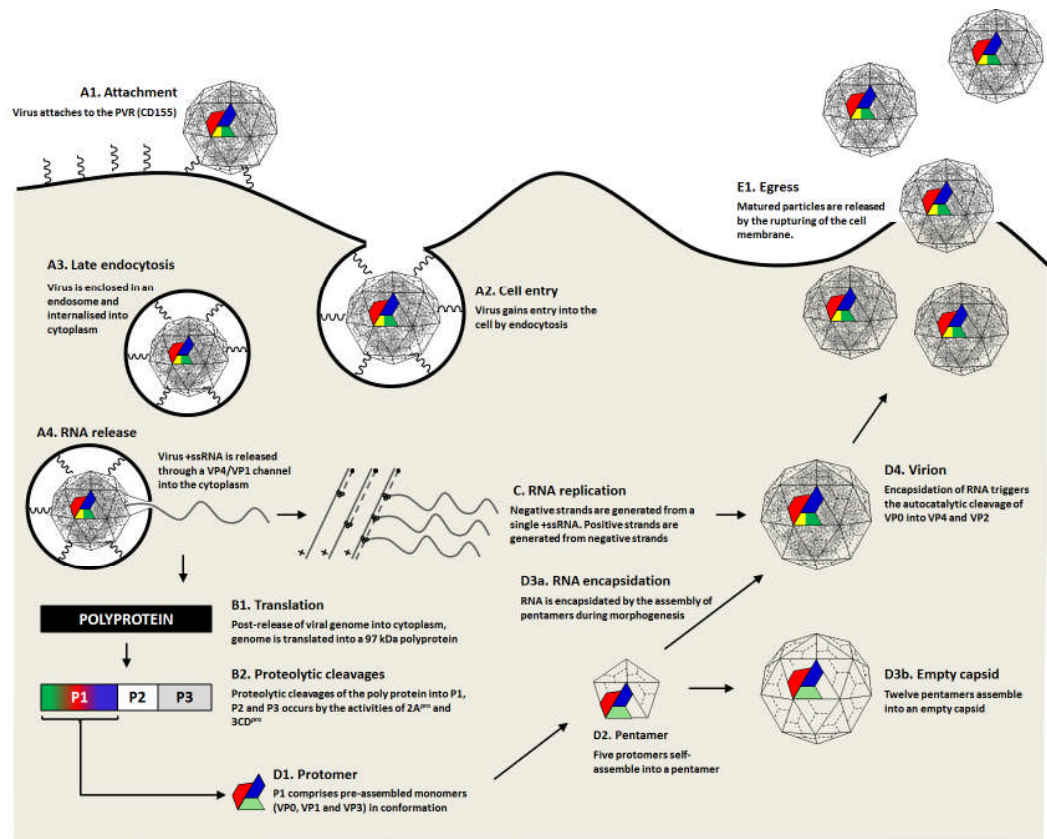
Figure 1.8. Replication of PV. *(A) Cell entry. Virus attaches to host cellular receptor (CD155) and the genome is uncoated by receptor-dependent destabilization of virus capsid (B) Genome translation. Removal of VPg from viral RNA initiates translation by a cap-independent (IRES-mediated) mechanism. Proteolytic processing of the viral polyprotein by 2A^{pro} and 3CD^{pro} to generate structural and non-structural proteins. The P1 region is further cleaved into three capsid proteins VP1, VP2 and VP0 [a precursor of VP2 and VP4].* *(C) Genome Replication. Virus (mRNA) serves as template for complementary negative-strand synthesis, thereby producing a double-stranded RNA (replicative form, RF). Initiation of many positive strands from a single negative strand produces the partially single-stranded replicative intermediate. (D) Morphogenesis. Cleaved monomers exist as protomer, which assemble into pentamer and a provirion that encapsidates the RNA and is marked by the cleavage of VP0 into VP2 and VP4 (E) Egress. Lysis of the infected cell results in release of infectious progeny virions. Figure adapted from De-Jesus, 2007 (De Jesus, 2007).*

1.8.5. Possible solution to vaccine challenges

1.8.5.1.1. Virus-like particles (VLP) vaccines

Virus-like particles (VLPs) are self-assembled recombinant subunit vaccines of structural capsids proteins and/or envelopes that structurally mimic virus but lack the viral genome (RNA or DNA); therefore, they cannot replicate and thereby cause infection (Noad & Roy, 2003; Pushko *et al.*, 2013). Owing to their structural semblance to native viruses in molecular scaffolds, VLPs are able to elicit both humoral and cellular immune responses unaided and are suitable vaccine candidates (Pushko *et al.*, 2013).

VLP vaccines have been produce from viruses with single and multiple capsid proteins (Mohr *et al.*, 2013). Based on the structure of the parent virus (i.e. enveloped or non-enveloped virus), as well as its immunogenic sub-unit, VLPs are broadly categorised as non-enveloped and enveloped (Kushnir *et al.*, 2012). Non-enveloped VLPs are expressed through four main approaches that include: single viral antigen from single virus; multiple viral antigens from single virus; single target antigens from multiple viruses fused to a heterologous protein with the ability to self-assemble; and multiple target antigens from multiple viruses fused to a heterologous protein with the ability to self-assemble (Kushnir *et al.*, 2012; Rodriguez-Limas *et al.*, 2013). The non-enveloped VLP expression systems do not involve host-membrane incorporation, while enveloped VLPs involve a more complex system of host membranes incorporation (i.e. an envelope onto which target antigens are displayed) (Kushnir *et al.*, 2012) .

1.8.5.1.2. VLP expression systems

Co-expression and self-assemblage of enveloped and non-enveloped VLPs by recombinant cell-based (e.g. plant, yeast, insect, bacterial and mammalian), and cell-free systems (Kushnir *et al.*, 2012; Mohr *et al.*, 2013) (figure 1.10).
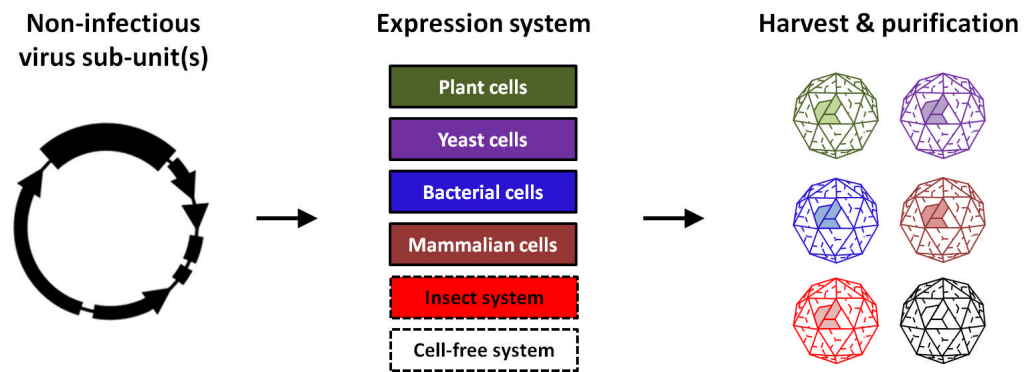
Figure 1.9. An overview of sub-unit VLP vaccine production. Generalised processes of VLP production include cloning of antigenic sub-unit(s) gene(s) into expression plasmids; protein expression of non-infectious antigenic sub-unit in plant, yeast, bacteria, mammalian cells or cell-free systems which permit post-expression modification/ assembly of expressed proteins. This is followed by harvest, purification and characterisation of expressed VLPs.

Each system is peculiar, with regards to complexity, protein modification, scale-up potential and cost (table 1.2). While plant expression offers a largescale, cost-effective production system that has accelerated interest and development in recent years (Lua *et al.*, 2014; Marsian & Lomonossoff, 2016), the bacterial system has been used most widely and it utilises non-pathogenic strains of gram positive (e.g. *Corynebacterium sp.*) and gram negative bacteria (e.g. *Escherichia coli*, *Pseudomonas fluorescence,* etc.) (Equbal *et al.*, 2013). Despite being a simple and inexpensive approach, bacteria-expressed proteins are often incorrectly folded (Noad & Roy, 2003) and issues of lipopolysaccharide (LPS)

contamination which have only been resolved by genetic modification (Mamat *et al.*, 2015).

Table 1.3. Potential yields of VLP expression systems

System	Yield (g/kg or L)	Reference
Plant		
Norwalk-like Virus capsid protein	0.8	(Santi *et al.*, 2008)
Hepatitis B virus core (HBc)	0.8	
Norwalk-like Virus capsid protein	0.34	(Huang *et al.*, 2009)
Bovine Papillomavirus type 1	0.183	(Love *et al.*, 2012)
Influenza virus HA	1.3	(Shoji *et al.*, 2012)
Papilloma virus L1	3	(Lua *et al.*, 2014)
Bacteria (*E. coli*)		
Polyomavirus VP1	4.3	(Liew *et al.*, 2010)
FMDV	0.05	(Xiao *et al.*, 2016)
HPV-16 L1	4.6	(Bang *et al.*, 2016)
Yeast (*P. pastoris*)		
Hepatitis B surface antigen	0.4	(Lua *et al.*, 2014)
Baculovirus		
Rotavirus VP2, VP6 and VP7	0.662	(Lua *et al.*, 2014)
EV71	0.171	(Lin *et al.*, 2015)
Influenza virus HA	0.062	(Meghrous *et al.*, 2009)
Mammalian cells		
Adeno-associated virus	0.5	(Lua *et al.*, 2014)
Cell-free		
Human Papillomavirus 58 L1	0.05	(Wang *et al.*, 2008)
Hepatitis B virus core (HBc)	0.356	(Bundy *et al.*, 2008)

Over the years, the yeast system has advanced from the use of *Saccharomyces cerevisiae* (Liu *et al.*, 2012d) to *Pichia pastoris* (Byme, 2015). It has produced the first commercialised and current hepatitis B VLP vaccine produced by GlaxoSmithKline (Engerix) and Merc and Co., Inc. (Recombivax). Similarly, the insect based system has also produced the current human papilloma virus VLP vaccine Cervarix by GlaxoSmithKline and Gardasil by Merc and Co., Inc.

(Minor, 1986). A range of other VLP vaccines are at various stages of development with 87 candidates currently undergoing clinical trials as listed on ClinicalTrials.gov (Health, 2016).

1.8.5.1.3.   Is a polio VLP vaccine possible?

Attempts have been made to express PV VLPs (pVLPs) in mammalian cells (Brautigam *et al.*, 1993b) and yeast cells (Ansardi *et al.*, 1991a); however, the expressed VLPs lost the native form of antigenicity. Expression in yeast appeared to be most promising (De Palma *et al.*, 2008b), owing to stabilising the VP1 pocket using a pyridazine analogue, pirodavir (ethyl 4-[2-(1-[6-methyl-3-pyridazinyl]-4-piperidinyl)ethoxy]benzoate) (De Palma *et al.*, 2008b; Rombaut & Jore, 1997b) (discussed further in chapters 5 and 6).

1.9.   Polio Eradication

Equipped with four strategic objectives as an endgame strategy (Minor, 2014), the GPEI and partners have sustained eradication efforts resulting in a reduction of polio from a global pandemic to residual pockets of infections in 3 endemic countries (i.e. Pakistan, Afghanistan and Nigeria) (Ghafoor & Sheikh, 2016). Globally, wt PV-2 has not been observed in circulation since 1999 while wt PV-3 was last seen in 2012 (De Palma *et al.*, 2008b; Initiative, 2013). Owing to the progress achieved towards polio eradication, as well as the challenges of reversion and recombination associated with OPV (Lukashev, 2010), in April 2016 there was a global switch from the trivalent OPV (tOPV) to a bivalent OPV (bOPV) that comprises PV-1 and PV-3 (Garon *et al.*, 2016; Pons-Salort *et al.*, 2016). Already, many countries use IPV, however, this will be closely followed-up by the complete replacement of OPV with IPV, globally (Hampton *et al.*, 2016; Patel *et al.*, 2015).

1.10. Study rationale

Post-eradication, immunisation will continue – this is in order to ensure against reintroduction of polio to a naïve population. Although the use of IPV avoids the biological concerns of OPV, its production involves the growth of large amounts of virus with the attendant risk of accidental release in a polio-free world (CDC, 2001; Sutter *et al.*, 2004); therefore, a virus-free (VLP) vaccine could be an ideal alternative, post-eradication. However, the instability of the EC (Basavappa *et al.*, 1994b) remains a barrier for a PV VLP vaccine.

1.11. Study objectives

The overall objective of this project is to develop a novel thermally-stable, PV-1 VLPs as novel vaccine candidates

Specific aims are to:

- Select thermally-stable PV mutants through thermal selection treatment.

- Characterise the effects of mutations on the stability of virus and natural empty particles.

- Describe how these thermally stable mutations evolved.

- Express the capsid proteins of stabilised PV as VLPs in recombinant plant and yeast expression systems.

- Isolate recombinantly expressed VLPs and assess their antigenic characteristics and thermal stability.

Chapter 2

Materials and method

2.1. General buffers, media and reagents

2.1.1. Luria-Bertani (LB) broth

10g NaCl

10g Tryptone

5g Yeast Extract

950 ml distilled water (dH$_2$O).

Autoclave on liquid cycle for 20 min at 15 psi. Allow solution to cool to 55°C,

and add relevant antibiotic (if needed).

2.1.2. LB Agar

To LB broth (section 2.1.1.), add 15 g/L agar before autoclaving.

2.1.3. 10 x TBE (Tris Borate Ethylenediaminetetraacetic [EDTA]) pH 8.3

108g Tris base

55g boric acid

9.3g EDTA (pH8.0)

Make up to 1 litre using dH$_2$O.

2.1.4. 50 x TAE (Tris Acetic Acid EDTA) pH 8.3 (1 litre)

242g Tris base

57.1ml Glacial Acetic Acid

100ml 0.5M EDTA (pH8.0)

Make up to 1 litre with dH$_2$O

2.1.5. Tris-buffer (1 M, pH=8.3, 6.3):

Add 121 g Tris base to 800 mL dH$_2$O. Adjust to required pH with HCl; make up

to 1 L with dH$_2$O and autoclave

2.1.6. TE-buffer (10 mM Tris, 1 mM EDTA, pH=8)

10 mL of Tris-buffer (1 M, pH=8)

2 mL of EDTA (0.5 M, pH=8)

Make up to 1 L with dH2O and autoclave

2.1.7. Dialysis buffer

10 mM N-(2-hydroxyethyl) piperazine-K-(2-ethane-sulfonic acid) (HEPES),

100 mM NaCl,

1 mM diaminoethanetetra-acetic acid (EDTA),

1 mM dithiothreitol (DTT),

pH 6.4

2.1.8. Agarose gel electrophoresis: loading dye

PROMEGA's Blue/ Orange 6X loading dye

0.4% orange G

0.03% bromophenol blue

0.03% xylene cyanol FF

15% Ficoll® 400

10mM Tris-HCl (pH 7.5)

50mM EDTA (pH 8.0)

2.1.9. Agarose gel electrophoresis: DNA marker 1 kb

PROMEGA's DNA ladder

A DNA ladder with 13 bands of fragments ranging from 250-10,000 base pairs;

the 1,000 and 3,000 bands have increased intensity to serve as reference points.

10mM Tris-HCl (pH 8.0),

1mM EDTA

2.1.10. Agarose gel electrophoresis: gel stain

Invitrogen's SYBR safe DNA gel stain-*safer substitute of ethidium bromide for staining DNA in agarose or acrylamide gels*

Fluorescence excitation maxima: 280 and 502 nm,

Emission maximum@ 530 nm

2.2.   Agarose Gel Electrophoresis of RNA

2.2.1.   Diethylpyrocarbonate [C6H10O5] (DEPC) –treated water

Dissolve DEPC in dH_2O to a ratio of 1:1000.

Autoclave on liquid cycle for 20 min at 15 psi. Allow solution to cool

2.2.2.   10x MOPS running buffer

200 mM MOPS

80 Mm Sodium Acetate

10 mM EDTA

Adjust pH to 7.0 using NaOH.

2.2.3.   RNA agarose Gel running buffer

Dilute 10x MOPS running buffer to 1x with DEPC-treated water

2.2.4.   RNA agarose Gel

1x MOPS running buffer

2% Formaldehyde (Sigma F8775-500ML)

0.8% pure agarose powder (Sigma BiC0-100)

Add agarose to MOPS and DEPC-treated water. Melt in a intermittently microwave (avoiding overspill). Cool to 50^oC, then add formaldehyde. Pour gel into cast tray with comb and leave to set.

2.3. Radio Immunoprecipitation assay (RIPA) buffer

50 mM Tris (pH 8.0)

150 mM NaCl

1% Triton X 100 or Nonidet P-40

0.5% sodium deoxycholate

0.1% SDS

1 L dH$_2$O

2.4. SDS-PAGE running buffer (10x)

30.2 g Tris base

144 g Glycine

10 g SDS

1 L dH$_2$O

2.5. SDS-PAGE transfer buffer (1x, 1 L)

To 100 ml of 10x SDS-running buffer (section 2.11), add 200 ml methanol and 700 ml d H$_2$O

2.6. SDS-PAGE stacking buffer (5%)

2.975 ml dH$_2$O

0.67 ml Acrylamide/Bis-acrylamide (30%/0.8% w/v)

1.25 ml 1.5 M Tris-HCl, pH 6.8

0.05 ml 10% (w/v) SDS

0.05 ml 10% (w/v) ammonium persulfate (APS)

0.005 ml TEMED

2.7. SDS-PAGE resolving buffer (15%)

2.2 ml dH$_2$O

5 ml Acrylamide/Bis-acrylamide (30%/0.8% w/v)

49

2.6ml 1.5 M Tris-HCl, pH 8.8

0.1 ml 10% (w/v) SDS

100 μl 10% (w/v) ammonium persulfate (APS)

4 μl TEMED

2.8. SDS-PAGE reference ladder

Bio-Rad Precision Plus Protein™ Dual Color Standards

A mixture of ten recombinant proteins (10–250 kD), including eight blue-stained bands and two pink reference bands (25 and 75 kD)

30% (w/v) glycerol

2% SDS

62.5 mM Tris, pH 6.8

50 mM DTT

5 mM EDTA

0.02% NaN_3

0.01% bromophenol blue

2.9. Autoradiography solutions

2.9.1. Gel fixing solution

250 ml Isopropanol

650 ml Water

100 ml Acetic acid

2.9.2. Amplify solution

GE healthcare Amersham amplify fluorographic reagent (NAMP100)

2.9.3. 10 x PBS (pH 7.4)

1.4 M NaCl

27 mM KCl

100 mM $Na_2HPO_4 \cdot 2\ H_2O$

18 mM KH$_2$PO$_4$

2.10. Cell Growth Medium

Dulbecco's Modified Eagles Medium (DMEM) SIGMA-D6429

10% Foetal calf serum (FCS)

100 units/ml penicillin

0.1 mg/ml streptomycin

1 % glutamine

2.11. Tris-Buffered Saline and Tween 20 (TBST)

50 mM Tris

150 mM NaCl

0.05% Tween 20

Adjust pH with HCl to pH 7.6

2.12. Chemo luminescence reagent

2.12.1. Solution 1

2.5 mM luminol

400 µM p-coumaric acid

100 mM Tris-HCl (pH 8.5)

2.12.2. Solution 2

0.018% H$_2$O$_2$

100 mM Tris-HCl (pH 8.5)

Prior to use, mix solution 1 and 2 in

2.13. PBS Tween-20 (0.2%)

To 1 X PBS, add TWEEN-20 to final concentration (v/v) of 0.2%

2.14. Crystal violet stain

40 ml 1% crystal violet

300 ml dH$_2$O

80 ml 95% ethanol

2.15. Blocking buffer

To 1x TBST, add 5% milk

2.16. Antibodies

2.16.1. Monoclonal antibodies

MAb 234 (anti-PV-1 VP-1 native [N-specific]), AbCam

MAb 237 (anti-PV-1 VP-1 native [N-specific]), AbCam

MAb 1588 (anti-PV-1 VP-1 non-native [H-specific]), AbCam

2.16.2. Polyclonal antibodies

Rab 3CD (Anti-PV-1 P3)

Sheep-16 [SH-16] (Anti PV-1 P1)

Rab 1A (anti-PV-1 VP1)

Rabbit anti-sheep IgG peroxidise conjugate (Sigma, S1265-2ML)

Donkey anti-sheep IgG [HRP] (Abcam, ab97125)

Rabbit anti-mouse IgG peroxidise conjugate (Sigma, A9044-2ML)

Goat anti-rabbit IgG peroxidise conjugate, (Sigma, A0545-1ML)

2.16.3. Nanobodies (VHH)

PVSP6A (Anti-PV-1 N-specific VHH)

PVSP7A (Anti-PV-1 H-specific VHH)

2.16.4. SuperScriptTM First-Strand Synthesis System for Reverse Transcription (RT)

1 µl Rev 1 primer (2 pmol/µl)

5 μl RNA template

1 μl dNTP mix (10 Mm)

4 μl FS buffer (5X)

2 μl M DTT (0.1)

2 μl SuperScript II RT

6 μl dH$_2$O (RNase free)

2.16.5. QIAGEN® Fast Cycling PCR

10 μl QIAGEN Fast Cycling master mix

(contains HotStarTaq Plus PCR Master Mix DNA Polymerase, 1x Fast Cycling

Buffer, 200 μM of each dNTP, Optimized Mg2+ concentration)

0.5 μM Reverse primer

0.5 μM forward primer

Template DNA (< 300 ng/20 μl reaction)

RNase-free water to a final volume of 20 μl

2.16.6. Primers

Adhering to the general principles of primer design (Dieffenbach *et al.*, 1993),

sets of PCR/ sequencing primers (Table 2.1) as well as mutagenesis primers

(Table 2.2.) were designed to comprise 18 – 24 nucleotides with a GC content of

40-60%, and melting temp (Tm) of 55-65°C.

Table 2.1. PCR/ Sequencing primers

Name	Sequence	Properties		
		Nt	GC%	Tm
P1 Reverse	CTTGGCCACTCAGGATGATT	20	50	65
P1 forward	TTAAAACAGCTCTGGGGTTGTAC	23	43	65
For 2	CAAACCAGTACCACCACGAAC	21	52	66
For 3	ACCGGTGACGGTGGTCCAGG	20	70	75
For 4	ATAATGGGTGCTCAGGTTTCAT	22	41	64
For 5	AAAACAGCCCCAATGCTAAAC	21	43	64
For 6	CGCCGTACCAGAGATGTGTC	20	60	68
For 7	GGATTAAGAAACATCACCCTGCC	23	48	66
For 8	TGTGGATCCATGATGGCAACT	21	48	67
For 9	GTGGGGGCGGCAACATCTAG	20	65	71
For 10	GCATGCCTTAAATCAAGTGTACCA	24	42	65
For 11	TGGATTACAAGGATGGTACGCT	22	45	66
For 12	CTCAGCAGATTAGCGACAAAAT	22	41	63
For 13	TCAGGAACACCAGGAAATTCTA	22	41	63
For 14	AGCATCCACAAACTCAAGCAG	21	48	66
For 15	GTCAACATCACCAGCCAGGT	20	55	68
For 16	AAAAGTTCAGAGACATTAGACCACAT	26	35	63
For 17	AGACAGACTTTGAGGAGGCAAT	22	45	66
For 18	TCACAAAAACCCAGGAGTGAT	21	43	64
For 19	GGACTAACTATGACTCCAGCTGACA	25	48	68
For 20	AGTCGAATTGGATTGGGTCAT	21	43	64
Rev 1	CTTGGCCACTCAGGATGATT	20	50	65
CYC1 3	GCGTGAATGTAAGCGTGAC			
AOX1 5'	GACTGGTTCCAATTGACAAGC			
PIC 3CD 1	ACCAATGACCTTTCCTGTGC			
PIC 3CD 2	TAAGGGTGGAATGCCTTCTG			
PV1 pr1	TTGGTGAGGAAAAACGAAGG			
PV1 pr2	AGCTAGTGGCCCTACCCATT			

Table 2.2. PV-1 mutagenized primers

Host genome sequences in capital letters and the mutated bases in small letters.

Name	Sequence	Properties		
		Nt	GC%	Tm
PV_R4034S_fwd	AATTATTATagtGATTCAGCTAGTAACGCGGC	32	38	68
PV_R4034S_rvs	AGCTGAATCactATAATAATTAATGGTGGTG	31	32	64
PV_D4045V_fwd	TCGAAACAGgtcTTCTCTCAAGACCCTTCCAAG	33	48	74
PV_D4045V_rvs	TTGAGAGAAgacCTGTTTCGAAGCCGCGTTAC	32	50	75
PV_F4046L_fwd	AAACAGGACctcTCTCAAGACCCTTCCAAGTTC	33	48	74
PV_F4046L_rvs	GTCTTGAGAgagGTCCTGTTTCGAAGCCGCG	31	58	77
PV_C3175A_fwd	AGCAACACCgcgTATCGGCAAACCATAGATGATAGTTTC	39	46	76
PV_C3175A_rvs	TTGCCGATAcgcGGTGTTGCTAATCCATGGC	31	55	78
PV_A1026T_fwd	TCTAGAGACactCTCCCAAACACTGAAGCCAG	32	50	74
PV_A1026T_rvs	GTTTGGGAGagtGTCTCTAGATGTTGCCGCCC	32	56	77
PV_ V1087A_fwd	GGTGCATGCgcgACCATTATGACCGTGGATAACC	34	56	78
PV_ V1087A_frvs	CATAATGGTcgcGCATGCACCCCGCGCGAAG	31	65	82
PV_ S1097P_fwd	AACCCAGCTcccACCACGAATAAGGATAAGC	31	52	75
PV_ S1097P_rvs	ATTCGTGGTgggAGCTGGGTTATCCACGGTC	31	58	78
PV_ I1194V_fwd	CCAGCCCGGgtcTCGGTACCGTATGTTGGTAT	32	59	79
PV_ I1194V_rvs	CGGTACCGAgacCCGGGCTGGAGCTGTTCCGT	32	69	84
F4046L_Pich_fwd	GCTAGTAAACAAGATttgTCACAAGAC	30	37	54
F4046L_ Pich_rvs	TGAAGGGTCTTGTGAcaaATCTTGTTT	30	33	57
A1026T_Pich_fwd	GCCACCTCCAGGGATacaCTTCCCAAC	30	59	66
A1026T_Pich_rvs	CTCTGTGTTGGGAAGtgtATCCCTGGA	30	52	63
V1087A_Pich_fwd	GCCAGGGGTGCTTGTgctACGATAATG	30	56	65
V1087A_Pich_rvs	GACAGTCATTATCGTagcACAAGCACC	30	48	60
I1194V_ Pich_fwd	ACAGCACCCGCTAGAgtgTCAGTGCCC	30	63	70
I1194V_ Pich_rvs	AACATAGGGCACTGAcacTCTAGCGGG	30	56	65

2.16.7. Formaldehyde (4%)

To 1 X PBS, add formaldehyde to final concentration (v/v) of 4%

2.16.8. MOPS gel buffer (10X)

EDTA (20 mM)

MOPS (200 mM)

Sodium acetate (50 mM)

Adjust pH to 7.0 using NaOH.

2.17. Cloning plasmids

2.17.1. pGEM T-easy

The pGEM T-easy vector used in this study was a commercial 3 kb plasmid with multiple cloning sites obtained from Promega (Robles, 1994). The vector encodes a β-lactamase gene and is thus, ampicillin selectable (100 mg/ ml). It also encodes a T7 and an SP6 RNA transcription initiation site, an SP6 RNA polymerase promoter, lac operons, a phage f1, pUC/M13 forward and reverse primer binding sites for sequencing. Inserts of about 3 kb with 3´ A-overhangs were cloned upstream a *lac* promoter after a single digest with *EcoR*I (NEB catalogue number R6011) or *Not*I (NEB catalogue number R6431) unique restriction enzymes.

2.17.2. pCR-XL TOPO

The pCR-XL TOPO vector applied to this study was a 7 kb commercial product from Thermo Fisher Scientific. It was encoded with the Zeocin and Kanamycin resistance genes, a M13 forward and reverse primer binding sites, T7 promoter regions, Lac promoter/operator region, multiple cloning sites, ccd B lethal gene ORF, and pUC origin. This was applied to inserts of about 6 kb with 3´ A-overhangs after a single digest with *EcoR*I (NEB catalogue number R6011) or *Not*I (NEB catalogue number R6431) unique restriction enzymes.

2.17.3. pCR-Blunt

A 3 kb pCR-Blunt commercial vector from Thermo Fisher Scientific was applied as a sub-cloning vector in this study. It was encoded with the Zeocin and Kanamycin resistance genes, a M13 forward and reverse primer binding sites, T7 promoter regions, Lac promoter/operator region, multiple cloning sites, ccd B lethal gene ORF, and pUC origin. This was applied to blunt-ended inserts after a

single digest with a *Stu*1 unique restriction enzyme (NEB catalogue number R0187S).

2.17.4. pT7RbzPV-1

An infectious clone of wt PV-1 (Mahoney strain) was used in this study was sourced from Bert Semler, University of California, USA, and was cloned downstream of a T7 RNA promoter to allow *in vitro* RNA synthesis. A hammerhead ribozyme was included at the 5' end resulting in production of an authentic infectious PV-1 RNA (Cornell *et al.*, 2004) (figure 2.1).
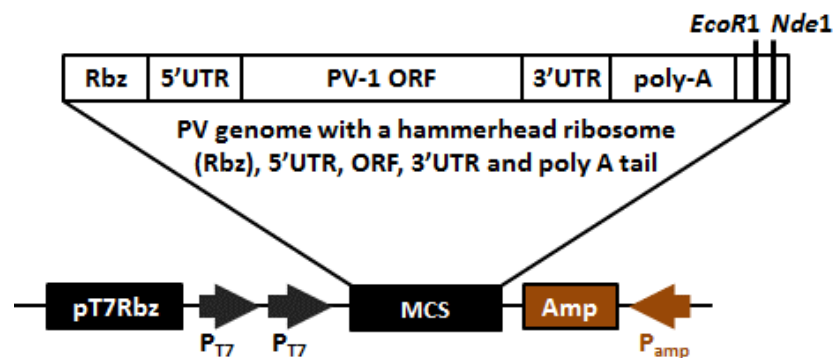
Figure 2.1. Schematics of PV infectious clone. Linear schematics of the wt infectious clone plasmid shooing the multiple cloning site (MCS) which begins with a hammerhead ribosome followed by the 5' UTR and the entire rest of the PV-1 genome including the 3' UTR and poly-A tail. EcoR1 and Nde1 unique restriction sites are also shown, which continue to the ampicillin resistant gene. The T7 promoters are also highlighted upstream the MCS.

2.17.5. pPINK-HC

The pPINK LC (7.7 kb) is a low copy number vector commercially supplied by Life Technologies (Cat. no. A11152). It encodes the ADE2 adenine knockout selection gene for *Pichia pastoris*, which is driven by an 82 bp ADE2 promoter. The plasmid backbone is based on pUC19 that encodes for Ampicillin (*bla*) resistance gene for selection in *E. coli*. It also encodes the AOX1 promoter and CYC1 transcription terminator for expression in yeast.

2.17.6. pPICZ-A

The non-secretory pPICZ-A vector was commercially supplied by Life Technologies (Cat. no. V190-20). It contains ADE2 adenine knockout selection gene for *Pichia pastoris* as well as the Zeocin resistance (Sh ble) gene to allow selection of the plasmid using Zeocin.

2.17.7. pPICK-A

The vector pPICK-A was obtained by modifying the commercial pPICZ-A vector by replacing the zeocine selectable marker gene (*Sh ble*) with a G418/ kanamycin selectable marker gene (*Tn903 Kam^R*). The *Tn903Kam^R* was commercially synthesised as a blunt-ended gene string with two unique restriction sites (*Mlu*I and *Not*I). The *Tn903Kam^R* was sub-cloned into pCR-Blunt and gene insert released by double digest using *Mlu*I and *Not*I restriction enzymes, which were also applied to release the *Sh ble* gene from pPICZA. The The *Tn903Kam^R* cassette was ligated into the pPICA backbone downstream the P$_{TEF1}$ and P$_{EM7}$ promoters to drive expression in yeast and *E. coli*, respectively (figure 2.2).
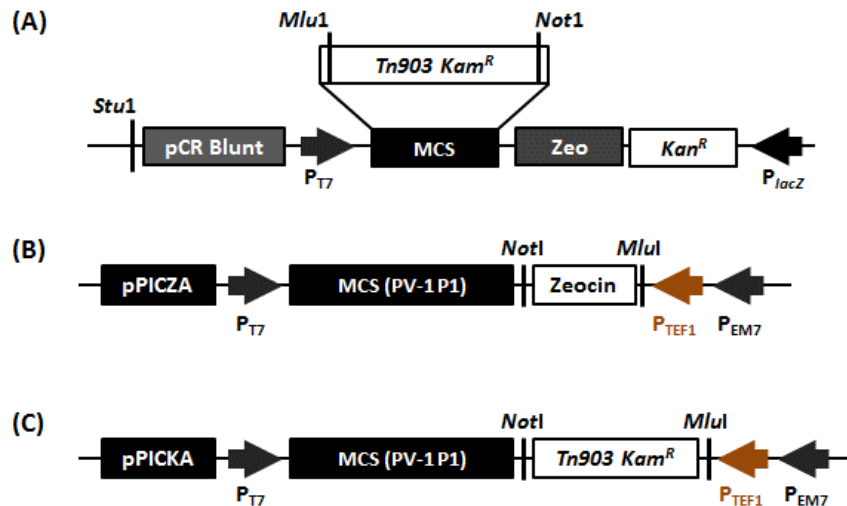
Figure 2.2. Schematics of plasmid cloning strategy. *Linear schematics of designed sub-cloning plasmid (pPCRBluntK), pPICZA and its modified version, pPICKA. The Pichia-optimised Tn903 Kam^R gene that confers G418 resistance in yeast and Kanamycin resistance to E. coli was synthesised as a blunt ended gene staring, flanked by the unique restriction sites, MluI and NotI. This was ligated into StuI-linearized sub-cloning vector, pCR-Blunt. The Zeocin-resistance gene (Sh ble^R) in pPICZA was dropped out replaced with unique restriction enzymes MluI and NotI and replaced with the propagated Tn903 Kam^R, which was also digested with MluI and NotI and gel-purified prior to ligation.*

2.18.   Cell culture methods

2.18.1. Cell line

HeLa Ohio cells, a continuous cell line, derived from human epithelial cell carcinoma of the cervix (Jones *et al.*, 1971) and mouse L-cells were obtained from the National Institute of Biological Standards and Control, UK.

2.18.2. Recovery of frozen cells

Vials of HeLa cells and mouse L-cells, cryopreserved at -80°C were removed and rapidly thawed at 37°C in a water bath. Cells were transferred to a T-25 Corning flask and made to a final volume of 5 ml with cell growth medium. After 24 hours of incubation at 37°C and 5% CO_2 in a humified cabinet, media

60

was changed to ensure removal of cryopreservant. At 80-90% confluence, cells were passed into a T-175 flask.

2.18.3. Maintenance of cell lines

Cells were grown by incubation at $37^{\circ}C$ in supplemented DMEM in a CO_2 cabinet. At 80-90% confluence, medium was removed and cells were washed with 1X PBS and detached from culture vessel by adding trypsin and incubating briefly at $37^{\circ}C$ with rocking. Trypsin was inoculated with equal volume of DMEM supplemented with 10% FBS and 20% of resulting cells was re-suspended in supplemented DMEM and re-incubated at $37^{\circ}C$ with 5% CO_2 in a humidified cabinet

2.18.4. Cryopreservation of cell line

Growth media was removed from cells, which were, thereafter, washed in 1X PBS and trypsinised thereafter. Trypsin was neutralised with equal volume of supplemented DMEM (as described in section 2.2.2 above). Cells were centrifuged at 1,500 rpm for 5 minutes and re-suspended in cryopreservant (10% DMSO and 90% FCS). Cell aliquots were stored at $-80^{\circ}C$.

2.19. Methods used in the thermal evolutional of PV-1 (Mahoney)

2.19.1. Virus propagation

L-cells cells were transfected with PV-1 RNA and the resulting viruses propagated by standard methods (Dulbecco & Vogt, 1954; Racaniello & Baltimore, 1981). Virus infectivity was determined by plaque assays, using HeLa monolayer cells (Dulbecco & Vogt, 1954). Virus titres were expressed as plaque forming units per millilitre (PFU/ml).

2.19.2. Virus concentration

PV-1 Virus was infected in a T-25 flask (as described in 2.3.1 above) till 100% cell death was observed. Cells were pelleted by centrifugation at 4,000 rpm for 10 minutes. Supernatant was recovered and stored at 4°C while pelleted cells were lysed with 100 µl of RIPA buffered and repeated freeze thawing (thrice). Released virus particles were separated (in supernatant) from lysed cell debris by centrifugation at 14,000 rpm for 10 minutes. Both supernatants (i.e. from cell pellet and cell debris) were pooled into a 5 ml Seton tube, loaded into a Beckman AH-650 swing bucket ultracentrifuge rotor and spun at 50,000 rpm for 1 hour to pellet virus particles. Supernatant was discarded and virus pellet suspended in 600 µl serum-free media.

2.19.3. Plaque assay

HeLa cells were propagated to 80% confluence and pre-washed with 1x PBS. Cells were trypsinised and neutralised. Cell suspension was diluted at a 1:1 ratio with Trypan blue and thoroughly mixed by pipetting up and down. A 10 µl volume of Trypan blue-cell suspension was loaded onto a chamber of a sterile haemocytometer with a cover slip in place and cells counted under the microscope. Each well (of a 6-well plate) was seeded to a final concentration of 3

x10^5 cells/ ml (or 1 x10^5 cells/ ml in a 6-well plate). Cells were grown to 100% confluence as monolayers on the bottom of the culture vessel and infected with 100 µl of a 10-fold serial dilution of concentrated virus. Cells were incubated at 37°C with 5% CO_2 for 1 – 2 hours. Each well was overlaid with 1% agarose in serum-free media and left for 10 minutes to solidify. After 48-hour incubation (at 37°C under 5% CO_2) solidified agarose was removed from each well, which was thereafter stained with 0.5 ml crystal violet for 2 minutes, decanted and virus plaques counted (Dulbecco & Vogt, 1954). Virus titres were expressed as plaque forming units per millilitre (PFU/ml).

2.19.4. Virus purification

Virus-infected HeLa cells or RNA-transfected L-cells were freeze-thawed and clarified by differential centrifugation. Supernatant was collected and virus pelleted though 30% (w/v) sucrose cushion at 300,000 xg (using a Beckman SW 55 Ti rotor) for 3.5 hours at 4°C. Virus pellet was re-suspended in phosphate buffered saline (PBS) and clarified by differential centrifugation. Supernatant was purified through 15-45% (w/v) sucrose density gradient by ultracentrifugation at 300,000 xg (using a Beckman SW 55 Ti rotor) for 50 minutes at 4°C (Basavappa *et al.*, 1994b). The peak fractions corresponding to virions and ECs were collected. Respective peak fractions were pooled, diluted and the particles pelleted by ultracentrifugation (using a Beckman SW 55 Ti rotor) at 300,000 xg for 2 hours at 4°C. Pellets were re-suspended in 300 µl PBS and re-clarified by centrifugation. Supernatants were re-purified through a second 15-45% sucrose gradient at 300,000 xg for 50 minutes at 4°C as described above.

2.19.5. Genome-free capsid preparation

Virus was propagated in cysteine/methionine-deficient media and radio-labelled with ^{35}S cysteine/methionine 2.75 hours post-infection/-transfection. At 3.25 hours post-infection, cells were treated with GuHCl at a final concentration of 2 mM to inhibit RNA replication and stimulate accumulation of genome-free ECs (Basavappa *et al.*, 1994b). ECs were purified through 15-45% sucrose density gradients (Basavappa *et al.*, 1994b) and detected by scintillation counting of gradient fractions (O'Brien & Newman, 1977).

2.19.6. 3H radio-labelled wt PV-1 (Mahoney)

A total of 0.4 x 10^6 HeLa cells propagated in a T-25 flask of HeLa were infected with *wt* PV-1 at MOI of 50 in 2 ml OptiMEM (1% HEPES) media. At 1 hour post infection (h.p.i.), virus RNA was radiolabelled with 100 µCi ^{3}H Uridine (Brandenburg *et al.*, 2007b) and cells were incubated at 37°C with rocking. Cells were harvested at 24 h.p.i. and cell debris was pelleted by centrifugation at 4,000 rpm for 10 minutes. Supernatant was supplemented with 0.5M NaCl-in-RSBEC buffer (100 mM Tris, 100 mM NaCl, 100mM MgCl$_2$) and virus concentrated by ultracentrifugation for 1 hour at 353,720 xg through 30% sucrose cushion. Virus pellet was re-suspended in 300 µl RSBEC buffer and purified through a 15-45% sucrose gradient by ultracentrifugation for 2.5 hours at 111,000 xg. Gradient was fractioned and ^{3}H-labelled RNA analysed by scintillation.

2.19.7. 35S Cys/Meth radio-labelled wt PV-1 (Mahoney)

Virus-infected HeLa cells or transfected L-cells were propagated in Cys/Meth – deficient RPMI media supplemented with 1% HEPES. At 2.45 hour post infection (h.p.i.), virus RNA was radiolabelled with 10 µCi/ ml ^{35}S Cys/Meth and cells were incubated at 37°C with rocking. Cells were harvested at 24 h.p.i. and

cell debris was pelleted by centrifugation at 4,000 rpm for 10 minutes. Supernatant was supplemented with 0.5M NaCl-in-RSBEC buffer (100 mM Tris, 100 mM NaCl, 100mM $MgCl_2$) and virus concentrated by ultracentrifugation for 1 hour at 353,720 xg through 30% sucrose cushion. Virus pellet was re-suspended in 300 µl RSBEC buffer and purified through a 15-45% sucrose gradient by ultracentrifugation for 2.5 hours at 111,000 xg. Gradient was fractioned and ^{3}H-labelled RNA analysed by scintillation.

2.19.8. Transmission electron microscopy

Purified virions and ECs were dialysed from sucrose fractions into dialysis buffer (10 mM HEPES, 100 mM NaCl, 1 mM EDTA, 1 mM DTT, pH 6.4) and visualised by negative staining transmission electron microscopy according to standard protocols (Miller, 1986).

2.20. Methods applied in the thermal evolution

2.20.1. Thermal stability assays

2.20.1.1. Thermal inactivation (TI50) assay

Virus samples were incubated at a range of temperatures for 30 minutes within a thermal cycler and immediately cooled to 4°C for 5 minutes. Heat-treated samples were titrated by plaque assays (Dulbecco & Vogt, 1954).

2.20.1.2. Thermal selection of virus mutants

Virus samples were heated for 30 minutes at temperatures resulting in 99.99% loss in titre. Surviving virus was propagated at 37°C in HeLa cells by standard methods and infectivity titres of pre- and post-heated samples were determined by plaque assays (Dulbecco & Vogt, 1954). Thermal selection was carried out sequentially until pre- and post-heated titres were approximately equal. Heat inactivation assays were repeated, followed by rounds of thermal selection at increasing temperatures of 51°C, 53°C and 57°C until there was a severe fitness cost.

2.20.1.3. Assessing the stability of thermal resistant mutants

Each thermo-resistant mutant was serially passaged a total of 5 times without heating and assayed respectively. Each passaged virus was thereafter heated and assayed. Post-heating virus titres were compared to *wt* virus titres after heating to same temperatures.

2.20.1.4. Particle Stability Thermal Release Assay (PaSTRy)

Thermal stability of the virus particles was further characterised by a thermo-fluorometric dual dye-binding assay using nucleic acid dye SYTO9 and protein-binding dye SYPRO Orange (both Invitrogen). Reactions of 50 μl containing 1.0 μg double-purified and de-salted virus fractions, 5 μM SYTO9, 150X

SYPRO orange and PaSTRy buffer (2mM HEPES, 200 mM NaCl, pH 8) were mixed and ramped from 25–95 °C with fluorescence reads taken at 1 °C intervals every 30 seconds within the Stratagene MX3005p qPCR system. The excitation (ex) and emission (em) band pass for SYPRO orange, were 492 and 585 nm, respectively and, 492 nm (ex) and 517 nm (em) for SYTO9(Walter *et al.*, 2012).
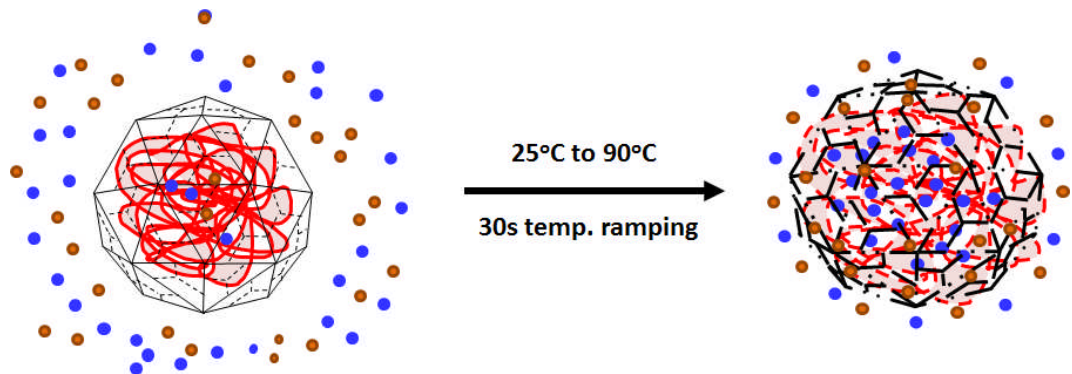
Figure 2.3 Particle stability thermal release assays (PaSTRy). This involves the use of dual dyes with differential scanning for SYTO9 nucleic acid-binding dye (blue solid balls) and SYPROorange protein-binding dyes (orange solid balls) under buffered conditions with continuous temperature ramping from 25–95 °C. Fluorescent reads are taken after a 1ºC increase every 30 seconds. Maximum fluorescence will occur at a melting temperature point where SYPROorange binds to the hydrophobic residues and SYTO9 accesses nucleic acid.

2.21. Gel electrophoresis methods

2.21.1. Agarose gel electrophoresis

A 0.8 % TBE (or TAE) agarose gel (containing 1:10,000 v/v SYBR® safe DNA gel stain) was sited in a gel tank containing 1x TBE (or TAE). Samples were mixed with 6X loading buffer (at a ratio 5:1) and loaded into wells. A charge of

90 V was applied to gel for 60 minutes. Bands were visualised under ultraviolet (UV) light, using the GenoDoc System (Syngene)

2.21.2. Agarose gel purification

A 0.8 % TBE (or TAE) agarose gel was run (as described in section 2.4.1 above). DNA fragments are excised from gel into a 1.5 ml microcentrifuge tube using a razor blade. DNA was purified using the Zymoclean^{TM} Gel DNA recovery kit. Excised gel was dissolved in 3 gel-volumes of agarose dissolving buffer (ADB) by heating at 55°C for 10 minutes. DNA fragment from melted agarose solution was transferred to a silica-based membrane column with subsequent washes and elution.

2.21.3. SDS-polyacrylamide gel electrophoresis (SDS-PAGE)

Proteins were analysed using a 15% acrylamide gel with a 5% stacking layer. Samples were added to 2x Laemmli SDS-PAGE loading buffer and boiled at 100°C for 10 minutes. Samples were loaded into gel wells and run in a 1x SDS-PAGE running buffer at 200V for 1 hour, in an electrophoresis tank.

2.21.4. Western blotting

Virus proteins were dissociated and separated by SDS-PAGE using standard protocols (Weber & Osborn, 2006) (section 2.4.3.). SDS-PAGE gel was soaked in ice-cold transfer buffer for 5 minutes. Gel tank was assembled in a vertical rig with polyvinylidene difluoride (PVDF) membrane, which had been pre-soaked in 100% methanol for 10 seconds followed by transfer buffer for 5 minutes. Electrophoretic transfer was carried out at 25 V for 90 minutes. Transferred proteins were immunoblotted with appropriate antibodies (section 2.6.5.) using standard protocols (Liu *et al.*, 2014).

2.21.5. Probing western blot with antibodies

Membrane with transferred proteins was blocked for 1 hour at room temperature with freshly prepared 5% milk in 1x TBST. Indirect antibody detection of target protein was carried out by an initial overnight incubation of transferred membrane in a 1/2000 dilution of a primary polyclonal antibody of rabbit origin (Rab 1A) with rocking at 4°C. After three 15-minute washes with 1 X TBST at room temperature, membrane was incubated in a labelled conjugated secondary (anti-rabbit) antibody (1/1000 dilution) at room temperature for 1 hour with shaking. Again the membrane was washed 3 x 15 minutes with 1 x TBST at room temperature before detection by photographic film in the presence of a chemiluminescent reagent (Thermo Scientific, Pierce ECL). Chemiluminescent substrate was added to the membrane for 1 minute at room temperature before exposure to X-ray film (Thermo Scientific, CL-XPosure Film).

2.21.6. Autoradiography

Radio-labelled proteins were separated by SDS-PAGE (section 2.4.3.). Proteins were fixed by soaking fixing solution (section 2.4.17.1) for approximately 30 minutes. Radio-isotope was amplified by soaking gel in fluorometric amplify solution (section 2.4.17.2) for 15 minutes followed by vacuum-drying onto filter paper at 80°C for 2 hours. Dried gels were exposed in close contact with an appropriate X-ray film at -80°C for at least 2 hours. After exposure, the film was developed according to the manufacturer's instructions (Circolo & Gulati, 2009).

2.22. Methods used in the analysis of virus antigenicity

2.22.1. Immunoprecipitation assay

2.22.1.1. Monoclonal antibodies

Radio-labelled virions and ECs were purified by sucrose density gradients as previously described (Basavappa *et al.*, 1994b) and incubated at a range of temperatures for 30 minutes. Particles were immunoprecipitated as described by Vrijsen *et al* (Vrijsen *et al.*, 1983), using a native anti-PV-1 monoclonal (mAb) antibodies (known as 234 mAb), which is known to bind intervals between pentamers at the 3-fold axis of the N form of the capsid, or non-native 1588 mAb (Minor, 1986; Osterhaus *et al.*, 1983; Rombaut *et al.*, 1990). Immunoprecipitated particles were counted by scintillation and analysed by SDS-PAGE and autoradiography according to standard protocols (Circolo & Gulati, 2009).

2.22.1.2. VHH nanobodies

Magnetic TALON beads were prewashed using wash buffer (50 mM NaH_2PO_4, 300 mM NaCl, Tween 20 to 0.01% (w/v), Methionine to 2%, and BSA to 0.01%, pH 8.0). Samples were pre-bound to nanobodies with shaking for 10 seconds and 1 hour incubation at room temperature. Pre-washed beads were added to sample and incubated at room temperature with continuous shaking. Beads were separated by magnet and boiled in SDS-loading buffer for 5 minutes. Proteins were separated by SDS-PAGE (Schotte *et al.*, 2012).

2.22.2. Enzyme-linked immunosorbent assay (ELISA)

Purified ECs and virions were heat-treated at a range of temperatures as previously described. Particle antigenicity was assayed by capture ELISA, using a purified polyclonal sheep (SH-16) antibody as capture. Monoclonal murine PV-1 antibodies Mab 234 and Mab 1588 were applied as primary antibodies to

identify native and non-native particles, respectively (Osterhaus *et al.*, 1983). An anti-mouse conjugated to HRP was used as secondary antibody. ELISA was carried out according to standard protocols (sections 2.5.4 and 2.5.7) (Gan & Patel, 2013).

2.22.3. Pulling down N-antigenic mutants for sequencing

Heated virus particles were immunoprecipitated using native (N-234) monoclonal murine PV-1 antibodies (section 2.6.1). After three washes of the immune complex (IC) with PBS containing 0.2% TEEWN-20, virus RNA was extracted, reverse transcribed and amplified (sections 2.6.1, 2.6.2 and 2.6.3). Amplified nucleic acid was gel purified and sequenced by Beckman Cogenics and aligned as described in section 2.6.7.

2.22.4. Assessing genetic stability

Mutants were serially passaged five times without selection pressure. Serially passaged samples were then heated at respective selection temperature (51°C, 53°C and 57°C). Pre-heated and post-heated virus samples were assayed for infectivity.

2.23. Methods used in virus RNA studies

2.23.1. Virus RNA extraction

2.23.1.1. Qiagen RNeasy kit

Virus RNA was extracted using the Qiagen RNeasy plus universal protocol. Initial cell membrane disruption and homogenisation was carried with phenol (7:1 v/v ratio) – containing RNase-inactivating guanidine thiocyanate. After a breif incubation of homogenate at room temperature, and the elimination of genomic DNA, further membrane disruption was carried out with chloroform. After a cold centrifugation to separate sample into phases, the upper, aqueous RNA-containing phase was precipitated with diethylpyrocarbonate (DEPC)-treated ethanol; captured onto a silica membrane; washed in 2 steps and then eluted.

2.23.1.2. Phenol-chloroform extraction and ethanol precipitation

Native virion particles were immunoprecipitated and total RNA extracted by guanidinium thiocyanate-phenol-chloroform methods (Chomczynski & Sacchi, 2006).

2.23.2. Reverse transcription of virus RNA into cDNA

In vitro reverse transcription of the P1 region of the virus genome was carried out using the Invitrogen SuperScript II protocol. A 12 µL reaction containing reverse primer (specific to the P1 region of PV-1), extracted RNA, dNTP Mix (10 mM each) and Sterile, distilled water was heated to 65°C for 5 min and quick chilled on ice. After a brief centrifugation to collect sample at the bottom of the tube, reaction buffer (250 mM Tris-HCl, pH 8.3; 375 mM KCl; 15 mM $MgCl_2$) and 0.1 M DTT were added, and the reaction incubated at 42°C for 2 min. Two hundred units of SuperScript II reverse transcriptase were added and the reaction

was made up to a final volume of 20 μL and then incubated at 42°C for 50

minutes. The reaction was thereafter inactivated by heating at 70°C for 15

minutes.

2.23.3. Amplification of cDNA by Polymerase Chain Reaction (PCR)

A total of <200 ng of cDNA, 0.5 μM forward and reverse primers (specific to the

P1 region of PV-1) were made up to a 20 μL PCR reaction of the the QIAGEN

Fast Cycling PCR Kit, which contains a master mix of HotStarTaq *Plus* PCR

DNA Polymerase, KCl and $(NH_4)2.SO_4$, 200 μM of each dNTP, and optimized

$Mg2+$ concentrations. PCR cycling conditions were shown in Table 2.3 below

Table 2.3 PCR cycling protocol

Step	Temperature (°C)	Time	No. of cycles
Initial denaturing	95	5 minutes	1
Denaturing	96	5 seconds	
Primer annealing	59	5 seconds	30
Extension	68	1 minute 45 seconds	
Final extension	72	1 minute	1

2.23.4. Cloning amplicons into plasmids

2.23.4.1. pGEM T-easy vector

PCR amplicon were gel-purified through TBE agarose (as described in 2.4.2 above) and ligated into linearized pGEM T-easy vectors with a single 3´-terminal thymidine at both ends and transformed into high-efficiency competent DH5α cells in LB-ampicillin broth to a final volume of 1ml. A total volume of 200μl transformation culture was plated on LB-ampicillin agar and incubated overnight at 37°C.

2.23.4.2. pCR-XL TOPO vector

PCR amplicons were gel-purified through TAE agarose (as described in section 2.4.2 above). Amplicons were ligated into linearized pCR-XL TOPO vectors and transformed into high-efficiency competent XL-10 gold cells in the presence of Kanamycin and incubated overnight at 37°C.

2.23.5. Plasmid preparation from overnight cultures

Single colonies from overnight cultures of pGEM T-easy vector-transformed cells were picked into LB/Amp broth (100 μg/ml ampicillin) or colonies from overnight cultures of pCR-XL TOPO vector-transformed cells were picked into LB/Kam broth (100 μg/ml kanamycin). Plasmid recovery was carried out using the QIAprep Spin Miniprep Kit (Qiagen). Cells were pelleted from a 10 ml culture and re-suspended in buffer containing RNase A. This is followed by an alkaline lysis of bacterial cells, which is followed by the neutralisation, precipitation and adsorption of plasmid DNA onto a silica membrane, respectively. Plasmid DNA are thereafter washed and eluted. A single digest using *EcoRI* releases the insert and can be viewed on an agarose gel. Plasmid was sequenced by Beckman Cogenics using sequencing primers.

2.23.6. Virus sequencing

Reverse-transcribed cDNA was amplified by PCR using copy-proof Phusion DNA polymerase, a 5'-UTR upstream [Forward] primer and P1-specific downstream [Reverse] primer, following standard protocols. PCR-amplicons were gel-purified and sequenced. A-tailing of PCR amplicons was carried out followed by cloning into the high copy number pGEMT-easy vector plasmid (Chen *et al.*, 2009). Individual colonies were sequenced for confirmation Plasmid was sequenced by Beckman Cogenics using sequencing primers.

2.23.7. Sequence alignment of individual virus mutants

Alignment of sequenced reactions was carried out using the ClustalW program, designed and made available from the European Molecular Biological Laboratory, European Bioinformatics Institute, at

http://www.ebi.ac.uk/Tools/msa/clustalw2/

2.24.   Methods applied to plant expression

2.24.1.   Plasmid Constructs

Codon-optimized plasmid constructs of PV53δ and PV57δ for *Nicotiana benthamiana* were commercially synthesised with flanking restriction sites for *Age*I and *Xho*I. Genes were cloned into separate pEAQ-*HT* (Sainsbury *et al.*, 2009) expression vectors producing pEAQ-HT-PV53δ, pEAQ-HT-PV57δ and pEAQ-*HT*-3CD. The *HyperTrans* mutation of the vector carrying 3CD was subsequently removed to give rise to produce pEAQ-3CD vector. *Agrobacterium tumefaciens* LBA4404 were transformed with the constructs by electroporation and propagated at 28°C in Luria-Bertani media containing 50 µg/ml kanamycin and 50 µg/ml rifampicin.

2.24.2.   Transient expression

Agrobacterium tumefaciens containing the respective constructs were grown to stable phase in Luria-Bertani medium supplemented with the appropriate antibodies. Cultures were pelleted by centrifugation at 2500 x g and re-suspended in MMA buffer (10 mM MES, pH 5.6, 10mM $MGCl_2$, 100 µM acetosyringone) to an OD_{600} of 0.8 (for pEAQ-HT-PV53δ and pEAQ-HT-PV57δ, respectively) and 0.4 (for pEAQ-3CDo). The bacteria were mixed in 1:1 ratio and left at room temperature for 0.5–3 hours prior to infiltration. The suspensions were pressure infiltrated into 3 week old *Nicotiana benthamina* leaves as described by Thuenemann et al. (Thuenemann *et al.*, 2013). Plants were grown in glasshouses maintained at 25 °C with supplemental lighting to guarantee 16 hours of daylight and watered daily for 6-7 days.

2.24.3. Extraction and purification

Infiltrated leaf tissue was weighed and homogenized using a Waring (Torrington, CT) blender with 3 x volume of extraction buffer (0.2 M Na_2HPO_4, 0.2 M NaH_2PO_4) plus added protease inhibitor (Roche, Welwyn Garden City, UK) and then filtered through Miracloth (Calbiochem). The crude extract was centrifuged at 9,500 x g for 15 min at 4°C following filtration over a 0.45 µm syringe filter (Sartorius). The clarified extract was then purified over a sucrose cushion (1 ml 70% and 5 ml 25%) at 167,000 x g for 3 h at 4°C and the lower fraction was retrieved. Sucrose was removed by dialysis using PD10 desalting columns (GE Healthcare) and the volume of the sample reduced using Amicon Centrifugal Filter Units (Millipore). The sample was further purified by centrifugation through a Nycodenz gradient (20% -60%) in a TH641 ultracentrifuge swing-out rotor (Sorvall) at 247,103 x g for 24h and 4°C. VLPs were collected by piercing the side of the tube with a needle and PD10 desalting columns (GE Healthcare) were used to remove the Nycodenz and the samples concentrated using Amicon Centrifugal Filter Units (Millipore).

2.25. Methods applied to yeast expression

2.25.1. Plasmid constructs

The *Pichia*-optimised codon sequences for a non-cleavable 3CD mutant was cloned into pPINK-LC plasmid (see section 2.2.5), while the P1 region for the *Pichia*-optimised codon sequences of wt PV-1 and thermally-stable PV57δ was cloned into pPICZ-A vector (see section 2.2.6).

A study has demonstrated that protein expression using *P. pastoris* vectors is achievable using G-418 sulphate as the primary selectable marker by replacing the Zeocin-resistant marker gene (*Sh ble*) with a G-418selectable marker gene (*Tn903 Kam^R*) (Papakonstantinou *et al.*, 2009). The pPICZAPVP1 constructs were modified to a pPICKAPVP1 (section 2.2.7).

2.25.2. Transient expression

Yeast cells (*Pichia pastoris*) were grown up in YPD media and transformed with *Pichia*-optimised plasmid clones of 3CD (pPINK-HC-3CD) by electroporation. Transformed yeast cells were grown on Pichia-adenine-dropout (PAD) plates to select for yeast cells expressing the ADE2 gene. Positive colonies were screened for the presence of 3CD and grown in the presence of glycerol (BGMY) media for 24 hours. The expression of 3CD was initiated in the presence of methanol (BMMY) for 48 hours.

Chapter 3

Improving PV capsid stability by thermal selection

3. De-stabilising a metastable 160S particle

PV (PV) protects its genomic RNA by encapsidation into a 160S metastable particle (Hogle, 2002b). In order to replicate, the metastable particle has to be destabilised and its RNA released into a receptive host by means of a systematic capsid-destabilising processes (Basavappa *et al.*, 1994a; Levy *et al.*, 2010; Marc *et al.*, 1989). Preliminary events to this process involve attachment of the 160S particle to the host-specific receptor (PVR or CD155), which binds within a depression in the capsid surface termed the canyon. This event occurs without structural or conformational changes (Belnap *et al.*, 2000b) and is followed by transporting the particles within an endocytic vesicles. However, in order to release the genome the PVR attachment triggers a capsid expansion that results in a 135S particle (Basavappa *et al.*, 1998b). The pocket factor, which resides within a VP1 cavity underlying the canyon is released and the PVR moves deeper into the canyon (Hogle, 2002b). By means of biochemical and structural studies it has been shown that the internalised VP4 and the N-terminus of VP1 are externalised, possibly creating a pore-like channel through which the viral RNA is delivered into the cell (Fricks & Hogle, 1990; Tuthill *et al.*, 2006; Tuthill *et al.*, 2010). Real-time cell imaging and virus infectivity assays have also shown that these events occur within vesicles about 100–200 nm below the plasma membrane (Brandenburg *et al.*, 2007a).

3.1. Instability of the PV EC

Post cell-entry, the PV genome is translated into a polyprotein that is cleaved by virus-encoded proteases [$2A^{pro}$ and $3C^{pro}$/ $3CD^{pro}$] into three protein precursors, P1, P2 and P3 (Parsley *et al.*, 1999b); further proteolytic cleavage of P1 reveal three structural proteins, VP1, VP3 and, VP0 (a precursor of VP2 and VP4). At

early stages of PV morphogenesis, VP1, VP3 and VP0 exist as a protomer (Jiang *et al.*, 2014; Mueller *et al.*, 2005; Wien *et al.*, 1996); five protomers assemble to form a pentamer, and 12 pentamers assemble into an 80S procapsid or a fully mature virion in an event mapped by the cleavage of VP0 into VP2 and VP4 (Jiang *et al.*, 2014).

Prior to attaining its metastable state, the 80S PV EC is reinforced by a network of internal N-termini of VP1, VP3 and VP0. After RNA encapsidation in the 160S particle, VP0 is cleaved into VP2 and VP4 (i.e. the N-terminus of pre-cleaved VP0), which lies within the capsid shell as shown by X-ray chromatography (Hogle, 2002a). The released VP4 molecule rearrange to form a network on the inner surface of the capsid which contributes significantly to its stability (Basavappa *et al.*, 1994a).

3.2.   Roles of the PV EC

In many enteroviruses, ECs (which are antigenically identical to mature virions), are produced naturally during infection but their roles in the virus lifecycle are not fully understood (Hogle, 2002a; Jiang *et al.*, 2014). *In vitro* studies, suggested that in infected HeLa cells, ECs can be dissociated by heat and biochemical means into pentameric sub-units (Marongiu *et al.*, 1981; Onodera & Phillips, 1987) and may act as reservoirs of pentamers which can be chased into mature virion (Jacobson & Baltimor.D, 1968). A study however refutes this claim, suggesting that ECs are dead-end products of morphogenesis as shown using recombinantly-expressed bovine enterovirus (BEV) through biochemical assays. This study suggested that the assembly of EC from pentamers was most likely an irreversible function of inter-pentameric ionic strengths but however agrees that ECs may also be precursors of genome-packaged virion (Li *et al.*,

2012b). Recently a study carried out on EV71 suggested that ECs could also act as decoys by sequestering neutralising antibodies during the virus lifecycle (Shingler *et al.*, 2015).

3.3. Aim

Attempts have been made to produce PV-like particle (VLP) vaccines, PV ECs (PV ECs) have been produced in various recombinant expression systems (Ansardi *et al.*, 1991b; Brautigam *et al.*, 1993a; Rombaut & Jore, 1997a). However, wildtype PV ECs are very unstable and readily change antigenicity from a native form to a non-native or heated form (Basavappa *et al.*, 1994b) and are unable to elicite protective immune response.

The RdRp of RNA viruses are error prone and result in high mutation rates. This allows natural evolution, which can be rapidly driven by selection pressure (Elde, 2012; Karakasiliotis *et al.*, 2005) (discussed further in chapter 4). It was therefore hypothesised that if within a PV population, thermostable viruses exist at low levels, selecting for heat stability result to a more stable capsid. Therefore, this study sought to select, amplify and characterise thermostable mutant viruses. This approach has been attempted previously (Shiomi *et al.*, 2004) but the work here represents a more stringent and detailed analysis.

In this section, attempts to stabilise the EC of PV-1 by selecting for heat-resistant PV-1 mutants are discussed, highlighting the potential of selected stabilising mutations for the development of a synthetic PV VLP vaccine.

3.4. Selecting thermally-stable PV-1 mutants

Attempts to synthesise a native antigenic genome-free PV capsid as a VLP vaccine have been stalled by its antigenically unstable capsid (Basavappa *et al.*, 1994a). In an attempt to stabilise the virus capsid, heat-resistant virions were selected and then characterised by thermal inactivation assays. This involved an initial step of identifying the temperature at which over 99.9% of infectious titres were lost followed by cycles of thermal selection of surviving virus particles (Figure 3.1).
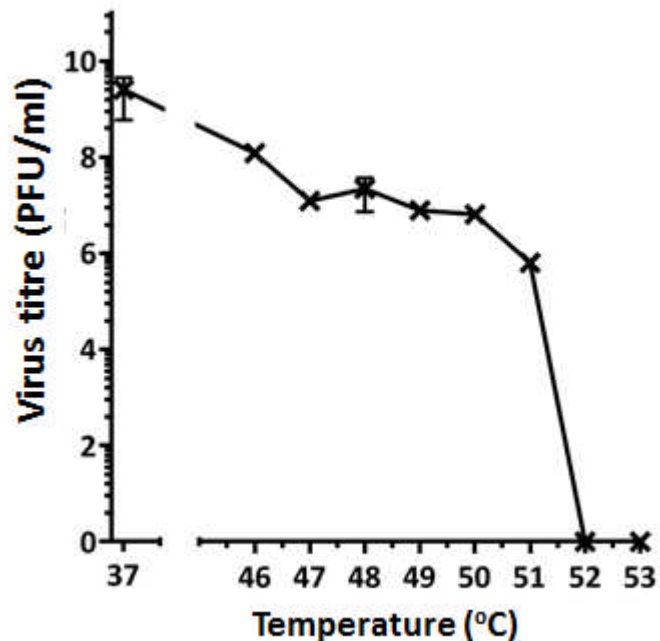
Figure 3.1. Thermal inactivation assay of wild type PV-1. *Wild-type PV-1 was incubated at a range of temperatures for 30 minutes and cooled to 4°C. Surviving pool of viruses was assayed for infectivity by plaque formation on HeLa cells. Figure shows that over 99.9% virus titres were lost at 51°C. n=3 ± S.D.*

Figure 3.1 shows that almost all the infectious virus was lost at $51^{\circ}C$ and therefore this temperature was chosen for initial selection. A sample of wt PV-1 was incubated at $51^{\circ}C$ followed by successive passage at $37^{\circ}C$ (Figure 3.2A). Thermal selection was repeated for 10 successive passages until the post-heated virus titre was aproximately equal to the pre-heated virus titre. This pool of thermally-selected PV-1 was termed VS51.

Thermal inactivation assays were again employed and $53^{\circ}C$ was identified as the next selection temperature. VS51 was subjected to thermal selection at $53^{\circ}C$ with 12 successive passages at $37^{\circ}C$ after each round of selection pressure. Pre- and post-heated virus titres were determined after each passage as previously described (Figure 3.2B). At the end of 12 cycles of thermal selection, the pool of selected virions was termed VS53.

The third selection was carried out at $57^{\circ}C$. A sample of VS53 was incubated at $57^{\circ}C$ with successive passage at $37^{\circ}C$ and infectivity titre was determined after each passage (Figure 3.2C). At the end of 10 successive cycles of selection, this pool of virion was termed VS57. In contrast to selection at VS51 and VS53, VS57 had a fitness cost of 1 $\log_{10}$ reduction in titre.
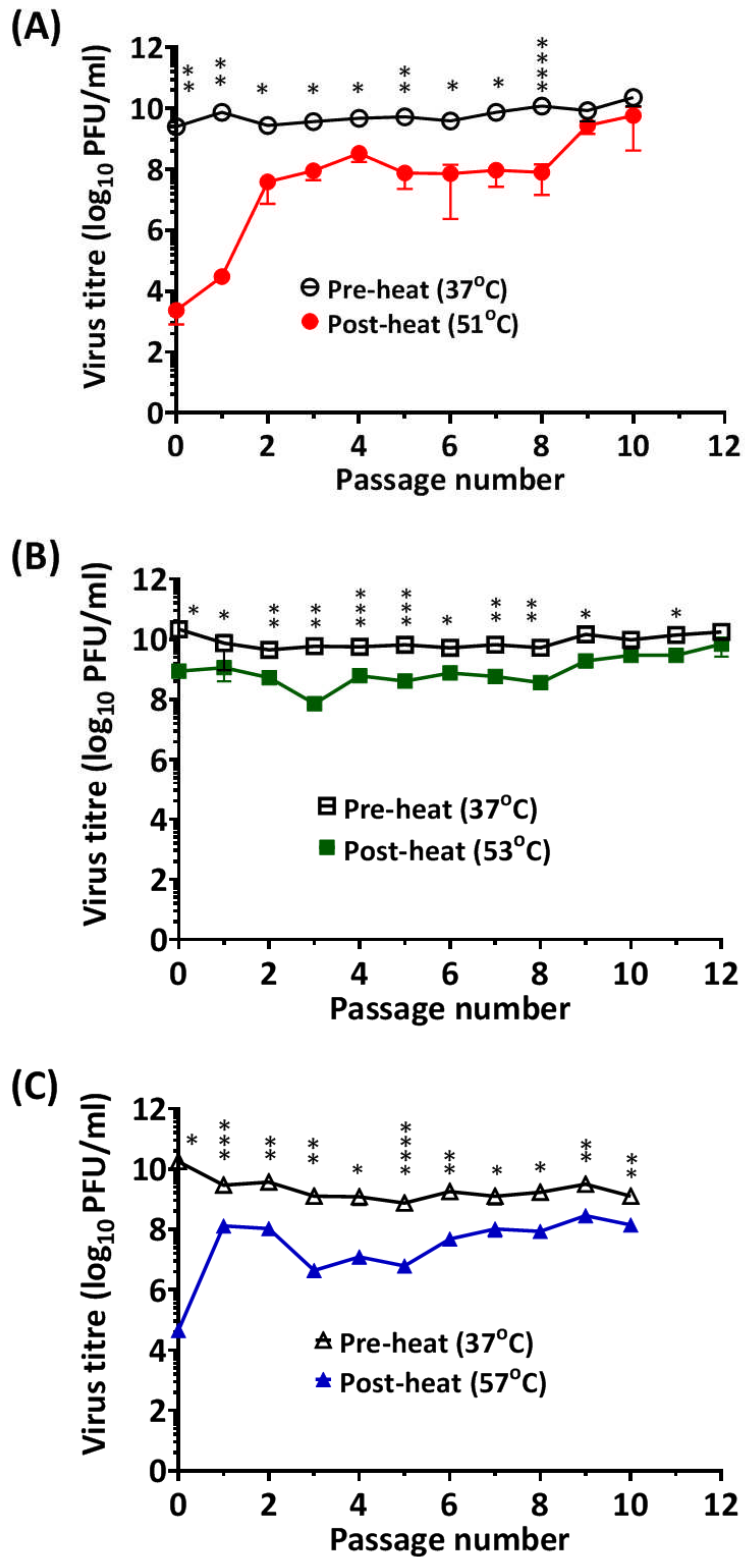
Figure 3.2. Thermal selection of heat-resistant PV through repeat passage. *(A) wt PV-1 was incubated at 51ºC for 30 minutes, which resulted in 99.99% loss of infectivity, and immediately cooled to 4ºC. The surviving pool of viruses was passaged at 37ºC. After each cycle of passage, virus titres (pre- and post-*

heating) were determined by plaque assays. Selection cycles were repeated until pre- and post-heated virus titres were approximately equal (n=3 ± S.D., *P<0.05, **P<0.001, ****P<0.00001) (B) After 10 cycles of thermal selection at 51°C and passage at 37°C, thermal pressure was increased to 53°C with 12 successive passages at 37°C. Pre- and post-heat titres were statistically-different from passage 0 until passage 9 and 11 (n=3 ± S.D. *P<0.05, **P<0.001, ***P<0.0001)). (C) After selection at 53°C, thermal selection pressure was subsequently increased to 57°C with 10 successive passages. Pre- and post-heat titres were statistically-differernt from passage 0 until passage 10 (n=3 ± S.D., *P<0.05, **P<0.001, ***P<0.0001), ****P<0.00001). Three titrations of the same selected pool were analysed at each temperature.

Owing to the gradual increase in selection pressure from 51°C to 57°C, three pools of viruses were selected and shown as able to withstand 30-minute incubation at 51°C, 53°C and 57°C, respectively, without significant loss in infectivity titres, as determined by plaque assays.

3.4.1. Thermal resistance of heat-selected PVs

The ability of VS51, VS53 and VS57 to withstand elevated temperatures was assessed by thermal inactivation assays. This measures instability as a function of temperature as assessed by loss of infectivity (figure 3.3).
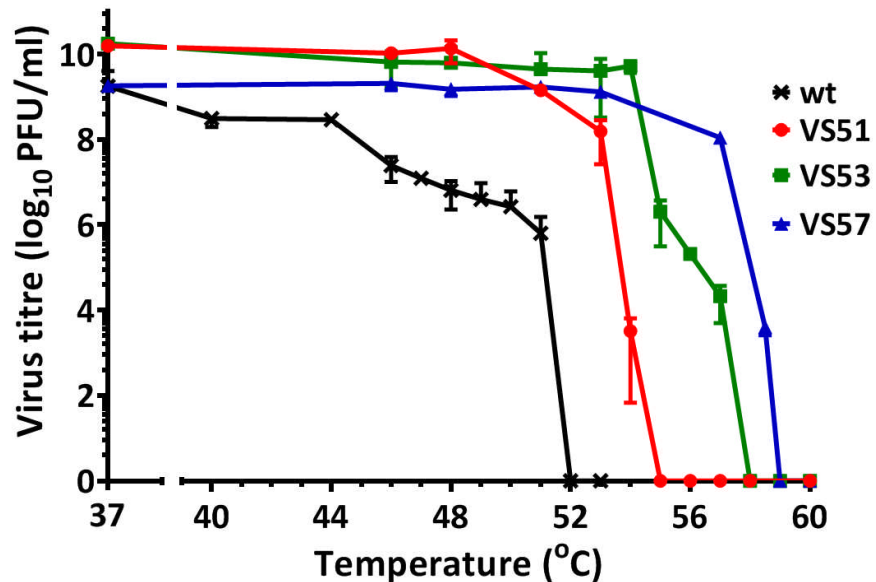
Figure 3.3. Thermal resistance profile of heat-selected PV-1 pools. (A) Pools of PV-1 selected at 51ºC (VS51), 53ºC (VS53) and 57ºC (VS57) were incubated at a range of temperatures between 37ºC and 60ºC for 30 minutes and immediately cooled to 4ºC. Titres were determined by plaque assays on HeLa cells. Data represent titres at each temperature (n=3 ± S.D., P <0.0001).

Thermal inactivation assays showed that VS51, VS53 and VS57 were still infectious at higher temperatures than wt. Particle stability thermal release assays (PaSTRy) were also applied to assess the thermal stability of the virus particles without directly assessing infectivity (Walter *et al.*, 2012). The PaSTRy assay employees the use of two fluorescent dyes: SYTO9, which binds nucleic acid and indicates accessibility to the viral RNA; and SYPROorange, which binds hydrophobic amino acid residues and indicates unfolding/ denaturation of the capsid proteins (figure 3.4).
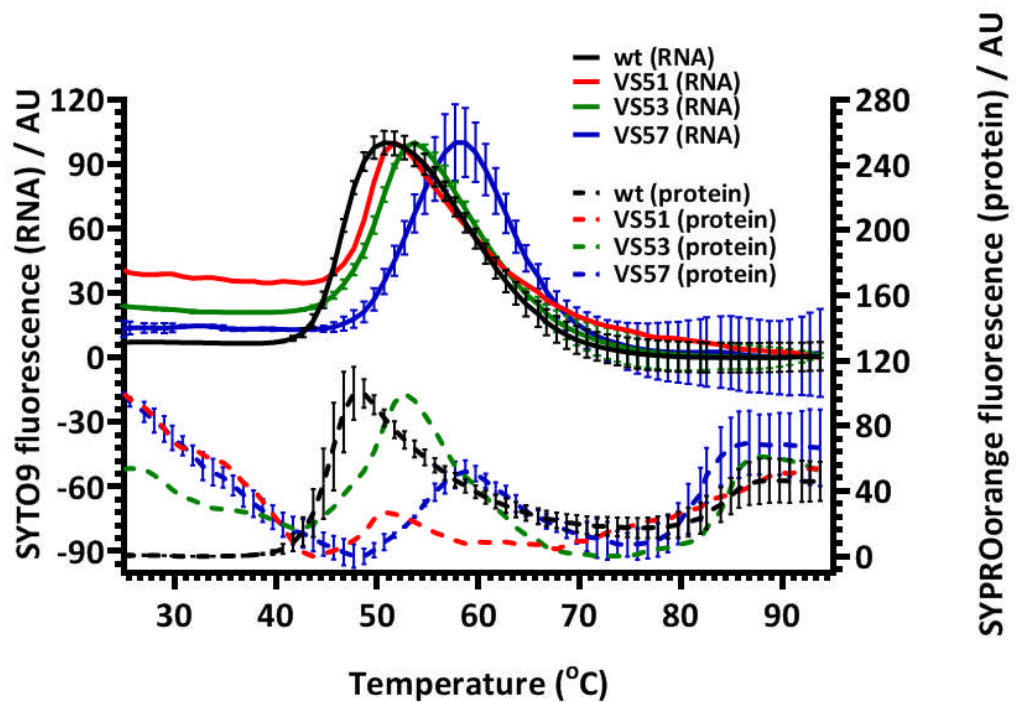
Figure 3.4. Particle stability thermal release assays (PaSTRy). Wild type PV-1 and thermal-selected virus samples were propagated in HeLa cells with respective selection pressure. Virus samples were pelleted through 30% sucrose cushions and purified through two 15-45% sucrose density gradients. Differential scanning fluorometric assays (PaSTRy) were set up using SYTO9 nucleic acid-binding dye and SYPROorange protein-binding dye (Walter et al., 2012). Graph shows Relative fluorescence of SYTO9 as solid lines (n=3 ± S.D., P<0.0001) and Relative fluorescence of SYPRO orange as broken (n=3 ± S.D., p<0.001). Error bars on B and C are omitted for clarity.

Maximal fluorescence of SYTO9 is shown to have occurred at 51ºC (wt), 52ºC (VS51), 54ºC (VS53) and 58ºC (VS57). SYPROorange had two patterns of binding to hydrophobic residues of capsid proteins at 48ºC (WT), 51ºC (VS51), 53ºC (VS53) and, 59ºC (VS57) as well as at approximately 85ºC for all viruses. Both SYTO9 and SYPROorange PaSTRy assays confirm the observations from

infectious thermal inactivation and demonstrate thermally-stable virus pools can withstand elevated temperatures compared to wt PV-1 (Figure 3.4).

The results suggest that thermal stability may be associated with a synchronised temperature for RNA release (T_R) and first protein melting temperature, (T_m), both of which occur before thermal inactivation of infectivity. Data further showed that wt PV-1 had distinct T_R and T_m occurring within 5°C-range, while selected mutants had an increasing T_m and T_R, with both events coinciding in the most stable but least fit of all three virus pools (i.e. VS57). Comparatively, Hepatitis A virus (HAV), being a more thermal stable picornavirus, was shown to have a higher PaSTRy T_R than T_m by Wang et al, 2015 (Wang *et al.*, 2015). This suggests that as PV attains higher thermal stability, RNA release and capsid dissociation may occur as a synchronized event.

3.5. Generating ECs of PV

Studies have shown that addition of guanidine hydrochloride (GuHCl) to virus infected cells inhibits RNA synthesis and leads to an accumulation of genome-free ECs (Basavappa *et al.*, 1998a; Jacobson & Baltimor.D, 1968; Jiang *et al.*, 2014). PV ECs were generated by GuHCl-treatment and adopted as a model for PV VLPs, however, these are antigenically unstable, as discussed above. The effect of GuHCl was assessed by infecting HeLa cells with wt PV-1 and incubating at 37ºC under 5% CO_2. A sample was treated with 2mM GuHCl at 3.25 h.p.t. and cells were incubated at 37ºC under 5% CO_2 for 24 hours. Virus particles were harvested by freeze-thawing cells and clarification of cellular debris by centrifugation and supernatants titrated by plaque assays on HeLa cells (figure 3.5)
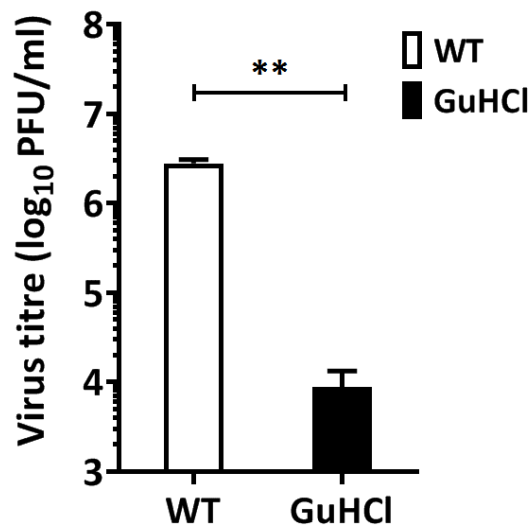
Figure 3.5. Inhibiting PV-1 RNA synthesis by GuHCl-treatment Viral RNA was transfected into L-cells and incubated at 37ºC under 5% CO_2. Samples were treated with 2mM GuHCl at 3.25 h.p.t. and virus titrated for infectivity by plaque assay using HeLa cells (n=3, **P<0.001).

In order to identify the EC particles, wt PV-1, VS51, VS53 and VS57 were propagated in L-cells by transfection. Capsid proteins were radio-labelled with [^{35}S]-(Cys/Met) at 2.75 hours post-transfection (h.p.t.) when virus-induced shutdown of cellular protein synthesis had occurred. Cells were incubated at 37°C under 5% CO_2 and treated with 2mM GuHCl at 3.15 h.p.t. thereby, generating ECs *In vitro*. GuHCl-treated and non-treated virus particles were harvested by freeze-thawing cells and clarification of cellular debris by centrifugation. Supernatants were clarified by centrifugation at 4,000 rpm and pelleted through a 30% sucrose cushion by ultracentrifugation at 40,000 rpm for 3.5 hours in a Beckman SW 40 Ti rotor. Pellets were purified through 15-45% sucrose density gradients by ultracentrifugation at 50,000 rpm for 50 minutes in the same rotor (see section 2.4.4). Gradients were fractioned from bottom to top and 3% of fractions were counted by scintillation for [^{35}S]-radio-activity (figure 3.2A). Virion and EC peaks were harvested and a fraction boiled in SDS loading buffer prior to SDS-PAGE and autoradiography (figure 3.6B). Virion and EC fractions were also dialysed into dialysis buffer (section 2.1.7) and visualised by negative staining transmission electron microscopy and (figure 3.6C).
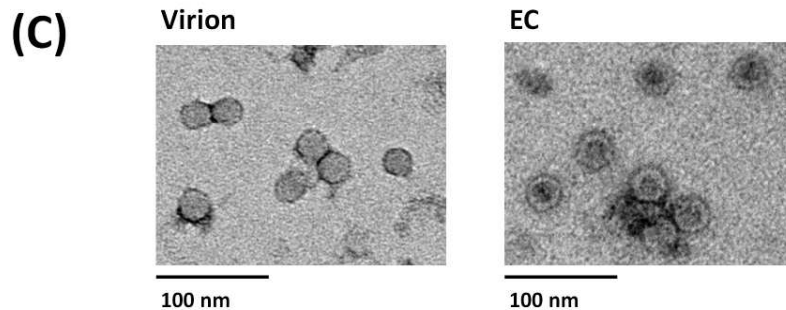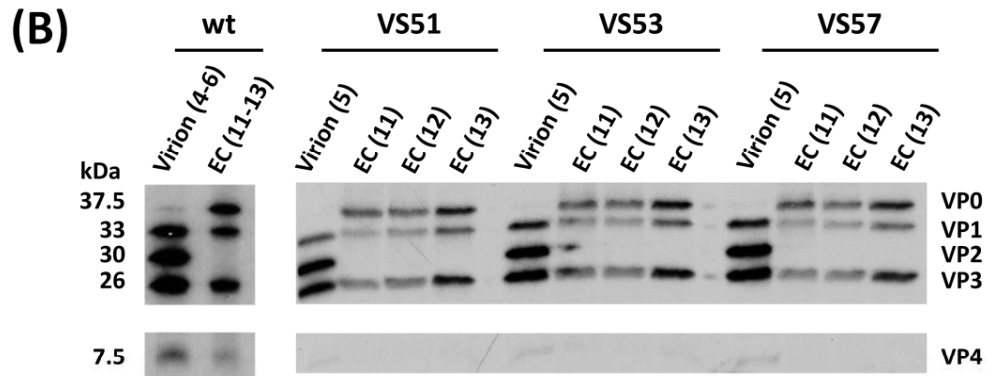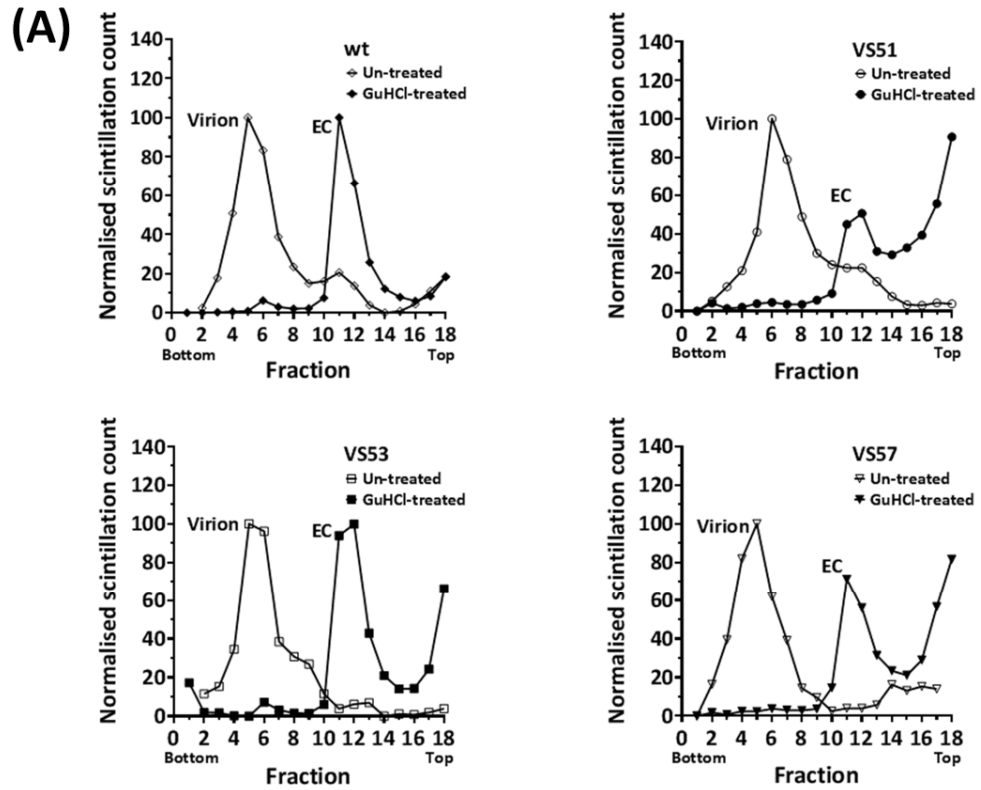
Figure 3.6. Generation and purification of full virion and genome-free ECs.
Viral RNA of with wt, VS51, VS53 and VS57, respectively were transfected into L-cells and radio-labelled with [^{35}S]-Cys/Met at 2.75 h.p.t. and incubated at 37°C under 5% CO$_2$. For EC preparation, 2mM GuHCl was added at 3.15 h.p.t.

Samples were harvested, respectively and particles purified by ultracentrifugation through 15-45% sucrose gradient. (A) Scintillation counts of fractions of 15-45% sucrose density gradients of wt, VS51, VS53 and VS57. Gradients were fractioned into 300 µl fractions and 3% of each fraction was counted by scintillation. (B) Autoradiograph of proteins from virion and EC sucrose density gradient peak fractions of wt, VS51, VS53 and VS57. Samples from virion and EC peaks were boiled in SDS loading buffer. Proteins were separated by SDS polyacrylamide gel electrophoresis, and ^{35}S-(Cys/ Met) radio-labelled virus bands were detected by autoradiography. (C) Electron micrographs of virion and EC peaks of wt. Virion and EC peaks were harvested and dialysed into 10 mM HEPES, 100 mM NaCl, 1 mM EDTA, 1 mM DTT, pH 6.4, and visualised by negative staining transmission electron microscopy. Size bar = 100 nm

GuHCl had an inhibitory effect on virus replication evidenced by a 1,000-fold loss in virus titres. The untreated sample in figure 3.1B shows two peaks in the positions expected for virion and naturally generated EC in the untreated sample with the latter much smaller. A larger peak corresponding to EC was detected in the guanidine-treated sample. Electron micrographs (figure 3.6C) shows dense full virions particles that do not take up the stain in the virion, and less dense EC particles that take up the stain. The autoradiograph images of virion peaks show cleaved products of VP0 (i.e. VP2, and VP4), while EC lane shows non-cleaved VP0.

3.5.1. Thermal stability of virions and ECs of heat-selected PV-1.

When heated at temperatures above 50°C, wt PV has been shown (by means of structural and biological data) to undergo an antigenic switch from a native (N) to a non-native or heated (H) form due to loss of VP4 followed by RNA release (Breindl, 1971; Le Bouvier, 1955). Wildtype PV-1 was radio-labelled with [^{35}S]-cys/met and purified by a density gradient. Purified virus was then heat-treated and re-purified through a second sucrose density gradient (Figure 3.7).
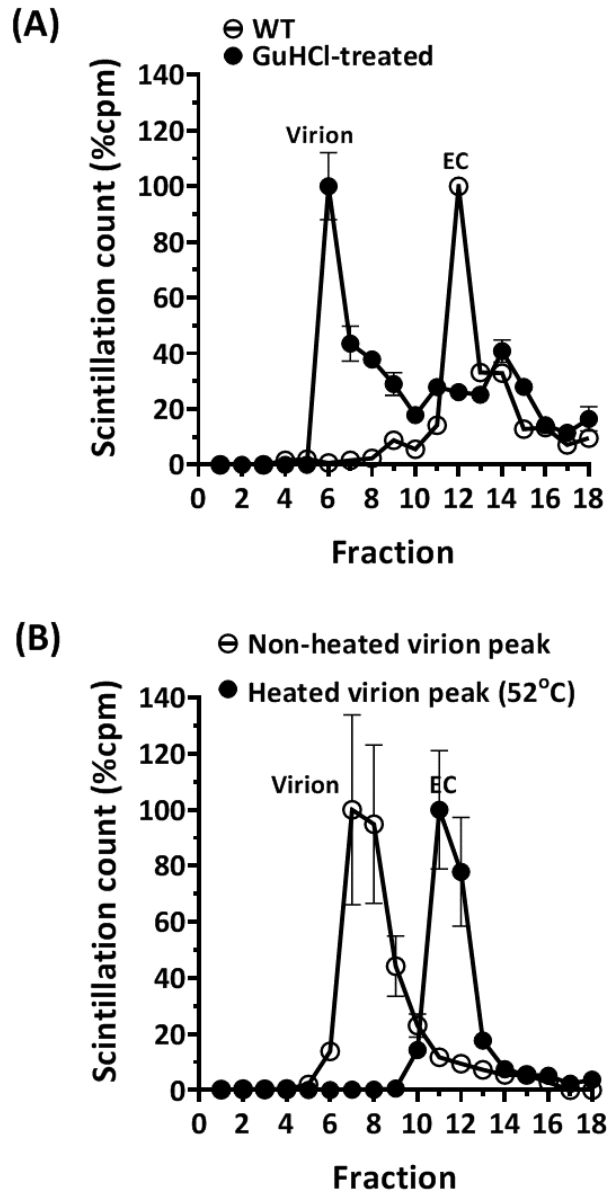
Figure 3.7 Effects of heat treatment on wt virion. *Wildtype PV-1 was propagated in the presence of [^{35}S]-Cys/Met radio-label with and without GuHCl-treatment. Cell lysates were clarified and supernatants pelleted through 30% sucrose cushions. Pellets were re-suspended in PBS and purified through pre-formed 20 – 60% Nycodenz gradients by ultracentrifugation at 30,000 rpm for 30 hours. (A) Gradient fractions were counted by scintillation and, showed peaks corresponding to virions and ECs. (B) The peaks in figure A were de-salted by gel filtration chromatography and the virus peak filtrate was heated at 52ºC for 30 minutes before a second purification through 15-45% sucrose gradient. The heat-treated virion peak yielded a peak corresponding to ECs (n=2± S.D.)*

Result suggests that GuHCl- and 52°C heat-treatment of virion particles for 30 minutes results in 80S EC particles. In an attempt to assess the binding pattern of the hydrophobic residues of EC under PaSTRy conditions, heat-treated virion peaks as well GuHCl-treated peaks purified through a second sucrose gradient were assayed for stability by PaSTRy assay (Figure 3.8).
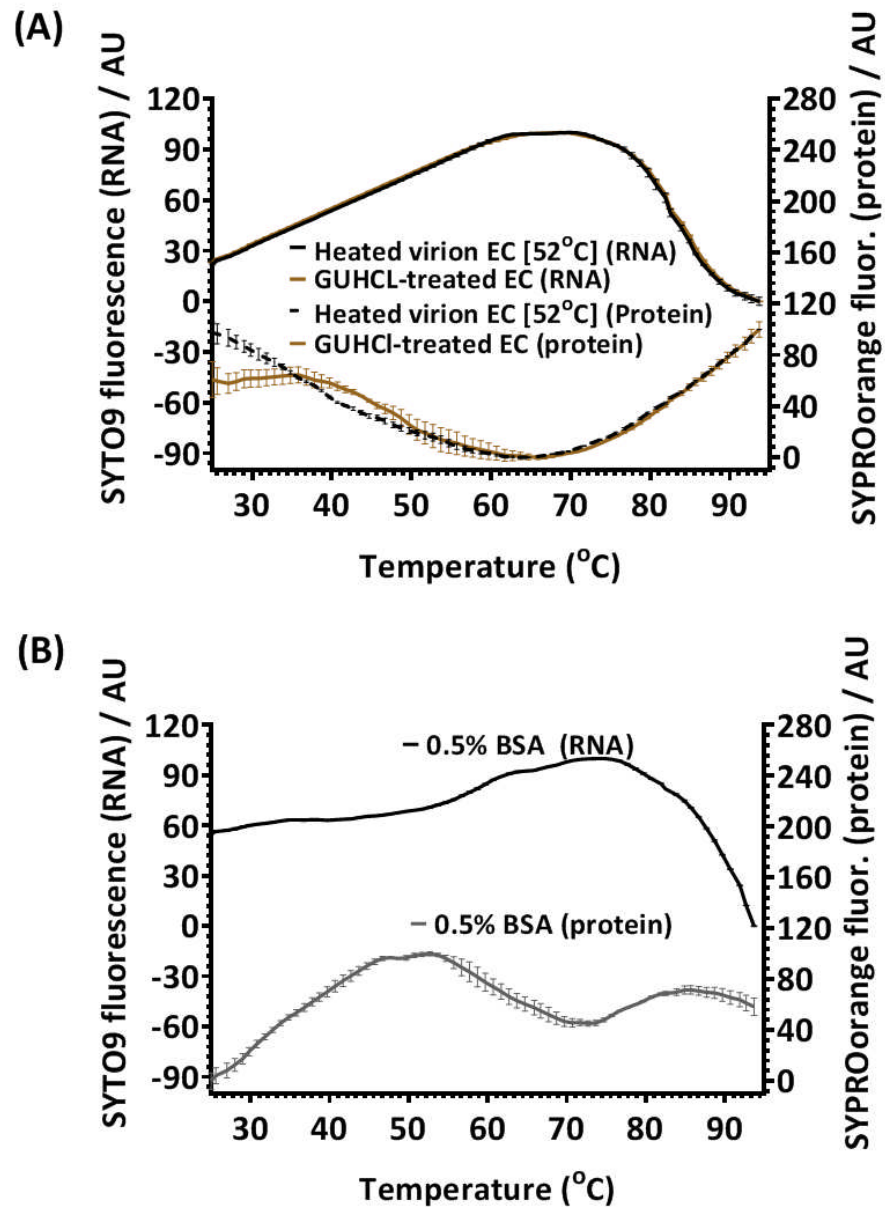
Figure 3.8. Analysis of heat- and GuHCl-treated virion by PaSTRy. *Wildtype PV-1 was propagated with and without GuHCl-treatment and respectively purified through pre-formed 20 – 60% Nycodenz gradients by ultracentrifugation at 30,000 rpm for 30 hours. Gradient peak fractions that correspond to virion was heat-treated and purified through 15-45% sucrose gradient. GuHCl-treated EC peak gradient was also purified through 15-45% sucrose gradient. (A) Gradient fractions that correspond to EC from heat- and GuHCl-treated samples were dialysed and assayed by PaSTRy using the SYTO9 and SYPROorange dyes. (B) 0.5% bovine serum albumin (BSA) was also analysed by PaSTRy. (n=2± S.D.)*

RNA PaSTRy profile however suggests that constant binding of Syto9 to (residual) nucleic acid component within the EC may have occurred as compared to 0.5% BSA profiles. Binding of hydrophobic residues however suggest that in the absence of RNA, capsid T_m could be highly altered.

3.5.2.   Antigenic stability of virions and ECs of heat-selected PV-1.

Although virion particles undergo antigenic changes at elevated temperatures (figure 3.7), ECs undergo conformational changes that result in an antigenic switch at temperatures below 10ºC (Basavappa *et al.*, 1994a). Hypothetically, thermally selected viruses should have stabilised ECs at physiological temperature. In order to investigate this hypothesis, [^{35}S]-Cys/Met radio-labelled virions or ECs of wt PV-1, VS51, VS53 and VS57 were generated and purified by sucrose density gradients. Purified virions were treated at a range of temperatures. Particles were immunoprecipitated with either of two monoclonal antibodies that recognise native PV-1 particles (mAb243) and non-native PV-1 particles (mAb1588) (Minor, 1986; Osterhaus *et al.*, 1983; Rombaut *et al.*, 1990). The temperature at which 50% of the native antigenic particles were converted to the non-native form was quantified by scintillation counting of immunoprecipitated [^{35}S]-Cys/Met radio-labelled particles (Figure 3.9).

(A) Virion antigenicity

(B) EC antigenicity

(C)
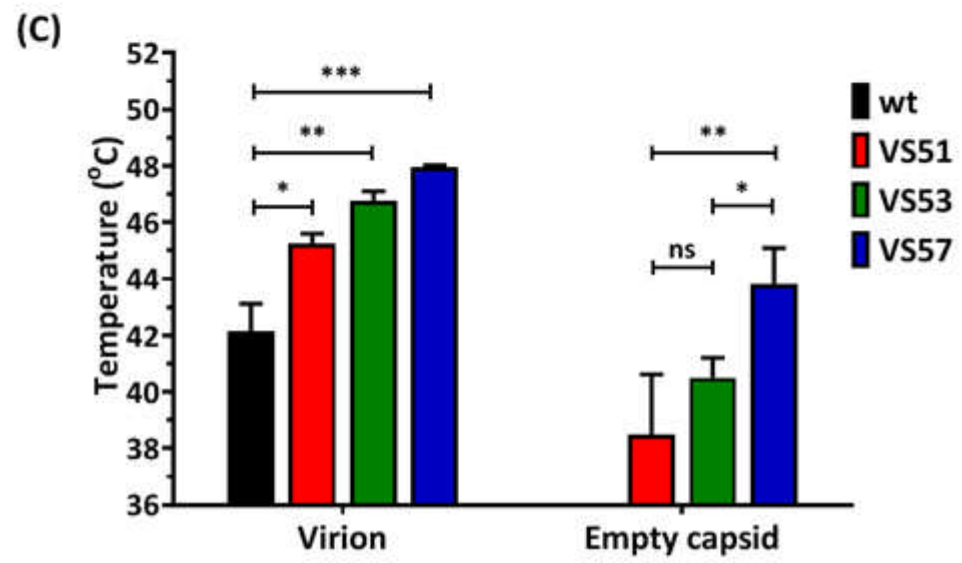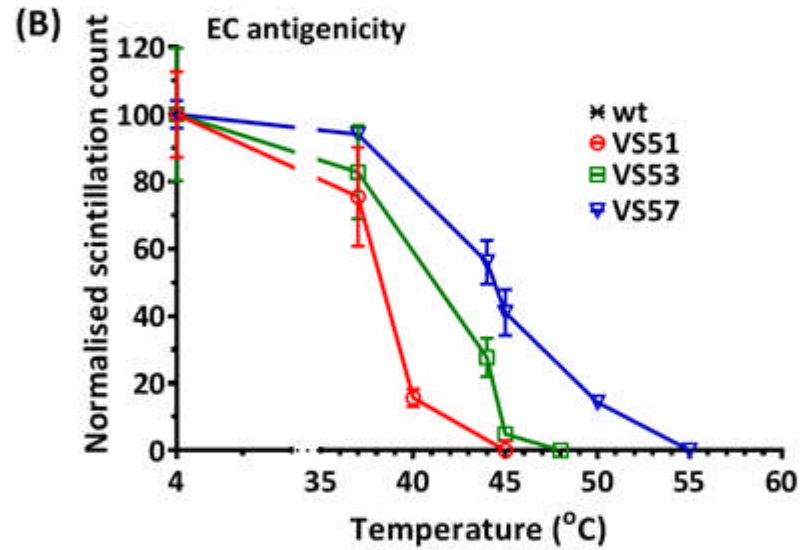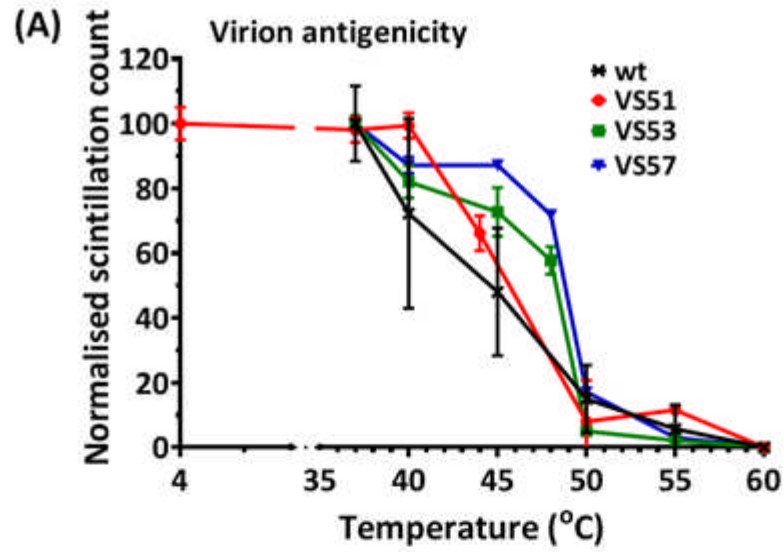
Figure 3.9. Antigenic stability profile of heat-selected PV-1 pools. Heat-selected virus samples were radio-labelled with [^{35}S]-Cys/Met and purified through 15-45% sucrose gradients by ultracentrifugation at 303,200 xg for 1 hour. Virion and EC peaks were identified by scintillation counting. Virion and EC fractions were harvested and incubated at a range of temperatures for 30 minutes and then cooled to 4°C. Heat-treated N-specific particles were immunoprecipitated using mAb 234 antibodies. Figures show (A) Normalised scintillation counts of heat-treated virion (n=3 ± S.D., P <0.05) (B) Normalised scintillation counts of heat-treated EC particles (n=3 ± S.D.). It was not possible to compare values to wt as these convert completely to the H/C form at 10^{0}C. (C) The temperatures at which 50% of the N/D antigenicity was converted to the H/C form were estimated and compared to wt (*P<0.05, **P<0.001, ***P<0.0001) of virion particles of selected viruses (VS51, VS53 and VS57) compared to wt.

Wild-type virions lost 50% N-antigenicity at 42°C and showed complete switch from N-H antigenicity at 50°C as previously published (Breindl, 1971; Lebouvier, 1955; Shiomi *et al.*, 2004). In comparison, VS51, VS53 and VS57 lost 50% N-H antigenicity at 45 ^{o}C, 47 ^{o}C and 48 ^{o}C, respectively (Figure 3.5). Wild-type PV-1 ECs did not retain native antigenicity above 10°C as expected. Thermally selected viruses had ECs with enhanced stability, with antigenic switches occurring at 37 ^{o}C (VS51), 41 ^{o}C (VS53), and 44 ^{o}C (VS57) (Figure 3.9). Together, these data demonstrate that both full virions and ECs of the thermally-selected viruses had increased native antigenic stability at elevated temperatures.

3.6. Further selection of heat-resistant viruses

Owing to the high error rates of their RdRp, RNA viruses are known to have high mutation rates and exist as a population made up of a quasispecies of genetically-linked viruses which are distributed around a consensus sequence (Andino & Domingo, 2015b; Vignuzzi *et al.*, 2006). In order to select for more thermally-stable viruses, VS57 was incubated at 58°C for 30 minutes and cooled to 4°C immediately. HeLa cells at 80% confluence were infected with heat-treated virus at an MOI of 1 and incubated at 37°C for 48 hours. Neutral red stain was used to visualise plaques. A total of 12 individual plaques were selected and re-suspended in serum-free DMEM. Selected plaques were propagated in individual wells of a 12-well vessel of HeLa cells until total cell death was observed. Propagated virus plaque samples were assayed for temperature-resistance post-incubation at 58°C, 60°C and 62°C (figure 3.10).
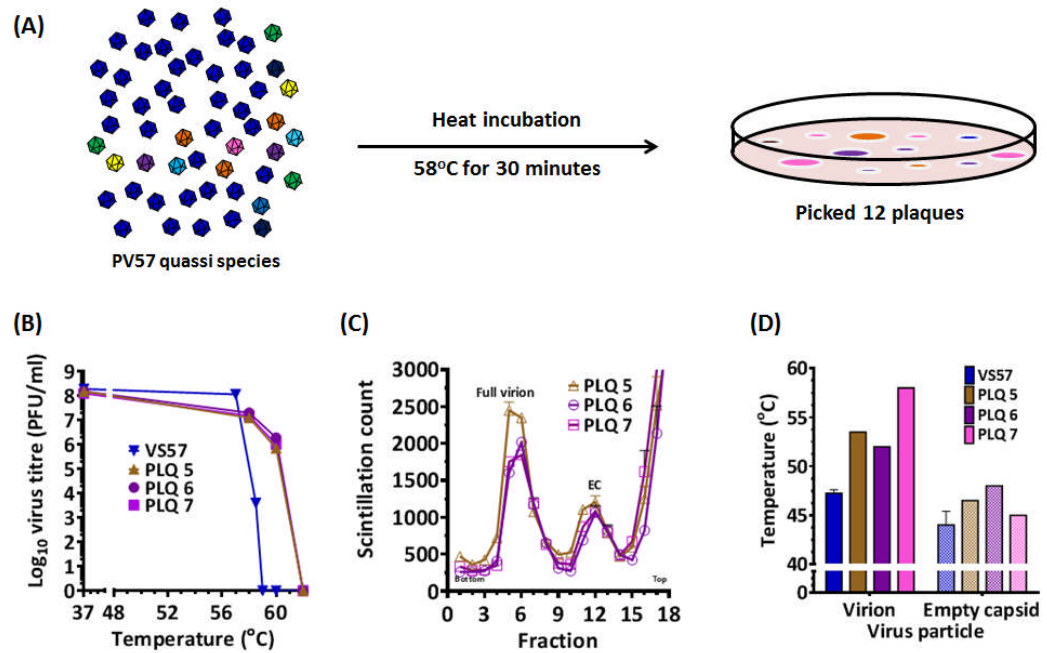
Figure 3.10. Selecting more thermally-stable viruses. (A) VS57 was incubated at 57°C and a plaque assay was undertaken using HeLa cells. Twelve individual plaques of VS57 were randomly selected and propagated in HeLa cells. (B) Plaque virus samples were incubated at 58°C, 60°C and 62°C and assayed for infectious titres (C) Plaques were propagated in HeLa cells, , radio-labelled with [^{35}S]-Cys/Met and purified through a gradient. (D) Gradient peak fractions were assayed for antigenicity by IP along other mutant virus samples. N=2 ± S.D.

Results show that three plaque (PLQ 5, PLQ 6 and PLQ 7) could withstand incubation at 60°C for 30 minutes but lost infectious titres about 62°C. This shows that thermally-selected virus VS57 still comprises a quasi species of virus, some of which may be more thermally stable than VS57. However, PLQ5, PLQ6 and PLQ 7 readily reverted back to wt VS57 after 3 selection cycles and could not be taken any further.

3.7. Identification of mutations in the structural proteins of heat-selected PV-1.

In order to identify the capsid mutations that occurred in the thermally-selected virus pools (VS51, VS53 and VS57), genomic RNA was extracted. The P1 region was amplified by reverse transcription PCR purified and sequenced. Alongside sequenced PCR amplicons, individual vector clones of PCR amplicons were randomly selected and also sequenced. Nucleotide sequences of thermally selected viruses VS51, VS53 and VS57 were aligned against wt PV-1 (Mahoney). This revealed various non-synonymous capsid mutations VP1, VP3 and VP4 (Table 3.1).

Table 3.1. Non-synonymous capsid mutations.

Selected virus	Capsid mutation
VS51	V1087A, I1194V
VS53	A1026T, V1087A, I1194V & F4046L
VS57	V1087A, S1097P, I1194V, C3175A, R4034S & D4045V

Nomenclature of residues follows the picornavirus crystalline numbering for the structural region. The first and last alphabets represent the original amino acid and substituted amino acids, respectively (e.g. V1001A represent a substitution of valine to alanine). The first number represents the viral protein within the P1region, while t he remaining three digits represent the residue position (e.g. 1001, 2001, 3001 and 4001reporesent the first residues of VP1, VP2, VP3 and VP4)

The positions of capsid mutations of VS51, VS53 and VS57 were modelled into the structural models of PV-1 (Mahoney) (PDB ID: 1ASJ) (Wien *et al.*, 1997) using PyMOL (Table 3.2 and Figure 3.11). In addition, PV serotypes were aligned (Toyoda *et al.*, 1984a) and compared to identified mutations.

Table 3.2 Positions of mutations within virus capsid.

Mutation	Residue position	PV-2 (Sabin)	Pv-3 (Leon)
A1026T	VP1: Internal surface of the virus capsid; close to the N-terminus of VP1.	S	S
V1087A	VP1: B strand of the VP1 β-barrel; outer surface of the virus pocket.	*	*
S1097P	VP1: Capsid surface at the 5-fold interpentameric vertex. Reissued resides on B-C loop of the VP1 β-barrel.	P	P
I1194V	VP1: Within the virus pocket; G strand of the VP1 β-barrel.	*	*
C3175A	VP3: Surface G-H loop of the VP3 β-barrel. A capsid surface residue, located on the Surface G-H loop of the VP3 β-barrel. It is situated between monomers within a pentamer.	*	*
R4034S	VP4: Internally located in virus capsid.	*	K
D4045V	VP4: Internally located in virus capsid	*	*
F4046L	VP4: Internally located in virus capsid	*	Y

* = residue homology between wt PV-1 and respective serotype (i.e. PV-2 and/ or PV-3). The nomenclature of residues follows the picornavirus crystalline numbering for the structural region. The first and last alphabets represent the original amino acid and substituted amino acids, respectively (e.g. V1001A represent a substitution of valine to alanine). The first number represents the viral protein within the P1region, while t he remaining three digits represent the residue position (e.g. 1001, 2001, 3001 and 4001reporesent the first residues of VP1, VP2, VP3 and VP4)

The mutation that occurred on the 97th VP1 residue was a substitution that is found in wt PV-2 and PV-3 (i.e. S1097P), which are more stable than wt PV-1. S1097 lies on the 5-fold inter-pentameric vertex of the external surface of the viral capsid. As a result of the selection at 57°C, this residue was mutated to a proline as occurs in PV-2 and PV-3. It has been shown that VP1 pocket residues V87 and I194 are highly conserved among the three PV serotypes (Toyoda *et al.*, 1984a). Mutations occurring on these residues (V1087A and I1194V) were consistent in all 3 thermally-selected virus pools. One mutation (S1097P) was identified on an external residue that lies on the 5-fold inter-pentameric vertex. All other mutations were shown to occur on inter-subunit residues within the viral capsid.
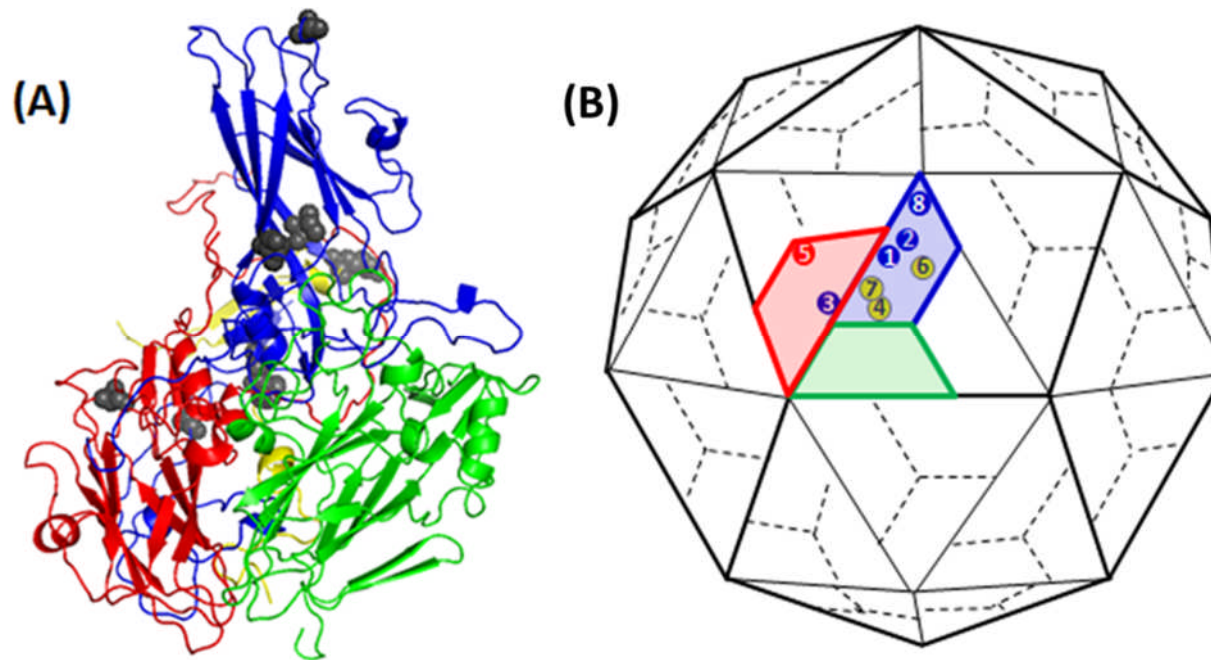
Figure 3.11. PV genome, showing position of common mutations. *(A) Ribbon model of a PV-1 protomer, showing assembled capsid proteins with already cleaved VP0. Positions of selected mutations are represented as black spheres on capsid proteins VP4 (yellow), VP3 (red) and VP1 (blue). (B) Cartoon modelling of PV-1 virion, showing positions of thermal selected mutations. Most mutations occurred on residues lying on the internal surface of the capsid. Figures are not drawn to scale.*

3.8. Discussion

In the course of PV morphogenesis, the switch from native antigenic 160S particles to the 135S intermediates or 80S EC particles has been reported to be as a result of conformational changes associated with capsid surface features actively associated with the BC-loop of the VP1 β-barrel (Basavappa *et al.*, 1998b; Lin *et al.*, 2013a; Wiegers & Dernick, 1985). The instability of ECs has significantly limited the possibility of a PV VLP vaccine, which may be an alternative to current OPV and/ or IPV options for a polio-free world (CDC, 2001; Sutter *et al.*, 2004).

In an attempt to increase the thermal stability of PV-1 ECs, cycles of thermal selection of virions at increasing temperatures of 51°C, 53°C and 57°C were attempted followed by picking individual plaques from a selected pools of virus. Three thermally stable candidates (VS51, VS53 and VS57) were able to withstand elevated temperatures without losing infectivity or genetic stability. Increased capsid stability were confirmed by biological infectivity assays, biochemical assays as well as immunoassays. All three assays suggest substantial increase in PV-1 capsid stability. As a result of this increased stability, ECs generated from thermally-selected virions were antigenically stable and could withstand elevated temperatures up to 45°C.

A total of 8 mutations were identified by sequencing of the (P1) region of selected pools of viruses (VS51, VS53 and VS57). Two VP1 mutations (V1087A and I1194V) were present in all three selected virus candidates. A previous study had reported the occurrence of V1087A mutation after PV-1 was selected at 50°C, but there was no analysis of the effect of this mutation on the EC (Shiomi *et al.*, 2004). A study has shown that selection of drug-resistant PV mutants

against a pocket-binder [V-073] that inhibits uncoating in all PV serotypes (Oberste *et al.*, 2009) resulted in isolates with mutations in the VP1 residue 194 (or 192 in corresponding PV-3) from its wt residue into methionine or phenylalanine among all serotypes with reduced thermal stability (Liu *et al.*, 2012a). It is however interesting to note that thermally-stable virus pools evolved with a combination of I1194V and V1087A were shown here to have antigenically stable ECs.

VP1 residues 87 and 194 both lie within the capsid pocket on the B- and G-strands of the VP1 β-barrel, respectively. Based on their proximity, to antigenic binding sites on the BC-loop (Lin *et al.*, 2013b), residue interactions on the B- and G-strands could have a regulatory effect on the antigenic conformation of the capsid (Minor, 1986; Vanderwerf *et al.*, 1983). Since these changes were from larger side-chains to smaller side-chain residues, this may have an effect on the size of the capsid pocket and its ability to retain the pocket factor at higher temperatures than wt since it has been shown that substitutions with larger residues in the pockets of enterovirus 71 and Coxsackievirus A16 make the viruses more thermolabile (Kelly *et al.*, 2015). This is consistent with data reported for other enteroviruses including PV-3 (Katpally & Smith, 2007; Mosser *et al.*, 1994; Shepard *et al.*, 1993).

Increasing the thermal selection pressure resulted in detection of an internal VP4 mutation (F4046L) and an additional VP1 mutation (T1026A). Further increase appeared to lead to reversion of these two additional mutations and detection of additional VP4 mutations on residues 46 and 34 (i.e. D4045V and R4034S). This highlights an important capsid-stabilising role of the internally embedded VP4 which hitherto, exists as the N-terminus of the uncleaved VP0 prior to cleavage.

Thus, the uncleaved VP0 could contribute to the stability of the PV EC by mutations on three residues in two combinations (i.e. F4046L and a combination of D4045V and R4034S). It would however be necessary to characterise the effects of these selected mutations individually, and in various combinations.

Chapter 4

Capturing an evolving virus by thermal selection

4.1.Enteroviruses and PV

Owing to the high rates of mutation among RNA viruses (Andino & Domingo, 2015a; Lauring *et al.*, 2013a; Sanjuán *et al.*, 2010), dynamics may have contributed to a larger family of picornaviruses (Knowles, 2012a). The *Enterovirus* genus is made up of highly ubiquitous members of similar nucleotide fingerprints. As a picornavirus, PV shares genomic and symptomatic similarities with some close relatives such as Enterovirus C105 (Horner *et al.*, 2015), Coxsackievirus B (Yui & Gledhill, 1991), Coxsackievirus A, EV71 and Echoviruses (Muehlenbachs *et al.*, 2015). Through recombination events among various enteroviruses, attenuated viruses (such as PV serotypes) have been able to regain virulence and cause disease (Kew *et al.*, 2005; Rakoto-Andrianarivelo *et al.*, 2007).

4.1.1. Evolution of PV serotypes

There are three PV serotypes, known to possess about 71% nucleotide homology (Toyoda *et al.*, 1984b). While the origin of the PV serotypes remains a mystery, molecular analysis could help understand some relationships that exist among the serotypes. An alignment of serotype sequences deposits from the National Centre for Biotechnology Information (NCBI) was carried out on PV-1 [V01149.1], PV-2 [AY177685.1] and PV-3 [AY184221.1], to highlight areas of genomic variations using the CLC viewer tool based on CLUSTAL OMEGA (figure 4.1).

111
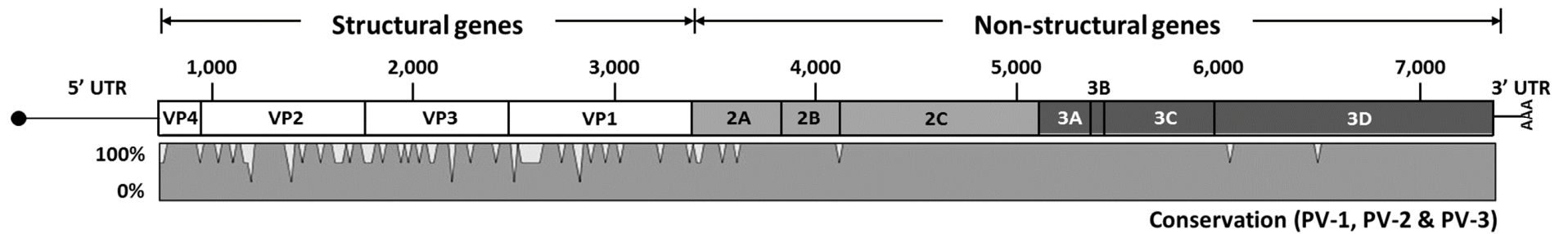
Figure 4.1. Gene conservation among PV serotypes. *Genome sequences of PV-1 [V01149.1], PV-2 [AY177685.1] and PV-3 [AY184221.1] were aligned using the CLC viewer. Figure shows a cartoon structure of the PV genome, superimposed on a graph plot of the aligned genome sequences. Graph shows highly conserved non-structural [P2 and P3] regions (Knowles et al., 2012; Adams et al., 2013, 2014, 2015; ICTV)*

PV has been shown to have a high mutation rate (Acevedo *et al.*, 2014; Sanjuan *et al.*, 2010), which varies at different regions of the genome. Figure 4.1 suggests that genomic variations among the PV serotypes lie mainly around the structural region, which has been reported as distinct for antigenic responses and the basis of serotype distinction (Hogle, 2002b; Minor *et al.*, 1986; Rossmann *et al.*, 2002a). Within the structural region, the internally embedded VP4 (the smaller product of cleaved VP0) was also shown to be highly conserved. VP4 is known to form an internal network with the N-terminus of the other structural proteins on the inner surface of the capsid, and plays a significant role in virion stability (Basavappa *et al.*, 1994b; Hogle, 2002a; b).

In order to elucidate the evolution of each of the serotypes, analysis of available genome sequences was carried out using the structural region of 100 randomly selected genome sequences each of PV-1, PV-2 and PV-3, respectively (Table 4.1). A color-coded pairwise identity matrix was generated as a PV-serotype homology chart, using the Sequence Demarcation Tool (SDT) (figure 4.2) (Muhire *et al.*, 2014). The SDT utilises a genome-based Pairwise Sequence Comparison (PASC) web tool, which applies local and global alignment algorithms (Bao *et al.*, 2012; 2014) as recommended by the International Committee on Taxonomy of Viruses (ICTV). SDT analysis was carried out using multiple sequence alignment [MAFFT] program (Katoh *et al.*, 2002; Pais *et al.*, 2014) (figure 4.2A and 4.2B).

Table 4.1. Ascension numbers of PV serotypes.

PV-1	AF065158.1, KJ170532.1, KJ170531.1, KJ170530.1, KJ170529.1, KJ170528.1, KJ170527.1, KJ170526.1, KJ170525.1, KJ170524.1, KJ170523.1, KJ170522.1, KJ170521.1, KJ170520.1, KJ170519.1, KJ170518.1, KJ170517.1, KJ170516.1, KJ170515.1, KJ170514.1, KJ170513.1, KJ170512.1, KJ170511.1, KJ170510.1, KJ170509.1, KJ170508.1, KJ170507.1, KJ170506.1, KJ170505.1, KJ170504.1, KJ170502.1, KJ170501.1, KJ170500.1, KJ170499.1, KJ170498.1, KJ170497.1, KJ170496.1, KJ170495.1, KJ170494.1, KJ170493.1, KJ170492.1, KJ170491.1, KJ170490.1, KJ170489.1, KJ170488.1, KJ170487.1, KJ170486.1, KJ170485.1, KJ170484.1, KJ170483.1, KJ170482.1, KJ170481.1, KJ170480.1, KJ170479.1, KJ170478.1, KJ170477.1, KJ170476.1, KJ170475.1, KJ170459.1, KJ170458.1, KJ170457.1, KJ170456.1, KJ170455.1, KJ170454.1, KJ170453.1, KJ170452.1, KJ170451.1, KJ170450.1, KJ170448.1, KJ170447.1, KJ170446.1, KJ170445.1, KJ170441.1, KJ170440.1, KJ170439.1, KJ170438.1, KJ170437.1, KJ170436.1, KU866422.1, KT353719.1, KR259355.1, HM537002.1, AF462419.1, EU794962.1, EU794961.1, EU794960.1, EU794959.1, EU794958.1, EU794957.1, EU794956.1, EU794955.1, EU794954.1, EU794953.1, GQ984141.1, AY184219.1, AJ416942.1, AJ430385.1, V01148.1, V01149.1, V01150.1
PV-2	KJ170575.1, KJ170574.1, KJ170573.1, KJ170572.1, KJ170571.1, KJ170568.1, KJ170567.1, KJ170566.1, KJ170565.1, KJ170564.1, KJ170563.1, KJ170562.1, KJ170561.1, KJ170560.1, KJ170559.1, KJ170558.1, KJ170557.1, KJ170556.1, KJ170554.1, KJ170553.1, KJ170552.1, KJ170551.1, KJ170549.1, KJ170548.1, KJ170547.1, KJ170546.1, KJ170545.1, KJ170537.1, KJ170535.1, KJ170534.1, KJ170533.1, KU598890.1, KU598887.1, KU598886.1, KU372652.1, KM433732.1, KR817066.1, KR817065.1, KR817064.1, KR817063.1, KR817062.1, KR817061.1, KJ419277.1, KJ419276.1, KJ419275.1, KJ419274.1, KJ419273.1, KF322152.1, KF656732.1, HF913428.1, JX275380.1, JX275292.1, JX275273.1, JX275266.1, JX275257.1, JX275238.1, JX275206.1, JX275191.1, JX275168.1, JX275166.1, JX275164.1, JX275141.1, JX275071.1, JX275053.1, JX275032.1, JX275015.1, JX275008.1, JX274995.1, JX274991.1, JX274989.1, JX274988.1, JX274982.1, JX274981.1, JX274980.1, HQ738303.1, HQ738290.1, HQ738288.1, HQ738287.1, AY278552.1, AY278549.1, AY184220.1, HM107834.1 ,HM107832.1, FJ460224.1, FJ460223.1, FJ517649.1, FJ517648.1, EU566949.1, EU566948.1, EU566945.1, EU566940.1, EU566938.1, EU566936.1, DQ890386.1, DQ890385.1, FJ898290.1, DQ205099.1, AY238473.1, D00625.1, M12197.1
PV-3	KJ170619.1, KJ170613.1, KJ170598.1, KJ170597.1, KJ170591.1, KJ170588.1, HQ738302.1, KJ170668.1, KJ170663.1, KJ170658.1, KJ170654.1, KJ170652.1, KJ170651.1, KJ170642.1, KJ170641.1, KJ170640.1, KJ170638.1, KJ170637.1, KJ170636.1, KJ170635.1, KJ170632.1, KJ170631.1, KJ170630.1, KJ170629.1, KJ170628.1, KJ170627.1, KJ170626.1, KJ170623.1, KJ170622.1, KJ170621.1, KJ170620.1, KJ170618.1, KJ170615.1, KJ170612.1, KJ170604.1, KJ170595.1, KJ170594.1, KJ170579.1, KJ170577.1, AY184221.1, KJ170661.1, KJ170657.1, KJ170656.1, KJ170655.1, KJ170653.1, KJ170643.1, KJ170634.1, KJ170625.1, KJ170624.1, KJ170614.1, KJ170603.1, KJ170587.1, KJ170578.1, HQ738299.1, KJ170669.1, KJ170667.1, KJ170664.1, KJ170662.1, KJ170660.1, KJ170659.1, KJ170639.1, KJ170576.1, HQ738300.1, KJ170670.1, KJ170672.1, KJ170671.1, KJ170666.1, KJ170633.1, KJ170665.1, KJ170674.1, KJ170675.1, KJ170673.1, KJ170676.1, GU180608.1, KJ170677.1, FJ460227.1, HM537008.1, HM537007.1, FJ460226.1, HM537010.1, AB205395.1, AF334949.1, HM537011.1, HM537009.1, AF334953.1, AF334952.1, AF334951.1, AF334950.1, KR259358.1, FJ859183.1, FJ859184.1, HQ738298.1, HQ738291.1, GU256222.1, HQ738301.1, HQ738296.1, EU684057.1, X00925.1, X00596.1, K01392.1

114
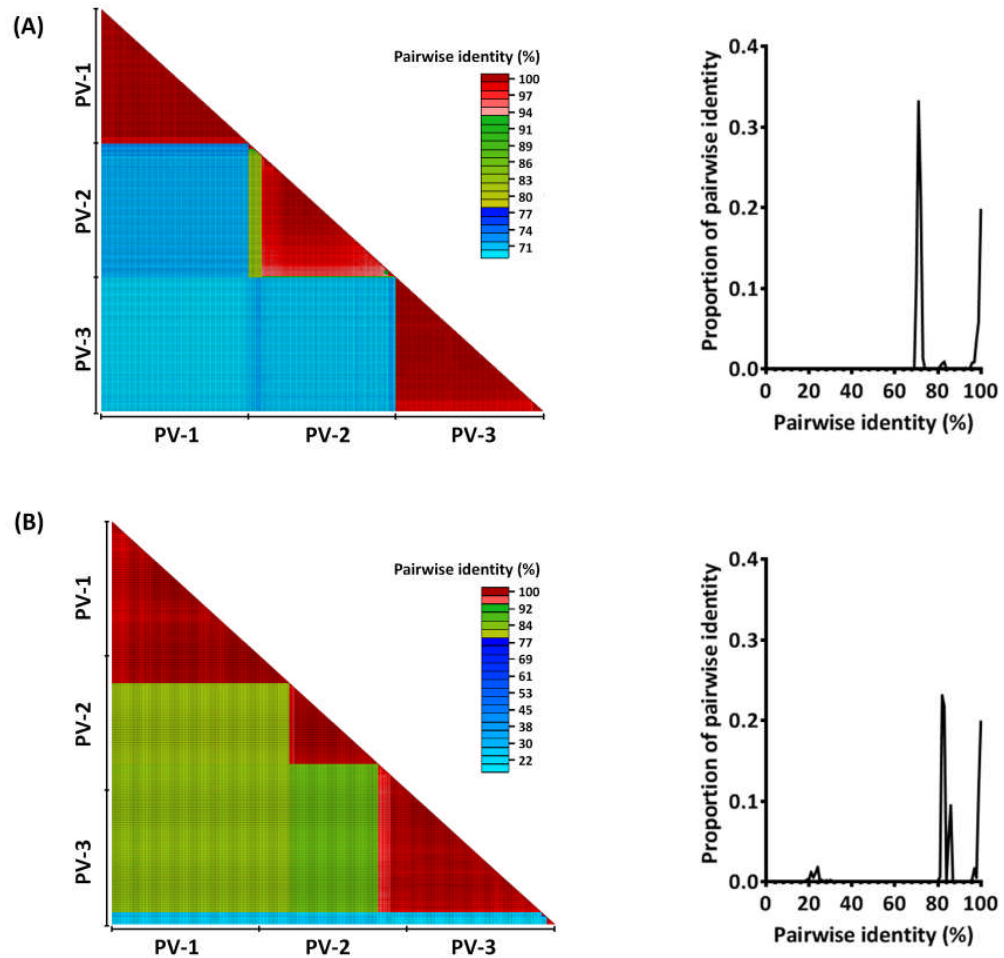
Figure 4.2 Relationship among PV serotypes (A) Colour-coded pairwise identity matrix of PV serotypes. Serotype nucleotide sequence of the structural (P1) region of 100 isolates of PV-1, PV-2 and PV-3, respectively, were aligned by PASC, using the SDT software. Each box represents a pair of sequences aligned using MAFFT algorithms and expressed as colour-coded percentages as shown in the key. Graph shows about 71% nucleotide homology within the structural region. Homology plot of the proportion of isolates sharing identical sequences are also shown on the right panel. Serotypes share about 71% homology. (B.) Colour-coded pairwise identity matrix of PV serotypes. Translated nucleotide sequences the structural (P1) region of 100 isolates of PV-1, PV-2 and PV-3. Sequence alignment was carried out using PASC. Each box represents a pair of sequences aligned using MAFFT algorithms and expressed as colour-coded percentages as shown in the key. Homology plot of the proportion of isolates sharing identical sequences are also shown on the right panel. Serotypes share about 82% homology (N=300)

Pairwise analysis of the entire genome showed that PV-2 and PV-3 share the greatest homology (80-90%), followed by PV-1 and PV-3 (77-80%) (figure not shown), however a pairwise analysis of the structural genes, which are the basis for serotype distinction, suggest a homology of about 71% at the nucleotide level and 82% at the protein level. Based on inter-serotypic homology, a phylogenetic tree was also constructed to depict the likely trends of evolution among the PV serotypes (figure 4.3C). Phylogenetic analysis further suggest that the PV serotypes evolved from a common ancestor (figure 4.3) through evolutionary events that were spaced out between serotypes, with the farthest evolutionary distance between PV-1 and PV-2.
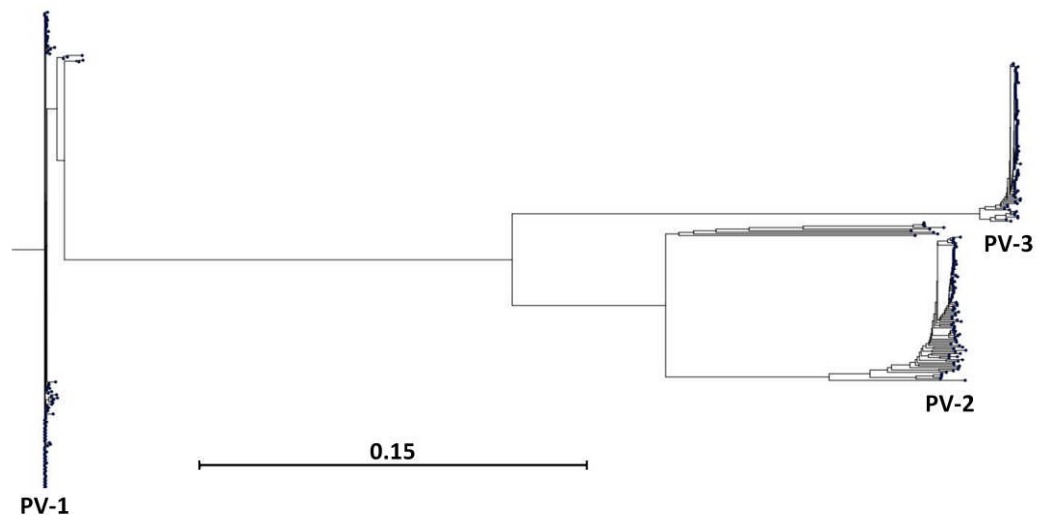
Figure 4.3 Evolution of PV serotypes. *A rooted phylogenetic tree of PV serotypes, showing an evolutionary relationship among 100 isolates of each PV serotypes. Horizontal lines represent evolutionary lineages over time with a scale bar of 0.15 representing the mutation rate (N=300)*

Data further shows that a common ancestor to all three PV serotypes may have evolved distinct serotypes over time through diverse evolutional processes (Holmes, 2011; Koonin *et al.*, 2015) such as antibody responses and bottle neck adaptations. This be seen as an adaptive strategy to prevent extinction. One of

such evolutionary strategies has been linked to the low fidelity of the PV RNA-dependent-RNA polymerase (RdRp) (Campagnola *et al.*, 2015) and recombination among serotypes as well as with other enteroviruses (Andino & Domingo, 2015a; Gregori *et al.*, 2016; Zhang *et al.*, 2010). However, such events are usually restricted to the non-structural regions of the genome and have not been shown as directly impacting serotype specificity. Studies have reported the occurrence of PV serotypes that possess inter-serotypic chimeric structural proteins which have been linked to recombination events among/ between serotypes (Blomqvist *et al.*, 2003; Combelas *et al.*, 2011; Kyriakopoulou *et al.*, 2006; Liu *et al.*, 2000; Martin *et al.*, 2002; Mueller *et al.*, 2009). A chimeric model of PV-1 and PV-3 was attempted *in vitro* by Minor *et al*, with the ability to be recognised by polyclonal PV-3 antibodies and PV-1 MAbs but with diminished fidelity (Minor *et al.*, 1990). Such PV chimeras reportedly isolated from a child (Martín *et al.*, 2002) and a China sewage (Tao *et al.*, 2010) are antigenically reactive to a single PV serotype, respectively. There remains no empirical data that describes the natural occurrence of a multi-serotype recombinant chimera that can be neutralised by more than one PV serotype antibody (figure).

4.1.2. Section aim

In the previous chapter, thermally-stable PV-1 populations were selected at increasing temperatures of 51°C (VS51), 53°C (VS53), and 57°C (VS57) through repeated cycles of heat treatment followed by passaging surviving population at 37°C. After ten, twelve and ten cycles of selection, respectively, genetically stable populations of thermally-stable viruses had evolved with two (V1087A and I1194V), four (A1026T, V1087A, I1194V and F4046L) and six (V1087A,

117

S1097P, I1194V, C3175A, R4034S and D4045V) mutations, respectively. While the evolution of the PV serotypes is not fully understood, in this chapter, the evolution of the thermally-stable mutants is examined by capturing intermediate viruses in a bid to understanding how these viruses evolved under selection pressure.

4.2. Selecting genetically stable PV pools

Owing to a high rate of mutation, an RNA virus population is made up of a quasi-species of genetically-linked viruses which are distributed around a consensus sequence (Lauring *et al.*, 2013b). Such populations are genetically robust and able to withstand external pressure such as population bottlenecks (Fares, 2015; Lauring *et al.*, 2013b). In order to assess the genetic stability of the population of thermally-selected viruses described in section 3, recovered pools of viruses were serially passaged five times in the absence of selection pressure. Serially-passaged viruses were then incubated at the temperature of selection and titrated by plaque assays (figure 4.4).
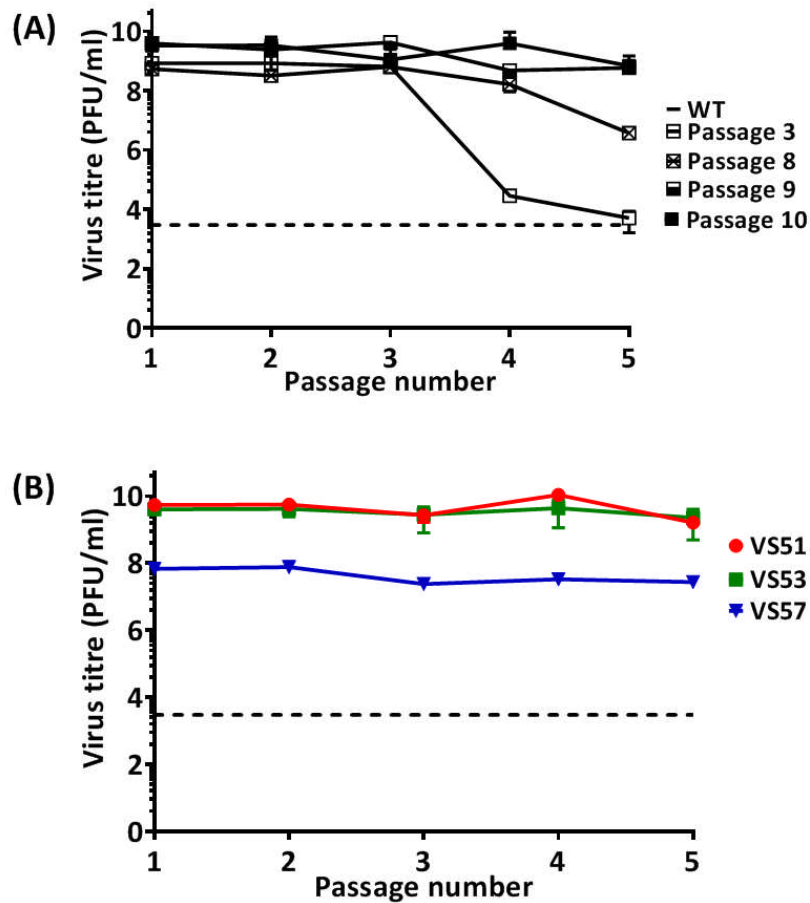
Figure 4.4. Genetic stability of intermediate passages. *VS51 is a pool of viruses selected over 10 cycles of thermal selection at 51ºC. VS53 and VS57 were selected over 12 and 10 cycles at 53ºC and 57ºC, respectively. (A) Intermediate passages of VS51 (i.e. passages 3, 8, 9 and 10) were serially passaged five times in the absence of selection pressure. Post-passage, each pool of was heat-treated at 51ºC and titrated by plaque assay. Broken lines represent the titres of wt PV-1 after heat treatment at 51ºC for 30 minutes. (B) Fitness cost of selected virus pools VS51, VS53 & VS57. After respective selection cycles, VS51, VS53 and VS57 were serially passaged five times in the absence of selection pressure. Post-passage, each pool of selected virus was heat-treated at the respective selection temperature (i.e. 51ºC, 53ºC, and 57ºC, respectively) and titrated for infectivity by plaque assay (n = 2 ± S.D.). As a control, WT PV-1 was heated to 51ºC and also titrated (broken lines). Selected virus pools did not lose infectivity titres after serial passage. This suggests that pool of viruses comprise a stable population of heat-resistant particles.*

Data shows that at early cycles of selection, virus pools rapidly lost thermal stability, however after about 10 selection cycles, virus pools had evolved genetically stable populations that could withstand the selection pressure. This phenotypic characteristic was observed in all three virus pools selected.

4.2.1. Population growth kinetics

While some viruses have successfully immortalised their existence by targeting host germlines (Bock & Stoye, 2000; Spence *et al.*, 1989), other viruses (especially RNA viruses) relentlessly adapt to their constantly changing environments within a host or across a plethora of hosts (Agudelo-Romero *et al.*, 2008; Elena *et al.*, 2009), such as the influenza viruses (dos Reis *et al.*, 2011; Taubenberger & Kash, 2010). These adaptations are largely driven by their high mutation rates, which has been linked to a balance between evolutionary constraints, fitness cost and rates of replication (Belshaw *et al.*, 2008). With the use of a one-step growth curves, the rate of viral replication was examined in order to assess the fitness cost of thermal selection on replication kinetics (Figure 4.5).
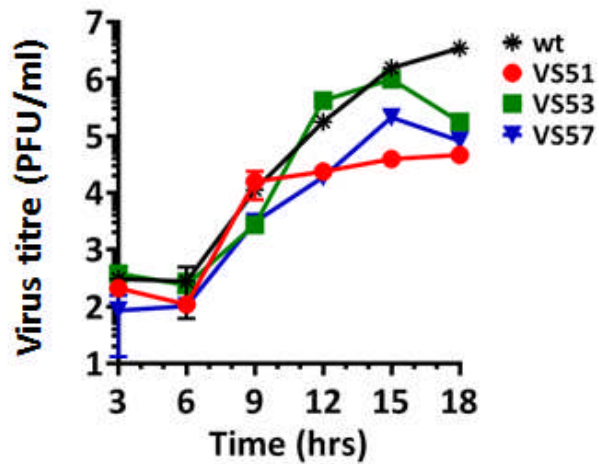
Figure 4.5. Growth kinetics of selected viruses. HeLa cells were propagated to confluence. After two washes with 1x PBS, cells were infected with wt PV-1, VS51, VS53 and VS57 at 0.1 MOI. To facilitate virus attachment to receptor (PVR), cells were incubated at room temperature with rocking for 20 minutes. Post-attachment, cells were washed twice with PBS and media replaced. Cells were incubated at 37°C under 5% CO_2. At 3-hour intervals, supernatant and cells were harvested and cells lysed by freeze-thawing in RIPA buffer. Supernatant and cell lysate were titrated by plaque assay (n = 2 ± SD).

Initial rates of replication were similar but overall yield of VS51 and VS 57 was reduced.

4.3. Thermal evolution of heat-resistant polioviruses

In order to elucidate the evolutionary trend of thermally-selected viruses, the viral RNA was extracted from each pool of recovered virus as follows. Ten selection cycles at 51°C resulted to pools termed VS51.1 to VS51.9 and VS51 from which RNA were extracted. Twelve selection cycles at 53°C were termed VS53.1 to VS53.11 and VS53 from which RNA were extracted. Ten selection cycles at 57°C, were termed VS57.1 to VS57.9 and VS57 from which RNA were extracted. The P1 (capsid) region of the extracted genome was reverse-transcribed, amplified by PCR and sequenced. Figures 4.6 and 4.7 however show the percentage pairwise identity and evolutionary trend of consensus mutations over the cycles of selection.
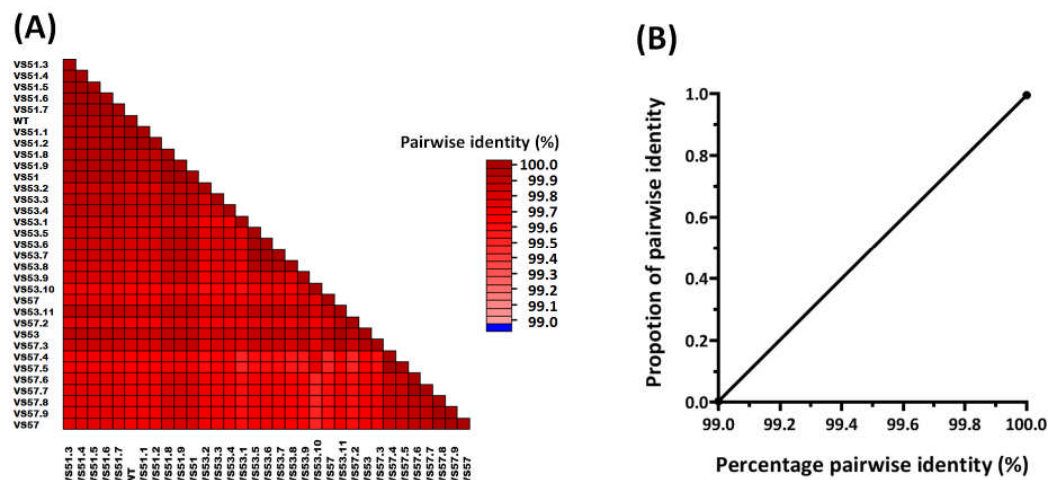
Figure 4.6. Percentage pairwise identity. *(A) Colour-coded pairwise identity matrix of all passages at 51°C (VS51.1 to VS51.9 and VS51), 53°C (VS53.1 to VS53.11 and VS53), and 57°C (VS57.1 to VS57.9 and VS57) aligned by SDT. Each box represents a pair of sequences aligned using MAFFT algorithms and expressed as colour-coded percentages as shown in the key. (B) Pairwise identity proportion graph.*
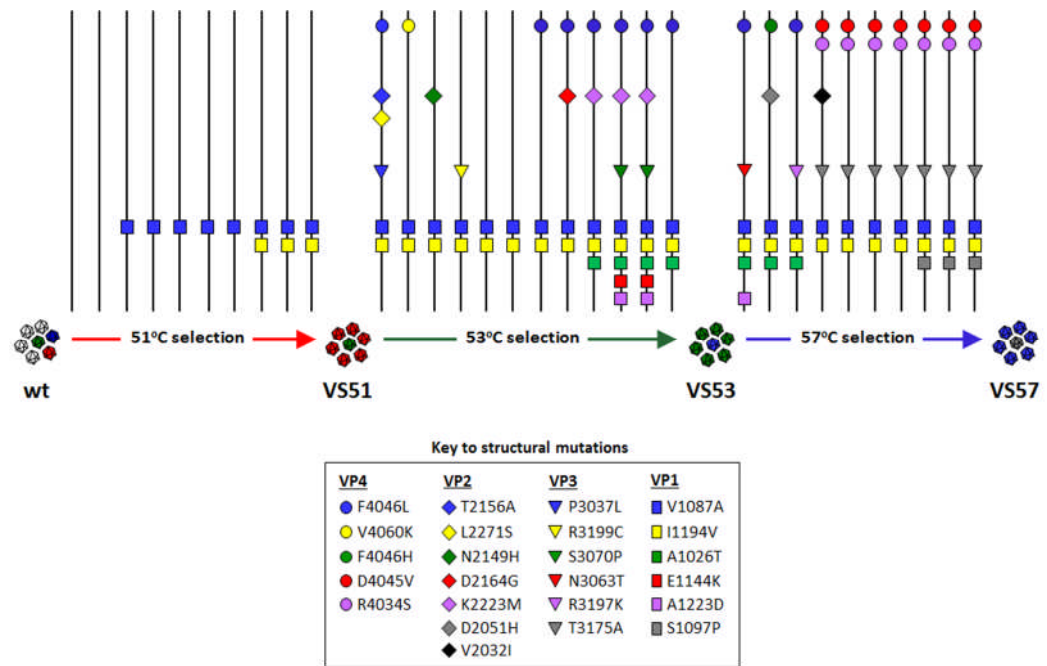
Figure 4.7. Thermal evolution of PV-1 mutations. *Following the thermal selection, virus RNA was extracted from intermediate pools of selected viruses at at 51ºC (VS51.1 to VS51.9 and VS51), 53ºC (VS53.1 to VS53.11 and VS53), and 57ºC (VS57.1 to VS57.9 and VS57). The viral capsid (P1) region was reverse-transcribed and PCR-amplified. The P1-amplicon of each virus pool was Sanger-sequenced and aligned against the wt PV-1 sequence by ClastalOmega. Solid black vertical lines represent wt sequences of the capsid proteins. Non-synonymous mutations are presented as coloured shapes of capsid proteins, VP4 (●), VP2 (◆), VP3 (▲) and VP1 (■). Horizontal arrows represent temperatures of selection at 51 ºC (red arrow), 53 ºC (green arrow) and 57 ºC (blue arrow). White capsids represent the wild type viruses, red capsids represent VS51 consensus mutations, and green capsids represent VS53 consensus mutations while blue capsids represent VS57 consensus mutations. Other colours represent quasispecies variation*

Two common pocket mutations (V1087A and I1194V) occurred in all selected virus pools (VS51, VS53 and VS57). Indeed, these were the only mutations identified in the VS51 pool. Figure 4.8 shows that at early stages of selection cycle at 51ºC, the VP1 pocket mutation V1087A was the first to appear within the virus pool after three selection cycles. At the eight selection cycle, a second

VP1 pocket mutation, I1194V evolved along with V1087A and both mutations were maintained in subsequent cycles. This suggests that these two mutations may play important roles in stabilising the capsid. An increase in the selection pressure from 51°C to 53°C resulted to some VP2 mutations. There was a switch in the consensus mutations after some cycles of selection at 53°C which resulted to an additional VP1 mutation (A1026T) as well as a VP4 mutation (F4046L). These sets of additional mutations were maintained as consensus within the virus population over into few cycles of selection at 57°C. At the fourth selection cycle at 57°C, a VP3 mutation was observed. This was in addition to the two common VP1 mutations as well as a switch in other VP1 and VP4 mutations i.e. S1097 P became the consensus as against A1026T while D4045V and R4034S became consensus VP4 mutation replacing F4046L. These alternating consensus mutations suggest the occurrence of an evolving population of viruses from genetically robust pools (figure 4.8).
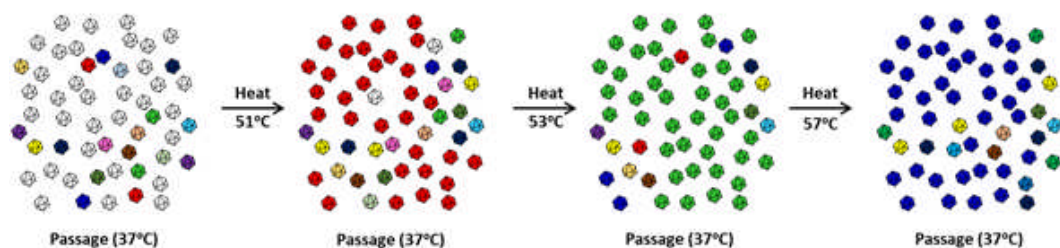
Figure 4.8. Working modelmodel of thermal evolution of thermally-stable viruses. The pool of viruses (VS51, VS53 and VS57) which survived the thermal pressure were sequenced after heat-treatment and prior to passaging. White capsids represent the wild type viruses, red capsids represent PV51 consensus mutations, and green capsids represent PV53 consensus mutations while blue capsids represent PV57 consensus mutations.

With these results, we have shown that the wildtype population existed as a quasi-species of sequences that revolved around the wt; in addition, within this population also existed viruses with sequences that corresponded to the VS51, VS53 and VS57 consensus, as well as a range of others. The gradual increase in selection pressure slowly created a bottleneck effect that selected thermally fit viruses which dominated the recovered pools.

Secondly, two common VP1 pocket mutations (i.e. V1087A and I1194V) which were observed in most pools of viruses are hypothesised to play important roles in the thermal stability of the viruses.

4.4.Characterisation of common pocket mutations, V1087A and I1194V

Previously, it was hypothesised that the two common mutations (V1087A and I1194V) may play important roles in stabilising the viral capsid. In order test this hypothesis, these mutations were introduced into an infectious clone of wt PV-1 by site-directed mutagenesis, generating PV-I1194V and PV-V1087A (also termed PV51δ). A combination of both mutations was also constructed and termed PV51. *In vitro* transcripts were generated from these infectious clones. In order to prevent reversion due to multiple infectious cycles, single-round cycles of infection were carried out by transfecting mouse L-cells with transcript RNA. Capsid proteins radio-labelled with ^{35}S (Cys/Met). Infectious clones of wt, PV-V1087A and PV51 yielded infectious viral particles, while PV-I1194V did not (Figure 4.9A). Supernatants and cell lysate were harvested and purified by sucrose density gradients. Virion peak fractions were immunoprecipitated using native (N)-specific (mAb 234) and non-native (H)-specific (mAb 1588) monoclonal anti-PV-1 antibodies. N-specific immunoprecipitated particles were identified by scintillation counts (figure 4.9B) and western blots (figure 4.9C and 4.9D). All RNA transcripts produced non-structural proteins, 3D and 3CD. H-specific particles were also immunoprecipitated from RNA transcripts of wt, VS51 and PV-V1087A (data not shown), however, PV-I1194V had no immunoprecipitated [N- or H-specific] particles and it therefore appears that this mutation may have affected virus production.
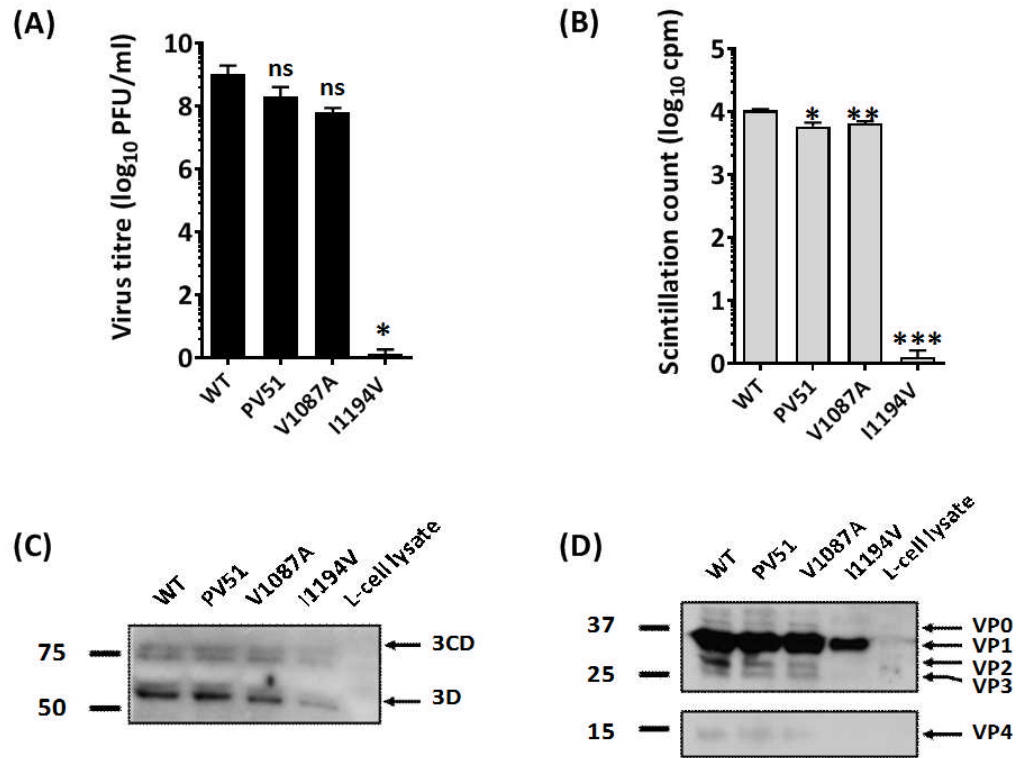
Figure 4.9. Characterising common pocket mutations, V1087A and I1194V.
The two common mutations that occurred in all mutants were re-introduced by site-directed mutagenesis into an infectious clone of wt PV-1 individually and in combination (PV51). Viral RNA was generated by T7 transcription. A total of 5×10^7 L-cells were transfected with 5 µg RNA and incubated at 37^oC. Virus proteins were radio-labelled with ^{35}S-(Cys/ Met) and purified by differential and sucrose gradient centrifugation. (A) Virus titres were determined by plaque assays on HeLa cells (n = 3 ± S.D., *P<0.05). (B) Virions were immunoprecipitated with N/D specific (Mab 234) and H/C specific (Mab1588) monoclonal antibodies and counted by scintillation. The sum of the radioactivity in immunoprecipitated particles from 30% of virus peak fractions is presented and compared to wt (n=3 ±S.D. *P<0.05, **P<0.001, ***P<0.0001). Transfected cell lysates were blotted against (C) anti-3CD and (D) polyclonal P1 antibody (SH-16).

4.5. Improving capsid stability of selected viruses by rational design

In this section, the roles of two VP1 mutations (I1194V and V1087A) as well as other mutations selected at 51°C, 53 °C and 57 °C, were characterised individually and in various combinations for thermal stability.

4.5.1. Testing VS51 mutations

Constructs PV-I1194V, PV-V1087A (also termed PV51δ) and a combination of both mutations PV51 were generated by site-directed mutagenesis. L-cells were transfected with RNA transcripts of mutants. Harvested viruses were assessed for thermal inactivation by plaque assays. Temperatures at which infectivity was lost are shown in figure 4.10.
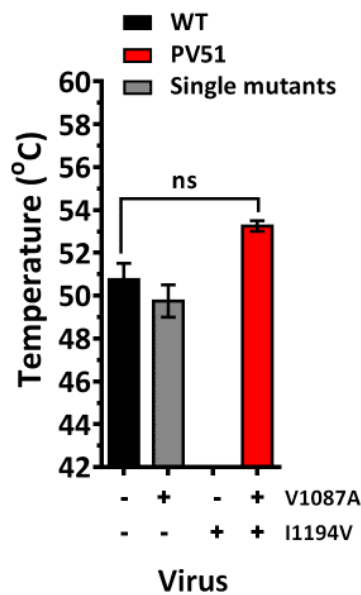
Figure 4.10. Inactivation temperatures of combination of mutations found in PV51. Capsid mutations selected at 51°C were introduced into PV-1 infectious clones and RNA transcript generated by T7 transcription. L-cells were transfected with mRNA by electroporation. After 24 hours, Cells were lysed by freeze-thawing and virus particles were harvested by centrifugation at 4,000 rpm for 10 minutes. Virus samples were incubated at temperature range from 40°C – 60 °C and cooled to 4°C. Virus titres were determined by plaque assays using HeLa cells. Graph shows the temperature at which infectious titres were lost. n = 2 ± S.D.

Mutant construct PV-V1087A was approximately as stable as wt PV-1 but less stable than PV51 which is a combination of I1194V and V1087A. Although, differences in thermal resistance profiles of these mutants were not statistically significant, the biological effect of the temperatures of thermal inactivation remains significant.

4.5.2. Testing VS53 mutations

Mutant constructs of VS53 (i.e. using mutations A1026T, I1194V, V1087A and F4046V) were generated by site-directed mutagenesis. Individual constructs (PV-A1026T, PV-I1194V, PV-V1087A and PV-F4046V), as well as construct having combinations were generated (PV-A1026T/F4046V). In order to assess the effect of I1194V, a construct having all mutations was generated and termed PV53, while PV53δ was a construct without I1194V. In order to avoid a second round infection, L-cells were transfected with RNA generated from cloned contructs. Infectious viral particles were assessed for thermal inactivation by plaque assays (figure 4.11).
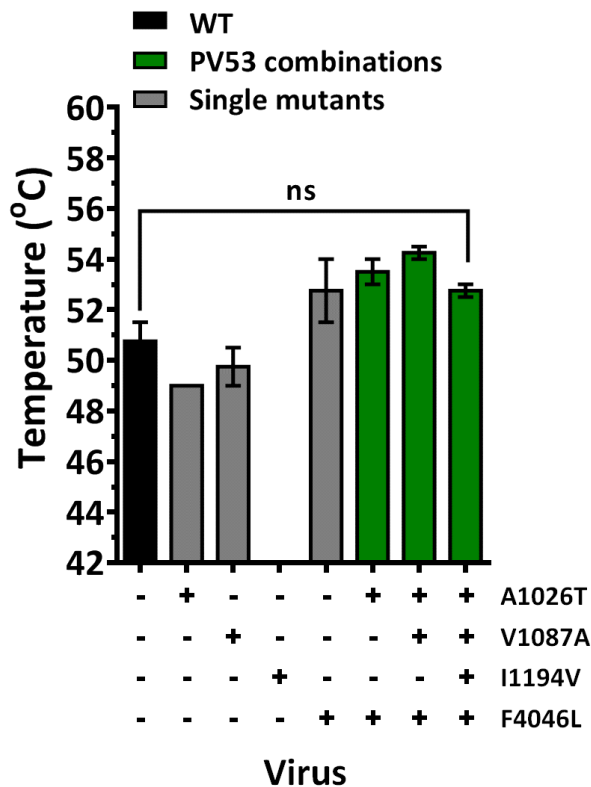
Figure 4.11. Inactivation temperatures of combination of mutations found in PV53. Capsid mutations selected at 53°C were introduced into PV-1 infectious clones and RNA transcript generated by T7 polymerisation. L-cells were transfected with mRNA by electroporation. After 24 hours, Cells were lysed by freeze-thawing and virus particles were harvested by centrifugation at 4,000 rpm for 10 minutes. Virus samples were incubated at temperature range from 40°C – 60 °C and cooled to 4°C. Virus titres were determined by plaque assays using HeLa cells. Graph shows the temperature at which infectious titres were lost. N=2 ± S.D.

Although four mutations were selected at 53°C, various combinations of these mutations conferred different degrees of thermal stability to virion particles. Introducing these mutations individually, F4046L was the only mutations shown to be more stable than the wt virus. A combination of A1026T and F4046L also showed remarkable stability than the wt virus and was comparable to all four mutations present. However, of all mutant constructs, PV53δ (which is a

combination of all four mutations selected but without I1194V) was the most thermally stable combination of mutations selected at 53°C. There was no statistical significance in these thermal inactivation profiles.

4.5.3. Testing VS57 mutations

Using VS57 selected mutations (i.e. V1087A, S1097P, I1194V, C3175A, R4034S & D4045V), mutants construct were generated by site-directed mutagenesis. Individual constructs (PV-V1087A, PV-S1097P, PV-I1194V, PV-C3175A, PV-R4034S & PV-D4045V), as well as construct having combinative mutations were generated by site-directed mutagenesis. In order to assess the effect of I1194V on a construct having all mutations (i.e. PV57), a construct without I1194V was also generated and termed PV57δ. Mouse L-cells were transfected with RNA generated from cloned contructs, to prevent second round infections. Infectious viral particles were assessed for thermal inactivation by plaque assays (figure 4.12).
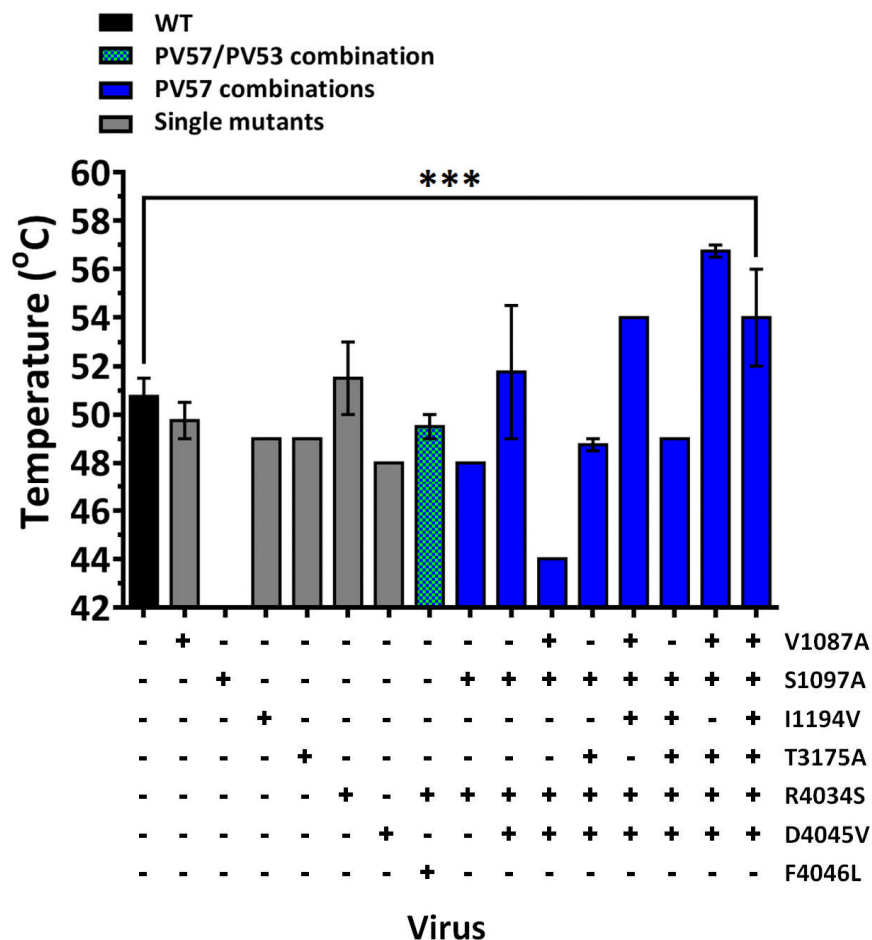
Figure 4.12. Inactivation temperatures of combination of mutations found in PV57. Capsid mutations selected at 57°C were introduced into PV-1 infectious clones and RNA transcript generated by T7 transcription. L-cells were transfected with mRNA by electroporation. After 24 hours, Cells were lysed by freeze-thawing and virus particles were harvested by centrifugation at 4,000 rpm for 10 minutes. Virus samples were incubated at temperature range from 40°C – 60 °C and cooled to 4°C. Virus titres were determined by plaque assays using HeLa cells. Graph shows the temperature at which infectious titres were lost. N=2 ± S.D. (***P<0.0001)

Of all the mutations selected at 57°C, PV- R4034S showed enhanced thermal stability than the wild type virus. A dual combination of the most thermally stable mutation selected at 53°C [F4046L] and the most thermally stable individual mutant selected at 57°C [R4034S] resulted to a construct (PV-

F4046L/R4034S), which was less stable than the wild type virus. Similarly, a combination of the most stable VP4 mutation [R4034S] selected at 57°C with a less stable VP1 mutation (S1097P) also selected at 57°C yielded a dual construct termed PV- R4034S/S1097P, which was stable mutant than wt. However, when the co-evolved VP4 mutation [D4045V] was added to this dual combination construct, the triple mutant construct termed PV-R4034S/S1097P/D4045V was more stable than wt PV-1 with comparable thermal resistant properties to a combination with all six mutations (i.e. PV57).

Mutant combinations with and without the two common mutations (i.e. I1194V and V1087A) had varied thermal stability in various constructs. In order to determine the effect these two mutations have in combination, a construct of VS57 was designed without I1194V and V1087A mutations and termed PV-PV-S1097P/C3175A/R4034S/D4045V. This mutant construct was shown to be less stable than wt. A mutant construct of mutations selected in VS57 without I1194V only was termed PV57δ and was the most stable combination of mutations selected at 57°C. In order to assess the effect of the VP3 mutation, a construct of VS57 was designed without the VP3 mutation [C3175A] and was shown to be less stable than PV57δ but more stable than the wt virus. Results were statistically significant.

4.5.4. Phenotypic characteristics of rationally-designed and selected mutants

Small plaque (SP) phenotypes have been reported to have resulted to temperature sensitive and replication-deficient polioviruses (Bellocq *et al.*, 1987; Burgon *et al.*, 2009; Kanda & Melnick, 1959) as well as some other picornaviruses such as West Nile virus (Jia *et al.*, 2007), EV71 (Phuektes *et al.*, 2011), Coxsackie B virus (Ramsingh *et al.*, 1995), Bunyamwera and Ngari viruses (Odhiambo *et al.*, 2014), etc. During the production of live Dengue viral vaccine, SP is an empirical phenotypic criteria that indicates attenuation (Goh *et al.*, 2016). In order to determine the plaque morphology of mutants, plaque assays were set up and resulting plaques measured using a graduated rule. Figure 4.13 shows the various plaque sizes observed.

Blank   Normal   Small
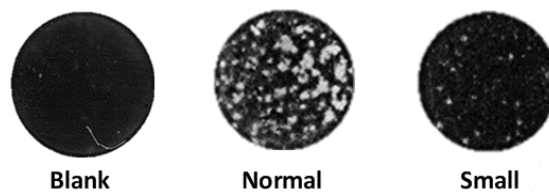
Figure 4.13. Plaque morphology. L-cells were transfected with various mutant constructs. HeLa cells were infected with harvested virus and plaques stained with crystal violet. Various plaque sizes were observed among mutant virus constructs.

Two variants of plaques were observed among mutant constructs: the normal plaque sizes which were similar to the wild-type virus plaques was the most common plaque morphology observed, while a tiny plaque morphology was observed in two mutant constructs (figure 4.14).
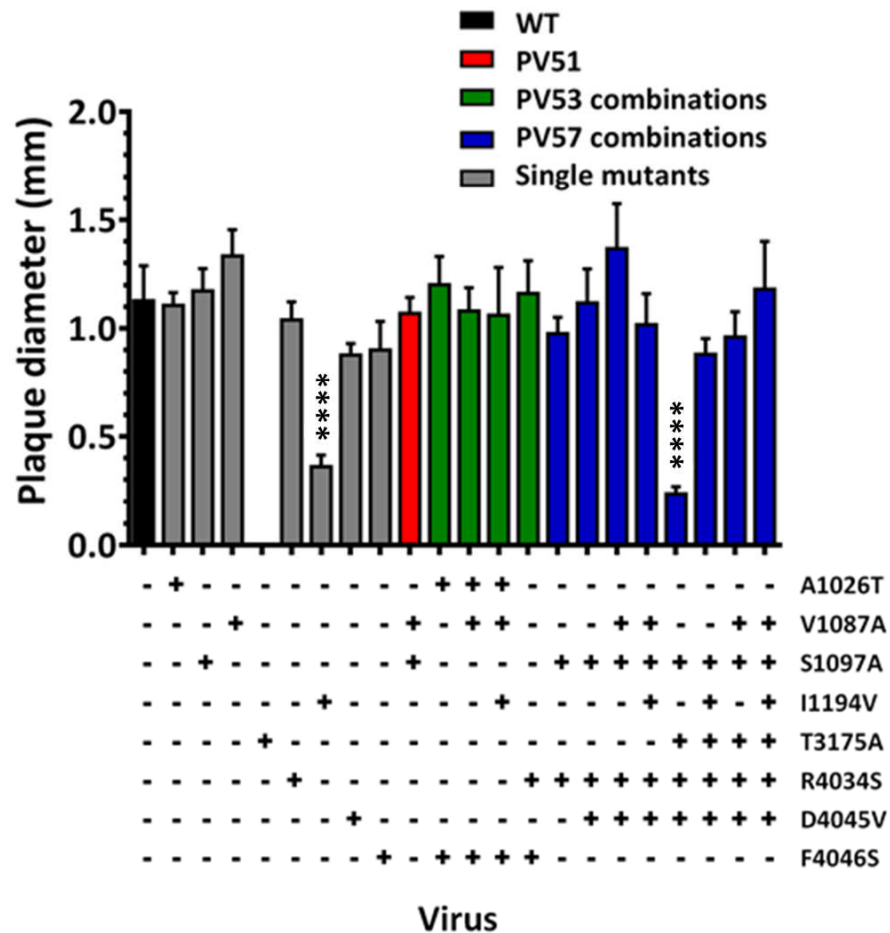
Figure 4.14. Plaque morphology (sizes). *Mouse L-cells were transfected with T7-transcripts of SDM-generated mutants and incubated at 37°C under 5% CO_2. Plaque assays of propagated virus were set up on HeLa cells. Variation in plaque diameters was determined by graduated rule measurements; n = 20 ± S.D. (****P<0.00001)*

Most viruses had plaque sizes of about 1mm diameter. Two variations of small plaques were observed with mutant PV-R4034S as well as a PV57 mutant construct without the two common mutations (I1194V and V1087A).

4.6.Effects of pocket mutation on selected mutants PV51, PV53 and PV57

The VP1 pocket mutation V1087A has been reported to increase the thermal stability of PV-1 and PV-2 when heated for prolonged period (Shiomi *et al.*, 2004). This mutation was introduced into a wt PV-1 infectious clone (section 2.) and RNA generated by T7 transcription. Infectious virus particles were generated by transfecting mouse L-cells with mRNA. By means of thermal inactivation assays, our findings suggest that V1087A reduced the thermal stability of PV-1 when heated for 30 minutes at elevated temperatures, but in combination with I1194V, enhanced the thermal stability. Since the mutation I1194V has been shown to play a vital role in capsid stability of PV51, we sought to investigate its effect on selected viruses in their respective combination. Using site-directed mutagenesis, clones of PV51, PV53 and PV57 were constructed with and without (δ) mutation I1194V (Table 4.2).

Table 4.2. Infectious clones. Mutants were constructed by site-directed mutagenesis into an infectious clone of wt PV-1 using identified combinations. Mutation I1194 was included and excluded from reconstructed viruses.

Mutant	Amino acid substitutions
PV- I1194V	I1194V
PV51δ (PV-V1087A)	V1087A
PV51	V1087A, I1194V
PV53δ	A1026T, V1087A & F4046L
PV53	A1026T, V1087A, I1194V & F4046L
PV57δ	V1087A, S1097P, C3175A, R4034S & D4045V
PV57	V1087A, S1097P, I1194V, C3175A, R4034S & D4045V

RNA was generated by T7 *In vitro* transcription and L-cells were transfected with mutagenised transcripts. Infective titres were determined by plaque assays using HeLa cells (Figure 4.16). It was observed that maintaining the wildtype

I1194 residue in PV51 and PV53 decreased the virion titres 4- and 13-fold, respectively (n=2 ± SD), however, maintaining the wt I1194 residue in PV57 increased the virus titres 40-fold (Figure 4.15).
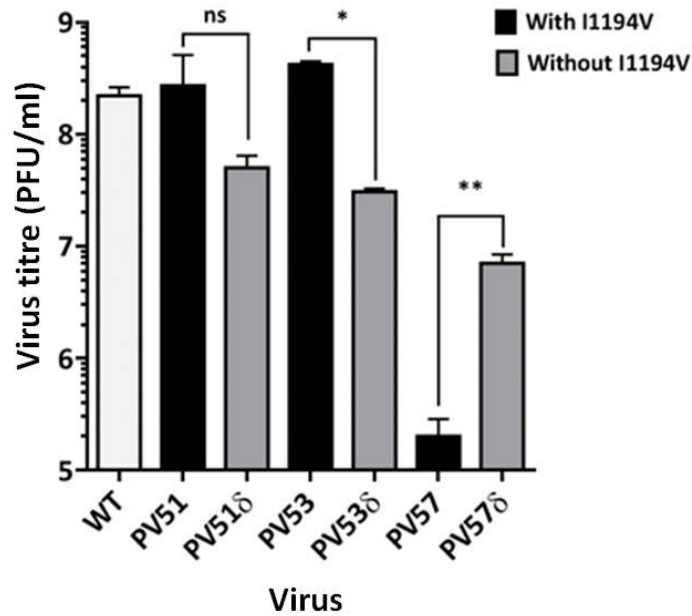
Figure 4.15. *Infectivity titres of SDM-generated mutants. Mutant viruses were constructed with and without I1194V mutation. Transcript mRNA was generated by T7 transcription. A total of 1×10^7 Mouse L-cells were transfected with 5 µg viral mRNA. Post-transfection, supernatant was harvested and cells were freeze-thawed. Virion titres were determined by plaque assays using HeLa cells. (*p<0.05, **p<0.001). n=2 ± S.D.*

Result suggests that in mutant PV53, the wildtype I1194 residue significantly reduced the virus yield, but this wildtype I1194 residue significantly increased the yield in PV57.

4.7. Thermal stability profiles of mutant viruses

Using thermal inactivation assays, virus produced by RNA transfection were shown to loose infectivity at 52°C (wt), 53°C (PV51), 54°C (PV53) and 56 ^{o}C (PV57) (Figure 4.18A). It was further observed that PV51 with the wildtype I1194 residue was more thermally stable than with the mutant V1194 residue (PV51δ). Similarly, PV53δ (i.e. PV53 with the wildtype I1194 residue) could withstand higher temperatures than its alternative with the mutant V1194 residue. Mutant PV57 with the wildtype I1194 and mutant V1194 residue had approximately similar inactivation temperatures (figure 4.16).
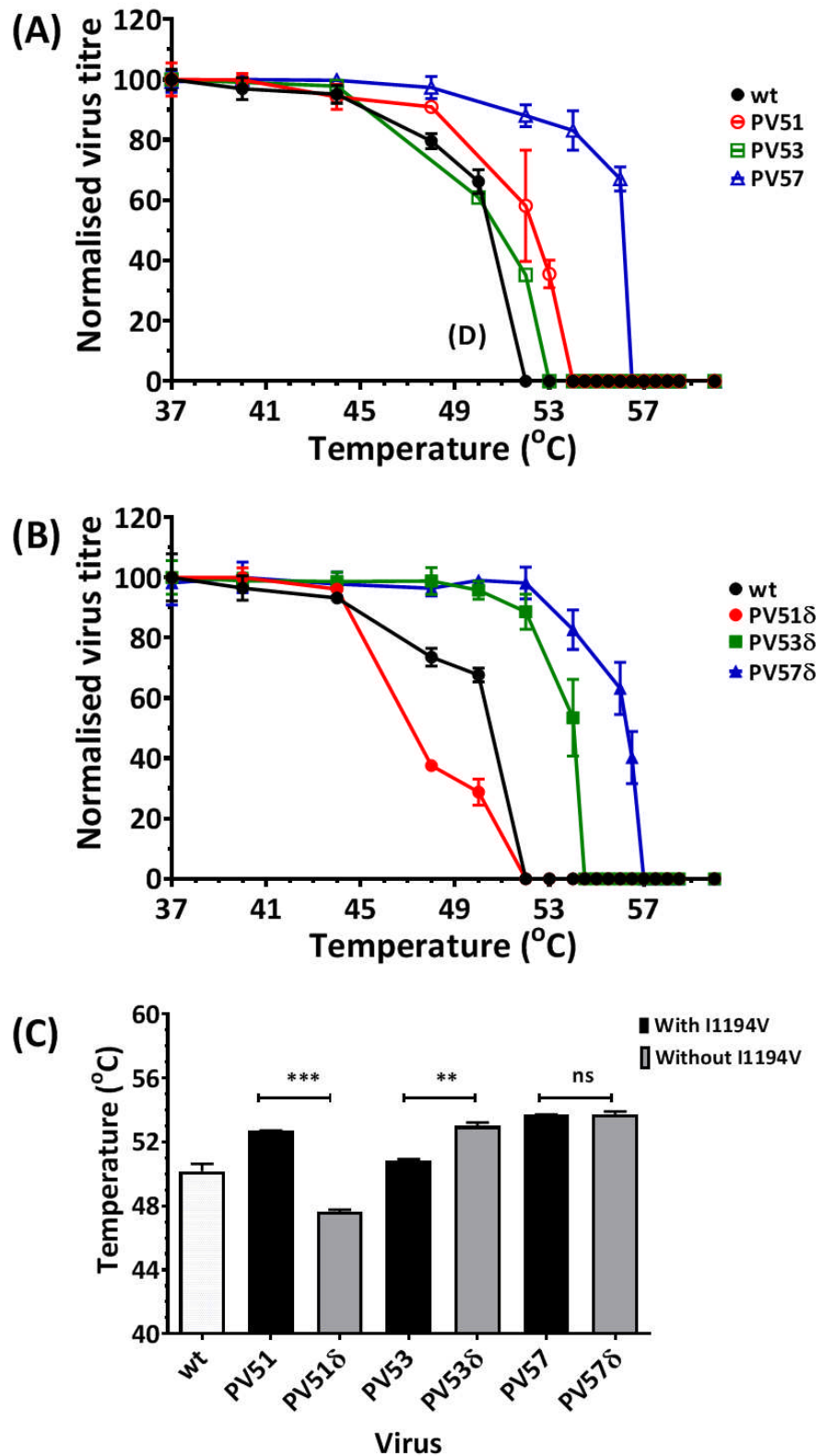
Figure 4.16. Thermal inactivation profile of virus mutants with and without I1194V. *Mutant viruses were constructed individually and in combinations by SDM, with and without I1194V. PV51δ (V1087A); PV53δ (A1026T, V1087A & F4046L) and PV57δ (V1087A, S1097P, C3175A, R4034S & D4045V) were*

generated and compared with constructs where I1194V was present i.e. PV51 (V1087A, I1194V); PV53 (A1026T, V1087A, F4046L, I1194V) and PV57 (V1087A, S1097P, C3175A, R4034S, D4045V, I1194V. A total of 1 x 10^7 mouse L-cells were transfected with 5 µg of in vitro transcribed RNA. Post-transfection, supernatant was harvested and cells freeze-thawed. Samples were heat-treated at a range of temperatures and virus titres were determined by plaque assays using HeLa cells (A) Normalised thermal inactivation assays for SDM mutants without I1194V (n=3 ± S.D., P<0.00001). (B) Input virus titres (n=3 ± S.D., *P<0.05, **P<0.001). (C) The IC$_{50}$ temperature values for thermal inactivation curves of mutants with and without I1194V (n=3 ± S.D., **P<0.001, ***P<0.0001)

4.7.1. Thermal stability profiles of candidate mutant viruses

Owing to the effects of I1194V demonstrated above, PV51, PV53δ and PV57δ were taken forward for more detailed analysis. Antigenicity profiles of virion particles (Figure 4.18A) showed that PV53δ and PV57δ were significantly ($P<0.001$) more thermally-stable than PV51 and both were significantly ($P<0.00001$) more thermostable than wt virion. The antigenic switches of virions occurred at 44°C (PV51), 49°C (PV53δ) and 50°C (PV57δ). EC antigenicity profiles (Figure 4.19B) also showed that PV57δ was significantly more thermally-stable than PV53δ ($P<0.05$) and PV51 ($P<0.0001$). For the corresponding ECs of PV51, PV53δ and PV57δ, antigenic switches occurred at 38°C, 42°C and 45°C respectively. Since the wt EC is antigenically unstable, current IPV vaccine (i.e. BRP vaccine) was used as control (Figure 4.19C). Results showed that although PV51 was significantly ($P<0.001$) less stable than BRP both PV53δ and PV57δ were as stable as BRP (Figure 4.19D).
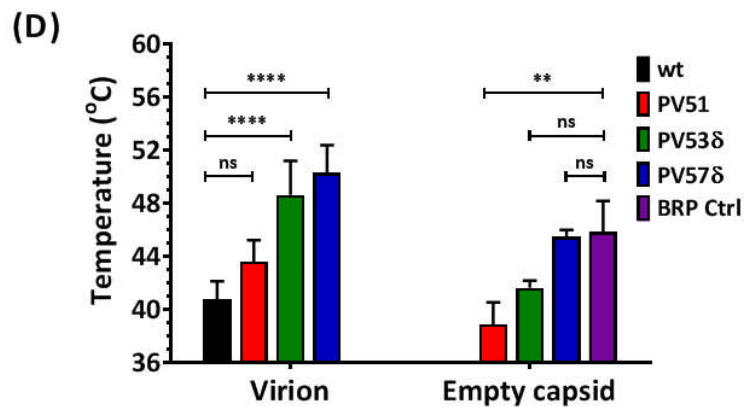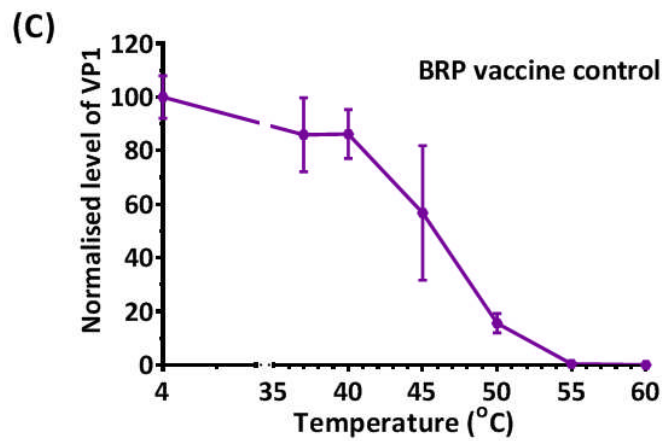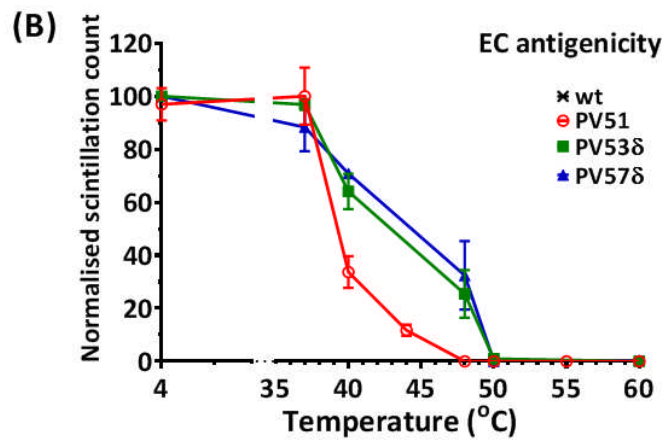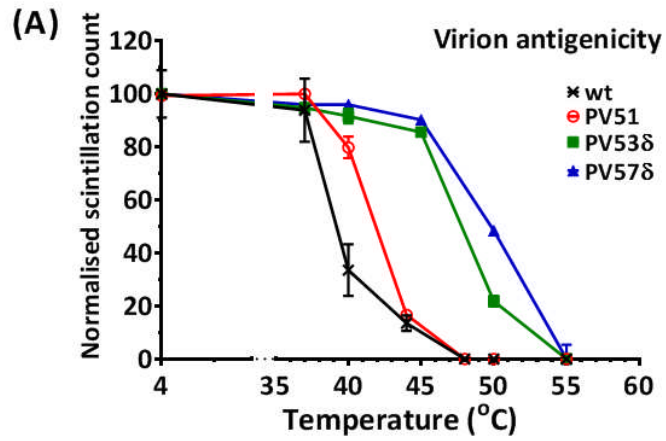
Figure 4.17 Thermal stability profile of virus mutants. Mutations identified by thermal selection were introduced by SDM into an infectious clone of wt PV-1, individually and in combinations with and without mutation I1194V. Wt was included for comparison. Transcribed RNAs were transfected into L-cells to recover infectious virus and ECs were accumulated by GuHCl treatment at 3.15 hours post-transfection. Harvested particles were purified through 15-45% sucrose density gradients. Sucrose was removed by dialysis, and virions and ECs were dialysed out of sucrose and incubated at a range of temperatures (from 37ºC to 60ºC) for 30 minutes and cooled to 4ºC for 5 minutes before titration by plaque assays using HeLa cells. (A) Immunoprecipitation assay for heat-treated virions (B) Immunoprecipitation assay for heat-treated ECs using N/D specific (Mab234) monoclonal antibodies. (C) Immunoprecipitation assay for heat-treated BRP vaccine controls, using N/D specific (Mab234) monoclonal antibodies. Samples were immunoblotted with anti-VP1 Millipore mAb 8650. Figure shows normalised average of semi-quantitative densitometric plots of VP1 band intensities using ImageJ. (n= 3 ± S.D.) (D) Temperatures at which 50% native (N/D) antigenicity was lost. n=3 ± S.D., for virus, data is compared to wt, for EC, to BRP (**P<0.001, ****P<0.00001).

4.8. Discussion

Through bottlenecks (i.e. perturbations or external pressures) the genetic diversity of a population of viruses is often largely diminished, the effect of which may be difficult to predict (Manrubia et al., 2005). In the previous chapter, the selection of thermally-stable PV-1 mutants through increasing temperatures of $51^{\circ}C$, $53^{\circ}C$ and $57^{\circ}C$ was described.

Virus population studies have shown that transitional mutations are more likely changes than transversional mutations, however transversional mutations are more likely to cause non-synonymous mutations with potentially more dramatic effects (Carter & Sanford, 2012; Tanaka et al., 1993). The data presented in figure 4.7 agrees with the submission that stability between transitional and transversional mutations is more attainable at higher frequencies of mutation (Acevedo et al., 2014).

Although the exclusion of I1194V and V1087A from PV53 and PV57 did not result to mutants that were less thermally stable than wt, V1087A may have evolved mutants with enhanced stability in both combinations. This suggests that the VP4 mutations selected at $53^{\circ}C$ (F4046L) and $57^{\circ}C$ (a combination of R4034S with D4045V) may also play important roles in the capsid stability through a different mechanism possibly from within the internal network of the capsid. Reduced thermal-stability as observed by thermal inactivation assays of the combination PV-F4046L/R4034S suggests that since mutation F4046L selected at $53^{\circ}C$, while D4045V was selected at $57^{\circ}C$, a combination of both mutations (F4046L and R4034S) could out-select the virus, hence it may not have been an evolutional combination for thermal stability.

145

The two key VP1 mutations (V1087A and I1194V) that evolved in early cycles of selection and were maintained as a consistent pair in all selected candidates. Shiomi et al, (2004), reported the occurrence of V1087A as a heat-resistant mutation able to withstand 50°C (Shiomi *et al.*, 2004). Although they did not show the effect of this mutation on the EC, our findings further suggests better fitness of V1087A in combination with I1194V resulted in an antigenically stable EC. Studies have reported the destabilising effects of mutations on VP1 position 194 in PV-1, PV-2 and PV-3 (Kouiavskaia *et al.*, 2011; Liu *et al.*, 2012b). Our data suggests that mutating this residue to a valine affected assembly, however, when in combination with V1087A, there was a compensation for infectivity that further enhanced capsid stability.

Since the overall frequencies of transition and transversion mutations stabilised at higher selection pressures (as shown in figure 4.7), the evolutional trend of mutations suggest a bottleneck effect of selection from a genetically robust population of viruses. This was corroborated by the randomly selected plaques from VS57 pool of viruses that had been kept under selection at 57°C, which were shown to be more thermally stable than VS57 but reverted to VS57 phenotype after 2 cycles of selection (section 3). Results further suggest that VP2 mutations may have played transitional roles within the evolving population during thermal selection at 53 °C.

The position of residue 87 on the B-strand of the VP1 β-barrel and residue 194 on the G-strand both within the capsid pocket may play a vital role to the EC stability, relative to the flexible BC-loop (residues 95-105) (Lin *et al.*, 2013a), which is a known neutralising antibody binding site (Minor *et al.*, 1986; Vanderwerf *et al.*, 1983). Studies have further shown that heating 160S particles

resulted to expansions that created a larger distance on the antigenic- BC loop residues in an event that coincides with loss in native antigenicity (Belnap *et al.*, 2000a; Lin *et al.*, 2013a). Therefore, our first hypothesised model for capsid stability suggests that both pocket mutations (V1087A and I1194V) may have stabilised the surface features, by preventing conformational changes at the antigenic binding sites. Further selection of VS51 evolved a virus with two mutations, one being on VP4 (46 F/L) and a second on VP1 (26 T/A). Further selection led to more internal mutations as well as an interpentameric VP3 mutation (T3175A), which in combination, stabilised the EC structure further at even higher temperatures than the wt 160S virion particles. Owing to the inability of PV/I1194V to assemble particles, we assessed the effect of omitting this mutation in PV53 and PV57 mutants (i.e. PV53δ and PV57δ). Our findings suggest that in the absence of I1194V, PV53δ and PV57δ had better capsid stabilities. This may further suggest the de-stabilising effect of mutations on the highly conserved residue VP1194 on the virus fitness.

Chapter 5

Generating stable type-1 PV-like particles (VLPs) of thermally-stable mutants, PV53δ and PV57δ, in two recombinant expression systems

5.1. VLP expression in recombinant systems

Virus-like particles (VLPs) are self-assembled recombinant structural capsids proteins and/or envelopes (Noad & Roy, 2003; Pushko *et al.*, 2013). VLPs vary in size, structure and properties and are capable of invoking a strong and long-lasting immune responses, making them suitable vaccine candidates (Pushko *et al.*, 2013). VLP vaccines remain the safest of viral vaccines, because they lack the viral genome and are therefore non-infectious; and they do not require the use of live virus at any stage of production (figure 5.1). They also have the potential of producing relatively higher yield than other vaccines (depending on the expression system) (Peyret H. P., 2015). VLPs can be more immunogenic than other vaccines, inducing very high titres of neutralising antibodies. This is because they are self-assembled highly ordered structures that mimic the live organism by presenting repetitive epitopes that could activate and/ or stimulate [B- and T-] cell-mediated immune responses (Chen & Lai, 2013).
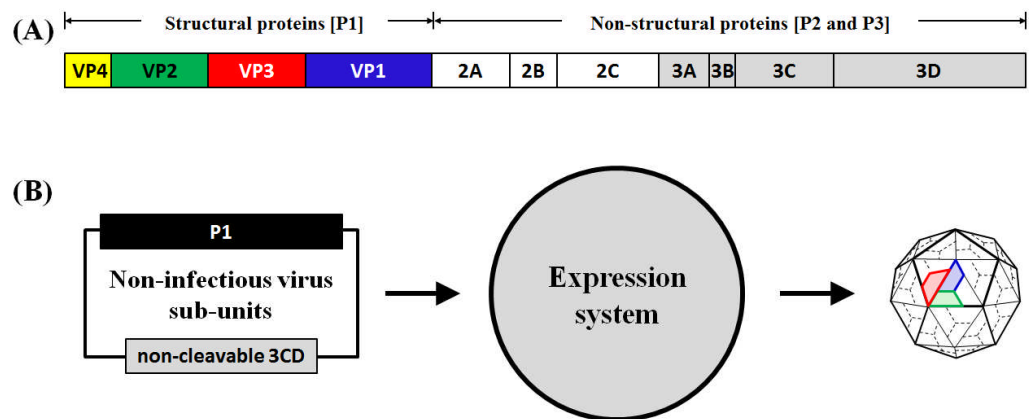
Figure 5.1. Schematic of a pathogen VLP expression system. *(A) Cartoon image of the PV genome, showing the structural P1 region comprising non-cleaved VP0, VP3 and VP1. The P2 non-structural region as well as the P3 region, which comprises the P1-processing 3C or 3CD are also shown. Figure are not drawn to scale. (B) Recombinant expression of VLPs from virus subunits involve use of an expression system. Figure shows the schematic of typical expression system for a non-enveloped, self-assembling VLP, showing the processing flow from cloning virus subunits into expression of self-assembled VLPs such e.g. PV.*

VLP vaccines have been successfully produced though various cell-based expression systems including bacterial (Liew *et al.*, 2010; Tan *et al.*, 2004; Zhang *et al.*, 2016b), insect (Koch *et al.*, 1995; Lopez-Macias *et al.*, 2011), mammalian (Tree *et al.*, 2001), plants (Kapusta *et al.*, 1999; Thanavala *et al.*, 2005), yeast (Saraswat *et al.*, 2016; Zhang *et al.*, 2015), as well as cell-free systems (Almeida *et al.*, 1975; Bhattacharya & Mazumder, 2011; Morein *et al.*, 1979).

5.1.1. Potential expression systems for recombinant VLP

The choice of an expression system is largely dependent on the virus structure, morphogenesis and antigenic conformation (Kushnir *et al.*, 2012). These characteristics determine what kind of VLP expression systems may be most

suitable as well as whether or not such VLPs could exist as chimeric or distinct vaccines. Other considerable factors include immunogenicity of VLP, production potential of expression system, regulatory requirements and vaccine target host (i.e. human or animal). Of the available expression systems, yeast remains a well-established and regulated VLP expression system for human vaccines (Kushnir *et al.*, 2012; Peyret H. P., 2015). Applications have advanced from *S. cerevisiae* to high-level expressing methanol-inducers, *P. pastoris* (Ahmad *et al.*, 2014; Cregg *et al.*, 1985). Owing to the production potential at very low costs, the plant-based expression system has fast gained popularity (Phan & Conrad, 2016; Rybicki, 2014) and possibly become the ideal expression system for VLP vaccines.

5.1.2. Generating recombinantly expressed PV VLPs

In the course of the PV lifecycle, post-translation of the PV RNA into a polyprotein, $2C^{pro}$ and $3C^{pro}$, both play important roles in processing of the poly protein into sub-units (figure 5.2.), followed by the morphogenesis of the P1 sub-units into a capsid. As these events proceed, $3C^{pro}$ plays an important role in the shutdown of host-protein synthesis (Clark *et al.*, 1993; Yalamanchili *et al.*, 1997) and therefore is known to be cytotoxic in a recombinant assays (Baum *et al.*, 1991). Studies have shown that inserting a serine close to the 3C/3D junction of the polyprotein precursor ($3CD^{pro}$) precludes its autocatalytic cleavage into 3C and 3D, thus, making it less cytotoxic but still proteolytic (Bert L. Semler & Ypma-Wong, 1987; Graham *et al.*, 2004). With the use of a mutagenised non-cleavable 3CD, it has also been shown that proteolytic cleavage of polyprotein P1 into VP0, VP3 and VP1 is most efficiently carried out by the multifunctional $3CD^{Pro}$ (Parsley *et al.*, 1999a).
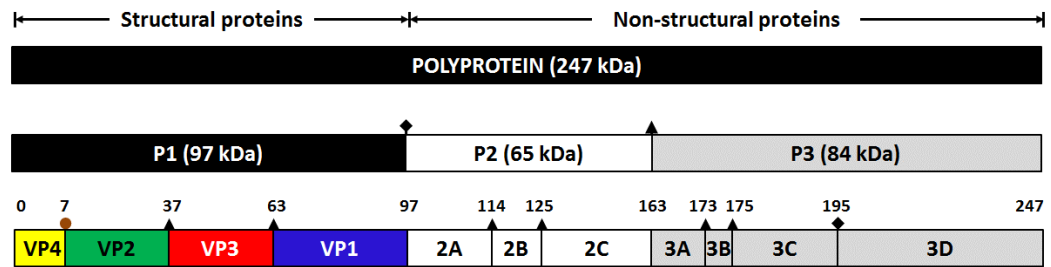
Figure 5.2. PV cleavage map. *Showing a schematic representations of translated polyprotein (247 kDa), post-cleavage sizes of P1 (97 kDa), P2 (65 kDa) and P3 (84 kDa), as well as proteolytic and autocatalytic cleavages of P1, P2 and P3 with relative sizes indicated in kilo Daltons (kDa). Cleavage positions by 3C^{pro} or 3CD^{pro} (▲), 2A^{pro} (◆) and a virion maturation autocatalytic event (●) are also indicated. Figure not drawn to scale.*

In this chapter, the expression of VLPs of the thermally-stable mutants, PV53δ and PV57δ, which were shown to be more thermally stable mutant combinations in recombinant systems is discussed. The plant VLP expression was carried out in collaboration with Johanna Marsian and George Lomonossoff at the John Innes Centre (JIC), Norwich, UK. The VLP expressions in recombinant yeast (*P. pastoris*) of these mutants as a stable PV VLP is also discussed.

5.2. Plant-based expression of PV53δ and PV57δ VLPs

In order to facilitate proteolytic cleavage of P1 into VP0, VP3 and VP1, *Agrobacterium tumefaciens* was co-transformed with *Nicotiana benthamiana* codon-optimised plasmid clones of non-cleavable mutant 3CD (pEAQ-*HT*-3CD) along with plasmid clones of the P1 region of thermally-stable mutants PV53δ and PV57δ (i.e. pEAQ-HT-PV53δ and pEAQ-HT-PV57δ, respectively) (Sainsbury *et al.*, 2009). The leaves of 3-week old *Nicotiana benthamina* were pressure-infiltrated with positively selected tansformants (Thuenemann *et al.*, 2013) and grown at 25 °C with 16 hours supplemental daylight and daily watering for 6-7 days. Plants were harvested by mechanical disruption and filtered through Miracloth. Crude extracts were clarified by centrifugation at 9,500 xg for 15 min at 4°C and filter-sterilised through a 0.45 µm syringe filter (Figure 5.3). Levels of expression were as high as 8 mg/ kg of *N. benthamina*.

This work was undertaken by Johanna Massena and George Lomonossoff at the John Innes Centre, Norwich.
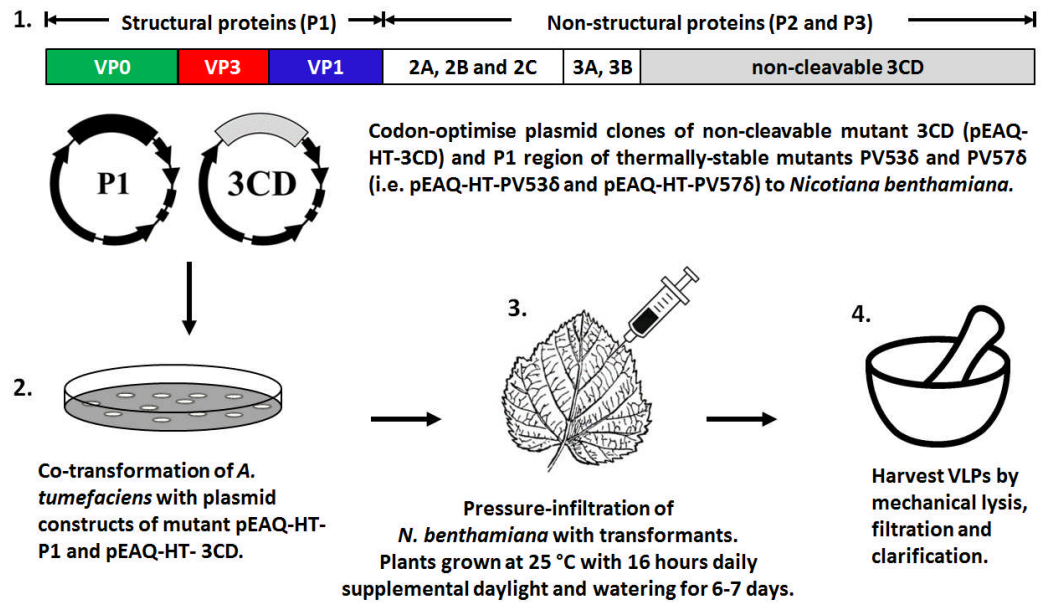
Figure 5.3. A schematic workflow of plant expression of PV-1 VLPs *showing (1) PV genome highlighting the P1 and non-cleavable 2CD region in black and grey, respectively. Genes were codon-optimised to Nicotiana benthamina and cloned into plasmid construct. (2) Agrobacterium tumefaciens was co-transformed with P1 and 3CD plasmids. (3) Transformants were pressure-infiltrated into Nicotiana benthamina and propagated at 25ºC for 6-7 days. (4) Self-assembled VLPs were harvested by mechanical lysis of plant, filtration of lysate and clarification of filtrate.*

5.2.1. Detection of plant-expressed VLPs using PV-1 N-specific nanobodies

Owing to the high cross-reactivity of available anti-PV-1 N- and H-specific MAbs with yeast proteins (data not shown), therefore an alternative screening method for self-assembled PV-1 particles was developed. VHH (also known as Nanobodies®) are alternative heavy chain antibodies found in camelids. They are made up of only a single-domain and are the smallest known antigen-binding fragments (Kontermann, 2010; Wesolowski *et al.*, 2009). The use of VHH has gained fast acceptance in scientific and clinical research applications (Spiess *et al.*, 2015), due to their robust-affinity, ability to access conventionally-inaccessible structures plus their tolerance of low/high-pH and wide temperature ranges (de Marco, 2011; Spiess *et al.*, 2015). A group of highly specific anti-PV-1 VHHs have been selected and characterised as good binders of native and non-native PV particles (Thys *et al.*, 2010). Two of these N- (PVSP6A) and H-specific (PVSP7A) VHHs have also been successfully applied to immuno-capture assays (Schotte *et al.*, 2012) for the purification of PV-1 particles.

Plant-expressed filtrates (PL-PV53δ and PL-PV57δ) were pelleted through 30% sucrose cushion by ultracentrifugation at 167,000 x g for 3 h at 4°C. PL-PV53δ and PL-PV57δ pelettes were re-suspended in PIPES buffer and immunoprecipitated using the anti-PV-1 N- (PVSP6A) and H-specific (PVSP7A) nanonobodies (Schotte *et al.*, 2012). An inactivated trivalent PV BRP vaccine with European Pharmacopoeia (EP) Reference Standard was applied as control. Immunoprecipitated particles were immunoblotted against anti-VP0 rabbit polyclonal and anti-VP1 MAb antibodies (figure 5.4). BRP was included as a control.
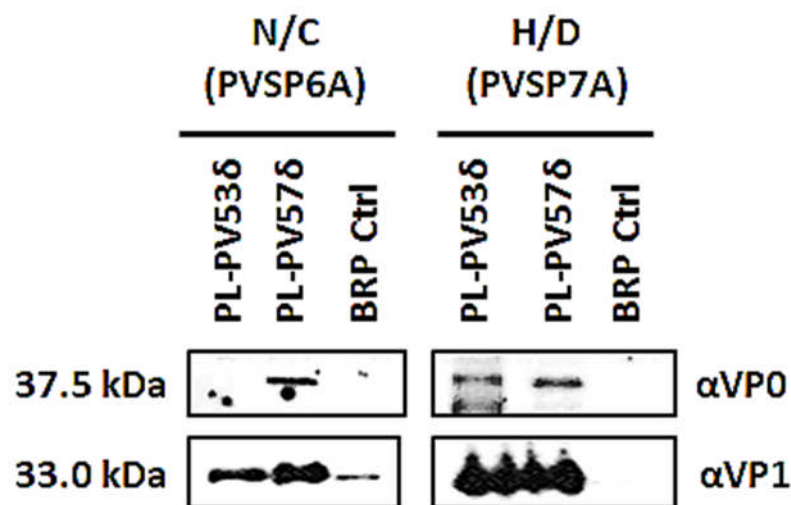
Figure 5.4. Immunoprecipitation of VLPs. *Material was immunoprecipitated using N-specific anti-PV-1 nanonbodies (PVSP6A) and H-specific anti-PV-1 nanobodies (PVSP7A) and immobilised onto HRP-conjugated IgG magnetic beads. Following a single wash step, beads were seperated from supernatant and boiled in SDS-loading buffer. Proteins were seperated by SDS-PAGE and immunoblotted against anti-VP0 rabbit polyclonal and anti-VP1 mouse monoclonal antibody (Millipore 8650). BRP vaccine controls were shown on lanes 3 and 6. Figure shows N- and H-specific VP0 bands of about 37.5 kDa on PV53δ and PV57δ lanes, BRP does not contain VP0. N- and H-specific VP1 bands of about 33 kDa are also shown on all lanes.*

Results show that plant-expressed PL-PV53δ and PL-PV57δ both had bands at sizes corresponding to VP0, although this was less visible in N-antigenic PL-PV53δ, while BRP vaccines standards had no VP0 bands. However, BRP, PL-PV53δ and PL-PV57δ all had VP1 bands as shown in the figure 5.4.

5.2.2. Assessing antigenicity of PL-PV53δ and PL-PV57δ VLPs

In order to confirm the self-assembly of VLPs, sucrose-clarified materials (PL-PV53δ and PL-PV57δ) were purified through 15-45% sucrose gradient. With the use of a polyclonal SH-16 capture antibody, N-specific (234 MAb) and H-specific (1588 MAb) primary antibodies and anti-mouse HRP conjugate secondary antibodies, gradient fractions were assayed for antigenicity by capture ELISA (figures 5.5A-C). Gradient peak fractions were dialysed from sucrose and analysed by negatively stained electron microscopy (figures 5.5D and 5.5E).
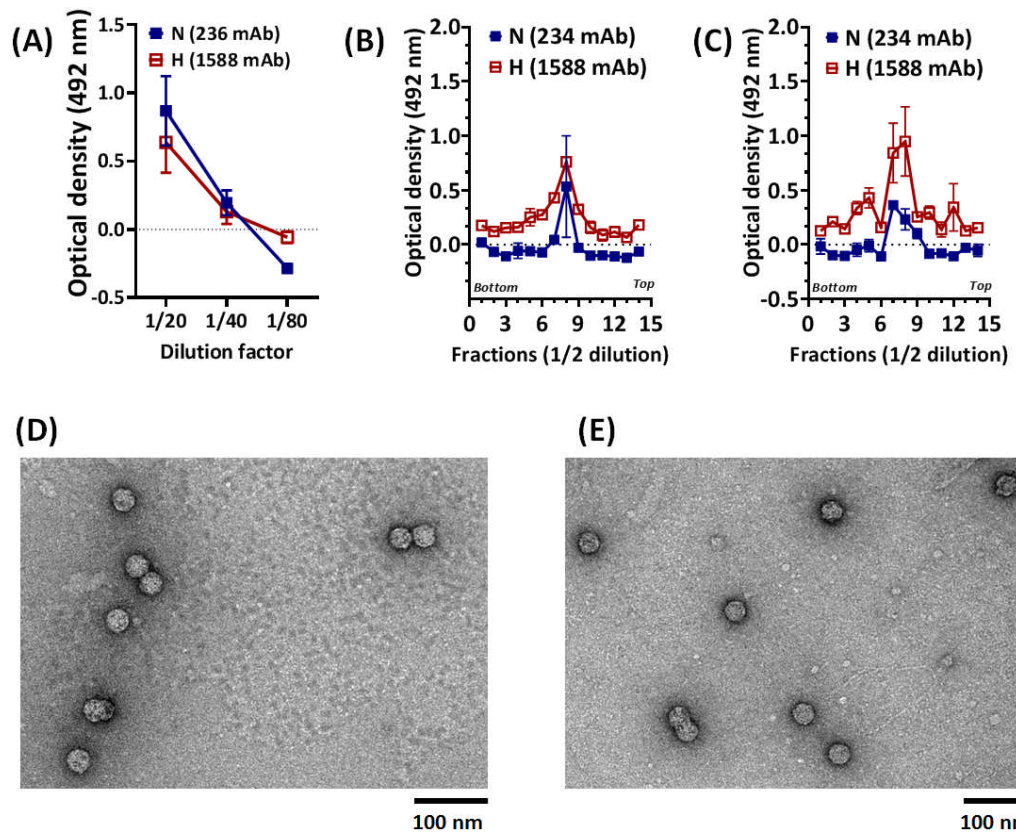
Figure 5.5. Plant-expressed VLPs. Harvested particles were clarified by ultracentrifugation at 167,000 x g for 3 h at 4°C. Pellets were purified through 15-45% sucrose density gradients by ultracentrifugation at 50,000 rpm for 50 minutes in a Beckman SW 55 Ti rotor. Gradients were fractioned from bottom (left) to top (right). A total of 50 μl of each fraction was assayed by ELISA in a 1:2 dilution using polyclonal SH-16 capture antibody, N-specific (234 MAb) and H-specific (1588 MAb) as primary antibodies and anti-mouse HRP conjugate as secondary antibodies. Figures show Standardised BRP ELISA diluents (A), gradient ELISA plots of PL-PV53δ (B) and PL-PV57δ (C) Gradient peaks were dialysed into PBS and analysed by negatively stained electron microscopy at a magnification of 30,000x. Electron micrographs show assembled VLPs of PL-PV53δ (D) and PL-PV57δ (E). n= 2 ± S.D.

Electron micrographs of particles purified by density gradients suggest that the 3CD-processed expressions of the P1 region of PV53δ and PV57δ self-assembled into VLPs in plant. Approximate diameter of capsids also suggests that these VLPs have diameters of approximately 30 nm, which is typical of picornavirus VLPs (Table 5.1, Figures 5.5C and 5.5D).

Table 5.1. Measurements of PV diameters

Source	Particle (n)	Mean diameter (±S.D.)
HeLa cell-derived	Virion (20)	28 (± 3.1)
	EC (20)	32 (± 2.5)
Plant-expressed VLPs	PL-53 (11)	32 (± 4.7)
	PL-57 (11)	30 (± 3.8)

n = 20 ± SD

5.2.3. Thermal stability of plant-expressed VLPs

In order to determine the antigenic stability of plant-expressed PL-PV53δ and PL-PV57δ VLPs with reference to inactivated BRP vaccine standards, samples of PL-PV53δ, PL-PV57δ and BRP vaccine controls were incubated at a range of temperature (from 22°C to 60°C) for 30 minutes and cooled to 4°C. With the use of a polyclonal SH-16 capture antibody, N-specific 234 MAb as primary antibody and anti-mouse HRP conjugate as secondary, samples were assayed for antigenicity by capture ELISA (figures 5.6A and 5.6B). Samples were further immunoprecipitated using N-specific PVSP6A VHH followed by immunoblot assays against N-specific anti-VP0 PAb and anti-VP1 MAb, respectively (figures 5.6C and 5.6D).
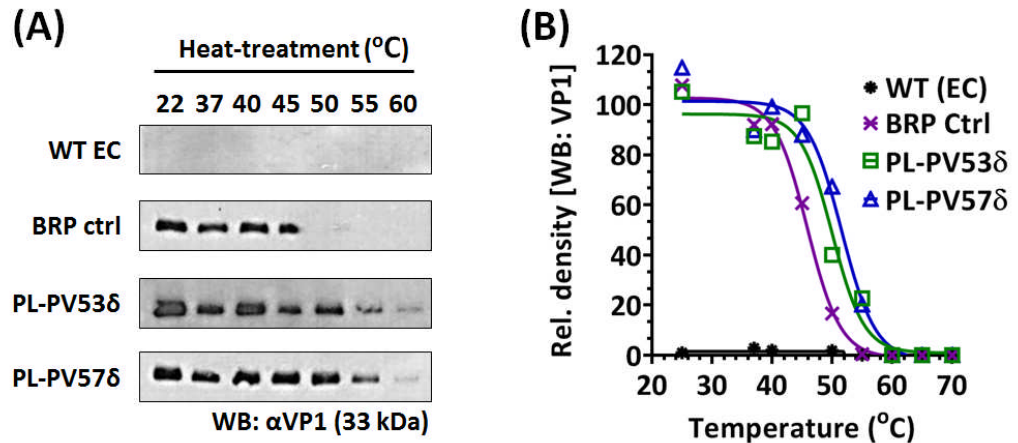
Figure 5.6. Antigenic stability of PL-PV53δ, PL-PV57δ VLPS. *Harvested particles were clarified by ultracentrifugation at 167,000 x g for 3 h at 4°C. Pellets were re-suspended in 1x PBS and incubated at a range of temperatures from 22 – 60 °C. Using N-specific anti-PV-1 nanonbodies (PVSP6A), samples were immobised onto HRP-conjugated IgG magnetic beads. Following a single wash step, beads were seperated from supernatant and boiled in SDS-loading buffer. Proteins were seperated by SDS-PAGE and immunoblotted against anti-VP1 MAb. Figure shows (A) Immunoblots of immunoprecipitated samples us against anti-PV-1 VP1 MAb (B) densinometric plots of 33 kDa VP1 bands shown on [A]. n = 2 ± S.D.*

As shown by immunoblots (figure 5.6), immunoprecipitated plant-expressed VLPs, PL-PV53δ and PL-PV57δ were more stable than current inactivated PV vaccine BRP controls.

5.2.4. How empty are the plant-expressed VLPs PL-PV53δ and PL-PV57δ

Studies have shown that PV ECs are EM stain-penetrable, while densely packed cores of virion particles are not (Boublik & Drzeniek, 1977; Li *et al.*, 2012a) (see figure 3.1C), however, the plant-expressed VLPs appeared to exclude stain (figure 5.5). The "empty" status of the VLPs was also analysed by optical density (OD) 260/280 ratio (Sommer *et al.*, 2003) (figure 5.7B) and by differential scanning fluorometric assays (PaSTRy) using SYTO9 nucleic acid-binding dye and SYPROorange protein-binding dye (Walter *et al.*, 2012) PaSTRy assay (Table 5.2 and figure 5.7). GuHCl-generated EC and virion samples of wt PV were also assayed as controls.

Table 5.2. The absorbence of VLPs were determined by OD

Source	Sample	Absorbance (260/280 ratio)
HeLa cell-derived	Virion	1.8
	EC	1.6
Plant-expressed VLPs	PL-53	1.3
	PL-57	1.4
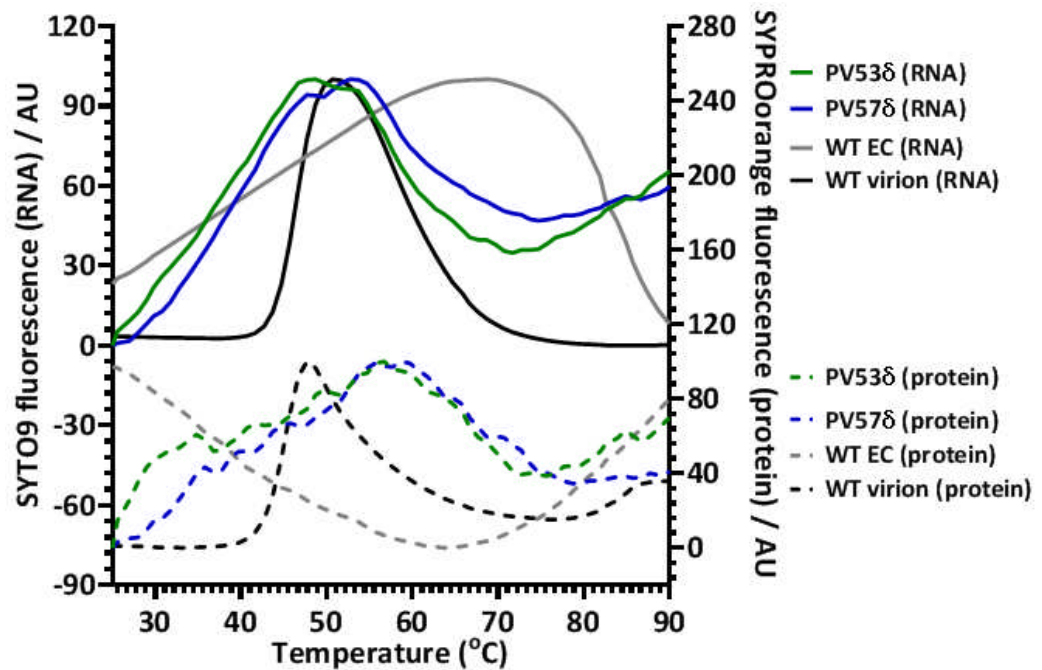
Figure 5.7. PaSTRy assay of plant-expressed LVPs. *Wild type PV-1 virion and EC as well as plan-expressed VLPs were purified through 15-45% sucrose density gradients. Respective peak fractions were assayed for fluorescence by a dual dye-binding thermofluor assay (PaSTRy) that employs the use of differential scanning for SYTO9 nucleic acid-binding dye and SYPROorange protein-binding dyes under buffered conditions with continuous temperature ramping from 25– 95 °C. Fluorescent reads are taken after a 1ºC increase every 30 seconds. Graph shows relative fluorescence of SYTO9 (solid lines) and SYPROorange (dotted lines) at temperature range.*

As shown by PaSTRy, PV-1 ECs do not have a virion-like SYTO9 [binding] fluorescence pattern (figure 5.8). Protein binding [SYPOOrange] pattern however shows a dip as shown in figure 5.7A. However, plant-expressed VLPs suggest that, although particles are PV genome-free, VLPs may package some nucleic acid fragments. Ratios OD 260/280, however suggest that particles may be similar to ECs.

5.3. Yeast expression

The production of VLP vaccines in recombinant yeast expression systems is well advanced with a number of yeast-expressed vaccines for animals, two licenced for human (i.e. HPV and HBV), and a number of other human VLP vaccines candidates at various stages se.g. pre-clinical trials of HIV and proof of principles for an immunogenic Dengue VLP vaccine (Kushnir *et al.*, 2012). A remarkable feat in this advancement was the discovery of a methanol auxotroph, *Pichia pastoris*, which has largely replaced the standard *Saccharomyces cerevisiae* expression system. This is largely due to the high growth rate, quick turnaround low cost of production, scalability, ability to produce post-translational modifications, and generally less complexities in the *P. pastoris* expression system (Weinacker *et al.*, 2013). Expression of non-infectious PV-1 VLPs have been attempted by co-transforming the P1 and 3CD coding regions into a recombinant *S. cerevisiae* (Rombaut & Jore, 1997b), however, there still remains no successful PV VLP vaccine candidate.

5.3.1. Expressing non-cleavable 3CD in P. pastoris

In order to express the thermally-stable PV57δ in *P. pastoris*, a non-cleavable PV-1 3CD mutant (Bert L. Semler & Ypma-Wong, 1987) and the P1 region of PV57δ were codon-optimised to *P. pastoris* and commercially synthesised in zeocin-resistance pPINK and pPICzA vectors, respectively and flanked by unique restriction sites *Not*I and *Mlu*I on the 5' and 3' ends of the forward orientation. Plasmid construct pPINK-HT-3CD was transformed into *P. pastoris* and propagated in YPD media. Three colonies (9, 10 and 15) were selected and propagated in buffered glycerol-complex media (BMGY) at 28°C for 24 hours. Expression of 3CD proteins was induced by replacing the BMGY media with

buffered methanol-complex media (BMMY). Methanol was replenished every 24 hours and samples collected for analysis at various time intervals (figure 5.8).
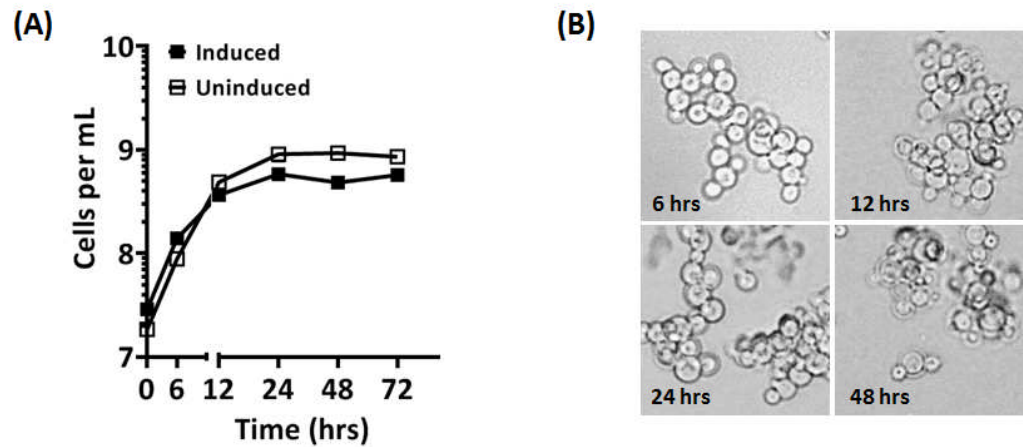
Figure 5.8. Expression of 3CD in P. pastoris. *WT Pichia pastoris strain 1 (pPINK kit, Invitrogen) was transformed with Pichia codon-optimised, linearised pPINK-LC-3CD (i.e. non-cleavable 3CD) plasmid. Expression of 3CD proteins was induced by replacing the BMGY media with buffered methanol-complex media (BMMY). Methanol was replenished every 24 hours and samples collected for analysis at various time intervals. Figure shows (A) Growth curve of induced and un-induced protein-expressing colony 9 (B) Light micrograph of trypan blue-stained yeast cells, post-induction. Cells were stained with 0.4% trypan blue at 1:2 dilution and viewed under a light microscope at 400x magnification.*

Growth pattern of yeast cells as analysed by OD_{600} shows a lag phase, exponential phase and a stationary (figure 5.8A). Wet-preparation microscopy showed light cells represent dividing yeast cells, while dark cells represent dead yeast cells which take up the dye (figure 5.8B). Both results suggest that yeast-expressing cells followed a normal growth pattern and reached optimal numbers after 24 hours of propagation. It further suggests un-induced cells had higher numbers than induced cells.

Samples of induced and un-induced yeast cell were collected at 48 and 72 hours post-induction. Cells were lysed by NaOH-treatment and re-suspended in SDS-loading buffer. Samples were analysed by SDS-PAGE and western blot against an anti-PV-1 3CD polyclonal antibody. HeLa cells were infected with wt PV-1 and harvested at 6 and 20 hours post-infection (h.p.i.) and also analysed as positive ccontrols for expression of 3 CD (Figure 5.9).
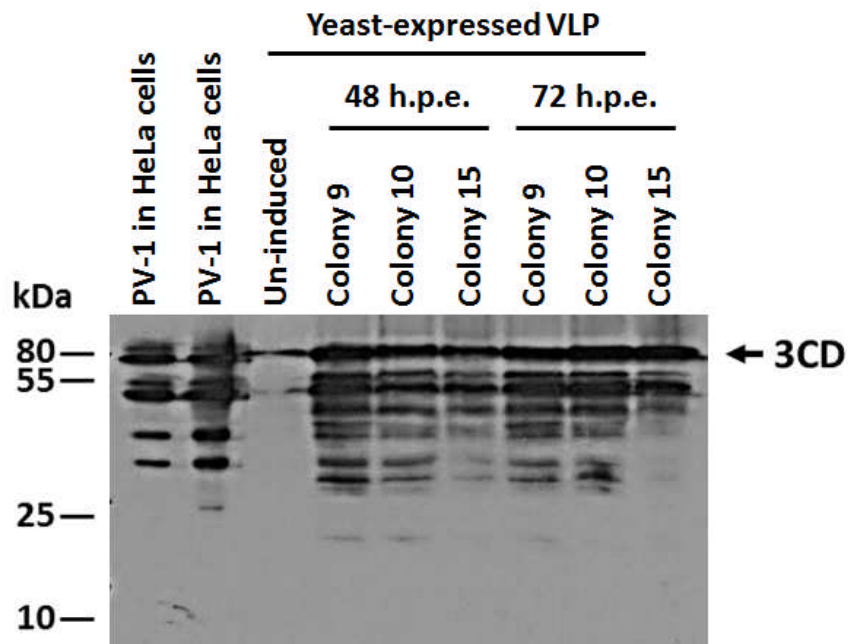
Figure 5.9. 3CD-expression in P. pastoris. Harvested samples of P. pastoris were lysed by NaOH treatment followed by boiling in SDS-loading buffer. Proteins were seperated by SPS-PAGE and immuno-blotted against 3CD. HeLa-cells infected with wt PV-1 werer also analysed on lanes 1 and 2 represeting 6 h.p.i. and 20 h.p.i., respectively. Figure shows 3CD bands on all lanes of methanol-induced yeast colonies.

Figure also suggests that *P. pastoris* tansformants expressed non-cleavable 3CD as shown by bands that correspond to sizes of non-cleaved 3CD in the 3 colonies analysed. Additional bands of cleaved 3CD were also seen.

5.3.2. VLP expression in P. pastoris:

Figure 5.10 shows an overview of the VLP expression system in recombinant *P. pastoris*.
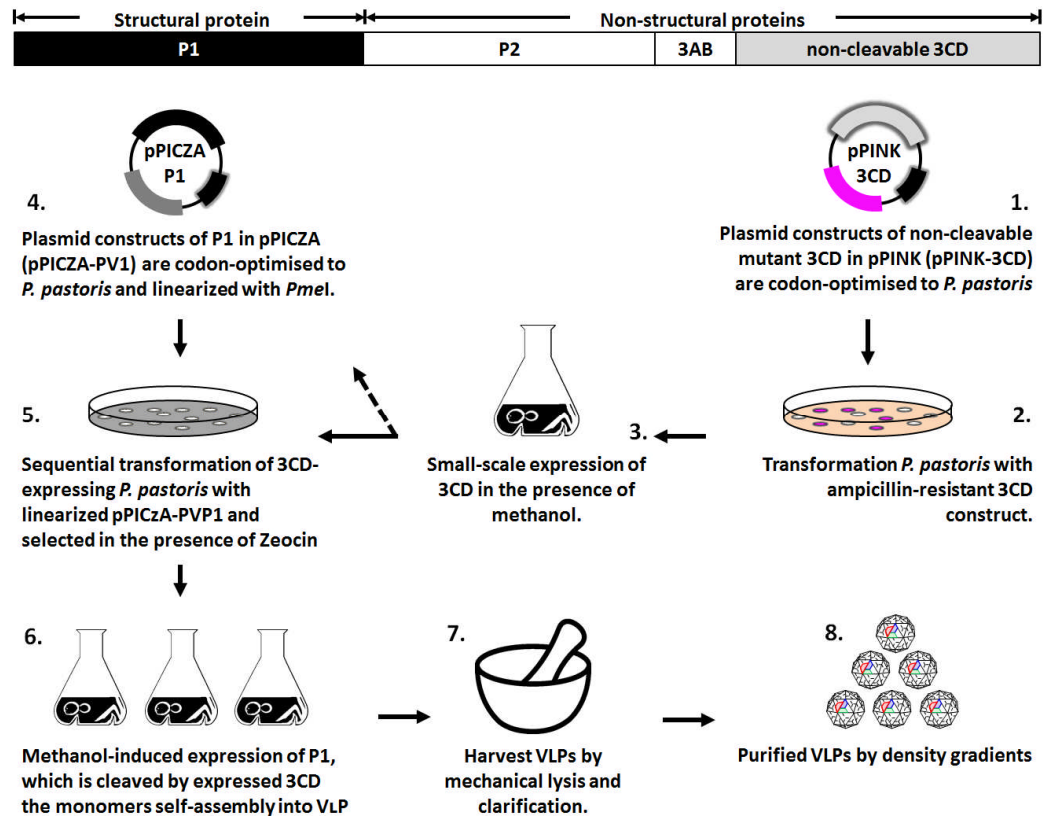
Figure 5.10. Yeast expression of PV57δ and PV57δ VLPs. *The PV genome highlighting the P1 [in black] and non-cleavable 3CD [in grey]. (1) A plasmid construct of a non-cleadable mutant 3CD cloned into pPINK-HT vector and codon-optimised to Pichia pastoris. (2) Competent P. pastoris were transformed with pPINK-HT-3CD. Zeocin-resistant pink colonies were selected. (3) Expression of 3CD in non-secretory P. pastoris was induced with methanol (4) The P1 region is cloned into Zeocin-resistant gene pPICzA and codon-optimised to P. pastoris. (5) Sequential transformation of 3CD-expressing P. pastoris with pPICzA-P1PV. (6) Transformed cells will be propagated in the presence of glycerol and protein expression induced in the presence of methanol at 28ºC for 72 hours with daily methanol replenishment. (7) Self-assembled VLPs will be harvested mechanical lysis and clarification (8) VLPs will be purified by density gradients.*

5.4. Cloning selectable marker for secondary transformation

Owing to the high cost of Zeocin for large-scale expression, a cheaper selectable alternative was sought for *P. pastoris* expressions. A study has demonstrated that protein expression using *P. pastoris* vectors is achievable using G-418 sulphate as the primary selectable marker by replacing the Zeocin-resistant marker gene (*Sh ble*) with selectable marker gene, *Tn903 Kam^R*, which also confers kanamycin-resistance in *E. coli* and G-418 resistance in yeast (Papakonstantinou *et al.*, 2009). Although the expression of *Tn903 Kam^R* in yeast and *E. coli* is initiated by GAPDH and *lac* Z promoters, respectively, (Agaphonov *et al.*, 2010) pPICzA vectors, initiate expression in yeast and *E. coli* using the TET7 and Em7 promoters, respectively.

5.4.1.1. Propagating Tn903 KamR gene in a sub-cloning vector (pCR-Blunt)

Prior to substitution of the zeocine marker gene *Sh ble* with the synthesised *Tn903 Kam^R* gene, a sub-cloning vector, designed with multiple cloning sites (pCR-Blunt), was cut downstream a T7 promoter at a unique restriction site using *Stu*I restriction enzyme. The *Tn903 Kam^R* was commercially synthesised with a non-phosphorylated blunt end and ligated into the linearized pCR-Blunt to yield pCR-BluntG418 construct, which was propagated in the presence of kanamycin (a selectable marker for pCR-Blunt). The presence of G418 insert was confirmed by diagnostic digest using *Not*I and *Mlu*I restriction enzymes (figure 5.9).
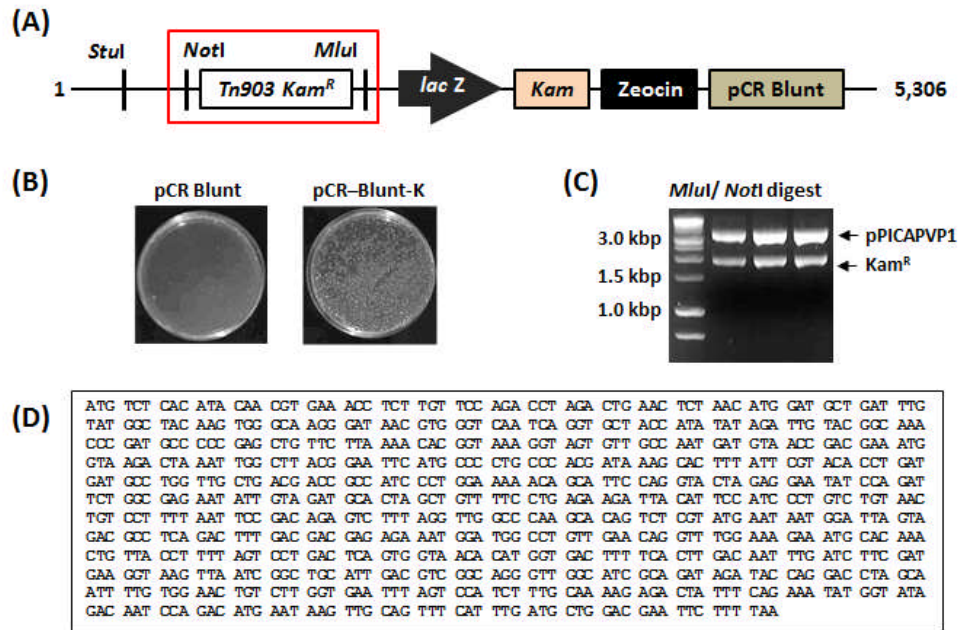
Figure 5.9. Sub-cloning the synthetic G-418 selectable marker gene (Tn903 KamR) into a pCR Blunt. *The G418 marker gene (Tn903 KamR) was codon-optimised to P. pastoris and commercially synthesised as a gene string flanked by NotI and MluI unique restriction sites on either side. (A) A schematic of plasmid constructs pCR Blunt – $^{MluI}G418^{NotI}$, showing the synthesised $^{MluI}G418^{NotI}$ insert (black), kanamycin selectable marker gene (light grey) and the remainder of the pCR Blunt plasmid (dark grey). Figure is not drawn to scale. (B) The synthetic KamR gene was ligated into a StuI-linearized sub-cloning vector (pCR Blunt) and transformed into E. coli DH5α competent cells in the presence of kanamycin. Figure shows linearized vector backbone without inserts and ligated transformants. (C) The presence of the KamR-insert was confirmed by diagnostic digest using NotI and MluI restriction enzymes followed by DNA agarose gel electrophoresis. (D) Sequenced colonies also confirmed the presence of KamR in the pCR-Blunt-K construct*

Positive colonies were also sequenced susing M13 primers to further confirm the presence of the G418 insert in the pCR-Blunt-K clones (figure 4D).

5.4.1.2. Converting pPICzA-PV57δP1 construct into pPICAG418-PV57δP1

In order to replace the zeocin-resistance gene (*Sh ble*) in pPICzA-PV57δP1 with the G418 selectable marker gene (*Tn903 Kam^R*), the band size that corresponded to *Kam^R* was excised and gel-purified from the DNA agarose gel of the double-digested pCR-BluntG418 clone. The pPICzA-PV57δP1 construct was also double digested with *Not*I and *Mlu*I. The band size that corresponded to the pPICA-PV57δP1 backbone was excised, gel-purified and de-phosphorylated. The gel-purified *Kam^R* gene was ligated into the de-phosphorylated vector backbone and transformed into *E. coli* DH5α competent cells and selected in the presence of G-418 sulphate (figure 5.9).
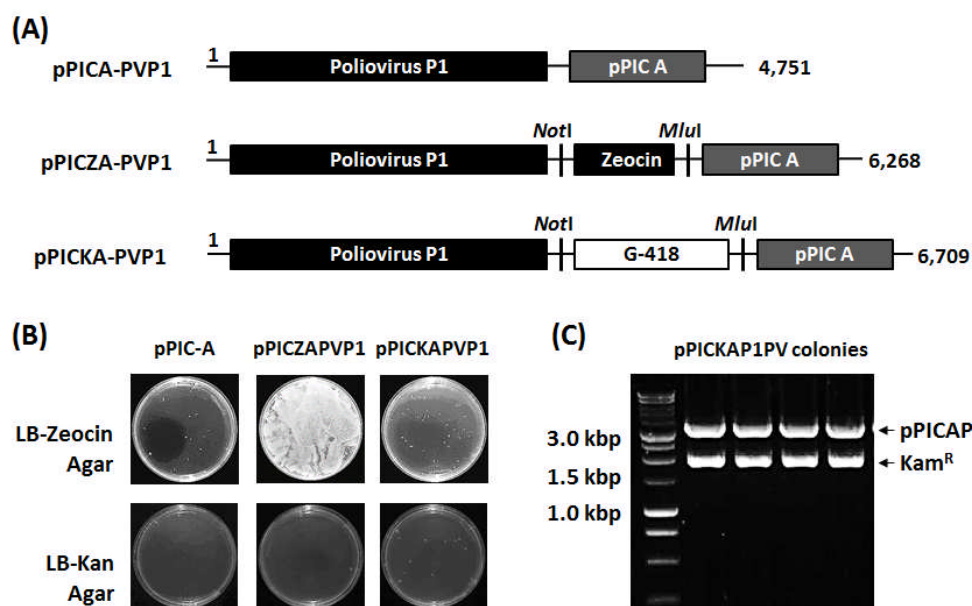
Figure 5.9. Replacing zeocin-resistant marker gene (Sh ble) in pPICzA with a G-418 selectable marker gene (Tn903 Kan^R). *The pPICzA-PV57δ plasmid construct was digested with NotI and MluI restriction enzymes and dephosphorylated. The gel-purified digested G-418 gene fragment was ligated into the dephosphorylated plasmid backbone to generate a pPICzA-G418-PV57δ construct. (A) Schematics of vector backbone without selection markers (pPICA-PVP1), plasmid construct with Zeocin as primary selectable marker (pPICzA-PVP1) and plasmid construct with G418 as primary selectable marker (pPICAKPVP1). Also shown are the PVP1 insert (black), Zeocin (dark grey), Kam^R (white), unique restriction sites NotI and MluI on either side of selectable marker genes, as well as the remainder of the pPIC A plasmid (light grey). Figure is not drawn to scale. (B) Vectors backbone were de-phosphorylated using caliph intestinal phosphate and selectable marker gene inserts were ligated using T4 DNA ligase. Competent DH5α cells were transformed with pPICA-PVP1, pPICzA-PVP1 and (pPICAKPVP1 constructs and selected in the presence of G418 sulphate (100 μg/ml) and Zeocin (25μg/ml), respectively. (C) Positive colonies from G-418 sulphate and Zeocin were screened by diagnostic digest using NotI and MluI restriction enzymes followed by DNA agarose gel electrophoresis. Figure shows band sizes that correspond to backbone vector with insert and respective selectable marker gene.*

The zeocine-resistant pPICzA-PV57δ construct yielded colonies in the presence of zeocine plates but did not yield colonies in the presence of G418 sulphate and vice versa for the G418 sulphate-resistant pPICzA-PV57δ construct. Corresponding band sizes from diagnostic digest using *Not*I and *Mlu*I restriction enzymes further corroborate this data. Colonies resistant to G418-sulphate were further sequenced and confirmed to be pPICKAPV57δ constructs. This process was also carrid out for the wt PV-1.

5.5. Discussion

In a polio-free world, the safest and ideal alternative to current polio vaccines would be a non-infectious, genome-free VLP vaccine, which would not require the use of life virus at any stage of production as do current OPV and IPV. Unfortunately, although immunogenic, the genome-free wt PV EC readily changes antigenicity from the native form to its non-native form at sub-physiological temperatures (Basavappa *et al.*, 1994b) even when expressed as VLPs in recombinant systems (Ansardi *et al.*, 1991c; Brautigam *et al.*, 1993b; Rombaut & Jore, 1997b). This antigenic switch (which can also be mimicked when the wt PV-1 virion is heated above 50°C), has been shown to be due to conformational changes at antigenic epitopes on the capsid (Le Bouvier, 1955; Shiomi *et al.*, 2004). In chapters three and four, the selection of three thermally-stable mutants was discussed. It was further shown that genome-free EC particles of thermally-selected mutants (generated by GuHCl-tretment) could retain the native form of antigenicity at temperatures above physiological degrees.

5.5.1. Plant expressed VLPs

Virus-like particles of two thermally-selected mutants (PV53δ and PV57δ) were expressed in recombinant *Nicotiana benthamiana* and harvested after 6 days at a high yield (i.e. mg/ ml). Plant-expressed VLPs were immunoprecipitate using the N-specific PVSP6A VHH, which have been shown [by cryo-electron microscopic analysis of VHH-PV complexes] to bind within the PV-1 canyon to sites that overlap the PVR-binding, thus inhibiting attachment and uncoating of PV particles (Schotte *et al.*, 2015; Thys *et al.*, 2010) thus, making them ideal for affinity purification of assembled particles.

172

The presence of anti-PV-1 N-specific VP-1 bands as shown by immunoblots on all lanes (including BRP vaccine controls), suggests that plant-expressed P1 region of PL-PV53δ and PL-PV57δ have been processed by mutant 3CD and self-assembled into particles having the native conformation. In the PV morphogenesis, virion particles do not have VP-0 present due to the cleavage of VP-0 into VP-2 and VP-4 at RNA encapsidation, however, the presence of non-cleaved VP-0 present in an assembled particle remains a hallmark of genome-free capsid EC or VLP particles (Hogle, 2002a; Jiang *et al.*, 2014). The presence of VP-0 bands in the immunoprecipitated PL-PV53δ and PL-PV57δ, but absent from the BRP vaccine controls (which are inactivated virion particles) suggest that the immunoprecipitated particles were genome-free VLPs. The plant-expressed VLPs were shown by immunoprecipitation assays to be more thermally stable than BRP vaccine controls.

5.5.2. Yeast-expressed VLPs

The use of P. pastoris has been largely influenced by its enabling post-translational modifications, quick turnaround, low production cost, scalability and less complexities (Weinacker *et al.*, 2013). Previous attempts to express wt PV-1 in *S. cerevisiae* resulted to loss in the native form of antigenicity due to the non-stable EC and were stabilised using a pyridazine analogue, pirodavir (ethyl 4-[2-(1-[6-methyl-3-pyridazinyl]-4-piperidinyl)ethoxy]benzoate) (De Palma *et al.*, 2008b; Rombaut & Jore, 1997b).

Chapter 6

Conclusion and future work

6.1. Thermal selection of antigenically stable PV-1

6.1.1. The potential of a PV VLP vaccine

Owing to the ability of OPV to revert to virulence as well as recombine with other enteroviruses to regain virulence (Liu *et al.*, 2013; WHO, 2005b) polio eradication strategies have resorted to the use of IPV. Further still, production of OPV as well as IPV require the stockpiling of live PV and as a result, the continued use and production of both vaccines post-eradication, constitutes a biological hazard. Ideally, a post-eradication PV vaccine should be PV genome-free, and would not require the use of live virus at any stage of production. The uses of subunit vaccines have been shown to meet these requirements for other viruses (Noad & Roy, 2003; Pushko *et al.*, 2013), however, antigenic epitopes across PV capsid subunits require a native conformation (Lin *et al.*, 2013b).

Although genome-free EC are produced naturally in the course of the PV life cycle (Hogle, 2002b; Jiang *et al.*, 2014), they readily change antigenicity from the N- to an H-form (Basavappa *et al.*, 1994b) and this has been a challenge for a PV VLP vaccine. The roles of PV EC are not fully understood, however, if stabilised, they could form the basis of a PV VLP vaccine.

This study applied an evolutionary selective approach to selecting for thermally-stable PV-1 that were were assayed by infectivity, thus aiming to ensure that the particles retained native conformation.

6.1.2. Thermal selection and bottlenecks

The thermal inactivation profile (figure 3.1) of the PV-1 suggests that this population comprised a quasi-species of viruses. Over 90% of the population lost infectivity at 46ºC, about 10% of the remaining population could withstand thermal stress between 47ºC and 50ºC, while the most thermally-stable viruses

175

within the pool (which comprised about 10% of the remaining) could withstand thermal stress up to 51°C. This data agrees with the theory of quasi-species which suggests that genetically-linked viruses are distributed around a consensus sequence [of the most fit genome] within a population of viruses (Lauring *et al.*, 2013b). Therefore the population of viruses was forced through temperature bottlenecks (Fares, 2015; Lauring *et al.*, 2013b) in a step-wise manner (figure 3.2) that captured evolving intermediates of three thermally stable pools of minority viruses [VS51, VS53 and VS57] within the wt population (Isakov *et al.*, 2015). Thermal inactivation profiles of VS51, VS53 and V557 further corroborate this submission suggesting that these pools of viruses represent populations.

Evolution of RNA viruses is a rapid process (Domingo & Holland, 1994) that is driven by a selection pressure (Andino & Domingo, 2015a). In this study, virus samples were incubated for 30 minutes at defined temperatures in order to select for thermally stable viruses. The selection pressure was increased gradually from 51°C through 53°C to 57°C in order to build up populations of thermally stable viruses, which may have been lost in the absence of a gradual build from 51°C. Using this approach VS57 was selected after a total of 32 cumulative selection cycles but at a fitness cost. This data further agrees with studies that suggest a fitness cost over selection (Andino & Domingo, 2015a; Belshaw *et al.*, 2008; Domingo, 2000; Domingo & Holland, 1994; Lázaro *et al.*, 2003).

6.1.3. Limitations of approach

As viruses evolve and adapt to their changing environment, there is usually a fitness cost (Crotty & Andino, 2002; Fares, 2015). Following cycles of infections, post-selection, thermally stable variants were selected whilst retaining

the ability to undergo full infectious cycles. Through this approach, only viruses that could complete an infectious cycle were selected and shown to be thermally and antigenically stable as corroborated by means of a biological (infectivity] assay (figure 3.4), biochemical (PaSTRy) assay (figure 3.5) and an antigenicity (immunoprecipitation) assay (figure 3.8). Owing to the increased thermal stability of the virion particles, EC particles of selected viruses VS51, V53 and VS57 could withstand temperatures above physiological while retaining the native antigenic conformation (figure 3.8). Non-infectious viruses were not selected through this approach.

6.1.4. Mutations and the PV capsid stability

Capsid-stabilising mutations were identified by sequencing the P1-region of the genome using the Sanger methods. The stabilising effects of V1087A have been referred to previously (Shiomi *et al.*, 2004). It has been shown that he 194th residue of VP1 is associated with loss of infectivity in PV-2 and PV-3 (Liu *et al.*, 2012c). It is however not fully understood how a combination of both mutations resulted to a thermally-stable EC. However, it is speculated that substitutions to smaller residues within the VP1 pocket of EV71 that correspond to similar substitutions in PV-1 may result in a thermally stable virus (Kelly *et al.*, 2015). The presence of both mutations [V1087A and I1194V] in all selected viruses (i.e. VS51, V53 and VS57) in addition to other mutations in V53 and VS57, however, suggests the importance of these mutations in stabilising the capsid.

6.1.5. Significance of mutations to serotype specificity

PV types 2 and PV-3 share the highest homology (figure 4.2) and have been shown to be more thermally-stable than PV-1 by prolonged incubation at 50°C (Youngner, 1957). However, of all mutations identified in the selected mutants, a

mutation that occurred in VS57 resulted to a conserved residue in PV-2 and PV-3 (i.e. S1097P) – a known H-antigenic antibody binding site.

6.1.6. Sub-conclusion

Through thermal selection, the PV-1 EC has been stabilised by selecting for thermally-stable viruses encoding structural mutations within the virus pocket, at inter-pentameric residues as well as inter-monomeric residues within the viral capsid. Selected variants were infectious and had thermally and antigenically stable ECs similar to IPV (Adeyemi *et al.*, 2016).

6.2. Thermally evolving PV-1

Recombination is also involved in the evolution of viruses. The occurrence of recombined virus chimeras in the presence or absence of genome replication also suggests that such events should not be overlooked (Simon-Loriere & Holmes, 2011) however, in the evolution of PV serotypes, recombination events may be significantly different (section 4.1.1). While recombination is a common occurrence among polioviruses and enteroviruses (Kew *et al.*, 2005; Lauring *et al.*, 2013b; Rakoto-Andrianarivelo *et al.*, 2007)., the lack of supportive data about the existence of antigenic chimeras of intra/inter-typical enteroviruses (Jenkins *et al.*, 1990; Martín *et al.*, 2002; Minor *et al.*, 1990; Tao *et al.*, 2010) suggest that recombination does not occur within the structural coding region of the PV genome.

6.2.1. Capturing an evolving population

The thermal section approach adopted in this study required growing the surviving virus after a prolonged heat-treatment. Using this approach, the aim was to select for thermally-stable infectious PV-1 by de-selecting thermally-labile and non-infectious variants. Post-selection, the serial passages of thermally-stable viruses suggested that selected thermally-stable populations were genetically stable (figure 4.4) although at a fitness cost (sections 3.6 and 4.21).

6.2.2. Alternative selection approaches

An alternative approach adopted by collaborators at the National Institute of Biological Standards and Control (NIBSC) involved the introduction of PV-3 IPV-attenuating mutations in combination with other identified thermal-stabilising mutations (Minor *et al.*, 1989). By means of deep sequencing, reverse

mutants were further selected from a pool of thermally-labile viruses and were shown to be thermally stable. Through their approach, Fox *et al*, 2017 (in press) were able to show that enhanced thermal stability resulted in loss of infectivity – which corroborates our findings with regards to the fitness cost (sections 3.6 and 4.21).

6.2.3. Sub-conclusion

This study suggests that PV51, PV53 and PV57 were present in the wt population and could be detected by deep sequencing the wt population. However, selected combinations that make-up PV51, PV53 and PV57 may not be readily easily identified by deep sequencing. By using our approach of gradually increasing the selection pressure, identified capsid-stabling mutations could be introduced into recombinant expression systems, for the synthesis of antigenically stable PV VLPs.

6.3. VLP expression

6.3.1. The need for a post-eradication polio vaccine

A major component of the polio endgame involves strategic proactive measures to address biosafety concerns of possible re-introduction of PV, post-eradication (Grassly, 2013; Orenstein *et al.*, 2002). Top on the agenda is the containment of PV within restricted access biomedical facilities (Wolff *et al.*, 2014). As a prelude to this, the replacement of tOPV with bOPV and mOPV (Garon *et al.*, 2016; Pons-Salort *et al.*, 2016) will be closely followed by a global switch from OPV to IPV (Hampton *et al.*, 2016; Patel *et al.*, 2015). All these measures, hint of a drive towards an entirely polio-free world. While these measures are entirely plausible, IPV production still requires the large-scale propagation of PV, which could inadvertently become biological hazards in a polio-free world.

Owing to its ability to replicate within the host gut (Dowdle & Birmingham, 1997) and thereby provide mucosal immunity (Holmgren & Czerkinsky, 2005) OPV prevents person-to-person transmission, and remains the most efficient outbreak-response vaccine (Duintjer Tebbens *et al.*, 2016; Thompson & Duintjer Tebbens, 2014). This was recently tested in the European outbreak of 2010 (Baicus, 2012a; WHO Country Office Tajikistan, 2010). This notwithstanding, its ability to revert to virulence as well as recombine with other enteroviruses to regain virulence (Kew *et al.*, 2005; Liu *et al.*, 2013; Lukashev, 2010; Rakoto-Andrianarivelo *et al.*, 2007; WHO, 2005b) makes the use of OPV a possible biological hazard, post-eradication of polio. As a result of the repetitiveness of antigenic epitopes that mimic the virion, VLP vaccines have been shown to elicit both humoral and cellular immune responses unaided (Chen & Lai, 2013; Pushko *et al.*, 2013).

6.3.2. Recombinant expressions

6.3.2.1. Plant expression

The high expression levels of N-antigenic PL-PV53δ and PL-PV57δ VLPs in recombinant plant systems make this approach ideal for scale up. The plant-expressed VLPs were shown to be more thermally-stable than current IPV vaccines, maintaining the N-antigenic conformation up to temperatures as high as 50°C (Figure 5.6).

In addition to its ability to regain virulence by reversion and recombination with other enteroviruses, (Liu *et al.*, 2013; WHO, 2005b), OPV can be inactivated at elevated temperatures (Rombaut *et al.*, 1994). This has informed the need to maintain a cold chain for its potency as a vaccine, which is a major challenge to developing economies (Kartoglu & Milstien, 2014) that has resulted in vaccine wastages (Shrivastava *et al.*, 2012; Yakum *et al.*, 2015). The use of thermally-stable vaccines has been recommended among other intervention strategies (Kartoglu & Milstien, 2014). If stabilised further, the thermally-stable VLP vaccine candidates would be most ideal post-eradication, in most climatic conditions.

6.3.2.2. Yeast expression

Expression of PV53δ and PV57δ in yeast (*P. pastoris*) is ongoing. Our approach involved the sequential transformation of the 3CD containing pPIK-HC and the P1 containing pPICZA under independent selectable markers (i.e. PAD and Zeocin, respectively). Owing to the high cost of Zeocin, we have sought to replace the Zeocin-resistance gene with an alternative selectable marker G418 which could further reduce the production cost at scale up.

6.3.3. Future work

6.3.3.1. Optimisation of the yeast-expression

Owing to the antigenically unstable wt PV-1 EC a non-secretory yeast expression strategy was adopted, however, a recent study suggests that secretory yeast-expressed Coxsackievirus A16 (CA16) VLPs were immunogenic in mice (Feng *et al.*, 2016). In addition, studies have also shown that multi-layered constructs of the P1 and 3CD separated by a repeat of the PAOX1 promoter within a single vector resulted in higher yields of EV71 (Zhang *et al.*, 2015) and CA16 (Zhang *et al.*, 2016a). As an alternate strategy to a multi-layered approach separation of the P1 and 3CD region by an IRES or 2A could also be attempted as a comparative measure for yield. Adoption of these approaches as a future strategy could reduce the production cost and time.

6.3.3.2. Stabilising the VP1 pocket

The use of capsid-stabilising drugs to enhance PV VLP stability was demonstrated with the use of pirodavir, which binds the VP1 hydrophobic pocket (Rombaut & Jore, 1997b). The use of other capsid-stabilising compounds such as NLD, ALD and GPP3 have also been demonstrated by binding to the EV71 pocket (De Colibus *et al.*, 2014). Such pocket-stabilising compounds could further stabilise the VLPs a future approach to enhancing the thermal stability of the expressed VLP vaccines.

6.3.4. Study limitations

The size of a virus capsid is suggested to be determined by the packaged genome size, both of which have been observed to be directly proportional among viruses (Kennedy & Parks, 2009; Lošdorfer Božič *et al.*, 2013; Zandi & van der Schoot, 2009). This phenomenon may be contributory to interactions between the nucleic acid and the capsid during morphogenesis of the virion capsids (Hesketh *et al.*, 2015; Jacobson & Baltimore, 1968; Rombaut *et al.*, 1986). However, the assembly of genome-free capsids as well as VLPs, has not been fully understood (Hesketh *et al.*, 2015). While this study has demonstrated that the recombinantly expressed PV VLPs were genome-free capsids in the native conformation, it has not been demonstrated that expressed VLPs have not packaged recombinant host nucleic material.

Although N-specific PV particles have been shown to be immunogenic (Ferguson *et al.*, 1993), this study has not shown immunogenicity data from the expressed VLPs; this is currently ongoing with collaborators at the NIBSC. While a PV VLP vaccine may be an ideal alternative for the virus-derived IPV and OPV, its ability to induce mucosal immune response has not been tested in this study.

6.4. Concluding remarks

This study has demonstrated the possibility of a genome-free thermally-stable polio VLP vaccine and has contributed to possible approaches of stabilising virion capsids in the design of future VLP vaccines. Two vaccine candidates have been expressed in recombinant plant systems and have been shown to be more thermally stable than current IPV.

The enhanced thermal stability of PL-PV53δ and PL-PV57δ over the excipient-free BRP vaccine standards, suggests that these VLPs would remain stable even in hot climates and may be ideal vaccine candidates.

References

Acevedo, A., Brodsky, L. & Andino, R. (2014). Mutational and fitness landscapes of an RNA virus revealed through population sequencing. *Nature* **505**, 686-+.

Adams, M. J., Lefkowitz, E. J., King, A. M. Q., Harrach, B., Harrison, R. L., Knowles, N. J., Kropinski, A. M., Krupovic, M., Kuhn, J. H., Mushegian, A. R., Nibert, M., Sabanadzovic, S., Sanfaçon, H., Siddell, S. G., Simmonds, P., Varsani, A., Zerbini, F. M., Gorbalenya, A. E. & Davison, A. J. (2016). Ratification vote on taxonomic proposals to the International Committee on Taxonomy of Viruses (2016). *Arch Virol* **161**, 2921-2949.

Adeyemi, O. O., Nicol, C., Stonehouse, N. J. & Rowlands, D. J. (2016). Increasing type-1 poliovirus capsid stability by thermal selection. *Journal of virology.*

Agaphonov, M., Romanova, N., Choi, E. S. & Ter-Avanesyan, M. (2010). A novel kanamycin/G418 resistance marker for direct selection of transformants in Escherichia coli and different yeast species. *Yeast* **27**, 189-195.

Agudelo-Romero, P., Carbonell, P., Perez-Amador, M. A. & Elena, S. F. (2008). Virus adaptation by manipulation of host's gene expression. *Plos One* **3**, e2397.

Ahmad, M., Hirz, M., Pichler, H. & Schwab, H. (2014). Protein expression in Pichia pastoris: recent achievements and perspectives for heterologous protein production. *Applied Microbiology and Biotechnology* **98**, 5301-5317.

Aldabe, R., Barco, A. & Carrasco, L. (1996). Membrane Permeabilization by Poliovirus Proteins 2B and 2BC. *J Biol Chem* **271**, 23134-23137.

Almeida, J. D., Brand, C. M., Edwards, D. C. & Heath, T. D. (1975). Formation of Virosomes from Influenza Subunits and Liposomes. *Lancet* **2**, 899-901.

Andino, R. & Domingo, E. (2015a). Viral quasispecies. *Virology* **479**, 46-51.

Andino, R. & Domingo, E. (2015b). Viral quasispecies. *Virology* **479-480**, 46-51.

Andino, R., Rieckhof, G. E., Achacoso, P. L. & Baltimore, D. (1993). Poliovirus RNA synthesis utilizes an RNP complex formed around the 5'-end of viral RNA. *The EMBO Journal* **12**, 3587-3598.

Andries, K., Dewindt, B., Snoeks, J., Willebrords, R., van Eemeren, K., Stokbroekx, R. & Janssen, P. A. (1992). In vitro activity of pirodavir (R 77975), a substituted phenoxy-pyridazinamine with broad-spectrum antipicornaviral activity. *Antimicrob Agents Chemother* **36**, 100-107.

Andries, K., Rombaut, B., Dewindt, B. & Boeye, A. (1994). Discrepancy between Infectivity and Antigenicity Stabilization of Oral Poliovirus

Vaccine by a Capsid-Binding Compound. *Journal of virology* **68**, 3397-3400.

Ansardi, D. C., Porter, D. C. & Morrow, C. D. (1991a). Coinfection with Recombinant Vaccinia Viruses Expressing Poliovirus-P1 and Poliovirus-P3 Proteins Results in Polyprotein Processing and Formation of Empty Capsid Structures. *Journal of virology* **65**, 2088-2092.

Ansardi, D. C., Porter, D. C. & Morrow, C. D. (1991b). Coinfection with Recombinant Vaccinia Viruses Expressing Poliovirus-P1 and Poliovirus-P3 Proteins Results in Polyprotein Processing and Formation of Empty Capsid Structures. *Journal of virology* **65**, 2088-2092.

Ansardi, D. C., Porter, D. C. & Morrow, C. D. (1991c). Coinfection with recombinant vaccinia viruses expressing poliovirus P1 and P3 proteins results in polyprotein processing and formation of empty capsid structures. *Journal of virology* **65**, 2088-2092.

Baicus, A. (2012a). History of polio vaccination. *World Journal of Virology* **1**, 108-114.

Baicus, A. (2012b). History of Polio vaccination. *World J Virol* **1**, 108-114.

Banerjee, R. & Dasgupta, A. (2001). Interaction of picornavirus 2C polypeptide with the viral negative-strand RNA. *J Gen Virol* **82**, 2621-2627.

Bang, H. B., Lee, Y. H., Lee, Y. J. & Jeong, K. J. (2016). High-Level Production of Human Papillomavirus (HPV) Type 16 L1 in Escherichia coli. *J Microbiol Biotechn* **26**, 356-363.

Bao, Y., Chetvernin, V. & Tatusova, T. (2012). PAirwise Sequence Comparison (PASC) and Its Application in the Classification of Filoviruses. *Viruses* **4**, 1318-1327.

Bao, Y., Chetvernin, V. & Tatusova, T. (2014). Improvements to pairwise sequence comparison (PASC): a genome-based web tool for virus classification. *Arch Virol* **159**, 3293-3304.

Barco, A. & Carrasco, L. (1998). Identification of regions of poliovirus 2BC protein that are involved in cytotoxicity. *Journal of virology* **72**, 3560-3570.

Barton, D. J. & Flanegan, J. B. (1997). Synchronous replication of poliovirus RNA: initiation of negative-strand RNA synthesis requires the guanidine-inhibited activity of protein 2C. *Journal of virology* **71**, 8482-8489.

Barton, D. J., O'Donnell, B. J. & Flanegan, J. B. (2001). 5′ cloverleaf in poliovirus RNA is a cis-acting replication element required for negative-strand synthesis. *The EMBO Journal* **20**, 1439-1448.

Basavappa, R., Gomez-Yafal, A. & Hogle, J. M. (1998a). The poliovirus empty capsid specifically recognizes the poliovirus receptor and undergoes some, but not all, of the transitions associated with cell entry. *Journal of virology* **72**, 7551-7556.

Basavappa, R., Gomez-Yafal, A. & Hogle, J. M. (1998b). The poliovirus empty capsid specifically recognizes the poliovirus receptor and undergoes some, but not all, of the transitions associated with cell entry. *Journal of virology* **72**, 7551-7556.

Basavappa, R., Syed, R., Flore, O., Icenogle, J. P., Filman, D. J. & Hogle, J. M. (1994a). Role and mechanism of the maturation cleavage of VP0 in poliovirus assembly: structure of the empty capsid assembly intermediate at 2.9 A resolution. *Protein science : a publication of the Protein Society* **3**, 1651-1669.

Basavappa, R., Syed, R., Flore, O., Icenogle, J. P., Filman, D. J. & Hogle, J. M. (1994b). ROLE AND MECHANISM OF THE MATURATION CLEAVAGE OF VPO IN POLIOVIRUS ASSEMBLY - STRUCTURE OF THE EMPTY CAPSID ASSEMBLY INTERMEDIATE AT 2.9-ANGSTROM RESOLUTION. *Protein Sci* **3**, 1651-1669.

Baum, E. Z., Bebernitz, G. A., Palant, O., Mueller, T. & Plotch, S. J. (1991). Purification, properties, and mutagenesis of poliovirus 3C protease. *Virology* **185**, 140-150.

Bellocq, C., Kean, K. M., Fichot, O., Girard, M. & Agut, H. (1987). Multiple Mutations Involved in the Phenotype of a Temperature-Sensitive Small-Plaque Mutant of Poliovirus. *Virology* **157**, 75-82.

Belnap, D. M., Filman, D. J., Trus, B. L., Cheng, N., Booy, F. P., Conway, J. F., Curry, S., Hiremath, C. N., Tsang, S. K., Steven, A. C. & Hogle, J. M. (2000a). Molecular tectonic model of virus structural transitions: the putative cell entry states of poliovirus. *Journal of virology* **74**, 1342-1354.

Belnap, D. M., McDermott, B. M., Filman, D. J., Cheng, N., Trus, B. L., Zuccola, H. J., Racaniello, V. R., Hogle, J. M. & Steven, A. C. (2000b). Three-dimensional structure of poliovirus receptor bound to poliovirus. *P Natl Acad Sci USA* **97**, 73-78.

Belsham, G. J. (2009). Divergent picornavirus IRES elements. *Virus Res* **139**, 183-192.

Belshaw, R., Gardner, A., RarnbaUt, A. & Pybus, O. G. (2008). Pacing a small cage: mutation and RNA viruses. *Trends Ecol Evol* **23**, 188-193.

Bert L. Semler, V. H. J., Patricia Gillis Dewalt, and & Ypma-Wong, M. F. (1987). Site-Specific Mutagenesis of cDNA Clones Expressing a Poliovirus Proteinase. *J Cell Biochem* **33**, 39-51.

Bhattacharya, S. & Mazumder, B. (2011). Virosomes: A Novel Strategy for Drug Delivery and Targeting. *Biopharm Int* **24**, S9-+.

Bienz, K., Egger, D. & Pasamontes, L. (1987). Association of polioviral proteins of the P2 genomic region with the viral replication complex and virus-induced membrane synthesis as visualized by electron microscopic immunocytochemistry and autoradiography. *Virology* **160**, 220-226.

Blomqvist, S., Bruu, A. L., Stenvik, M. & Hovi, T. (2003). Characterization of a recombinant type 3 type 2 poliovirus isolated from a healthy vaccinee and containing a chimeric capsid protein VP1. *J Gen Virol* **84**, 573-580.

Bock, M. & Stoye, J. P. (2000). Endogenous retroviruses and the human germline. *Curr Opin Genet Dev* **10**, 651-655.

Boros, Á., Kiss, T., Kiss, O., Pankovics, P., Kapusinszky, B., Delwart, E. & Reuter, G. (2013). Genetic characterization of a novel picornavirus distantly related to the marine mammal-infecting aquamaviruses in a

long-distance migrant bird species, European roller (Coracias garrulus). *The Journal of general virology* **94**, 2029-2035.

Boros, A., Pankovics, P., Adonyi, A., Phan, T. G., Delwart, E. & Reuter, G. (2014a). Genome characterization of a novel chicken picornavirus distantly related to the members of genus Avihepatovirus with a single 2A protein and a megrivirus-like 3 ' UTR. *Infect Genet Evol* **28**, 333-338.

Boros, Á., Pankovics, P., Knowles, N. J., Nemes, C., Delwart, E. & Reuter, G. (2014b). Comparative Complete Genome Analysis of Chicken and Turkey Megriviruses (Family Picornaviridae): Long 3′ Untranslated Regions with a Potential Second Open Reading Frame and Evidence for Possible Recombination. *Journal of virology* **88**, 6434-6443.

Bostina, M., Levy, H., Filman, D. J. & Hogle, J. M. (2011). Poliovirus RNA Is Released from the Capsid near a Twofold Symmetry Axis. *Journal of virology* **85**, 776-783.

Boublik, M. & Drzeniek, R. (1977). Structural Subunits of Poliovirus Particles by Electron-Microscopy. *J Gen Virol* **37**, 127-134.

Brandenburg, B., Lee, L. Y., Lakadamyali, M., Rust, M. J., Zhuang, X. & Hogle, J. M. (2007a). Imaging poliovirus entry in live cells. *Plos Biol* **5**, e183.

Brandenburg, B., Lee, L. Y., Lakadamyali, M., Rust, M. J., Zhuang, X. W. & Hogle, J. M. (2007b). Imaging poliovirus entry in live cells. *Plos Biol* **5**, 1543-1555.

Brautigam, S., Snezhkov, E. & Bishop, D. H. (1993a). Formation of poliovirus-like particles by recombinant baculoviruses expressing the individual VP0, VP3, and VP1 proteins by comparison to particles derived from the expressed poliovirus polyprotein. *Virology* **192**, 512-524.

Brautigam, S., Snezhkov, E. & Bishop, D. H. L. (1993b). Formation of Poliovirus-Like Particles by Recombinant Baculoviruses Expressing the Individual Vp0, Vp3 and Vp1 Proteins by Comparison to Particles Derived from the Expressed Poliovirus Polyprotein. *Virology* **192**, 512-524.

Breindl, M. (1971). Structure of Heated Poliovirus Particles. *J Gen Virol* **11**, 147-&.

Bubeck, D., Filman, D. J., Cheng, N. Q., Steven, A. C., Hogle, J. M. & Belnap, D. M. (2005). The structure of the poliovirus 135S cell entry intermediate at 10-Angstrom resolution reveals the location of an externalized polypeptide that binds to membranes. *Journal of virology* **79**, 7745-7755.

Büchen-Osmond, C. (2006). Picornaviridae. In *ICTVdB - The Universal Virus Database,*, p. 00.052. New York, USA: Columbia University.

Bundy, B. C., Franciszkowicz, M. J. & Swartz, J. R. (2008). Escherichia coli-based cell-free synthesis of virus-like particles. *Biotechnol Bioeng* **100**, 28-37.

Bunimovich-Mendrazitsky, S. & Stone, L. (2005). Modeling polio as a disease of development. *J Theor Biol* **237**, 302-315.

Burgon, T. B., Jenkins, J. A., Deitz, S. B., Spagnolo, J. F. & Kirkegaard, K. (2009). Bypass Suppression of Small-Plaque Phenotypes by a Mutation in Poliovirus 2A That Enhances Apoptosis. *Journal of virology* **83**, 10129-10139.

Burnet, F. M. & MacNamara, J. (1931). Immunological differences between strains of poliomyelitic virus. *Brit J Exp Pathol* **12**, 57-61.

Burr, H. S. (1942). Neural Mechanisms in Poliomyelitis. *The Yale Journal of Biology and Medicine* **14**, 565-565.

Byme, B. (2015). Pichia pastoris as an expression host for membrane protein structural biology. *Curr Opin Struc Biol* **32**, 9-17.

Campagnola, G., McDonald, S., Beaucourt, S., Vignuzzi, M. & Peersen, O. B. (2015). Structure-Function Relationships Underlying the Replication Fidelity of Viral RNA-Dependent RNA Polymerases. *Journal of virology* **89**, 275-286.

Carleton, H. A. (2011). Putting Together the Pieces of Polio: How Dorothy Horstmann Helped Solve the Puzzle. *The Yale Journal of Biology and Medicine* **84**, 83-89.

Carter, R. W. & Sanford, J. C. (2012). A new look at an old virus: patterns of mutation accumulation in the human H1N1 influenza virus since 1918. *Theor Biol Med Model* **9**.

Cassel (1913). Heine-Medin disease (Poliomyelitis and polioencephalitis acuta epidemica). *Deut Med Wochenschr* **39**, 2507-2509.

CDC (2001). Apparent global interruption of wild poliovirus type 2 transmission, pp. 222-224. Washington DC, USA: Center for Disease Control.

CDC (2009). *Epidemiology and Prevention of Vaccine-Preventable Diseases.* . Washington DC, USA: Public Health Foundation.

CDC (2012). Poliomyelitis. USA: CDC.

Chen, Q. & Lai, H. (2013). Plant-derived virus-like particles as vaccines. *Human Vaccines & Immunotherapeutics* **9**, 26-49.

Chen, S. B., Songkumarn, P., Liu, J. L. & Wang, G. L. (2009). A Versatile Zero Background T-Vector System for Gene Cloning and Functional Genomics. *Plant Physiol* **150**, 1111-1121.

Chomczynski, P. & Sacchi, N. (2006). The single-step method of RNA isolation by acid guanidinium thiocyanate-phenol-chloroform extraction: twenty-something years on. *Nature protocols* **1**, 581-585.

Circolo, A. & Gulati, S. (2009). Autoradiography and Fluorography of Acrylamide Gels. *Springer Protoc Hand*, 595-603.

Clark, M. E., Lieberman, P. M., Berk, A. J. & Dasgupta, A. (1993). Direct Cleavage of Human Tata-Binding Protein by Poliovirus Protease 3c Invivo and Invitro. *Mol Cell Biol* **13**, 1232-1237.

Combelas, N., Holmblat, B., Joffret, M. L., Colbere-Garapin, F. & Delpeyroux, F. (2011). Recombination between Poliovirus and Coxsackie A Viruses of Species C: A Model of Viral Genetic Plasticity and Emergence. *Viruses-Basel* **3**, 1460-1484.

Cornell, C. T., Perera, R., Brunner, J. E. & Semler, B. L. (2004). Strand-specific RNA synthesis determinants in the RNA-dependent RNA polymerase of poliovirus. *Journal of virology* **78**, 4397-4407.

Cregg, J. M., Barringer, K. J., Hessler, A. Y. & Madden, K. R. (1985). Pichia pastoris as a host system for transformations. *Mol Cell Biol* **5**, 3376-3385.

Cross, G. F. (1912). Acute anterior poliomyelitis in South West Norfolk. *Brit Med J* **1912**, 721-722.

Crotty, S. & Andino, R. (2002). Implications of high RNA virus mutation rates: lethal mutagenesis and the antiviral drug ribavirin. *Microbes Infect* **4**, 1301-1307.

Davis, M. P., Bottley, G., Beales, L. P., Killington, R. A., Rowlands, D. J. & Tuthill, T. J. (2008). Recombinant VP4 of human rhinovirus induces permeability in model membranes. *Journal of virology* **82**, 4169-4174.

De Colibus, L., Wang, X., Spyrou, J. A. B., Kelly, J., Ren, J., Grimes, J., Puerstinger, G., Stonehouse, N., Walter, T. S., Hu, Z., Wang, J., Li, X., Peng, W., Rowlands, D. J., Fry, E. E., Rao, Z. & Stuart, D. I. (2014). More-powerful virus inhibitors from structure-based analysis of HEV71 capsid-binding molecules. *Nature structural & molecular biology* **21**, 282-288.

de Crom, S. C. M., Rossen, J. W. A., van Furth, A. M. & Obihara, C. C. (2016). Enterovirus and parechovirus infection in children: a brief overview. *European Journal of Pediatrics* **175**, 1023-1029.

De Jesus, N. H. (2007). Epidemics to eradication: the modern history of poliomyelitis. *Virol J* **4**.

de Jong, A. S., de Mattia, F., Van Dommelen, M. M., Lanke, K., Melchers, W. J. G., Willems, P. H. G. M. & van Kuppeveld, F. J. M. (2008). Functional Analysis of Picornavirus 2B Proteins: Effects on Calcium Homeostasis and Intracellular Protein Trafficking. *Journal of virology* **82**, 3782-3790.

de Marco, A. (2011). Biotechnological applications of recombinant single-domain antibody fragments. *Microb Cell Fact* **10**.

De Palma, A. M., Pürstinger, G., Wimmer, E., Patick, A. K., Andries, K., Rombaut, B., De Clercq, E. & Neyts, J. (2008a). Potential Use of Antiviral Agents in Polio Eradication. *Emerg Infect Dis* **14**, 545-551.

De Palma, A. M., Vliegen, I., De Clercq, E. & Neyts, J. (2008b). Selective Inhibitors of Picornavirus Replication. *Med Res Rev* **28**, 823-884.

Dieffenbach, C. W., Lowe, T. M. J. & Dveksler, G. S. (1993). General Concepts for Pcr Primer Design. *Pcr Meth Appl* **3**, S30-S37.

Doedens, J. R., Giddings, T. H. & Kirkegaard, K. (1997). Inhibition of endoplasmic reticulum-to-Golgi traffic by poliovirus protein 3A: genetic and ultrastructural analysis. *Journal of virology* **71**, 9054-9064.

Doedens, J. R. & Kirkegaard, K. (1995). Inhibition of cellular protein secretion by poliovirus proteins 2B and 3A. *The EMBO Journal* **14**, 894-907.

Domingo, E. (2000). Viruses at the edge of adaptation. *Virology* **270**, 251-253.

Domingo, E. & Holland, J. (1994). Mutations and Rapid Evolution of RNA Viruses, pp. 161-184.

dos Reis, M., Tamuri, A. U., Hay, A. J. & Goldstein, R. A. (2011). Charting the Host Adaptation of Influenza Viruses. *Mol Biol Evol* **28**, 1755-1767.

Dove, A. W. & Racaniello, V. R. (2000). An antiviral compound that blocks structural transitions of poliovirus prevents receptor binding at low temperatures. *Journal of virology* **74**, 3929-3931.

Dowdle, W. R. & Birmingham, M. E. (1997). The biologic principles of poliovirus eradication. *J Infect Dis* **175**, S286-S292.

Duintjer Tebbens, R. J., Pallansch, M. A., Wassilak, S. G. F., Cochi, S. L. & Thompson, K. M. (2016). Characterization of outbreak response strategies and potential vaccine stockpile needs for the polio endgame. *BMC Infect Dis* **16**, 137.

Dulbecco, R. & Vogt, M. (1954). Plaque formation and isolation of pure lines with poliomyelitis viruses. *J Exp Med* **99**, 167-182.

Eggers, H. J. (1999). Milestones in early poliomyelitis research (1840 to 1949). *Journal of virology* **73**, 4533-4535.

Elde, N. C. (2012). Poliovirus Evolution: The Strong, Silent Type. *Cell Host Microbe* **12**, 605-606.

Elena, S. F., Agudelo-Romero, P. & Lalic, J. (2009). The evolution of viruses in multi-host fitness landscapes. *The open virology journal* **3**, 1-6.

Enders, J. F., Weller, T. H. & Robbins, F. C. (1949). Cultivation of the Lansing Strain of Poliomyelitis Virus in Cultures of Various Human Embryonic Tissues. *Science* **109**, 85-87.

Equbal, M. J., Srivastava, P., Agarwal, G. P. & Deb, J. K. (2013). Novel expression system for Corynebacterium acetoacidophilum and Escherichia coli based on the T7 RNA polymerase-dependent promoter. *Applied Microbiology and Biotechnology* **97**, 7755-7766.

Erasmus, M. (2011). Viral Infections of the Central Nervous System: Viral infections of the CNS are caused by a broad range of viruses. *Continuing Medical Education* **29**, 190-193.

Fares, M. A. (2015). Survival and innovation: The role of mutational robustness in evolution. *Biochimie* **119**, 254-261.

Feng, Q. J., He, Y. Q. & Lu, J. H. (2016). Virus-Like Particles Produced in Pichia Pastoris Induce Protective Immune Responses Against Coxsackievirus A16 in Mice. *Med Sci Monitor* **22**, 3370-3382.

Ferguson, M., Wood, D. J. & Minor, P. D. (1993). Antigenic Structure of Poliovirus in Inactivated Vaccines. *J Gen Virol* **74**, 685-690.

Fitzpatrick, M. (2006). The Cutter Incident: How America's First Polio Vaccine Led to a Growing Vaccine Crisis. *Journal of the Royal Society of Medicine* **99**, 156-156.

Flexner, S. (1910a). Lumbar puncture in poliomyelitis. *J Amer Med Assoc* **55**, 1397-1397.

Flexner, S. (1910b). Wanted: Specimens of nervous system from fatal cases of poliomyelitis. *J Amer Med Assoc* **55**, 878-878.

Flexner, S. & Amoss, H. L. (1914). LOCALIZATION OF THE VIRUS AND PATHOGENESIS OF EPIDEMIC POLIOMYELITIS. *The Journal of Experimental Medicine* **20**, 249-268.

Flexner, S. & Clark, P. F. (1911). Experimental poliomyelitis in monkeys - Ninth note - Immunity principles, effects of hexamethylenamin (uroiropin), early diagnosis, virus carriers. *J Amer Med Assoc* **56**, 585-587.

Flexner, S. & Lewis, P. A. (1910a). Epidemic poliomyelitis in monkeys - A mode of spontaneous infection. *J Amer Med Assoc* **54**, 535-535.

Flexner, S. & Lewis, P. A. (1910b). Experimental poliomyelitis in monkeys - Eight note: Further contributions to the subjects of immunization and serum therapy. *J Amer Med Assoc* **55**, 662-663.

Florea, N. R., Maglio, D. & Nicolau, D. P. (2003). Pleconaril, a novel antipicornaviral agent. *Pharmacotherapy* **23**, 339-348.

Forss, S. & Schaller, H. (1982). A tandem repeat gene in a picornavirus. *Nucleic Acids Res* **10**, 6441-6450.

Fricks, C. E. & Hogle, J. M. (1990). Cell-induced conformational change in poliovirus: externalization of the amino terminus of VP1 is responsible for liposome binding. *Journal of virology* **64**, 1934-1945.

Frost, W. H. (1913). *Epidemiologic studies of acute anterior poliomyelitis: I. Poliomyelitis in Iowa, 1910. II. Poliomyelitis in Cincinnati, Ohio, 1911. III. Poliomyelitis in Buffalo and Batavia, NY, 1912*: US Government Printing Office.

Gallei, A., Pankraz, A., Thiel, H. J. & Becher, P. (2004). RNA recombination in vivo in the absence of viral replication. *Journal of virology* **78**, 6271-6281.

Gan, S. D. & Patel, K. R. (2013). Enzyme immunoassay and enzyme-linked immunosorbent assay. *The Journal of investigative dermatology* **133**, e12.

Gard, S. (1960). Theoretical Considerations in the Inactivation of Viruses by Chemical Means. *Annals of the New York Academy of Sciences* **83**, 638-648.

Garon, J., Seib, K., Orenstein, W. A., Gonzalez, A. R., Blanc, D. C., Zaffran, M. & Patel, M. (2016). Polio endgame: the global switch from tOPV to bOPV. *Expert Review of Vaccines* **15**, 693-708.

Gebauer, F., de la Torre, J. C., Gomes, I., Mateu, M. G., Barahona, H., Tiraboschi, B., Bergmann, I., de Mello, P. A. & Domingo, E. (1988). Rapid selection of genetic and antigenic variants of foot-and-mouth

disease virus during persistence in cattle. *Journal of virology* **62**, 2041-2049.

Ghafoor, S. & Sheikh, N. (2016). Eradication and Current Status of Poliomyelitis in Pakistan: Ground Realities. *Journal of Immunology Research* **2016**, 6837824.

Glass, J. D., Samuels, O. & Rich, M. M. (2002). Poliomyelitis due to West Nile virus. *New Engl J Med* **347**, 1280-1281.

Gmyl, A. P., Belousov, E. V., Maslova, S. V., Khitrina, E. V., Chetverin, A. B. & Agol, V. I. (1999). Nonreplicative RNA recombination in poliovirus. *Journal of virology* **73**, 8958-8965.

Gmyl, A. P., Korshenko, S. A., Belousov, E. V., Khitrina, E. V. & Agol, V. I. (2003). Nonreplicative homologous RNA recombination: Promiscuous joining of RNA pieces? *Rna* **9**, 1221-1231.

Goh, K. C. M., Tang, C. K., Norton, D. C., Gan, E. S., Tan, H. C., Sun, B., Syenina, A., Yousuf, A., Ong, X. M., Kamaraj, U. S., Cheung, Y. B., Gubler, D. J., Davidson, A., St John, A. L., Sessions, O. M. & Ooi, E. E. (2016). Molecular determinants of plaque size as an indicator of dengue virus attenuation. *Sci Rep-Uk* **6**.

Goodfellow, I. (2011). The genome-linked protein VPg of vertebrate viruses - a multifaceted protein. *Current opinion in virology* **1**, 355-362.

Goodfellow, I. G., Kerrigan, D. & Evans, D. J. (2003). Structure and function analysis of the poliovirus cis-acting replication element (CRE). *Rna* **9**, 124-137.

Graham, K. L., Gustin, K. E., Rivera, C., Kuyumcu-Martinez, N. M., Choe, S. S., Lloyd, R. E., Sarnow, P. & Utz, P. J. (2004). Proteolytic cleavage of the catalytic subunit of DNA-dependent protein kinase during poliovirus infection. *Journal of virology* **78**, 6313-6321.

Grassly, N. C. (2013). The final stages of the global eradication of poliomyelitis. *Philosophical Transactions of the Royal Society B: Biological Sciences* **368**.

Gregori, J., Perales, C., Rodriguez-Frias, F., Esteban, J. I., Quer, J. & Domingo, E. (2016). Viral quasispecies complexity measures. *Virology* **493**, 227-237.

Guttman, N. & Baltimore, D. (1977). Morphogenesis of Poliovirus .4. Existence of Particles Sedimenting at 150s and Having Properties of Provirion. *Journal of virology* **23**, 363-367.

Hampton, L. M., Farrell, M., Ramirez-Gonzalez, A., Menning, L., Shendale, S., Lewis, I., Rubin, J., Garon, J., Harris, J., Hyde, T., Wassilak, S., Patel, M., Nandy, R., Chang-Blanc, D. & Eradication, G. P. (2016). Cessation of Trivalent Oral Poliovirus Vaccine and Introduction of Inactivated Poliovirus Vaccine - Worldwide, 2016. *Mmwr-Morbid Mortal W* **65**, 934-938.

Hansen, J. L., Long, A. M. & Schultz, S. C. (1997). Structure of the RNA-dependent RNA polymerase of poliovirus. *Structure* **5**, 1109-1122.

Harris, K. S., Xiang, W. K., Alexander, L., Lane, W. S., Paul, A. V. & Wimmer, E. (1994). Interaction of Poliovirus Polypeptide 3cd(Pro) with the 5'-Termini and 3'-Termini of the Poliovirus Genome - Identification of Viral and Cellular Cofactors Needed for Efficient Binding. *J Biol Chem* **269**, 27004-27014.

He, Y. N., Mueller, S., Chipman, P. R., Bator, C. M., Peng, X. Z., Bowman, V. D., Mukhopadhyay, S., Wimmer, E., Kuhn, R. J. & Rossmann, M. G. (2003). Complexes of poliovirus serotypes with their common cellular receptor, CD155. *Journal of virology* **77**, 4827-4835.

Health, N. I. o. (2016). ClinicalTrials.gov USA: National Institutes of Health.

Herold, J. & Andino, R. (2001). Poliovirus RNA Replication Requires Genome Circularization through a Protein–Protein Bridge. *Mol Cell* **7**, 581-591.

Hesketh, E. L., Meshcheriakova, Y., Dent, K. C., Saxena, P., Thompson, R. F., Cockburn, J. J., Lomonossoff, G. P. & Ranson, N. A. (2015). Mechanisms of assembly and genome packaging in an RNA virus revealed by high-resolution cryo-EM. *Nature Communications* **6**, 10113.

Hewitt, R. M. (1912). ON ACUTE POLIOMYELITIS (HEINE-MEDIN'S DISEASE). *Brit Med J* **1**, 719-721.

Hogle, J. M. (2002a). Poliovirus cell entry: common structural themes in viral cell entry pathways. *Annu Rev Microbiol* **56**, 677-702.

Hogle, J. M. (2002b). Poliovirus cell entry: Common structural themes in viral cell entry pathways. *Annu Rev Microbiol* **56**, 677-702.

Hogle, J. M., Chow, M. & Filman, D. J. (1985). 3-DIMENSIONAL STRUCTURE OF POLIOVIRUS AT 2.9 A RESOLUTION. *Science* **229**, 1358-1365.

Holmes, E. C. (2011). What Does Virus Evolution Tell Us about Virus Origins? *Journal of virology* **85**, 5247-5251.

Holmgren, J. & Czerkinsky, C. (2005). Mucosal immunity and vaccines. *Nat Med* **11**, S45-S53.

Horner, L. M., Poulter, M. D., Brenton, J. N. & Turner, R. B. (2015). Acute Flaccid Paralysis Associated with Novel Enterovirus C105. *Emerg Infect Dis* **21**, 1858-1860.

Horstmann, D. M. (1952). Poliomyelitis Virus in Blood of Orally Infected Monkeys and Chimpanzees. *P Soc Exp Biol Med* **79**, 417-419.

Horstmann, D. M. (1985). The Poliomyelitis Story - a Scientific Hegira. *Yale J Biol Med* **58**, 79-90.

Huang, Z., Chen, Q., Hjelm, B., Arntzen, C. & Mason, H. (2009). A DNA replicon system for rapid high-level production of virus-like particles in plants. *Biotechnol Bioeng* **103**, 706-714.

Iizuka, N., Kohara, M., Haginoyamagishi, K., Abe, S., Komatsu, T., Tago, K., Arita, M. & Nomoto, A. (1989). Construction of Less Neurovirulent Polioviruses by Introducing Deletions into the 5' Noncoding Sequence of the Genome. *Journal of virology* **63**, 5354-5363.

Initiative, G. P. E. (2013). Polio this week - As of 31 July 2013: Global Polio Eradication Initiative.

Isakov, O., Bordería, A. V., Golan, D., Hamenahem, A., Celniker, G., Yoffe, L., Blanc, H., Vignuzzi, M. & Shomron, N. (2015). Deep sequencing analysis of viral infection and evolution allows rapid and detailed characterization of viral mutant spectrum. *Bioinformatics* **31**, 2141-2150.

Jacobson, M. F. & Baltimor.D (1968). MORPHOGENESIS OF POLIOVIRUS .I. ASSOCIATION OF VIRAL RNA WITH COAT PROTEIN. *J Mol Biol* **33**, 369-&.

Jacobson, M. F. & Baltimore, D. (1968). Morphogenesis of Poliovirus .I. Association of Viral Rna with Coat Protein. *J Mol Biol* **33**, 369-+.

Jegouic, S., Joffret, M.-L., Blanchard, C., Riquet, F. B., Perret, C., Pelletier, I., Colbere-Garapin, F., Rakoto-Andrianarivelo, M. & Delpeyroux, F. (2009). Recombination between Polioviruses and Co-Circulating Coxsackie A Viruses: Role in the Emergence of Pathogenic Vaccine-Derived Polioviruses. *Plos Pathog* **5**, e1000412.

Jenkins, O., Cason, J., Burke, K. L., Lunney, D., Gillen, A., Patel, D., McCance, D. J. & Almond, J. W. (1990). An antigen chimera of poliovirus induces antibodies against human papillomavirus type 16. *Journal of virology* **64**, 1201-1206.

Jia, Y., Moudy, R. M., Dupuis, A. P., Ngo, K. A., Maffei, J. G., Jerzak, G. V. S., Franke, M. A., Kauffman, E. B. & Kramer, L. D. (2007). Characterization of a Small Plaque Variant of West Nile Virus Isolated in New York in 2000. *Virology* **367**, 339-347.

Jiang, P., Liu, Y., Ma, H. C., Paul, A. V. & Wimmer, E. (2014). Picornavirus morphogenesis. *Microbiology and molecular biology reviews : MMBR* **78**, 418-437.

John, T. J. (2001). Anomalous observations on IPV and OPV vaccination. *Dev Biol (Basel)* **105**, 197-208.

Jones, H. W., Mckusick, V. A., Harper, P. S. & Wuu, K. D. (1971). Gey,Go (1899-1970) - Hela Cell and a Reappraisal of Its Origin. *Obstet Gynecol* **38**, 945-&.

Jones, M. S., Lukashov, V. V., Ganac, R. D. & Schnurr, D. P. (2007). Discovery of a Novel Human Picornavirus in a Stool Sample from a Pediatric Patient Presenting with Fever of Unknown Origin. *J Clin Microbiol* **45**, 2144-2150.

Jurgens, C. K., Barton, D. J., Sharma, N., Morasco, B. J., Ogram, S. A. & Flanegan, J. B. (2006). 2Apro is a multifunctional protein that regulates the stability, translation and replication of poliovirus RNA. *Virology* **345**, 346-357.

Kanda, Y. & Melnick, J. L. (1959). Invitro Differentiation of Virulent and Attenuated Polioviruses by Their Growth Characteristics on Ms Cells. *J Exp Med* **109**, 9-&.

Kapusta, J., Modelska, A., Figlerowicz, M., Pniewski, T., Letellier, M., Lisowa, O., Yusibov, V., Koprowski, H., Plucienniczak, A. &

Legocki, A. B. (1999). A plant-derived edible vaccine against hepatitis B virus. *Faseb J* **13**, 1796-1799.

Karakasiliotis, I., Paximadi, E. & Markoulatos, P. (2005). Evolution of a rare vaccine-derived multirecombinant poliovirus. *J Gen Virol* **86**, 3137-3142.

Kartoglu, U. & Milstien, J. (2014). Tools and approaches to ensure quality of vaccines throughout the cold chain. *Expert Review of Vaccines* **13**, 843-854.

Katoh, K., Misawa, K., Kuma, K. & Miyata, T. (2002). MAFFT: a novel method for rapid multiple sequence alignment based on fast Fourier transform. *Nucleic Acids Res* **30**, 3059-3066.

Katpally, U. & Smith, T. J. (2007). Pocket Factors Are Unlikely To Play a Major Role in the Life Cycle of Human Rhinovirus. *Journal of virology* **81**, 6307-6315.

Kelly, J. T., De Colibus, L., Elliott, L., Fry, E. E., Stuart, D. I., Rowlands, D. J. & Stonehouse, N. J. (2015). Potent antiviral agents fail to elicit genetically-stable resistance mutations in either enterovirus 71 or Coxsackievirus A16. *Antiviral Research* **124**, 77-82.

Kemenesi, G., Zhang, D., Marton, S., Dallos, B., Görföl, T., Estók, P., Boldogh, S., Kurucz, K., Oldal, M., Kutas, A., Bányai, K. & Jakab, F. (2015). Genetic characterization of a novel picornavirus detected in Miniopterus schreibersii bats. *J Gen Virol* **96**, 815-821.

Kennedy, M. A. & Parks, R. J. (2009). Adenovirus Virion Stability and the Viral Genome: Size Matters. *Molecular Therapy: the Journal of the American Society of Gene Therapy* **17**, 1664-1666.

Kew, O. M., Sutter, R. W., de Gourville, E. M., Dowdle, W. R. & Pallansch, M. A. (2005). Vaccine-derived polioviruses and the endgame strategy for global polio eradication. In *Annu Rev Microbiol*, pp. 587-635. Palo Alto: Annual Reviews.

Kirchweger, R., Ziegler, E., Lamphear, B. J., Waters, D., Liebig, H. D., Sommergruber, W., Sobrino, F., Hohenadl, C., Blaas, D. & Rhoads, R. E. (1994). Foot-and-mouth disease virus leader proteinase: purification of the Lb form and determination of its cleavage site on eIF-4 gamma. *Journal of virology* **68**.

Kirienko A., P. A., Abdellatif I., Elbatrawy Y., Mostaf Z.M.A., Necc V (2011). Correction of poliomyelitis foot deformities with Ilizarov method. *Strat Traum Limb Recon* **6**, 107–120.

Kirkegaard, K. & Baltimore, D. (1986). The Mechanism of Rna Recombination in Poliovirus. *Cell* **47**, 433-443.

Kling, C. A., Wernstedt, W. E. & Pettersson, A. (1912). *Recherches sur le mode de propagation de la paralysie infantile épidémique (maladie de Heine-Medin).*

Knowles, N. J., Hovi, T, Hyypiä, T., King, A.M.Q., Lindberg, A.M., Pallansch, M.A., Palmenberg, A.C., Simmonds, P., Skern, T., Stanway, G., Yamashita, T. and Zell, R. (2012a). Picornaviridae. In *Virus Taxonomy: Classification and Nomenclature of Viruses: Ninth*

Report of the International Committee on Taxonomy of Viruses, pp. 855-880. Edited by A. M. Q. King, Adams, M.J., Carstens, E.B. and Lefkowitz, E.J. San Diego. USA: International Committee on Taxonomy of Viruses.

Knowles, N. J., Hovi, T, Hyypiä, T., King, A.M.Q., Lindberg, A.M., Pallansch, M.A., Palmenberg, A.C., Simmonds, P., Skern, T., Stanway, G., Yamashita, T. and Zell, R. (2012b). Picornaviridae. In *Virus Taxonomy: Classification and Nomenclature of Viruses: Ninth Report of the International Committee on Taxonomy of Viruses*, pp. 855-880. Edited by A. M. Q. King, Adams, M.J., Carstens, E.B. and Lefkowitz, E.J. San Diego.

Koch, G., Vanroozelaar, D. J., Verschueren, C. A. J., Vandereb, A. J. & Noteborn, M. H. M. (1995). Immunogenic and Protective Properties of Chicken Anemia Virus Proteins Expressed by Baculovirus. *Vaccine* 13, 763-770.

Kontermann, R. E. (2010). Alternative antibody formats. *Curr Opin Mol Ther* 12, 176-183.

Koonin, E. V., Dolja, V. V. & Krupovic, M. (2015). Origins and evolution of viruses of eukaryotes: The ultimate modularity. *Virology* 479, 2-25.

Kouiavskaia, D. V., Dragunsky, E. M., Liu, H. M., Oberste, M. S., Collett, M. S. & Chumakov, K. M. (2011). Immunological and pathogenic properties of poliovirus variants selected for resistance to antiviral drug V-073. *Antiviral therapy* 16, 999-1004.

Kushnir, N., Streatfield, S. J. & Yusibov, V. (2012). Virus-like particles as a highly efficient vaccine platform: Diversity of targets and production systems and advances in clinical development. *Vaccine* 31, 58-83.

Kyriakopoulou, Z., Kottaridi, C., Dedepsidis, E., Bolanaki, E., Levidiotou-Stefanou, S. & Markoulatos, P. (2006). Molecular characterization of wild-type polioviruses isolated in Greece during the 1996 outbreak in Albania. *J Clin Microbiol* 44, 1150-1152.

Landsteiner, K. & Levaditi, C. (1909). The transmission of infantile paralysis in monkeys. *Cr Soc Biol* 67, 592-594.

Lauring, A. S., Frydman, J. & Andino, R. (2013a). The role of mutational robustness in RNA virus evolution. *Nat Rev Micro* 11, 327-336.

Lauring, A. S., Frydman, J. & Andino, R. (2013b). The role of mutational robustness in RNA virus evolution. *Nat Rev Microbiol* 11, 327-336.

Lavinder, C. H., Freeman, A. W. & Frost, W. H. (1918). *Epidemiologic studies of poliomyelitis in New York City and the northeastern United States during the year 1916*: US Government Printing Office.

Lázaro, E., Escarmís, C., Pérez-Mercader, J., Manrubia, S. C. & Domingo, E. (2003). Resistance of virus to extinction on bottleneck passages: Study of a decaying and fluctuating pattern of fitness loss. *P Natl Acad Sci USA* 100, 10830-10835.

Le Bouvier, G. L. (1955). The modification of poliovirus antigens by heat and ultraviolet light. *Lancet* 269, 1013-1016.

Lebouvier, G. L. (1955). The Modification of Poliovirus Antigens by Heat and Ultraviolet Light. *Lancet* **2**, 1013-1016.

Levaditi, C. & Landsteiner, K. (1909). The transmission of poliomyelitis in chimpanzees. *Cr Hebd Acad Sci* **149**, 1014-1016.

Levy, H. C., Bostina, M., Filman, D. J. & Hogle, J. M. (2010). Catching a virus in the act of RNA release: a novel poliovirus uncoating intermediate characterized by cryo-electron microscopy. *Journal of virology* **84**, 4426-4441.

Ley, V., Higgins, J. & Fayer, R. (2002). Bovine Enteroviruses as Indicators of Fecal Contamination. *Applied and environmental microbiology* **68**, 3455-3461.

Li, C., Wang, J. C.-Y., Taylor, M. W. & Zlotnick, A. (2012a). In Vitro Assembly of an Empty Picornavirus Capsid follows a Dodecahedral Path. *Journal of virology* **86**, 13062-13069.

Li, C., Wang, J. C., Taylor, M. W. & Zlotnick, A. (2012b). In vitro assembly of an empty picornavirus capsid follows a dodecahedral path. *Journal of virology* **86**, 13062-13069.

Li, X., Lu, H.-H., Mueller, S. & Wimmer, E. (2001). The C-terminal residues of poliovirus proteinase 2Apro are critical for viral RNA replication but not for cis- or trans-proteolytic cleavage. *J Gen Virol* **82**, 397-408.

Liew, M. W. O., Rajendran, A. & Middelberg, A. P. J. (2010). Microbial production of virus-like particle vaccine protein at gram-per-litre levels. *J Biotechnol* **150**, 224-231.

Lin, J., Cheng, N., Hogle, J. M., Steven, A. C. & Belnap, D. M. (2013a). Conformational shift of a major poliovirus antigen confirmed by immuno-cryogenic electron microscopy. *Journal of immunology* **191**, 884-891.

Lin, J., Cheng, N. Q., Hogle, J. M., Steven, A. C. & Belnap, D. M. (2013b). Conformational Shift of a Major Poliovirus Antigen Confirmed by Immuno-Cryogenic Electron Microscopy. *J Immunol* **191**, 884-891.

Lin, S.-Y., Yeh, C.-T., Li, W.-H., Yu, C.-P., Lin, W.-C., Yang, J.-Y., Wu, H.-L. & Hu, Y.-C. (2015). Enhanced enterovirus 71 virus-like particle yield from a new baculovirus design. *Biotechnol Bioeng* **112**, 2005-2015.

Liu, F. X., Wu, X. D., Li, L., Liu, Z. S. & Wang, Z. L. (2013). Use of baculovirus expression system for generation of virus-like particles: Successes and challenges. *Protein Expres Purif* **90**, 104-116.

Liu, H.-M., Roberts, J. A., Moore, D., Anderson, B., Pallansch, M. A., Pevear, D. C., Collett, M. S. & Oberste, M. S. (2012a). Characterization of Poliovirus Variants Selected for Resistance to the Antiviral Compound V-073. *Antimicrob Agents Ch* **56**, 5568-5574.

Liu, H. M., Roberts, J. A., Moore, D., Anderson, B., Pallansch, M. A., Pevear, D. C., Collett, M. S. & Oberste, M. S. (2012b). Characterization of poliovirus variants selected for resistance to the antiviral compound V-073. *Antimicrob Agents Chemother* **56**, 5568-5574.

Liu, H. M., Roberts, J. A., Moore, D., Anderson, B., Pallansch, M. A., Pevear, D. C., Collett, M. S. & Oberste, M. S. (2012c). Characterization of Poliovirus Variants Selected for Resistance to the Antiviral Compound V-073. *Antimicrob Agents Ch* **56**, 5568-5574.

Liu, H. M., Zheng, D. P., Zhang, L. B., Oberste, M. S., Pallansch, M. A. & Kew, O. M. (2000). Molecular evolution of a type 1 wild-vaccine poliovirus recombinant during widespread circulation in China. *Journal of virology* **74**, 11153-11161.

Liu, Z., Tyo, K. E. J., Martínez, J. L., Petranovic, D. & Nielsen, J. (2012d). Different Expression Systems for Production of Recombinant Proteins in Saccharomyces cerevisiae. *Biotechnol Bioeng* **109**, 1259-1268.

Liu, Z. Q., Mahmood, T. & Yang, P. C. (2014). Western blot: technique, theory and trouble shooting. *North American journal of medical sciences* **6**, 160.

Lopez-Macias, C., Ferat-Osorio, E., Tenorio-Calvo, A., Isibasi, A., Talavera, J., Arteaga-Ruiz, O., Arriaga-Pizano, L., Hickman, S. P., Allende, M., Lenhard, K., Pincus, S., Connolly, K., Raghunandan, R., Smith, G. & Glenn, G. (2011). Safety and immunogenicity of a virus-like particle pandemic influenza A (H1N1) 2009 vaccine in a blinded, randomized, placebo-controlled trial of adults in Mexico. *Vaccine* **29**, 7826-7834.

Lošdorfer Božič, A., Šiber, A. & Podgornik, R. (2013). Statistical analysis of sizes and shapes of virus capsids and their resulting elastic properties. *Journal of Biological Physics* **39**, 215-228.

Love, A. J., Chapman, S. N., Matic, S., Noris, E., Lomonossoff, G. P. & Taliansky, M. (2012). In planta production of a candidate vaccine against bovine papillomavirus type 1. *Planta* **236**, 1305-1313.

Lua, L. H. L., Connors, N. K., Sainsbury, F., Chuan, Y. P., Wibowo, N. & Middelberg, A. P. J. (2014). Bioengineering virus-like particles as vaccines. *Biotechnol Bioeng* **111**, 425-440.

Lukashev, A. N. (2010). Recombination among picornaviruses. *Rev Med Virol* **20**, 327-337.

Lwoff, A. (1962). Thermosensitive Critical Event of Viral Cycle. *Cold Spring Harb Sym* **27**, 159-&.

MacLennan, C., Dunn, G., Huissoon, A. P., Kumararatne, D. S., Martin, J., O'Leary, P., Thompson, R. A., Osman, H., Wood, P., Minor, P., Wood, D. J. & Pillay, D. (2004). Failure to clear persistent vaccine-derived neurovirulent poliovirus infection in an immunodeficient man. *Lancet* **363**, 1509-1513.

Mamat, U., Wilke, K., Bramhill, D., Schromm, A. B., Lindner, B., Kohl, T. A., Corchero, J. L., Villaverde, A., Schaffer, L., Head, S. R., Souvignier, C., Meredith, T. C. & Woodard, R. W. (2015). Detoxifying Escherichia coli for endotoxin-free production of recombinant proteins. *Microbial Cell Factories* **14**, 57.

Manrubia, S. C., Escarmis, C., Domingo, E. & Lazaro, E. (2005). High mutation rates, bottlenecks, and robustness of RNA viral quasispecies. *Gene* **347**, 273-282.

Marc, D., Drugeon, G., Haenni, A. L., Girard, M. & van der Werf, S. (1989). Role of myristoylation of poliovirus capsid protein VP4 as determined by site-directed mutagenesis of its N-terminal sequence. *Embo J* **8**, 2661-2668.

Marongiu, M. E., Pani, A., Corrias, M. V., Sau, M. & La Colla, P. (1981). Poliovirus morphogenesis. I. Identification of 80S dissociable particles and evidence for the artifactual production of procapsids. *Journal of virology* **39**, 341-347.

Marschang, R. E. (2011). Viruses Infecting Reptiles. *Viruses* **3**, 2087-2126.

Marsian, J. & Lomonossoff, G. P. (2016). Molecular pharming — VLPs made in plants. *Curr Opin Biotech* **37**, 201-206.

Martin, J., Samoilovich, E., Dunn, G., Lackenby, A., Feldman, E., Heath, A., Svirchevskaya, E., Cooper, G., Yermalovich, M. & Minor, P. D. (2002). Isolation of an intertypic poliovirus capsid recombinant from a child with vaccine-associated paralytic poliomyelitis. *Journal of virology* **76**, 10921-10928.

Martín, J., Samoilovich, E., Dunn, G., Lackenby, A., Feldman, E., Heath, A., Svirchevskaya, E., Cooper, G., Yermalovich, M. & Minor, P. D. (2002). Isolation of an Intertypic Poliovirus Capsid Recombinant from a Child with Vaccine-Associated Paralytic Poliomyelitis. *Journal of virology* **76**, 10921-10928.

Martinez-Salas, E., Francisco-Velilla, R., Fernandez-Chamorro, J., Lozano, G. & Diaz-Toledano, R. (2015). Picornavirus IRES elements: RNA structure and host protein interactions. *Virus Res* **206**.

Marx, A., Glass, J. D. & Sutter, R. W. (2000). Differential diagnosis of acute flaccid paralysis and its role in poliomyelitis surveillance. *Epidemiol Rev* **22**, 298-316.

Meghrous, J., Mahmoud, W., Jacob, D., Chubet, R., Cox, M. & Kamen, A. A. (2009). Development of a simple and high-yielding fed-batch process for the production of influenza vaccines. *Vaccine* **28**, 309-316.

Melnick, J. L. (1947). Poliomyelitis Virus in Urban Sewage in Epidemic and in Nonepidemic Times. *Am J Hyg* **45**, 240-253.

Melnick, J. L. (1996). Current status of poliovirus infections. *Clinical Microbiology Reviews* **9**, 293-300.

Mikhejev.A & Ghendon, Y. (1974). Influence of Supraoptimal Temperature on Poliovirus Type-1 Mahoney Strain Reproduction. *Archiv Fur Die Gesamte Virusforschung* **45**, 65-77.

Miller, S. E. (1986). Detection and Identification of Viruses by Electron-Microscopy. *J Electron Micr Tech* **4**, 265-301.

Minor, P. (2014). The polio endgame. *Human Vaccines & Immunotherapeutics* **10**, 2106-2108.

Minor, P. D., Dunn, G., Evans, D. M. A., Magrath, D. I., John, A., Howlett, J., Phillips, A., Westrop, G., Wareham, K., Almond, J. W. & Hogle, J. M. (1989). The Temperature Sensitivity of the Sabin Type 3 Vaccine Strain of Poliovirus: Molecular and Structural Effects of a Mutation in the Capsid Protein VP3. *J Gen Virol* **70**, 1117-1123.

Minor, P. D., Ferguson, M., Evans, D. M., Almond, J. W. & Icenogle, J. P. (1986). Antigenic structure of polioviruses of serotypes 1, 2 and 3. *J Gen Virol* **67 (Pt 7)**, 1283-1291.

Minor, P. D., Ferguson, M., Katrak, K., Wood, D., John, A., Howlett, J., Dunn, G., Burke, K. & Almond, J. W. (1990). Antigenic Structure of Chimeras of Type-1 and Type-3 Poliovirus Involving Antigenic Site-1. *J Gen Virol* **71**, 2543-2551.

Minor, P. D., Ferguson, M., Evans, D.M.A., Almond, J.W., and Icenogle, J.P. (1986). Antigenic Structure of Polioviruses of Serotypes I, 2 and 3. *J Gen Virol* **67**, 1283-1291.

Mohr, J., Chuan, Y. P., Wu, Y., Lua, L. H. L. & Middelberg, A. P. J. (2013). Virus-like particle formulation optimization by miniaturized high-throughput screening. *Methods* **60**, 248-256.

Morales, M., Tangermann, R. H. & Wassilak, S. G. F. (2016). Progress Toward Polio Eradication - Worldwide, 2015-2016 (vol 65, pg 470, 2016). *Mmwr-Morbid Mortal W* **65**, 502-502.

Morein, B., Helenius, A., Simons, K. & Schirrmacher, V. (1979). Virus spike protein complexes and virosomes as effective subunit vaccines. *Advances in experimental medicine and biology* **114**, 811-816.

Mosser, A. G., Sgro, J. Y. & Rueckert, R. R. (1994). Distribution of drug resistance mutations in type 3 poliovirus identifies three regions involved in uncoating functions. *Journal of virology* **68**, 8193-8201.

Muehlenbachs, A., Bhatnagar, J. & Zaki, S. R. (2015). Tissue tropism, pathology and pathogenesis of enterovirus infection. *J Pathol* **235**, 217-228.

Mueller, J. E., Bessaud, M., Huang, Q. S., Martinez, L. C., Barril, P. A., Morel, V., Balanant, J., Bocacao, J., Hewitt, J., Gessner, B. D., Delpeyroux, F. & Nates, S. V. (2009). Environmental Poliovirus Surveillance during Oral Poliovirus Vaccine and Inactivated Poliovirus Vaccine Use in Cordoba Province, Argentina. *Applied and environmental microbiology* **75**, 1395-1401.

Mueller, S., Wimmer, E. & Cello, J. (2005). Poliovirus and poliomyelitis: a tale of guts, brains, and an accidental event. *Virus Res* **111**, 175-193.

Muhire, B. M., Varsani, A. & Martin, D. P. (2014). SDT: A Virus Classification Tool Based on Pairwise Sequence Alignment and Identity Calculation. *Plos One* **9**.

Murdin, A. D., Lu, H.-h., Murray, M. G. & Wimmer, E. (1992). Poliovirus antigenic hybrids simultaneously expressing antigenic determinants from all three serotypes. *J Gen Virol* **73**, 607-611.

Murray, M. G., Kuhn, R. J., Arita, M., Kawamura, N., Nomoto, A. & Wimmer, E. (1988). Poliovirus type 1/type 3 antigenic hybrid virus constructed in vitro elicits type 1 and type 3 neutralizing antibodies in rabbits and monkeys. *P Natl Acad Sci USA* **85**, 3203-3207.

Nagy, P. D., Zhang, C. & Simon, A. E. (1998). Dissecting RNA recombination in vitro: role of RNA sequences and the viral replicase. *The EMBO Journal* **17**, 2392-2403.

Nathanson, N. & Langmuir, A. D. (1995). The Cutter Incident - Poliomyelitis Following Formaldehyde-Inactivated Poliovirus Vaccination in the United-States during the Spring of 1955 (Reprinted from Am J Hyg, Vol 78, Pg 16-28, 1963). *Rev Med Virol* **5**, 126-131.

Nelson, A. L. (2010). Antibody fragments: Hope and hype. *mAbs* **2**, 77-83.

Newman, J. F. E., Rowlands, D. J. & Brown, F. (1973). Physicochemical Sub-Grouping of Mammalian Picornaviruses. *J Gen Virol* **18**, 171-180.

Ng, K. K. S., Arnold, J. J. & Cameron, C. E. (2008). Structure-Function Relationships Among RNA-Dependent RNA Polymerases. *Current topics in microbiology and immunology* **320**, 137-156.

Ng, T. F. F., Wellehan, J. F. X., Coleman, J. K., Kondov, N. O., Deng, X., Waltzek, T. B., Reuter, G., Knowles, N. J. & Delwart, E. (2015). A tortoise-infecting picornavirus expands the host range of the family Picornaviridae. *Arch Virol* **160**, 1319-1323.

Noad, R. & Roy, P. (2003). Virus-like particles as immunogens. *Trends Microbiol* **11**, 438-444.

O'Brien, R. T. & Newman, J. S. (1977). Inactivation of polioviruses and coxsackieviruses in surface water. *Applied and environmental microbiology* **33**, 334-340.

O'Reilly, E. K. & Kao, C. C. (1998). Analysis of RNA-dependent RNA polymerase structure and function as guided by known polymerase structures and computer predictions of secondary structure. *Virology* **252**, 287-303.

Oberste, M. S., Feeroz, M. M., Maher, K., Nix, W. A., Engel, G. A., Begum, S., Hasan, K. M., Oh, G., Pallansch, M. A. & Jones-Engel, L. (2013). Naturally Acquired Picornavirus Infections in Primates at the Dhaka Zoo. *Journal of virology* **87**, 572-580.

Oberste, M. S., Maher, K. & Pallansch, M. A. (2002). Molecular Phylogeny and Proposed Classification of the Simian Picornaviruses. *Journal of virology* **76**, 1244-1251.

Oberste, M. S., Moore, D., Anderson, B., Pallansch, M. A., Pevear, D. C. & Collett, M. S. (2009). In Vitro Antiviral Activity of V-073 against Polioviruses. *Antimicrob Agents Ch* **53**, 4501-4503.

Odhiambo, C., Venter, M., Limbaso, K., Swanepoel, R. & Sang, R. (2014). Genome Sequence Analysis of In Vitro and In Vivo Phenotypes of Bunyamwera and Ngari Virus Isolates from Northern Kenya. *Plos One* **9**.

Onodera, S. & Phillips, B. A. (1987). A Novel Method for Obtaining Poliovirus-14 S Pentamers from Procapsids and Their Self-Assembly into Virus-Like Shells. *Virology* **159**, 278-287.

Orenstein, W., Figueroa, J. P., Arita, I., Mohammad, A. J., Basu, R. N., Nkrumah, F. K. & Eradication, W. H. O. G. (2002). "Endgame" issues for the global polio eradication initiative. *Clin Infect Dis* **34**, 72-77.

Osterhaus, A. D. M. E., Vanwezel, A. L., Hazendonk, T. G., Uytdehaag, F. G. C. M., Vanasten, J. A. A. M. & Vansteenis, B. (1983). Monoclonal-Antibodies to Polioviruses - Comparison of Intratypic Strain Differentiation of Poliovirus Type-1 Using Monoclonal-Antibodies Versus Cross-Absorbed Antisera. *Intervirology* **20**, 129-136.

Pais, F. S.-M., Ruy, P. d. C., Oliveira, G. & Coimbra, R. S. (2014). Assessing the efficiency of multiple sequence alignment programs. *Algorithms for Molecular Biology : AMB* **9**, 4-4.

Pallansch M., R. R. (2007). Enteroviruses: Polioviruses, Coxsackieviruses, Echoviruses, and Newer Enteroviruses. . In *Field's Virology* pp. 839-893. Edited by P. H. M. Knippe D.M., Griffin D.E., Lamb R.A., Straus S.E., Martin M.A. and Roizman B. . USA: Lippincott Williams & Wilkins.

Panjwani, A., Strauss, M., Jackson, T., Chou, J.J., Rowlands, D.J., Stonehouse, N.J., Hogle, J.M., Tuthill, T.J. (2013). A capsid protein of a non-enveloped virus induces membrane permeability by the formation of a size-selective multimeric pore.

Papakonstantinou, T., Harris, S. & Hearn, M. T. W. (2009). Expression of GFP using Pichia pastoris vectors with zeocin or G-418 sulphate as the primary selectable marker. *Yeast* **26**, 311-321.

Parsley, T. B., Cornell, C. T. & Semler, B. L. (1999a). Modulation of the RNA binding and protein processing activities of poliovirus polypeptide 3CD by the viral RNA polymerase domain. *J Biol Chem* **274**, 12867-12876.

Parsley, T. B., Cornell, C. T. & Semler, B. L. (1999b). Modulation of the RNA binding and protein processing activities of poliovirus polypeptide 3CD by the viral RNA polymerase domain. *J Biol Chem* **274**, 12867-12876.

Patel, M., Zipursky, S., Orenstein, W., Garon, J. & Zaffran, M. (2015). Polio endgame: the global introduction of inactivated polio vaccine. *Expert Review of Vaccines* **14**, 749-762.

Pathak, H. B., Arnold, J. J., Wiegand, P. N., Hargittai, M. R. S. & Cameron, C. E. (2007a). Picornavirus genome replication - Assembly and organization of the VPg uridylylation ribonucleoprotein (initiaion) complex. *J Biol Chem* **282**, 16202-16213.

Pathak, H. B., Arnold, J. J., Wiegand, P. N., Hargittai, M. R. S. & Cameron, C. E. (2007b). Picornavirus Genome Replication: ASSEMBLY AND ORGANIZATION OF THE VPg URIDYLYLATION RIBONUCLEOPROTEIN (INITIATION) COMPLEX. *The Journal of biological chemistry* **282**, 16202-16213.

Paul, A. V., Peters, J., Mugavero, J., Yin, J., van Boom, J. H. & Wimmer, E. (2003). Biochemical and Genetic Studies of the VPg Uridylylation

Reaction Catalyzed by the RNA Polymerase of Poliovirus. *Journal of virology* **77**, 891-904.

Paul, A. V., van Boom, J. H., Filippov, D. & Wimmer, E. (1998). Protein-primed RNA synthesis by purified poliovirus RNA polymerase. *Nature* **393**, 280-284.

Paul, J. R. & Trask, J. D. (1935). THE NEUTRALIZATION TEST IN POLIOMYELITIS : COMPARATIVE RESULTS WITH FOUR STRAINS OF THE VIRUS. *The Journal of Experimental Medicine* **61**, 447-464.

Pelletier, J. & Sonenberg, N. (1988). Internal initiation of translation of eukaryotic mRNA directed by a sequence derived from poliovirus RNA. *Nature* **334**, 320-325.

Pettersson, R. F., Ambros, V. & Baltimore, D. (1978). Identification of a protein linked to nascent poliovirus RNA and to the polyuridylic acid of negative-strand RNA. *Journal of virology* **27**, 357-365.

Pevear, D. C., Tull, T. M., Seipel, M. E. & Groarke, J. M. (1999). Activity of pleconaril against enteroviruses. *Antimicrob Agents Ch* **43**, 2109-2115.

Peyret H. P., S. S. L. S., Stonehouse N. J. S., Rowlands D. J. R. (2015). History and Potential of Hepatitis B Virus core as a VLP vaccine platform. In *Viral Nanotechnology*, pp. 177-186. Edited by P. P. : Yury Khudyakov: CRC Press.

Phan, H. T. & Conrad, U. (2016). Plant-Based Vaccine Antigen Production. In *Vaccine Technologies for Veterinary Viral Diseases: Methods and Protocols*, pp. 35-47. Edited by A. Brun. New York, NY: Springer New York.

Phelps, N. B. D., Mor, S. K., Armien, A. G., Batts, W., Goodwin, A. E., Hopper, L., McCann, R., Ng, T. F. F., Puzach, C., Waltzek, T. B., Delwart, E., Winton, J. & Goyal, S. M. (2014). Isolation and Molecular Characterization of a Novel Picornavirus from Baitfish in the USA. *Plos One* **9**, e87593.

Phuektes, P., Chua, B. H., Sanders, S., Bek, E. J., Kok, C. C. & McMinn, P. C. (2011). Mapping genetic determinants of the cell-culture growth phenotype of enterovirus 71. *J Gen Virol* **92**, 1380-1390.

Pons-Salort, M., Burns, C. C., Lyons, H., Blake, I. M., Jafari, H., Oberste, M. S., Kew, O. M. & Grassly, N. C. (2016). Preventing Vaccine-Derived Poliovirus Emergence during the Polio Endgame. *Plos Pathog* **12**, e1005728.

Porter, A. G. (1993). Picornavirus Nonstructural Proteins - Emerging Roles in Virus-Replication and Inhibition of Host-Cell Functions. *Journal of virology* **67**, 6917-6921.

Pushko, P., Pumpens, P. & Grens, E. (2013). Development of Virus-Like Particle Technology from Small Highly Symmetric to Large Complex Virus-Like Particle Structures. *Intervirology* **56**, 141-165.

PUTNAM , J. J. & TAYLOR , E. W. (1893). Is Acute Poliomyelitis Unusually Prevalent This Season? *The Boston Medical and Surgical Journal* **129**, 509-510.

Racaniello, V. R. & Baltimore, D. (1981). Cloned Poliovirus Complementary-DNA Is Infectious in Mammalian-Cells. *Science* **214**, 916-919.

Raciniello, V. R. (2007). Picornaviridae: The virus and their replication. In *Field's Virology*, 5 edn, pp. 795-838. Edited by P. H. M. Knippe D.M., Griffin D.E., Lamb R.A., Straus S.E., Martin M.A. and Roizman B. USA: Lippincott Williams & Wilkins.

Rakoto-Andrianarivelo, M., Guillot, S., Iber, J., Balanant, J., Blondel, B., Riquet, F., Martin, J., Kew, O., Randriamanalina, B., Razafinimpiasa, L., Rousset, D. & Delpeyroux, F. (2007). Co-Circulation and Evolution of Polioviruses and Species C Enteroviruses in a District of Madagascar. *Plos Pathog* **3**, e191.

Ramsingh, A. I., Caggana, M. & Ronstrom, S. (1995). Genetic mapping of the determinants of plaque morphology of coxsackievirus B4. *Arch Virol* **140**, 2215-2226.

Robles, J. a. D., M. (1994). pGEM®-T Vector Systems troubleshooting guide. *Promega Notes* **45**, 2.

Rodriguez-Limas, W. A., Sekar, K. & Tyo, K. E. J. (2013). Virus-like particles: the future of microbial factories and cell-free systems as platforms for vaccine development. *Curr Opin Biotech* **24**, 1089-1093.

Rohll, J. B., Moon, D. H., Evans, D. J. & Almond, J. W. (1995a). The 3'-Untranslated Region of Picornavirus Rna - Features Required for Efficient Genome Replication. *Journal of virology* **69**, 7835-7844.

Rohll, J. B., Moon, D. H., Evans, D. J. & Almond, J. W. (1995b). The 3' untranslated region of picornavirus RNA: features required for efficient genome replication. *Journal of virology* **69**, 7835-7844.

Rohll, J. B., Percy, N., Ley, R., Evans, D. J., Almond, J. W. & Barclay, W. S. (1994). The 5'-Untranslated Regions of Picornavirus Rnas Contain Independent Functional Domains Essential for Rna Replication and Translation. *Journal of virology* **68**, 4384-4391.

Rombaut, B., Boeye, A., Ferguson, M., Minor, P. D., Mosser, A. & Rueckert, R. (1990). Creation of an Antigenic Site in Poliovirus Type-1 by Assembly of 14-S Subunits. *Virology* **174**, 305-307.

Rombaut, B. & Jore, J. P. (1997a). Immunogenic, non-infectious polio subviral particles synthesized in Saccharomyces cerevisiae. *J Gen Virol* **78 (Pt 8)**, 1829-1832.

Rombaut, B. & Jore, J. P. M. (1997b). Immunogenic, non-infectious polio subviral particles synthesized in Saccharomyces cerevisiae. *J Gen Virol* **78**, 1829-1832.

Rombaut, B., Verheyden, B., Andries, K. & Boeyé, A. (1994). Thermal inactivation of oral polio vaccine: contribution of RNA and protein inactivation. *Journal of virology* **68**, 6454-6457.

Rombaut, B., Vrijsen, R. & Boeye, A. (1983). Epitope Evolution in Poliovirus Maturation. *Arch Virol* **76**, 289-298.

Rombaut, B., Vrijsen, R. & Boeye, A. (1986). Assembly Factors in Poliovirus Morphogenesis. *Virology* **153**, 137-144.

Rossmann, M. G., He, Y. & Kuhn, R. J. (2002a). Picornavirus-receptor interactions. *Trends in microbiology* **10**, 324-331.

Rossmann, M. G., He, Y. N. & Kuhn, R. J. (2002b). Picornavirus-receptor interactions. *Trends Microbiol* **10**, 324-331.

Rowlands, D. J. (2003). Special issue - Foot-and-mouth disease - Preface. *Virus Res* **91**, 1-1.

Rybicki, E. P. (2014). Plant-based vaccines against viruses. *Virol J* **11**, 205.

Sabin, A. B. & Ward, R. (1941). THE NATURAL HISTORY OF HUMAN POLIOMYELITIS : I. DISTRIBUTION OF VIRUS IN NERVOUS AND NON-NERVOUS TISSUES. *The Journal of Experimental Medicine* **73**, 771-793.

Sabint, A. B. a. B., L.R. (1973). History of Sabin attenuated poliovirus oral live vaccine strains. *Journal of Biological Standardization* **1**, 115-l 118.

Sainsbury, F., Thuenemann, E. C. & Lomonossoff, G. P. (2009). pEAQ: versatile expression vectors for easy and quick transient expression of heterologous proteins in plants. *Plant Biotechnol J* **7**, 682-693.

Salk, J. E., Krech, U., Youngner, J. S., Bennett, B. L., Lewis, L. J. & Bazeley, P. L. (1954). Formaldehyde Treatment and Safety Testing of Experimental Poliomyelitis Vaccines. *American Journal of Public Health and the Nations Health* **44**, 563-570.

Sandoval, I. V. & Carrasco, L. (1997). Poliovirus infection and expression of the poliovirus protein 2B provoke the disassembly of the Golgi complex, the organelle target for the antipoliovirus drug Ro-090179. *Journal of virology* **71**, 4679-4693.

Sanjuan, R., Nebot, M. R., Chirico, N., Mansky, L. M. & Belshaw, R. (2010). Viral mutation rates. *Journal of virology* **84**, 9733-9748.

Sanjuán, R., Nebot, M. R., Chirico, N., Mansky, L. M. & Belshaw, R. (2010). Viral Mutation Rates. *Journal of virology* **84**, 9733-9748.

Santi, L., Batchelor, L., Huang, Z., Hjelm, B., Kilbourne, J., Arntzen, C. J., Chen, Q. & Mason, H. S. (2008). An efficient plant viral expression system generating orally immunogenic Norwalk virus-like particles. *Vaccine* **26**, 1846-1854.

Santti, J., Hyypiä, T., Kinnunen, L. & Salminen, M. (1999). Evidence of Recombination among Enteroviruses. *Journal of virology* **73**, 8741-8749.

Saraswat, S., Athmaram, T. N., Parida, M., Agarwal, A., Saha, A. & Dash, P. K. (2016). Expression and Characterization of Yeast Derived Chikungunya Virus Like Particles (CHIK-VLPs) and Its Evaluation as a Potential Vaccine Candidate. *PLoS Neglected Tropical Diseases* **10**, e0004782.

Schotte, L., Rombaut, B. & Thys, B. (2012). A Liquid Phase Affinity Capture Assay Using Magnetic Beads to Study Protein-Protein Interaction: The Poliovirus-Nanobody Example. *Jove-J Vis Exp*.

Schotte, L., Strauss, M., Thys, B., Halewyck, H., Filman, D. J., Bostina, M., Hogle, J. M. & Rombaut, B. (2014). Mechanism of Action and Capsid-Stabilizing Properties of VHHs with an In Vitro Antipolioviral Activity. *Journal of virology* **88**, 4403-4413.

Schotte, L., Thys, B., Strauss, M., Filman, D. J., Rombaut, B. & Hogle, J. M. (2015). Characterization of Poliovirus Neutralization Escape Mutants of Single-Domain Antibody Fragments (VHHs). *Antimicrob Agents Ch* **59**, 4695-4706.

Seipelt, J., Guarne, A., Bergmann, E., James, M., Sommergruber, W., Fita, I. & Skern, T. (1999). The structures of picornaviral proteinases. *Virus Res* **62**, 159-168.

Shepard, D. A., Heinz, B. A. & Rueckert, R. R. (1993). WIN 52035-2 inhibits both attachment and eclipse of human rhinovirus 14. *Journal of virology* **67**, 2245-2254.

Shingler, K. L., Cifuente, J. O., Ashley, R. E., Makhov, A. M., Conway, J. F. & Hafenstein, S. (2015). The Enterovirus 71 Procapsid Binds Neutralizing Antibodies and Rescues Virus Infection In Vitro. *Journal of virology* **89**, 1900-1908.

Shiomi, H., Urasawa, T., Urasawa, S., Kobayashi, N., Abe, S. & Taniguchi, K. (2004). Isolation and characterisation of poliovirus mutants resistant to heating at 50 degrees C for 30 min. *J Med Virol* **74**, 484-491.

Shoji, Y., Farrance, C. E., Bautista, J., Bi, H., Musiychuk, K., Horsey, A., Park, H., Jaje, J., Green, B. J., Shamloul, M., Sharma, S., Chichester, J. A., Mett, V. & Yusibov, V. (2012). A plant-based system for rapid production of influenza vaccine antigens. *Influenza and Other Respiratory Viruses* **6**, 204-210.

Shrivastava, A., Gupta, N., Upadhyay, P. & Puliyel, J. (2012). Caution needed in using oral polio vaccine beyond the cold chain: Vaccine vial monitors may be unreliable at high temperatures. *The Indian Journal of Medical Research* **135**, 520-522.

Simmonds, P. (2006). Recombination and selection in the evolution of picornaviruses and other Mammalian positive-stranded RNA viruses. *Journal of virology* **80**, 11124-11140.

Simmonds, P. & Welch, J. (2006). Frequency and Dynamics of Recombination within Different Species of Human Enteroviruses. *Journal of virology* **80**, 483-493.

Simon-Loriere, E. & Holmes, E. C. (2011). Why do RNA viruses recombine? *Nat Rev Micro* **9**, 617-626.

Smellie, J. M. (1933). A Review of the Use of Immune Serum in Acute Poliomyelitis. *Arch Dis Child* **8**, 75-83.

Smyth, M. S. & Martin, J. H. (2002). Picornavirus uncoating. *Molecular Pathology* **55**, 214-219.

Solomon, T. & Willison, H. (2003). Infectious causes of acute flaccid paralysis. *Curr Opin Infect Dis* **16**, 375-381.

Sommer, J. M., Smith, P. H., Parthasarathy, S., Isaacs, J., Vijay, S., Kieran, J., Powell, S. K., McClelland, A. & Wright, J. F. (2003). Quantification of adeno-associated virus particles and empty capsids by optical density measurement. *Mol Ther* **7**, 122-128.

Spence, S. E., Gilbert, D. J., Swing, D. A., Copeland, N. G. & Jenkins, N. A. (1989). Spontaneous germ line virus infection and retroviral insertional mutagenesis in eighteen transgenic Srev lines of mice. *Mol Cell Biol* **9**, 177-184.

Spiess, C., Zhai, Q. T. & Carter, P. J. (2015). Alternative molecular formats and therapeutic applications for bispecific antibodies. *Mol Immunol* **67**, 95-106.

Stanway, G. (1990). Structure, Function and Evolution of Picornaviruses. *J Gen Virol* **71**, 2483-2501.

Stewart, F. W. & Haselbauer, P. (1928). Virus neutralization experiments with Rosenow's and Pettit's antipoliomyelitic sera. *The Journal of experimental medicine* **48**, 449.

Strauss, M., Schotte, L., Thys, B., Filman, D. J. & Hogle, J. M. (2016). Five of Five VHHs Neutralizing Poliovirus Bind the Receptor-Binding Site. *Journal of virology* **90**, 3496-3505.

Strebel, K. & Beck, E. (1986). A second protease of foot-and-mouth disease virus. *Journal of virology* **58**.

Sun, D., Chen, S., Cheng, A. & Wang, M. (2016). Roles of the Picornaviral 3C Proteinase in the Viral Life Cycle and Host Cells. *Viruses* **8**, 82.

Sutter, R. W., Caceres, V. M. & Mas Lago, P. (2004). The role of routine polio immunization in the post-certification era. *Bull World Health Organ* **82**, 31-39.

Sweeney, T. R., Cisnetto, V., Bose, D., Bailey, M., Wilson, J. R., Zhang, X., Belsham, G. J. & Curry, S. (2010). Foot-and-mouth disease virus 2C is a hexameric AAA+ protein with a coordinated ATP hydrolysis mechanism. *J Biol Chem* **285**, 24347-24359.

Takegami, T., Kuhn, R. J., Anderson, C. W. & Wimmer, E. (1983). Membrane-dependent uridylylation of the genome-linked protein VPg of poliovirus. *P Natl Acad Sci USA* **80**, 7447-7451.

Tan, M., Zhong, W. M., Song, D., Thornton, S. & Jiang, X. (2004). E. coli-expressed recombinant norovirus capsid proteins maintain authentic antigenicity and receptor binding capability. *J Med Virol* **74**, 641-649.

Tanaka, T., Kato, N., Hijikata, M. & Shimotohno, K. (1993). Base Transitions and Base Transversions Seen in Mutations among Various Types of the Hepatitis-C Viral Genome. *Febs Lett* **315**, 201-203.

Tao, Z., Wang, H., Xu, A., Zhang, Y., Song, L., Zhu, S., Li, Y., Yan, D., Liu, G., Yoshida, H., Liu, Y., Feng, L., Chosa, T. & Xu, W. (2010). Isolation of a recombinant type 3/type 2 poliovirus with a chimeric capsid VP1 from sewage in Shandong, China. *Virus Res* **150**, 56-60.

Taubenberger, J. K. & Kash, J. C. (2010). Influenza Virus Evolution, Host Adaptation and Pandemic Formation. *Cell Host Microbe* **7**, 440-451.

Thanavala, Y., Mahoney, M., Pal, S., Scott, A., Richter, L., Natarajan, N., Goodwin, P., Arntzen, C. J. & Mason, H. S. (2005). Immunogenicity in humans of an edible vaccine for hepatitis B. *Proc Natl Acad Sci U S A* **102**, 3378-3382.

Thompson, A. A. & Peersen, O. B. (2004). Structural basis for proteolysis-dependent activation of the poliovirus RNA-dependent RNA polymerase. *The EMBO Journal* **23**, 3462-3471.

Thompson, K. M. & Duintjer Tebbens, R. J. (2014). Modeling the dynamics of oral poliovirus vaccine cessation. *J Infect Dis* **210**.

Thuenemann, E. C., Lenzi, P., Love, A. J., Taliansky, M., Becares, M., Zuniga, S., Enjuanes, L., Zahmanova, G. G., Minkov, I. N., Matic, S., Noris, E., Meyers, A., Hattingh, A., Rybicki, E. P., Kiselev, O. I., Ravin, N. V., Eldarov, M. A., Skryabin, K. G. & Lomonossoff, G. P. (2013). The use of transient expression systems for the rapid production of virus-like particles in plants. *Curr Pharm Des* **19**, 5564-5573.

Thys, B., Schotte, L., Muyldermans, S., Wernery, U., Hassanzadeh-Ghassabeh, G. & Rombaut, B. (2010). In vitro antiviral activity of single domain antibody fragments against poliovirus. *Antivir Res* **87**, 257-264.

Toyoda, H., Kohara, M., Kataoka, Y., Suganuma, T., Omata, T., Imura, N. & Nomoto, A. (1984a). Complete Nucleotide-Sequences of All 3 Poliovirus Serotype Genomes - Implication for Genetic-Relationship, Gene-Function and Antigenic Determinants. *J Mol Biol* **174**, 561-585.

Toyoda, H., Kohara, M., Kataoka, Y., Suganuma, T., Omata, T., Imura, N. & Nomoto, A. (1984b). Complete nucleotide sequences of all three poliovirus serotype genomes. Implication for genetic relationship, gene function and antigenic determinants. *Journal of molecular biology* **174**, 561-585.

Tree, J. A., Richardson, C., Fooks, A. R., Clegg, J. C. & Looby, D. (2001). Comparison of large-scale mammalian cell culture systems with egg culture for the production of influenza virus A vaccine strains. *Vaccine* **19**, 3444-3450.

Trevelyan, B., Smallman-Raynor, M. & Cliff, A. D. (2005). The spatial structure of epidemic emergence: geographical aspects of poliomyelitis in north-eastern USA, July–October 1916. *Journal of the Royal Statistical Society Series A, (Statistics in Society)* **168**, 701-722.

Trono, D., Pelletier, J., Sonenberg, N. & Baltimore, D. (1988). Translation in mammalian cells of a gene linked to the poliovirus 5' noncoding region. *Science* **241**, 445-448.

Tuthill, T. J., Bubeck, D., Rowlands, D. J. & Hogle, J. M. (2006). Characterization of Early Steps in the Poliovirus Infection Process: Receptor-Decorated Liposomes Induce Conversion of the Virus to Membrane-Anchored Entry-Intermediate Particles. *Journal of virology* **80**, 172-180.

Tuthill, T. J., Groppelli, E., Hogle, J. M. & Rowlands, D. J. (2010). Picornaviruses. *Current topics in microbiology and immunology* **343**, 43-89.

Underwood, M. (1789). Debility of the Lower Extremities. In *A Treatise on the Diseases of Children, with General Directions for the Management of Infants from Birth* London: J. Mathews.

Van Dyke, T. A. & Flanegan, J. B. (1980). Identification of poliovirus polypeptide P63 as a soluble RNA-dependent RNA polymerase. *Journal of virology* **35**, 732-740.

van Kuppeveld, F. J., Hoenderop, J. G., Smeets, R. L., Willems, P. H., Dijkman, H. B., Galama, J. M. & Melchers, W. J. (1997). Coxsackievirus protein 2B modifies endoplasmic reticulum membrane and plasma membrane permeability and facilitates virus release. *The EMBO journal* **16**, 3519-3532.

Vanderwerf, S., Wychowski, C., Bruneau, P., Blondel, B., Crainic, R., Horodniceanu, F. & Girard, M. (1983). Localization of a Poliovirus Type-1 Neutralization Epitope in Viral Capsid Polypeptide-Vp1. *P Natl Acad Sci-Biol* **80**, 5080-5084.

Vignuzzi, M., Stone, J. K., Arnold, J. J., Cameron, C. E. & Andino, R. (2006). Quasispecies diversity determines pathogenesis through cooperative interactions in a viral population. *Nature* **439**, 344-348.

Vrijsen, R., Rombaut, B. & Boeye, A. (1983). A Simple Quantitative Protein-a Micro-Immunoprecipitation Method - Assay of Antibodies to the N-Antigen and H-Antigen of Poliovirus. *J Immunol Methods* **59**, 217-220.

Walter, T. S., Ren, J., Tuthill, T. J., Rowlands, D. J., Stuart, D. I. & Fry, E. E. (2012). A plate-based high-throughput assay for virus stability and vaccine formulation. *Journal of virological methods* **185**, 166-170.

Wang, C., Jiang, P., Sand, C., Paul, A.V. and Wimmer, E. (2012). Alanine Scanning of Poliovirus 2CATPase Reveals New Genetic Evidence that Capsid Protein/2CATPase Interactions Are Essential for Morphogenesis. *J Virol* **86**, 9964-9975.

Wang, X., Liu, J., Zheng, Y., Li, J., Wang, H., Zhou, Y., Qi, M., Yu, H., Tang, W. & Zhao, W. M. (2008). An optimized yeast cell-free system: Sufficient for translation of human papillomavirus 58 L1 mRNA and assembly of virus-like particles. *J Biosci Bioeng* **106**, 8-15.

Wang, X., Ren, J., Gao, Q., Hu, Z., Sun, Y., Li, X., Rowlands, D. J., Yin, W., Wang, J., Stuart, D. I., Rao, Z. & Fry, E. E. (2015). Hepatitis A virus and the origins of picornaviruses. *Nature* **517**, 85-88.

Weber, K. & Osborn, M. (2006). SDS-PAGE to determine the molecular weight of proteins: The work of Klaus Weber and Mary Osborn - The reliability of molecular weight determinations by dodecyl sulfate-polyacrylamide gel electrophoresis (reprinted from J.Biol. Chem. vol. 244, pg. 4406-4412, 1969). *J Biol Chem* **281**.

Weinacker, D., Rabert, C., Zepeda, A. B., Figueroa, C. A., Pessoa, A. & Farías, J. G. (2013). Applications of recombinant Pichia pastoris in the healthcare industry. *Brazilian Journal of Microbiology* **44**, 1043-1048.

Weller, T. H. & Robbins, F. C. (1950). Cultivation of the Lansing Strain of Poliomyelitis Virus in Cultures of Various Human Embryonic Tissues. *Am J Dis Child* **79**, 1133-1134.

Weller, T. H., Robbins, F. C. & Enders, J. F. (1949). Cultivation of Poliomyelitis Virus in Cultures of Human Foreskin and Embryonic Tissues. *P Soc Exp Biol Med* **72**, 153-155.

Wesolowski, J., Alzogaray, V., Reyelt, J., Unger, M., Juarez, K., Urrutia, M., Cauerhff, A., Danquah, W., Rissiek, B., Scheuplein, F., Schwarz, N., Adriouch, S., Boyer, O., Seman, M., Licea, A., Serreze, D. V., Goldbaum, F. A., Haag, F. & Koch-Nolte, F. (2009). Single domain antibodies: promising experimental and therapeutic tools in infection and immunity. *Med Microbiol Immun* **198**, 157-174.

WHO (2005a). Case definitions for the four diseases requiring notification in all circumstances under the International Health Regulations.

WHO (2005b). Cessation of routine oral polio vaccine (OPV) use after global polio eradication: framework for national policy makers in OPV-using countries. Geneva: World Health Organization.

WHO (2013). Poliomyelitis. In *Fact sheet* p. Poliomyelitis fact sheet: The World Health Organisation.

WHO Country Office Tajikistan, W. R. O. f. E., European Centre for Disease Prevention and Control (2010). Outbreak of poliomyelitis in Tajikistan in 2010: risk for importation and impact on polio surveillance in Europe? *Euro surveillance : bulletin Europeen sur les maladies transmissibles = European communicable disease bulletin* **15**.

Wickman, I. (1911). Acute poliomyelitis and polyneuritis. *Z Gesamte Neurol Psy* **4**, 54-66.

Wickman, I. (1980). On the Epidemiology of Heine-Medins Disease. *Rev Infect Dis* **2**, 319-327.

Wiegers, K. J. & Dernick, R. (1985). Evidence for Conformational-Changes of Poliovirus Precursor Particles during Virus Morphogenesis. *J Gen Virol* **66**, 1037-1044.

Wien, M. W., Chow, M. & Hogle, J. M. (1996). Poliovirus: New insights from an old paradigm. *Structure* **4**, 763-767.

Wien, M. W., Curry, S., Filman, D. J. & Hogle, J. M. (1997). Structural studies of poliovirus mutants that overcome receptor defects. *Nature structural biology* **4**, 666-674.

Wolff, C., Roesel, S., Lipskaya, G., Landaverde, M., Humayun, A., Withana, N., Ramamurty, N., Tomori, O., Okiror, S. O., Salla, M. & Dowdle, W. (2014). Progress Toward Laboratory Containment of Poliovirus After Polio Eradication. *J Infect Dis* **210**, S454-S458.

Xiang, W., Harris, K. S., Alexander, L. & Wimmer, E. (1995). Interaction between the 5'-terminal cloverleaf and 3AB/3CDpro of poliovirus is essential for RNA replication. *Journal of virology* **69**, 3658-3667.

Xiao, Y., Chen, H.-Y., Wang, Y., Yin, B., Lv, C., Mo, X., Yan, H., Xuan, Y., Huang, Y., Pang, W., Li, X., Yuan, Y. A. & Tian, K. (2016). Large-

scale production of foot-and-mouth disease virus (serotype Asia1) VLP vaccine in Escherichia coli and protection potency evaluation in cattle. *BMC Biotechnology* **16**, 56.

Yakum, M. N., Ateudjieu, J., Walter, E. A. & Watcho, P. (2015). Vaccine storage and cold chain monitoring in the North West region of Cameroon: a cross sectional study. *BMC Research Notes* **8**, 145.

Yalamanchili, P., Datta, U. & Dasgupta, A. (1997). Inhibition of host cell transcription by poliovirus: cleavage of transcription factor CREB by poliovirus-encoded protease 3Cpro. *Journal of virology* **71**, 1220-1226.

Youngner, J. S. (1957). Thermal Inactivation Studies with Different Strains of Poliovirus. *The Journal of Immunology* **78**, 282-290.

Ypmawong, M. F., Dewalt, P. G., Johnson, V. H., Lamb, J. G. & Semler, B. L. (1988). Protein 3cd Is the Major Poliovirus Proteinase Responsible for Cleavage of the P1 Capsid Precursor. *Virology* **166**, 265-270.

Yui, L. A. & Gledhill, R. F. (1991). Limb Paralysis as a Manifestation of Coxsackie-B Virus-Infection. *Dev Med Child Neurol* **33**, 427-438.

Zandi, R. & van der Schoot, P. (2009). Size Regulation of ss-RNA Viruses. *Biophys J* **96**, 9-20.

Zeichhardt, H., Otto, M. J., Mckinlay, M. A., Willingmann, P. & Habermehl, K. O. (1987a). Inhibition of Poliovirus Uncoating by Disoxaril (Win-51711). *Virology* **160**, 281-285.

Zeichhardt, H., Otto, M. J., Mckinlay, M. A., Willingmann, P. & Habermehl, K. O. (1987b). Inhibition of Poliovirus Uncoating in Acidic Organelles by Disoxaril (Win-51711). *Eur J Cell Biol* **43**, 66-66.

Zhang, C., Ku, Z. Q., Liu, Q. W., Wang, X. L., Chen, T., Ye, X. H., Li, D. P., Jin, X. & Huang, Z. (2015). High-yield production of recombinant virus-like particles of enterovirus 71 in Pichia pastoris and their protective efficacy against oral viral challenge in mice. *Vaccine* **33**, 2335-2341.

Zhang, C., Liu, Q., Ku, Z., Hu, Y., Ye, X., Zhang, Y. & Huang, Z. (2016a). Coxsackievirus A16-like particles produced in Pichia pastoris elicit high-titer neutralizing antibodies and confer protection against lethal viral challenge in mice. *Antivir Res* **129**, 47-51.

Zhang, P., Mueller, S., Morais, M. C., Bator, C. M., Bowman, V. D., Hafenstein, S., Wimmer, E. & Rossmann, M. G. (2008). Crystal structure of CD155 and electron microscopic studies of its complexes with polioviruses. *P Natl Acad Sci USA* **105**, 18284-18289.

Zhang, Y., Wang, Z. F., Zhan, Y., Gong, Q., Yu, W. T., Deng, Z. B., Wang, A. B., Yang, Y. & Wang, N. D. (2016b). Generation of E-coli-derived virus-like particles of porcine circovirus type 2 and their use in an indirect IgG enzyme-linked immunosorbent assay. *Arch Virol* **161**, 1485-1491.

Zhang, Y., Zhu, S. L., Yan, D. M., Liu, G. Y., Bai, R. Y., Wang, D. Y., Chen, L., Zhu, H., An, H. Q., Kew, O. & Xu, W. B. (2010). Natural Type

3/Type 2 Intertypic Vaccine-Related Poliovirus Recombinants with the First Crossover Sites within the VP1 Capsid Coding Region. *Plos One* **5**.